AD_____

Award Number: DAMD17-98-1-8260

TITLE: A Novel Apoptotic Protease Activated in Human Breast Cancer Cells After Poisoning Topoisomerase I

PRINCIPAL INVESTIGATOR: David Boothman, Ph.D.

CONTRACTING ORGANIZATION: Case Western Reserve University
Cleveland, Ohio 44106-7006

REPORT DATE: October 1999

TYPE OF REPORT: Annual

PREPARED FOR: U.S. Army Medical Research and Materiel Command, Fort Detrick, Maryland 21702-5012

NOTICE

USING GOVERNMENT DRAWINGS, SPECIFICATIONS, OR OTHER DATA INCLUDED IN THIS DOCUMENT FOR ANY PURPOSE OTHER THAN GOVERNMENT PROCUREMENT DOES NOT IN ANY WAY OBLIGATE THE U.S. GOVERNMENT. THE FACT THAT THE GOVERNMENT FORMULATED OR SUPPLIED THE DRAWINGS, SPECIFICATIONS, OR OTHER DATA DOES NOT LICENSE THE HOLDER OR ANY OTHER PERSON OR CORPORATION; OR CONVEY ANY RIGHTS OR PERMISSION TO MANUFACTURE, USE, OR SELL ANY PATENTED INVENTION THAT MAY RELATE TO THEM.

LIMITED RIGHTS LEGEND

Award Number: DAMD17-98-1-8260
Organization: Case Western Reserve University

Those portions of the technical data contained in this report marked as limited rights data shall not, without the written permission of the above contractor, be (a) released or disclosed outside the government, (b) used by the Government for manufacture or, in the case of computer software documentation, for preparing the same or similar computer software, or (c) used by a party other than the Government, except that the Government may release or disclose technical data to persons outside the Government, or permit the use of technical data by such persons, if (i) such release, disclosure, or use is necessary for emergency repair or overhaul or (ii) is a release or disclosure of technical data (other than detailed manufacturing or process data) to, or use of such data by, a foreign government that is in the interest of the Government and is required for evaluational or informational purposes, provided in either case that such release, disclosure or use is made subject to a prohibition that the person to whom the data is released or disclosed may not further use, release or disclose such data, and the contractor or subcontractor or subcontractor asserting the restriction is notified of such release, disclosure or use. This legend, together with the indications of the portions of this data which are subject to such limitations, shall be included on any reproduction hereof which includes any part of the portions subject to such limitations.

THIS TECHNICAL REPORT HAS BEEN REVIEWED AND IS APPROVED FOR PUBLICATION.

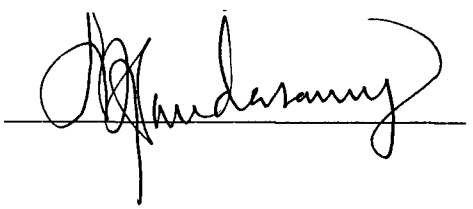

11/02/00

REPORT DOCUMENTATION PAGE

Form Approved
OMB No. 074-0188

1. AGENCY USE ONLY (Leave blank)	2. REPORT DATE	3. REPORT TYPE AND DATES COVERED
	October 1999	Annual (15 Sep 98 - 14 Sep 99)

4. TITLE AND SUBTITLE
A Novel Apoptotic Protease Activated in Human Breast Cancer Cells After Poisoning Topoisomerase I

5. FUNDING NUMBERS
DAMD17-98-1-8260

6. AUTHOR(S)
David Boothman, Ph.D.

7. PERFORMING ORGANIZATION NAME(S) AND ADDRESS(ES)
Case Western Reserve University
Cleveland, Ohio 44106-7006

e-mail:
dab30@po.cwru.edu

8. PERFORMING ORGANIZATION REPORT NUMBER

3. SPONSORING / MONITORING AGENCY NAME(S) AND ADDRESS(ES)
U.S. Army Medical Research and Materiel Command
Fort Detrick, Maryland 21702-5012

10. SPONSORING / MONITORING AGENCY REPORT NUMBER

11. SUPPLEMENTARY NOTES

12a. DISTRIBUTION / AVAILABILITY STATEMENT
Distribution authorized to U.S. Government agencies only (proprietary information, Oct 99). Other requests for this document shall be referred to U.S. Army Medical Research and Materiel Command, 504 Scott Street, Fort Detrick, Maryland 21702-5012.

12b. DISTRIBUTION CODE

13. ABSTRACT *(Maximum 200 Words)*

The goal of this grant is to clone the unknown protease activated by the active anti-breast cancer agent, ß-lapachone (ß-lap). The research team showed for the first time that ß-lap requires NQ01, a two-electron reduction enzyme elevated in many human breast cancers, for activation. The team then characterized the unknown apoptotic protease activated in human breast cancer cells by ß-lap, defining endpoints which will be essential for the ultimate isolation of this novel apoptotic protease. The unknown protease: (a) is a non-caspase cytsteine protease; (b) cleaves p53, lamin B, and PARP (atypically) in an NQ01-dependent manner at a time co-incident with calpain activation (appearance of an 18 kDa active form and its movement into the nucleus by confocal microscopy); and (c) is calcium-dependent (e.g., the proteolytic cleavage of PARP or p53 was blocked by co-administration of EGTA or EDTA), and the drug causes massive NQ01-dependent calcium influx within 3 mins posttreatment with 5-8 µM ß-lap;. Furthermore, significant progress has been made in developing reagents that will be required for the cloning of this novel noncaspase cysteine protease. The new hypothesis being tested is that ß-lap activates calpain, which then triggers DNA fragmentation and apoptosis.

14. SUBJECT TERMS
Breast Cancer, Apoptosis, ATP loss, ß-Lapachone, Calcium, Calpain, NQ01, PARP Cleavage.

15. NUMBER OF PAGES
187

16. PRICE CODE

17. SECURITY CLASSIFICATION OF REPORT	18. SECURITY CLASSIFICATION OF THIS PAGE	19. SECURITY CLASSIFICATION	20. LIMITATION OF ABSTRACT
Unclassified	Unclassified	Unclassified	Limited

FOREWORD

Opinions, interpretations, conclusions and recommendations are those of the author and are not necessarily endorsed by the U.S. Army.

__XX_Where copyrighted material is quoted, permission has been obtained to use such material.

__XX_Where material from documents designated for limited distribution is quoted, permission has been obtained to use the material.

__XX_Citations of commercial organizations and trade names in this report do not constitute an official Department of Army endorsement or approval of the products or services of these organizations.

__XX_In conducting research using animals, the investigator(s) adhered to the "Guide for the Care and Use of Laboratory Animals," prepared by the Committee on Care and use of Laboratory Animals of the Institute of Laboratory Resources, national Research Council (NIH Publication No. 86-23, Revised 1985).

_N/A_For the protection of human subjects, the investigator(s) adhered to policies of applicable Federal Law 45 CFR 46.

__XX_In conducting research utilizing recombinant DNA technology, the investigator(s) adhered to current guidelines promulgated by the National Institutes of Health.

__XX_In the conduct of research utilizing recombinant DNA, the investigator(s) adhered to the NIH Guidelines for Research Involving Recombinant DNA Molecules.

__XX_In the conduct of research involving hazardous organisms, the investigator(s) adhered to the CDC-NIH Guide for Biosafety in Microbiological and Biomedical Laboratories.

10-11-99

PI - Signature **Date:** October 14, 1999

TABLE OF CONTENTS:

INTRODUCTION: *Narrative that briefly (one paragraph) describes the subject, purpose, and scope of the research.*

Understanding and exploiting cell death processes in various human breast cancer cells following clinically useful anti-tumor drugs is a major focus in breast cancer research. The promise is that a better understanding of apoptotic and anti-apoptotic processes will allow improved anti-breast cancer efficacy of existing chemotherapeutic agents, as well as the development of additional efficacious drugs which elicit programmed cell suicide during treatment without inflamation. Apoptotic processes occurring in human breast cancer cells, particularly noncaspase-mediated cell death, are poorly understood. We discovered that a previously used drug for anti-trypanosomal therapies, ß-lapachone (ß-lap), is an active agent for the initiation and execution of apoptosis in a variety of human breast cancer cells in a p53-independent fashion. In the course of defining the compound's ability to cause cell death, we accomplished the following objectives or defined the following mechanism of action of the drug: (a) the primary intracellular target for ß-lap was NQ01, a two-electron reductase which was ionizing radiation-inducible; NQ01-containing cells were sensitive, NQ01-deficient cells were resistant; (b) interaction of the drug with NQ01 caused a futile cycling of the compound in which calcium homeostasis was altered within 3 mins and intracellular ATP levels decreased to <1% within 30 mins; (c) no evidence of caspase activation was detected in NQ01-containing breast cancer cells during ß-lap-mediated apoptosis; (d) an intracellular activation of a non-caspase cysteine protease was activated within 4-8 hours, concomitant with the appearance of DNA fragmentation, measured by TUNEL assays; (e) protease activation was concurrent with atypical cleavage of PARP, and cleavages of lamin B, p53 and degradation of pRb; (f) administration of dicoumarol (an NQ01 inhibitor) or calcium chelators (EGTA or EDTA) was able to prevent ß-lap-mediated apoptosis, and in the case of dicoumarol, cell lethality. The hypothesis currently being investigated is that ß-lap activates calpain, a noncaspase cysteine protease. The objective of the grant is to clone this unknown cyteine protease using a variety of strategies, including (1) substrate (PARP, p53 or lamin B) affinity chromatography; (2) previously described calpain isolation techniques; and (3) identification of specific ß-lap-mediated PARP cleavage sites, followed by use of these sites for the isolation of this ß-lap-activated, noncaspase cysteine protease. A complete understanding of the initiation and execution phases of ß-lap-mediated apoptosis should lead to improved therapy using this compound or more effective derivatives.

BODY OF GRANT UPDATE: *This section shall describe the research accomplishment associated with each Task outlined in the **approved** Statement of Work. Data presentation shall be comprehensive in providing a complete record of the research findings for the period of the annual/final report. However, appended publications and/or presentations **MAY** be substituted for a detailed description but **MUST** be referenced in the **BODY** of the report. If applicable, for each Task outlined in the Statement of Work, reference appended publications and/or presentations for details of result findings and tables and/or figures. The report shall include negative as well as positive findings, and also shall include any problems in accomplishing any of the tasks. Statistical tests of significance shall be applied to all data whenever possible. Figures and graphs referenced in the text shall be appended. The discussion shall include the relevance to the original hypothesis. Recommended changes or future work to better address the research topic may also be included, although changes to the original statement of work must be approved by the Grants Officer.*

F:* Previous *Statement of Work and Accomplishments Made.

Grant Objective:* *To test the hypothesis that expression of a novel apoptotic protease in human breast cancer cells directly correlates with the efficacy of ß-lap. The objectives of this grant are being accomplished as follows:

Specific Aim #1: Clone the unknown apoptotic protease, which is activated by ß-lap and whose activity correlates with toxicity after acute drug exposures *(Years 0-2).*

ß-Lap activates a noncaspase cysteine protease during apoptotic cell death. Previous research defined the DNA unwinding enzyme, Topoisomerase I (Topo I), as a potentially important intracellular target for the apoptosis-active drug, ß-lap. However, the efficacy of inhibition or activation of Topo I by ß-lap *in vivo* was **never established. In fact, to date no intracellular target for this compound has been established.**

In order to determine the key enzymatic target for ß-lap, we first established a number of intracellular proteolytic reactions that occur in a temporal sense during ß-lap-mediated apoptosis in MCF-7:WS8 breast cancer cells. Since activation of pre-existing zymogens is common-place during apoptosis and specific apoptotic substrates are known [e.g., poly(ADP-ribosyl) polymerase (PARP), lamin B, the retinoblastoma protein (pRb)], we examined proteolytic cleavage reactions occurring *in vivo* in four human breast cancer cell lines at various times after ß-lap (4-8 μM) treatment (Pink et. al., Exp. Cell Research, In Revision, enclosed). Typical cleavage of pRb and lamin B (Fig. 1) were observed at 8 h posttreatment with 4-8 μM ß-lap (Pink et. al., Exp. Cell Research, In Revision, enclosed). In contrast, an atypical cleavage of PARP (appearance of a ~60 kDa PARP polypeptide) was observed in ß-lap-treated MCF-7 cells (Fig. 2, Pink et. al., Exp. Cell Research, In Revision, enclosed), co-incident with lamin B and pRb cleavage (Fig. 1). Furthermore, cleavage of p53 in T47D human breast cancer cells was also found (Pink et. al., Exp. Cell Research, In Revision, enclosed). The cleavage events described above occurred in ß-lap-treated MCF-7 or T47D cells regardless of cell cycle or p53 status, strongly suggesting that DNA Topoisomerase II-alpha (which is cell cycle regulated, present in G_2/M and S-phases and absent in G_0/G_1 cells) was not a determinant in ß-lap-mediated toxicity. Also, we noted that MDA-MB-468 and MDA-MB-231 cells were fairly resistant to ß-lap treatment found (Pink et. al., Exp. Cell Research, In Revision, enclosed).

We next examined the effects of various specific and nonspecific enzyme inhibitors on ß-lap-mediated toxicity using the specific protein cleavage events *in vivo* described above. We discovered that iodoacetamide (I) and N-ethylmaleimide (N), global inhibitors of cysteine proteases, prevented PARP cleavage in ß-lap-treated MCF-7:WS8 cells (see Fig. 7, Pink et. al., Exp. Cell Research, In Revision, enclosed). In contrast, global inhibitors of caspases (i.e., zVAD-fmk, zAAD-fmk, and zFA-fmk) did not block atypical ß-lap-mediated PARP cleavage in MCF-7:WS8 cells. In addition, inhibitors of granzyme B, cathepsins D and L, trypsin and chymotrypsin-like proteases did not prevent ß-lap-mediated atypical PARP cleavage. Furthermore, calpeptin, calpain inhibitor III, and leupeptin (Figs. 2 and 3) also did not block ß-lap-mediated apoptosis and concomitant proteolyses *in vivo*. We concluded from these data that ß-lap treatment of certain sensitive human breast cancer cells caused the activation of a noncaspase cysteine protease during apoptosis; cells were demonstrated to be apoptotic by DNA fragmentation TUNEL assays (Pink et. al., Exp. Cell Research, In Revision, enclosed).

NQ01 is the major intracellular target for ß-lap. We extended our studies using inhibitors to more specific enzymes. The structural similarities between ß-lap and menadione and 1,2-naphthoquinones suggested that either one-electron reduction enzymes (p450 or b5R) or two-electron reductases (e.g., NQ01) may be involved in the toxification or detoxification of ß-lap. Administration of dicoumarol, a fairly specific inhibitor of NQ01, prevented ß-lap-mediated apoptosis, ß-lap-mediated proteolysis (e.g., atypical PARP cleavage), and ß-lap-induced cell death (see Figs. 1,2 and 4, Pink et. al., J. Biol. Chem., submitted, enclosed). Furthermore, NQ01 levels appeared to correlate well with overall sensitivity to ß-lap: MCF-7:WS8>T47D>>>MDA-MB-468 cells. MCF-7 cells contained the greatest levels of NQ01, with T47D cells containing significantly lower levels and NQ01 level absent in MDA-MB-468 cells (see Fig. 3, Pink et. al., J. Biol. Chem., submitted, enclosed). Furthermore, we noticed that MDA-MB-468 cells were fairly resistant to ß-lap and co-administration of dicoumarol with ß-lap did not affect the minimal toxicity caused by this drug in these cells.

To further demonstrate that MDA-MB-468 cells were resistant to ß-lap due to their lack of expression of NQ01, we then transfected these cells with CMV-controlled NQ01. Stable NQ01-expressing human MDA-MB-468 breast cancer transfectants were compared to cells containing pcDNA vector alone to their sensitivity to ß-lap with or without dicoumarol co-administration. As expected, NQ01-containing MDA-MB-468 transfectants were sensitive to ß-lap and this sensitivity was completely prevented by co-administration of dicoumarol. ß-Lap-mediated apoptosis and it's associated proteolyses (e.g., p53 and PARP cleavage events) *in vivo* in MDA-MB-468 transfectants were also prevent by dicoumarol. Surprisingly, the responses of NQ01-containing compared to NQ01-deficient MDA-MB-468 cells to menadione exposures were opposite those of ß-lap. NQ01-expressing MDA-MB-468 cells were extremely resistant to menadione-induced apoptosis, PARP cleavage and lethality due to the known detoxification of this drug by NQ01. Dicoumarol co-administration with menadione increased the sensitivity of NQ01-expressing MDA-MB-468 cells to this drug, in direct opposition to the protective effects of dicoumarol on ß-lap-mediated cell death. These data showed that

ß-lap targets NQ01 for its lethal effects in human breast cancer cells. Furthermore, NQ01 detoxifies menadione, but enhances ß-lap toxicity.

ß-Lap undergoes NQ01-dependent futile cycling to initiate cell death. The opposing lethality data using coadministration of dicoumarol with menadione or ß-lap in NQ01-containing MCF-7:WS8, T47D or transfected MDA-MB-468 cells strongly suggested that NQ01 detoxified menadione, but strongly enhanced ß-lap-mediated apoptosis and lethality. In NQ01 enzyme assays without the addition of cytochrome C, we noticed the continual cycling of ß-lap, as measured by the loss of NAD(P)H over time. Addition of menadione to S100 cell extracts or in purified NQ01 enzymatic assays led to one reaction cycling detoxification of menadione with the utilization of one mole NAD(P)H per one mole of menadione added. In contrast, one mole of ß-lap stimulated the loss of 5-8 moles of NAD(P)H in enzyme assays without the addition of cytochrome C. The activities above were completely prevented by administration of dicoumarol. These data strongly suggest that ß-lap undergoes futile cycling depleting cells of NAD(P)H, causing dramatic loss of energy in ß-lap-treated cells.

ß-Lap-activated proteolyses *in vivo* is calcium-dependent. The cleavage of p53 in ß-lap-treated, NQ01-containing human breast cancer cells strongly suggested that calpain was activated during apoptosis stimulated by this drug. Ionomycin treatment, which causes massive influx of calcium from the outside of the cell, of human breast cancer cells also induced an identical atypical PARP cleavage independent of NQ01 expression (Fig. 3). These data suggested to us that ß-lap-mediated apoptosis was calcium-dependent. Exposure of ß-lap-treated NQ01-expressing MDA-MB-468 or MCF-7 cells with EGTA or EDTA caused a suppression of ß-lap-mediated atypical PARP cleavage (Figs. 4-6). In addition EDTA or EGTA co-administration also suppressed ß-lap-mediated p53 cleavage (Fig. 7 and 8) and lamin B (Fig. 8) in MCF-7 cells. In contrast, treatment of MCF-7 cells with thapsigargin, an inhibitor of the intracellular membrane-bound calcium pump and stimulator of calcium release from ER and mitochondrial stores, caused typical caspase-mediated apoptosis as seen by the typical cleavage of PARP to its 89 kDa cleavage fragment from its full-length 113 kDa peptide. Finally, administration of BAPTA, an intracellular calcium chelator also prevented ß-lap-mediated p53 and atypical PARP cleavage events in MCF-7 (Fig. 10) or NQ01-expressing MDA-MB-468 cells (Fig. 11). EDTA or EGTA treatments of ß-lap-exposed NQ01-expressing cells also prevented the generation of ß-lap-mediated apoptosis (measured as TUNEL positive cells) (Figs. 12 and 13). Administration of EDTA also prevented ionomycin-induced apoptosis, but not apoptosis induced by staurosporin (STS) or topotecan (TPT) (Fig. 14). Thus, the atypical PARP cleavage, as well as p53 cleavage in ß-lap-treated NQ01-expressing human breast cancer cells was mediated by a calcium-dependent noncaspase cysteine protease, which we high suspect is calpain.

Accomplishment of Stated Tasks: Using the above data, we are now in a better position to complete the stated tasks of our grant. Although we were delayed a bit with the move of our laboratory to Case Western Reserve from the University of Wisconsin almost 8 months ago, we have completed a majority

of the stated tasks of Specific Aim #1. Furthermore, we now have genetic models with which to isolate the calcium-dependent, NQ01-dependent, noncaspase cysteine protease, which we now strongly suspect is calpain.

Task 1: Generation of PARP cDNA bacterial and mammalian expression vectors, and ^{35}S-methionine-labeled PARP protein, plus or minus histidine Tags.

We have generated his- as well as flag-tagged PARP cDNA mammalian expression vectors that can be propagated in bacterial cells. Using either wheat germ or rabbit reticulocyte *in vitro* transcription-translation systems, we have demonstrated that calpain treated in vitro synthesized 35S-methionine PARP protein leads to an identical atypical PARP cleavage fragment (Fig. 15), which is prevented by co-administration of calpastatin, addition of EDTA or EGTA, or calpain inhibitors (Fig. 16).

Task 2: Initiate ß-lap-activated apoptotic protease isolation using two simultaneous procedures and ß-lap-treated MCF-7:WS8 human breast cancer cells.

We then established stably transfected MCF-7 cells overexpressing his-tagged PARP. Treatment of these cells with ß-lap caused the expected appearance of a 60 kDa atypical PARP cleavage fragment from endogenous sources of protein and a slightly larger his-tagged PARP fragment from exogenous sources (Fig. 17). These cells will now be used in Specific Aim #2 as described below. The following Aims will be completed in Years 2 and 3.:

2A. Standard Protein Purification Procedure

1. Treat roller bottle-generated MCF-7:WS8 cells with ß-lap.
2. Confirm protease activation via endogenous PARP cleavage
3. Ammonium Sulfate Cuts Performed, active fractions pooled.
4. Mono-Q 16/10 FPLC
5. Mono-S 5/5 FPLC
6. Hydroxylapatite column chromatography
7. Superdex 200 26/60 gel filtration

*8. Active fractions pooled, analyzed by SDS-PAGE for atypical ^{35}S-PARP cleavage

9. In-gel PARP cleavage assay using cleavage site tetrapeptide fluorescent substrate generated from "Procedure B".

2B. Affinity Chromatographic Purification Procedure

1. PARP cleavage point determination and tetrapeptide syntheses

1a. Immunoprecipitation of PARP fragments using C-2-10 Antibody.

1b. *In vitro* ^{35}S-PARP cleavage±His tag, immunoprecipitation.

1c. PARP fragment purification and microsequencing.

1d. Cleavage site determined by computer analyses.

1e. Fluoromethylketone and fluorescent-tetrapeptide cleavage site-specific peptides made by CWRU. Several will be made as positive and negative controls for subsequent enzyme inhibition or activity assays.

1f. Confirmation of tetrapeptide-fmk blockage of atypical PARP cleavage and apoptotic protease activity using the tetrapeptide-fluorescent substrate.

1g. Mutagenization of PARP cDNA at cleavage site, in vitro translate, demonstrate no atypical PARP cleavage.

2. Construction of biotin-(streptavidin)-[X]-tetrapeptide-aldehyde.

3. DEAE Chromatographic Separation of ß-lap-treated MCF-7 cell extract, analyses of atypical cleavage activity using ^{35}S-methionine PARP.

4. Active fractions from "**Task #2B. 3**" are incubated with

5. biotin-[X]-tetrapeptide-aldehyde and bound to streptavidin-agarose beads and washed.

6. Apoptotic protease binding proteins are eluted with biotin.

*7. Eluted proteins are analyzed by SDS-PAGE, silver stained and assayed for ^{35}S-PARP cleavage.

The following Tasks may not be needed. The Specific Aims below may not be required should calpain be implicated. Calpain-negative cells, either deficient in calpain expression (mouse knock-out) or cells overexpressing dominant-negative calpain, will be used to explore the specific role of this one protease in ß-lap-sensitivity. Furthermore, using the cell models developed above we will also explore the signaling pathways between ß-la futile cycling and activation of the activation of calpain.:

Task 3: Production of polyclonal antisera using protein from (2A. *7) or (2B. *6) above.

Task 4: Microsequence purified apoptotic protease polypeptides from (2A. *7) or (2B. *6) above.

Task 5: Production of degenerative PCR probes corresponding to apoptotic protease amino acid sequences.

Task 6: Screen for ß-lap-activated apoptotic protease using antibodies from **Task #3** and PCR probes from **Task #5** in a sequential expression and cDNA hybridization approach.

Task 7: Screen for full-length ß-lap-activated apoptotic protease cDNA.

Task 8: Sequence and analyze the apoptotic protease DNA sequence.

Task 9: Subclone the apoptotic protease into the Tet-on response vector for **Aim #2.**

Task 10: Examine human breast cancer cells and patient tissue samples for ß-lap-activated apoptotic protease message, protein, and enzymatic activities.

Specific Aim #2: **Transfect sensitive (i.e., MCF-7) and resistant (i.e., MDA-MB-231) human breast cancer cells with sense and antisense expression vectors encoding the unknown protease to elucidate the role of this apoptotic death enzyme in drug resistance/sensitivities to ß-lap, or other Topo I poisons and DNA damaging agents (Years 2-3).**

Task 1: Transfect MCF-7:WS8 and MDA-MB-231 cells with Tet-on repressor cDNA and isolate doxycycline-responsive, low basal level subclones.

Task 2: Transfect Tet-on repressor-expressing subclones with doxycycline-responsive, sense- and antisense-oriented ß-lap-activated apoptotic protease expression vectors and double select (hygromycin and neomycin) clones.

Task 3: Examine cells generated in **Tasks #1-3** for apoptotic and survival responses to ß-lap, TPT, and other DNA damaging agents (such as ionizing radiation or Topo II-alpha poisons.

Task 4: Examine treated cells in **Task #4** for apoptotic cell death substrate cleavage and Caspase activities, as well as for the, now known, ß-lap (CPT + PDTC)-activated apoptotic protease.

Evidence for ß-lap-activated apoptosis mediated by calpain. We reasoned that if ß-lap stimulates NQ01-dependent calpain-mediated apoptosis, then the drug must cause significant alterations in calcium homeostasis. In collaboration with Drs. George Dubyiak (Dept. Biophysics, CWRU) and Clark Distelhorst (Hem//Onc., CWRU) we demonstrated that ß-lap treatment of NQ01-containing MCF-7:WS8 or MDA-MB-468 transfectants caused dramatic calcium influx within 3 mins as measured by FURA-2 binding (Fig. 18). Appropriate controls for the release of extracellular (ATP treatment) or intracellular (Thapsigargin) calcium were included (Figs. 19, 20). In contrast, calcium release was not evident in NQ01-deficient MDA-MD-468 parental or vector alone cells. Furthermore, treatment of MCF-7:WS8 or NQ01-expressing MDA-MB-468 transfectants with ß-lap caused the cleavage of p53 and atypical cleavage of PARP at the same time as the cleavage-dependent activation of calcium, as monitored by Western blot analyses of the appearance of the 18 kDa active subunit of calpain beginning at 8 hours. Furthermore, the appearance of these cleavage events at 8 hours

coincides with the initial appearance of TUNEL-positive, condensed-nuclei-containing apoptotic cells (not shown) at 8 hours post-ß-lap-treatment of NQ01 contain (MCF-7 or MDA-MB-468 transfectants) as opposed to parental or vector alone-containing MDA-MB-468 cells. The appearance of all the cleavage fragments described above in NQ01-containing cells was prevented by co-administration of dicoumarol, the NQ01 inhibitor. Furthermore using confocal microscopy, we noted the dramatic movement of cytosolic calpain into the nuclei of ß-lap-treated NQ01-expressing, but not NQ01-deficient, cells (Fig. 22). This movement of calpain into the nuclei of ß-lap-treated NQ01-expressing cells (Fig. 22) was prevented by dicoumoral co-administration, it coincided with the appearance at 4-8 hours posttreatment of atypical PARP cleavage, p53 cleavage and the appearance of the 18 kDa small subunit (active) form of calpain (Fig. 21), and was not a result of massive breakdown of the nuclear membrane since NQ01 (which is entirely cytosolic) remained cytosolic and the Ku70/Ku80 heterodimer (which is nuclear, not cleaved during apoptosis and was detected by Ab #162) remained nuclear. Furthermore, the movement of calpain from the cytoplasm to the nucleus was blocked by co-administration of dicoumarol (not shown).

ß-Lap exposure to NQ01-containing cells causes dramatic ATP depletion, which is not prevented by EDTA or EGTA. The loss of NAD(P)H in enzyme assays using NQ01-containing S100 cellular extracts or in purified NQ01 reactions, suggested that dramatic and rapid energy loss was occurring in NQ01-containing human breast cancer cells. We suspected that NQ01-mediated ß-lap futile cycling would lead to a dramatic loss of ATP within cells. Furthermore, we anticipated that such loss would be prevented by dicoumarol, but possibly not by EGTA or EDTA, since these would prevent calpain and apoptosis induction downstream but not affect the NQ01 enzyme. Using a luciferase assay, we demonstrated that NQ01-containing human breast cancer cells exhibited a dramatic loss in ATP within 30 mins posttreatment (Fig. 23). We estimate that less than 1% of the total ATP in control cells remain within 30 mins after a 4 hour pulse of 4-8 μM ß-lap. Administration of EDTA or EGTA had little affect of ATP loss mediated by ß-lap in MCF-7 cells. Interestingly, neither ionomycin or staurosporin (STS) caused ATP loss. These data are consistent with an NQ01-dependent futile cycling of ß-lap in that treated cells run out of energy. We are interested in the relationship between this futile cycling of the drug and release of calcium.

KEY RESEARCH ACCOMPLISHMENTS: Bulleted list of key research accomplishments emanating from this research.

We have accomplished the following objectives in the first year of this grant. We have determined that:

- NQ01 is the key determinant in ß-lap-mediated lethality.
- NQ01 is elevated in many human breast cancer cells and should be a useful target for ß-lap and its derivatives (Planchon et. al., Oncology Reports, 1999).
- ß-Lap stimulated apoptosis, as measured by TUNEL positive, G0/G1 cells, specific cleavage of key apoptotic substrates, i.e., PARP, pRb, p53, lamin B and calpain.
- ß-Lap causes calcium release.
- ß-Lap causes calpain movement from the cytosol to the nucleus.
- Atypical PARP cleavage is consistent with ß-lap-activated calpain-mediated apoptosis
- Dicoumarol and calcium chelators can protect cells from ß-lap-mediated apoptosis
- ß-Lap undergoes futile cycling which leads to calcium release and loss of energy. This combination is thought to prevent ATP-dependent caspase activation and supply the calcium needed to convert the inactive calpain zymogen to the 18 kDa active subunit.
- The necessary reagents, his- and flag-tagged PARP have been made and transfected into NQ01-containing cells for the isolation of ß-lap-activated apoptotic protease.
- Isolation of the protease is planned by three methods: -(1) isolation via PARP cleavage site; (2) isolation by standard biochemical methods in which PARP and p53 cleavage assays will be used, and (3) isolation of calpain using previously identified techniques- in ß-lap treated compared to ß-lap + dicoumarol-treated NQ01-expressing vs. NQ01-deficient human breast cancer cells.

REPORTABLE OUTCOMES: Provide a list of reportable outcomes to include:

– manuscripts, abstracts, presentations.

Manuscripts:

-Wuerzberger, S.M., Planchon, S.M., Pink, J.J., Bornmann, W. and **Boothman, D.A.** ß-Lapachone-induced apoptosis in MCF-7 human breast cancer cells. 1998; Cancer Res. 58: 1876-1885.

-Planchon, S., Wuerzberger, S., Pink, J.J., Robertson, K., Bornmann, W. and **Boothman, D.A.** bcl-2 protects against caspase 3-mediated apoptosis induced by ß-lapachone. 1999; Oncology Reports 6: 485-492.

-HL60 cells are NQ01-deficient and we suspect these cells are sensitive to free radical-mediated ß-lap responses.

-Separovic, D., Pink, J.J., Oleinick, N.L., Kester, M., **Boothman, D.A.,** McLoughlin, M., Pena, L.A., and Haimovitz-Friedman, A. Nieman-Pick human lymphoblasts are resistant to phthalocyanine 4-photodynamic therapy-induced apoptosis. 1999; Biomed Biophys. Res. Commun., 258: 506-512.

-Pink, J.J., Wuerzberger-Davis, S.M., Tagliarino, C., Planchon, S.M., Yang, X., Froelich, C.J., and Boothman, D.A. A novel noncaspase-mediated proteolytic pathway activated in breast cancer cells during ß-lapachone-mediated apoptosis. 1999; Exp. Cell Res., In Revision.

-Pink, J.J., Planchon, S.M., Tagliarino, C., Varnes, M.E., Siegel, D. and Boothman, D.A. NAD(P)H:quinone oxidoreductase (NQ01) activity is the principal determinant of ß-lapachone cytotoxicity. 1999; J. Biol. Chem., submitted.

-Mendonca, M.S., Howard, K.L., Farrington, D.L., Desmond, L.A., Temples, T.M., Mayhugh, B.M., Pink, J.J. and Boothman, D.A. Delay3ed apoptotic responses associated with radiation-induced neoplastic transformation of human hybrid cells. 1999; Cancer Res. 59: 3972-3979.

Abstracts:

EXPLOITATION OF AN IR-INDUCIBLE PROTEIN (XIP3) IN HUMAN CANCER CELLS USING ß-LAPACHONE. C. Tagliarino, J.J. Pink, S.M. Wuerzberger-Davis, S.M. Planchon, and D.A. Boothman. 11th Int Congress of Rad Res., Ireland, July 14-17, 1999. Paid for by grants from the Radiation Research Society to C.T. and D.A.B.

Presentations:

Invited Speaker, "Exploiting X-ray-inducible responses for improved therapy" Northern Illinois University, Dr. John Mitchell, host; Student's Choice Lecturer. *Feb. 4-6, 1999.*

Invited Speaker, "Exploiting radiation-inducible proteins for targeted apoptosis" Northern Illinois University, Host: Dr. James B. Mitchel, *Feb. 5, 1999.*

Invited Speaker, Exploiting IR-inducible Proteins For Therapy Against Breast Cancer, Midwest DNA Repair Conference, Ann Arbor, Michigan, *June 13, 1999.*

Invited Speaker, "Exploiting X-ray-inducible proteins for apoptotic chemotherapy" Essen, Germany (C. Streffer, host) *July 14-17, 1999.*

Invited Speaker, "A novel noncaspase-mediated apoptotic pathway induced by ß-lapachone: involvement of NQ01", Department of Radiation Oncology, University of Maryland, (W.F. Morgan, host) *October 23, 1999.*

Invited Speaker, Identification of a novel apoptotic pathway induced by ß-lapachone. Cleveland Clinic Lerner Research Institute. (A. Almasan, host) *November, 1999.*

Patents and licenses applied for and/or issued. None

Degrees obtained that are supported by this award.

Planchon, Sarah, M. Ph.D., Univ. Wisc.-Madison, Dept. Human Oncology, Dec. 1999.

Development of Cell Lines, Tissue or Serum Repositories:

-MDA-MB-468 NQ1-6, human NQ01-deficient cells stably transfected with CMV-directed NQ01.
-vector-alone MDA0-MB-468 cells.
-Stably transfected MCF-7:WS8 cells expressing caspase 3.

Informatics such as databases and animal models, etc. None

Funding applied for based on work supported by this award. In Prep.

Employment or research opportunities applied for and/or received on experiences/training supported by this award. None

CONCLUSIONS: Summarize the results to include the importance and/or implications of the completed research and when necessary, recommend changes on future work to better address the problem. A "so what section" which evaluates the knowledge as a scientific or medical product shall also be included in the conclusion of the annual and final reports.

The goal of this grant is to clone the unknown protease activated by the active anti-breast cancer agent, ß-lapachone (ß-lap). The research team showed for the first time that ß-lap requires NQ01, a two-electron reduction enzyme elevated in many human breast cancers, for activation. The team then characterized the unknown apoptotic protease activated in human breast cancer cells by ß-lap, defining endpoints that will be essential for the ultimate isolation of this novel apoptotic protease. The unknown protease: (a) is a non-caspase cytsteine protease; (b) cleaves p53, lamin B, and PARP (atypically) in an NQ01-dependent manner at a time co-incident with calpain activation (appearance of an 18 kDa active form and its movement into the nucleus by confocal microscopy); and (c) is calcium-dependent (e.g., the proteolytic cleavage of PARP or p53 was blocked by co-administration of EGTA or EDTA), and the drug causes massive NQ01-dependent calcium influx within 3 mins posttreatment with 5-8μM ß-lap;. Furthermore, significant progress has been made in developing reagents that will be required for the cloning of this novel noncaspase cysteine protease. The new hypothesis being tested is that ß-lap activates calpain, which then triggers DNA fragmentation and apoptosis.

We hypothesize that NQ01 could be exploited for breast cancer because (1) the enzyme is elevated in many human breast cancers and tumors can be rapidly assayed for overall levels prior to treatment; (2) the enzyme is induced by cytotoxic agents, such as ionizing radiation (e.g., it was isolated by our laboratory in 1993 as XIP3), and this attribute of the enzyme should be exploitable for improved radiotherapeutic strategies using ß-lapachone; and (3) the data implicates ß-lapachone for chemopreventive therapy against cancer, such as breast cancers, since NQ01 is an early known marker of neoplastic transformation of normal epithelial and other cell types.

REFERENCES: List all references pertinent to the report using a standard journal format such as *Science, Military Medicine,* etc.

1. Planchon, S. M., Wuerzberger, S., Frydman, B., Witiak, D. T., Hutson, P., Church, D. R., Wilding, G., and Boothman, D. A. (1995) *Cancer Res.* **55,** 3706-11
2. Wuerzberger, S. M., Pink, J. J., Planchon, S. M., Byers, K. L., Bornmann, W. G., and Boothman, D. A. (1998) *Cancer Res.* **58,** 1876-85
3. Li, C. J., Averboukh, L., and Pardee, A. B. (1993) *J. Biol. Chem.* **268,** 22463-8
4. Boothman, D. A., Greer, S., and Pardee, A. B. (1987) *Cancer Res.* **47,** 5361-6
5. Schuerch, A. R., and Wehrli, W. (1978) *Eur. J. Biochem.* **84,** 197-205
6. Docampo, R., Cruz, F. S., Boveris, A., Muniz, R. P., and Esquivel, D. M. (1979) *Biochem. Pharmacol.* **28,** 723-8
7. Boorstein, R. J., and Pardee, A. B. (1983) *Biochem. Biophys. Res. Commun.* **117,** 30-6
8. Boothman, D. A., Trask, D. K., and Pardee, A. B. (1989) *Cancer Res.* **49,** 605-12
9. Molina Portela, M. P., and Stoppani, A. O. (1996) *Biochem. Pharmacol.* **51,** 275-83
10. Frydman, B., Marton, L. J., Sun, J. S., Neder, K., Witiak, D. T., Liu, A. A., Wang, H. M., Mao, Y., Wu, H. Y., Sanders, M. M., and Liu, L. F. (1997) *Cancer Res.* **57,** 620-7
11. Vanni, A., Fiore, M., De Salvia, R., Cundari, E., Ricordy, R., Ceccarelli, R., and Degrassi, F. (1998) *Mutat Res* **401,** 55-63
12. Manna, S. K., Gad, Y. P., Mukhopadhyay, A., and Aggarwal, B. B. (1999) *Biochem. Pharmacol.* **57,** 763-74
13. Robertson, N., Haigh, A., Adams, G. E., and Stratford, I. J. (1994) *Eur. J. Cancer* **30A,** 1013-9
14. Cadenas, E. (1995) *Biochem. Pharmacol.* **49,** 127-40
15. Ross, D., Beall, H., Traver, R. D., Siegel, D., Phillips, R. M., and Gibson, N. W. (1994) *Oncol. Res.* **6,** 493-500
16. Rauth, A. M., Goldberg, Z., and Misra, V. (1997) *Oncol. Res.* **9,** 339-49
17. Ross, D., Siegel, D., Beall, H., Prakash, A. S., Mulcahy, R. T., and Gibson, N. W. (1993) *Cancer Met. Rev.* **12,** 83-101
18. Boothman, D. A., Meyers, M., Fukunaga, N., and Lee, S. W. (1993) *Proc. Natl. Acad. Sci. USA* **90,** 7200-4
19. Chen, S., Knox, R., Lewis, A. D., Friedlos, F., Workman, P., Deng, P. S., Fung, M., Ebenstein, D., Wu, K., and Tsai, T. M. (1995) *Mol. Pharmacol.* **47,** 934-9
20. Jaiswal, A. K., McBride, O. W., Adesnik, M., and Nebert, D. W. (1988) *J. Biol. Chem.* **263,** 13572-8
21. Radjendirane, V., Joseph, P., Lee, Y. H., Kimura, S., Klein-Szanto, A. J., Gonzalez, F. J., and Jaiswal, A. K. (1998) *J. Biol. Chem.* **273,** 7382-9
22. Marin, A., Lopez de Cerain, A., Hamilton, E., Lewis, A. D., Martinez-Penuela, J. M., Idoate, M. A., and Bello, J. (1997) *Br. J. Cancer* **76,** 923-9
23. Malkinson, A. M., Siegel, D., Forrest, G. L., Gazdar, A. F., Oie, H. K., Chan, D. C., Bunn, P. A., Mabry, M., Dykes, D. J., Harrison, S. D., and et al. (1992) *Cancer Res.* **52,** 4752-7
24. Belinsky, M., and Jaiswal, A. K. (1993) *Cancer Met. Rev.* **12,** 103-17
25. Joseph, P., Xie, T., Xu, Y., and Jaiswal, A. K. (1994) *Oncol. Res.* **6,** 525-32

26. Buettner, G. R. (1993) *Arch. Biochem. Biophys.* **300,** 535-43
27. Ross, D., Thor, H., Orrenius, S., and Moldeus, P. (1985) *Chemico-Biological Interactions* **55,** 177-84
28. Riley, R. J., and Workman, P. (1992) *Biochem. Pharmacol.* **43,** 1657-69
29. Siegel, D., Beall, H., Senekowitsch, C., Kasai, M., Arai, H., Gibson, N. W., and Ross, D. (1992) *Biochemistry* **31,** 7879-85
30. Prakash, A. S., Beall, H., Ross, D., and Gibson, N. W. (1993) *Biochemistry* **32,** 5518-25
31. Fitzsimmons, S. A., Workman, P., Grever, M., Paull, K., Camalier, R., and Lewis, A. D. (1996) *J. Natl. Cancer Inst.* **88,** 259-69
32. Beall, H. D., Murphy, A. M., Siegel, D., Hargreaves, R. H., Butler, J., and Ross, D. (1995) *Mol. Pharmacol.* **48,** 499-504
33. Hollander, P. M., and Ernster, L. (1975) *Arch. Biochem. Biophys.* **169,** 560-7
34. Hosoda, S., Nakamura, W., and Hayashi, K. (1974) *J. Biol. Chem.* **249,** 6416-23
35. Duthie, S. J., and Grant, M. H. (1989) *Br. J. Cancer* **60,** 566-71
36. Akman, S. A., Doroshow, J. H., Dietrich, M. F., Chlebowski, R. T., and Block, J. S. (1987) *J. Pharmacol. Exp. Ther.* **240,** 486-91
37. Thor, H., Smith, M. T., Hartzell, P., Bellomo, G., Jewell, S. A., and Orrenius, S. (1982) *J. Biol. Chem.* **257,** 12419-25
38. Siegel, D., McGuinness, S. M., Winski, S. L., and Ross, D. (1999) *Pharmacogenetics* **9,** 113-21
39. Gustafson, D. L., Beall, H. D., Bolton, E. M., Ross, D., and Waldren, C. A. (1996) *Mol. Pharmacol.* **50,** 728-35
40. Sambrook, J., Fritsch, E. F., and Maniatis, T. (1989) *Molecular Cloning-A Laboratory Manual*, Cold Spring Harbor Laboratory Press, Cold Spring Harbor
41. Pink, J. J., Bilimoria, M. M., Assikis, J., and Jordan, V. C. (1996) *Br. J. Cancer* **74,** 1227-36
42. Labarca, C., and Paigen, K. (1980) *Anal. Biochem.* **102,** 344-52
43. Siegel, D., Franklin, W. A., and Ross, D. (1998) *Clin Cancer Res* **4,** 2065-70
44. Hollander, P. M., Bartfai, T., and Gatt, S. (1975) *Arch. Biochem. Biophys.* **169,** 568-76
45. Strobel, H. W., and Dignam, J. D. (1978) *Methods Enzymol* **52,** 89-96
46. Beall, H. D., Mulcahy, R. T., Siegel, D., Traver, R. D., Gibson, N. W., and Ross, D. (1994) *Cancer Res.* **54,** 3196-201
47. Kaufmann, S. H., Desnoyers, S., Ottaviano, Y., Davidson, N. E., and Poirier, G. G. (1993) *Cancer Res.* **53,** 3976-85
48. Preusch, P. C., Siegel, D., Gibson, N. W., and Ross, D. (1991) *Free Radic. Biol. Med.* **11,** 77-80
49. Siegel, D., Gibson, N. W., Preusch, P. C., and Ross, D. (1990) *Cancer Res.* **50,** 7483-9
50. Keyes, S. R., Fracasso, P. M., Heimbrook, D. C., Rockwell, S., Sligar, S. G., and Sartorelli, A. C. (1984) *Cancer Res.* **44,** 5638-43
51. Hess, R., Plaumann, B., Lutum, A. S., Haessler, C., Heinz, B., Fritsche, M., and Brandner, G. (1994) *Toxicol. Lett.* **72,** 43-52
52. Boothman, D. A., and Pardee, A. B. (1989) *Proc. Natl. Acad. Sci. USA* **86,** 4963-7

53. Boothman, D. A., Wang, M., Schea, R. A., Burrows, H. L., Strickfaden, S., and Owens, J. K. (1992) *Int. J. Radiat. Oncol. Biol. Phys.* **24,** 939-48

54. Nelson, W. G., and Kastan, M. B. (1994) *Mol. Cell. Biol.* **14,** 1815-23

55. Kubbutat, M. H., and Vousden, K. H. (1997) *Mol. Cell. Biol.* **17,** 460-8

56. Squier, M. K., and Cohen, J. J. (1997) *J. Immunol.* **158,** 3690-7

57. Wood, D. E., and Newcomb, E. W. (1999) *J. Biol. Chem.* **274,** 8309-15

58. Squier, M. K., Sehnert, A. J., Sellins, K. S., Malkinson, A. M., Takano, E., and Cohen, J. J. (1999) *J. Cell. Physiol.* **178,** 311-9

59. Wefers, H., and Sies, H. (1983) *Archives of Biochemistry & Biophysics* **224,** 568-78

60. Bellomo, G., Jewell, S. A., and Orrenius, S. (1982) *J. Biol. Chem.* **257,** 11558-62

61. Iyanagi, T. (1990) *Free Radical Research Communications* **8,** 259-68

62. Molina Portela, M. P., Fernandez Villamil, S. H., Perissinotti, L. J., and Stoppani, A. O. (1996) *Biochem. Pharmacol.* **52,** 1875-82

63. Docampo, R., Cruz, F. S., Boveris, A., Muniz, R. P., and Esquivel, D. M. (1978) *Arch Biochem Biophys* **186,** 292-7

64. Chau, Y. P., Shiah, S. G., Don, M. J., and Kuo, M. L. (1998) *Free Radic Biol Med* **24,** 660-70

65. Zhao, Q., Yang, X. L., Holtzclaw, W. D., and Talalay, P. (1997) *Proc. Natl. Acad. Sci. USA* **94,** 1669-74

66. Jaiswal, A. K. (1994) *J. Biol. Chem.* **269,** 14502-8

67. Boorstein, R. J., and Pardee, A. B. (1984) *Biochem. Biophys. Res. Commun.* **118,** 828-34

68. Fornace, A. J., Jr., Alamo, I., Jr., and Hollander, M. C. (1988) *Proc Natl Acad Sci U S A* **85,** 8800-4

69. Williams, J. B., Wang, R., Lu, A. Y., and Pickett, C. B. (1984) *Arch. Biochem. Biophys.* **232,** 408-13

70. Farber, E. (1984) *Can J Biochem Cell Biol* **62,** 486-94

APPENDICES: Attach all appendices that contain information that supplements, clarifies or supports the text. Examples of appendices include journal articles, reprints of manuscripts and abstracts, a curriculum vitae, patent applications, study questionnaires, and surveys, etc.

Appendix Items

-Wuerzberger, S.M., Planchon, S.M., Pink, J.J., Bornmann, W. and **Boothman, D.A.** ß-Lapachone-induced apoptosis in MCF-7 human breast cancer cells. 1998; Cancer Res. 58: 1876-1885.

-Pink, J.J., Wuerzberger-Davis, S.M., Tagliarino, C., Planchon, S.M., Yang, X., Froelich, C.J., and Boothman, D.A. A novel noncaspase-mediated proteolytic pathway activated in breast cancer cells during ß-lapachone-mediated apoptosis. 1999; Exp. Cell Res., In Revision.

-Pink, J.J., Planchon, S.M., Tagliarino, C., Varnes, M.E., Siegel, D. and Boothman, D.A. NAD(P)H:quinone oxidoreductase (NQ01) activity is the principal determinant of ß-lapachone cytotoxicity. 1999; J. Biol. Chem., submitted.

-Mendonca, M.S., Howard, K.L., Farrington, D.L., Desmond, L.A., Temples, T.M., Mayhugh, B.M., Pink, J.J. and Boothman, D.A. Delay3ed apoptotic responses associated with radiation-induced neoplastic transformation of human hybrid cells. 1999; Cancer Res. 59: 3972-3979.

-Separovic, D., Pink, J.J., Oleinick, N.L., Kester, M., **Boothman, D.A.,** McLoughlin, M., Pena, L.A., and Haimovitz-Friedman, A. Nieman-Pick human lymphoblasts are resistant to phthalocyanine 4-photodynamic therapy-induced apoptosis. 1999; Biomed Biophys. Res. Commun., 258: 506-512.

BINDING: Because all reports are entered into the Department of Defense Technical Reports Database collection and are microfiched, it is recommended that all reports be bound by stapling the pages together in the upper left hand corner. All reports shall be prepared in camera ready copy (legible print, clear photos/illustrations) for microfiching. Figures should include legends and all figures and tables should be clearly marked.

FINAL REPORTS: All final reports must include a bibliography of all publications and meeting abstracts and a list of personnel (not salaries) receiving pay from the research effort.

NOTE: IF ALL OF THE ABOVE ELEMENTS ARE NOT MET, THE REPORT WILL BE CONSIDERED UNACCEPTABLE AND WILL BE RETURNED FOR REWRITE.

HELPFUL HINTS:

1. **Please proof all reports for errors.**

2. Please provide supporting data, i.e. tables, figures, graphs, etc.

3. **Ensure all publications published as a result of effort acknowledges the work supported by USAMRMC. Copies of all publications supported by the USAMRMC are to be provided with reports.**

Manuscripts/Reprints, Abstracts

A copy of manuscripts or subsequent reprints resulting from the research shall be submitted to the USAMRMC. An extended abstract suitable for publication in the Proceedings of the Breast Cancer Research Program is required in relation to a DOD BCRP meeting tentatively planned for 2002. The extended abstract shall (1) identify the accomplishments since award and (2) follow instructions to be prepared by the USAMRMC and promulgated at a later date. The extended abstract style will be dependent on the discipline.

Figure Legends

Figure 1. **Proteolysis of proteins in ß-lapachone (ß-lap)-treated MCF-7 cells.** Log-phase MCF-7 cells were exposed to 5 μM ß-lap for 4 h as previously described by our laboratory (4,8,52,). Cells were then allowed to grow in the absence of drug and at various times whole cell extracts were prepared and analyzed for steady state levels of proteins by Western immunoblot assays. Cleavage of pRb, lamin B and other proteins were then monitored.

Figure 2. **Lack of inhibition of ß-lap-mediated apoptosis by various inhibitors.** Cells were treated with or without ß-lap and co-administered inhibitors at the indicated drug concentrations as described in Figure 1.

Figure 3. **Effect of various inhibitors on the appearance of atypical PARP cleavage caused by ß-lap treatment.** Cells were treated and analyzed as described in Figure 1.

Figure 4. **EDTA or EGTA inhibits atypical PARP cleavage during ß-lap-mediated apoptosis in MCF-7 cells.** Cells were treated as described in Figure 2.

Figure 5. **EDTA or EGTA inhibits atypical PARP cleavage during ß-lap-mediated apoptosis in MCF-7 cells.** Cells were treated as decribed in Figure 4. EDTA and EGTA controls were included.

Figure 6. EDTA or EGTA inhibits NQ01-dependent atypical PARP cleavage during ß-lap-mediated apoptosis.

Figure 7. **EDTA prevents p53 cleavage during ß-lap-mediated apoptosis in MCF-7 cells.**

Figure 8. **EDTA or EGTA prevents lamin B cleavage in MCF-7 cells during ß-lap-mediated apoptosis.**

Figure 9. **Thapsigargin (TG) does not cause atypical PARP cleavage or cleavage of p53 in MCF-7 cells as does ß-lap.**

Figure 10. **BAPTA partially prevents ß-lap-mediated atypical PARP cleavage and p53 celavage in MCF-7 cells, but not in NQ01-deficient MDA-MB-468 cells.**

Figure 11. **Administration of calcium can not restore atypical PARP cleavage and p53 cleavage during ß-lap-mediated apoptosis in NQ01-expressing cells.** Exposure to high

dose calcium appeared to cause atypical PARP cleavage and p53 cleavage in a process that appears independent of NQ01.

Figure 12. **EDTA or EGTA can partially prevent apoptosis in ß-lap-treated MCF-7 cells.** Cells were treated with 5 μM ß-lap with or without EDTA or EGTA. Apoptosis was monitored by TUNEL assays.

Figure 13. **NQ01-dependent apoptosis mediated by ß-lap treatment.** Cells were treated as described in Figure 12.

Figure 14. **Effect of calcium chelators on ß-lap-mediated apoptosis in MCF-7 or NQ01-expressing MDA-MB-468 transfectants.**

Figure 15. **Calpain treatment of *in vitro* transcribed and translated full-length PARP (113 kDa) results in an identical atypical PARP cleavage fragment as observed in ß-lap-treated MCF-7 cells.**

Figure 16. **Effect of known calpain inhibitors on enzyme-mediated atypical PARP cleavage using *in vitro* transcribed/translated full length PARP.**

Figure 17. **Establishment of stably transfected MCF-7 cells with his-tagged PARP.** Treatment of his-tagged PARP-expressing MCF-7 transfectants with ß-lap resulted in atypical PARP cleavage as observed with the endogenous protein.

Figure 18. **Changes in intracellular calcium in ß-lap-treated MCF-7:WS8 cells.** Calcium changes were monitored by FURA-2 binding as described in the text.

Figure 19. **NQ01-dependent, ß-lap-induced changes in intracellular calcium in MCF-7 or NQ01-expressing MDA-MB-468 transfectants following exposure to 5 μM ß-lap.** Appropriate controls for extracellular (ATP treatment) and intracellular (thapsigargin, TG) calcium changes were included.

Figure 20. **NQ01-dependent calcium changes.**

Figure 21. **Apparent activation of calpain concomitant with atypical PARP fragmentation and p53 cleavage.**

Figure 22. **Movement of calpain into the nuclei of ß-lap-treated, NQ01-expressing human breast cancer cells.**

Proteolysis of Proteins in β-Lapachone Treated MCF-7 Cells

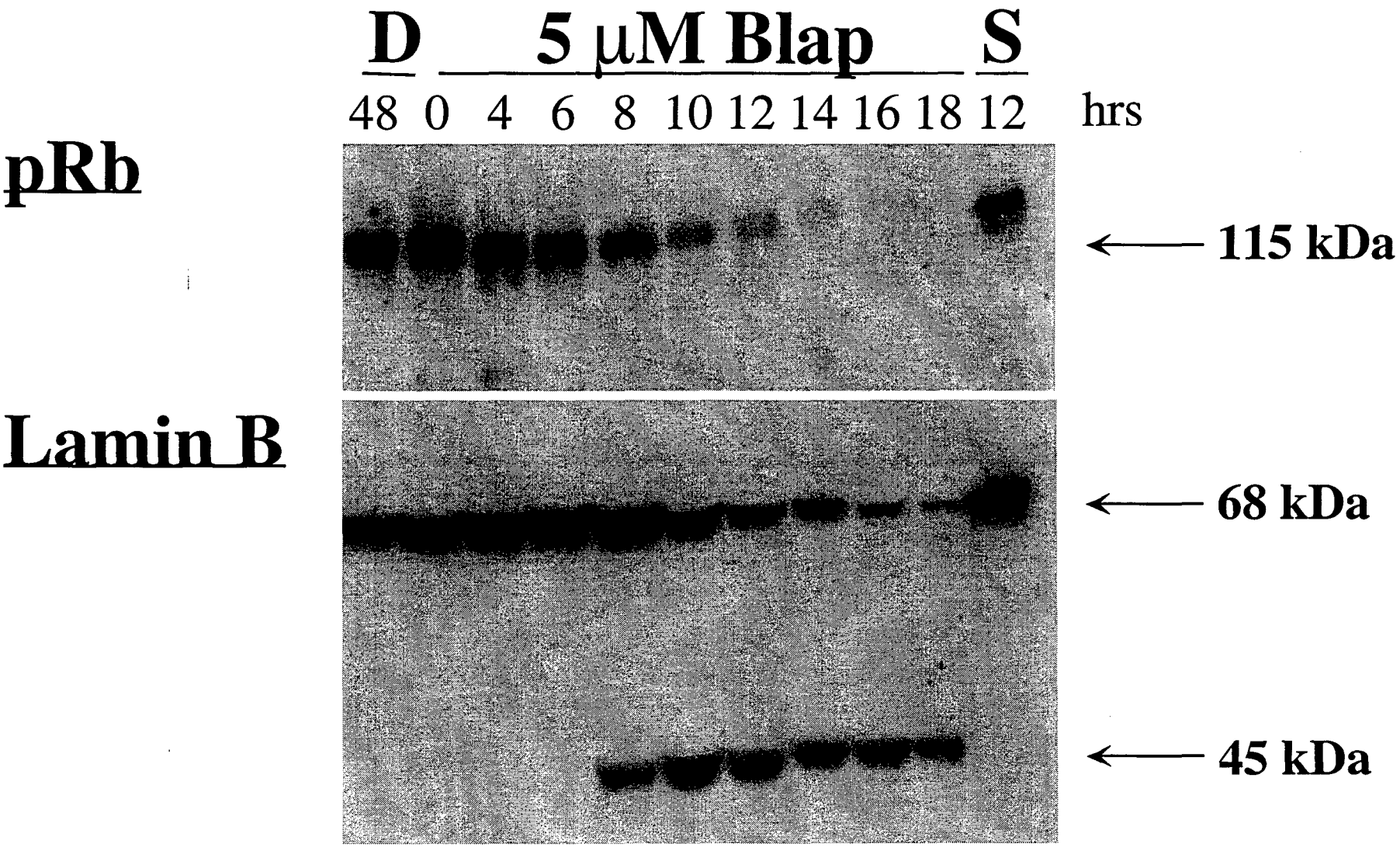

Figure 1

Figure 2

Inhibitors with Varying Blap Conc. at 24 hr

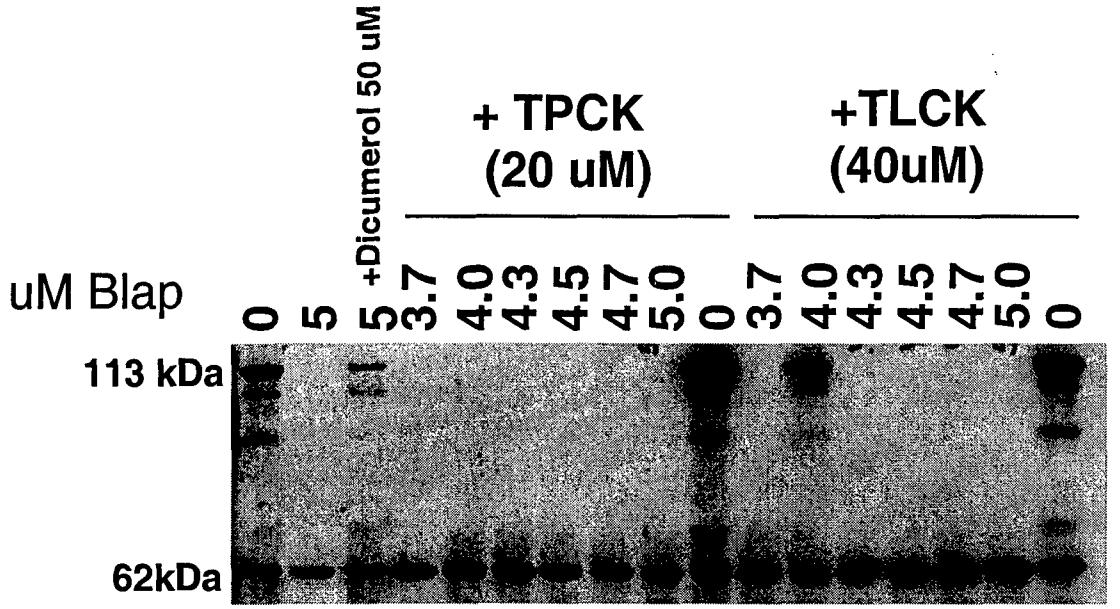

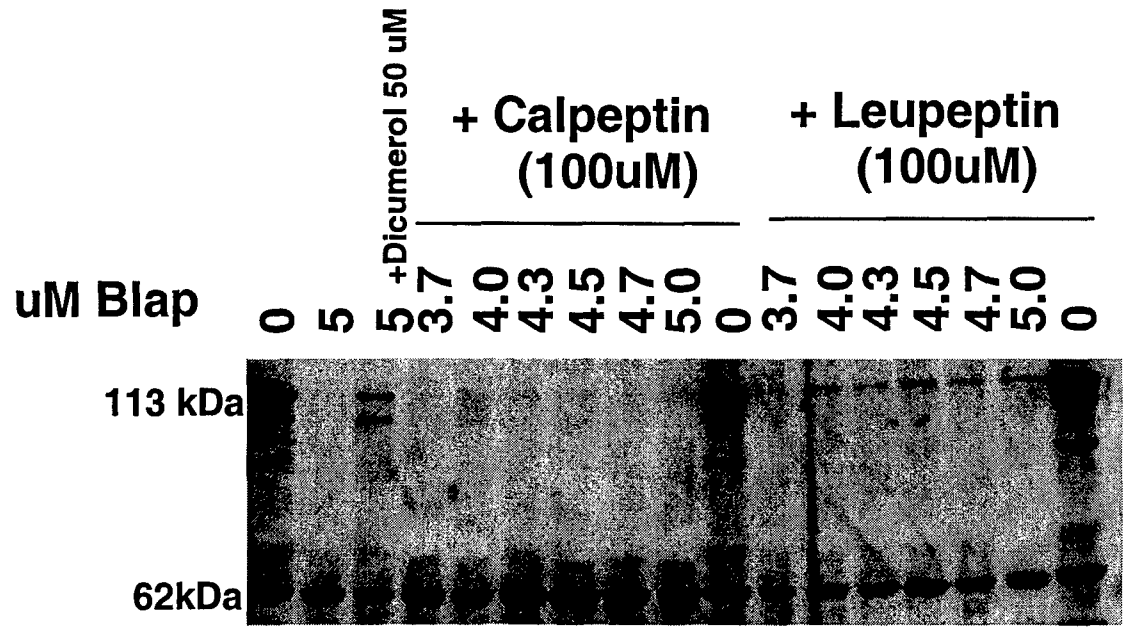

Blap8a
1/11/99

PARP Cleavage analysis of Inhibitors with Varying Blap Conc. at 24 hr

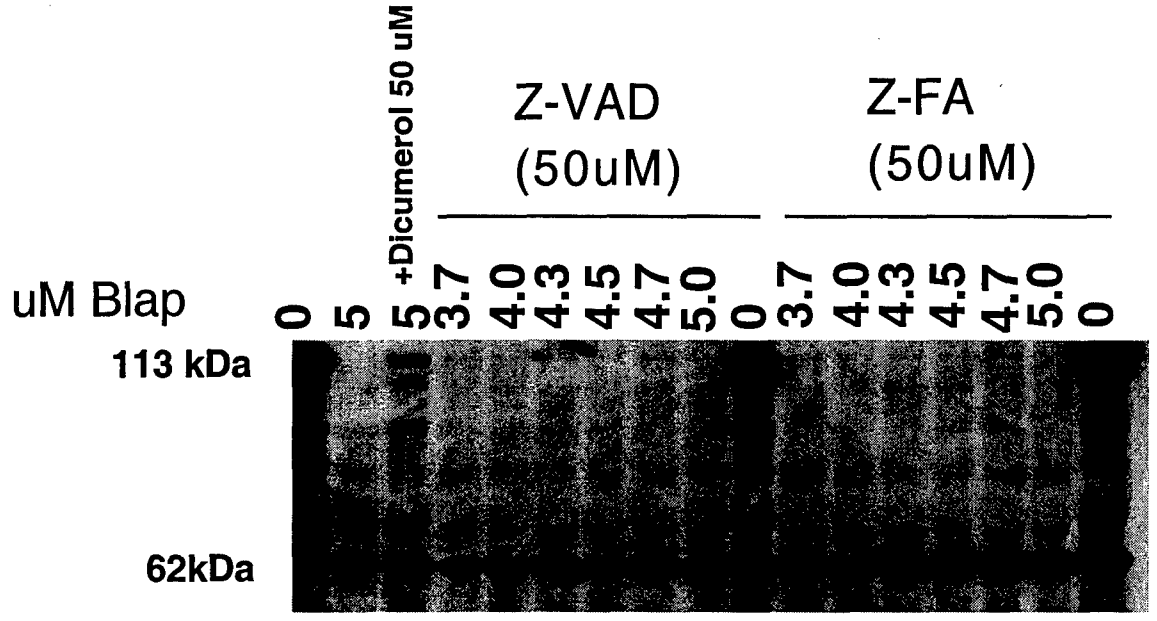

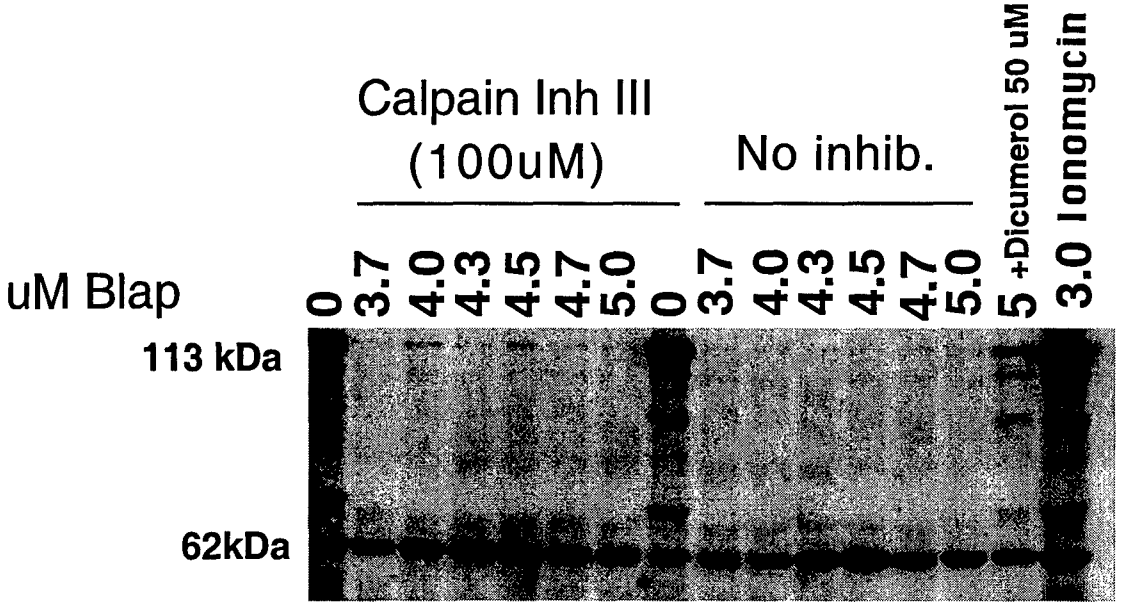

blap8b
1/14/99

PARP Substrate Proteolysis is Calcium Dependent

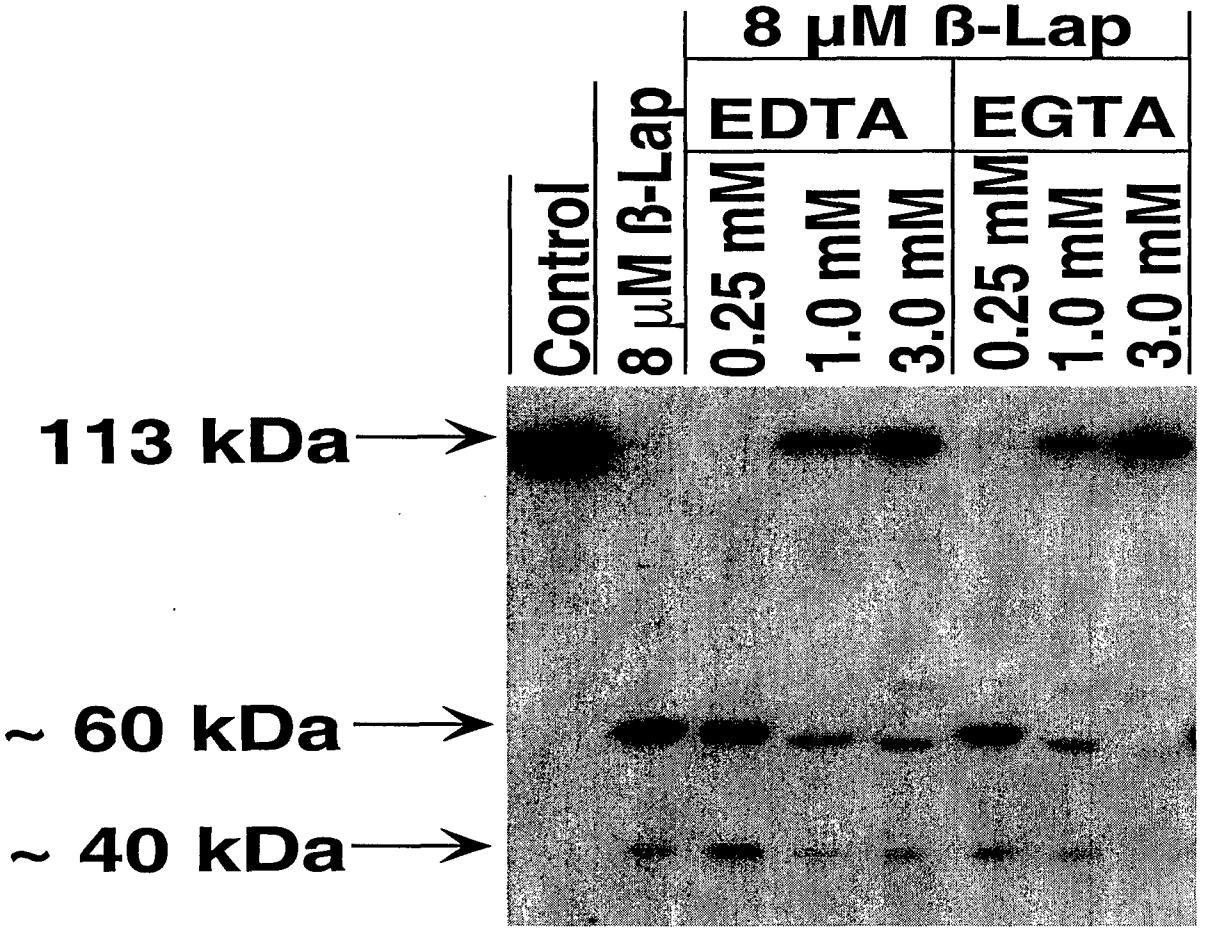

PARP cleavage with 5uM Blap in the presence of EDTA or EGTA

5 uM Blap 8hr | 5 uM Blap 24 hr | No Blap

EDTA EGTA EDTA EGTA EDTA EGTA

0 .25 1 3 .25 1 3 .25 1 3 .25 1 3 .25 1 3 .25 1 3 mM

EGTA/EDTA Before, during after Blap treatment

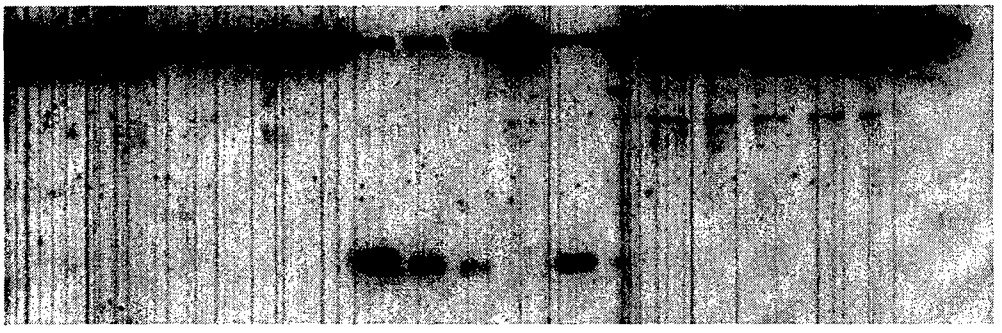

5 uM Blap 8hr | 5 uM Blap 24 hr | No Blap

5 uM Blap 24 hr EDTA EGTA EDTA EGTA EDTA EGTA

.25 1 3 .25 1 3 .25 1 3 .25 1 3 .25 1 3 .25 1 3 mM

EGTA/EDTA Before and during Blap treatment complete media afterwards

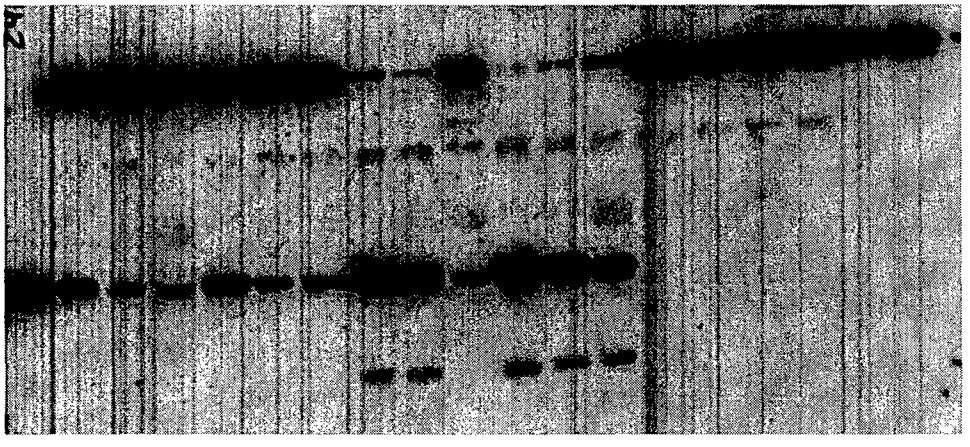

Blap12
2/28/99

Figure 6

PARP Cleavage With 8 uM Blap in the presence of EDTA or EGTA

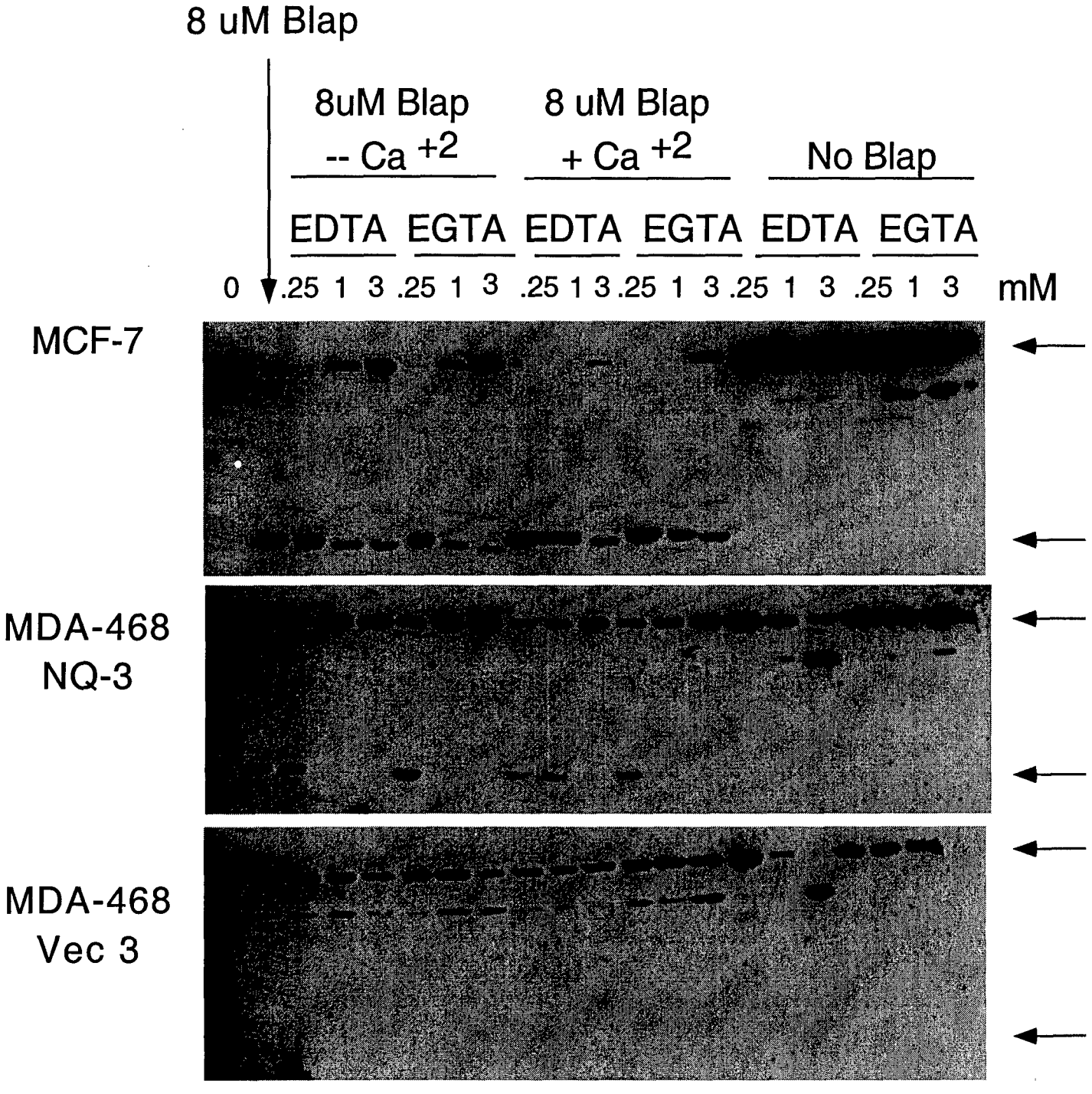

Blap12R
3/3/99

Figure 7

p53Cleavage With 8 uM Blap in the presence of EDTA or EGTA in MCF-7 Cells

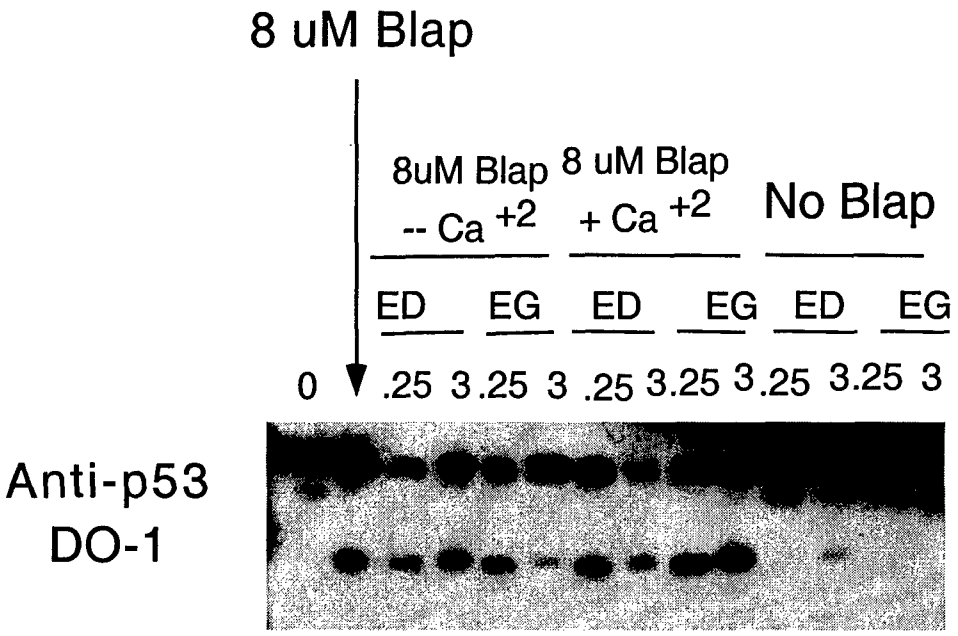

Blap12Ra
3/22/99

Figure 8

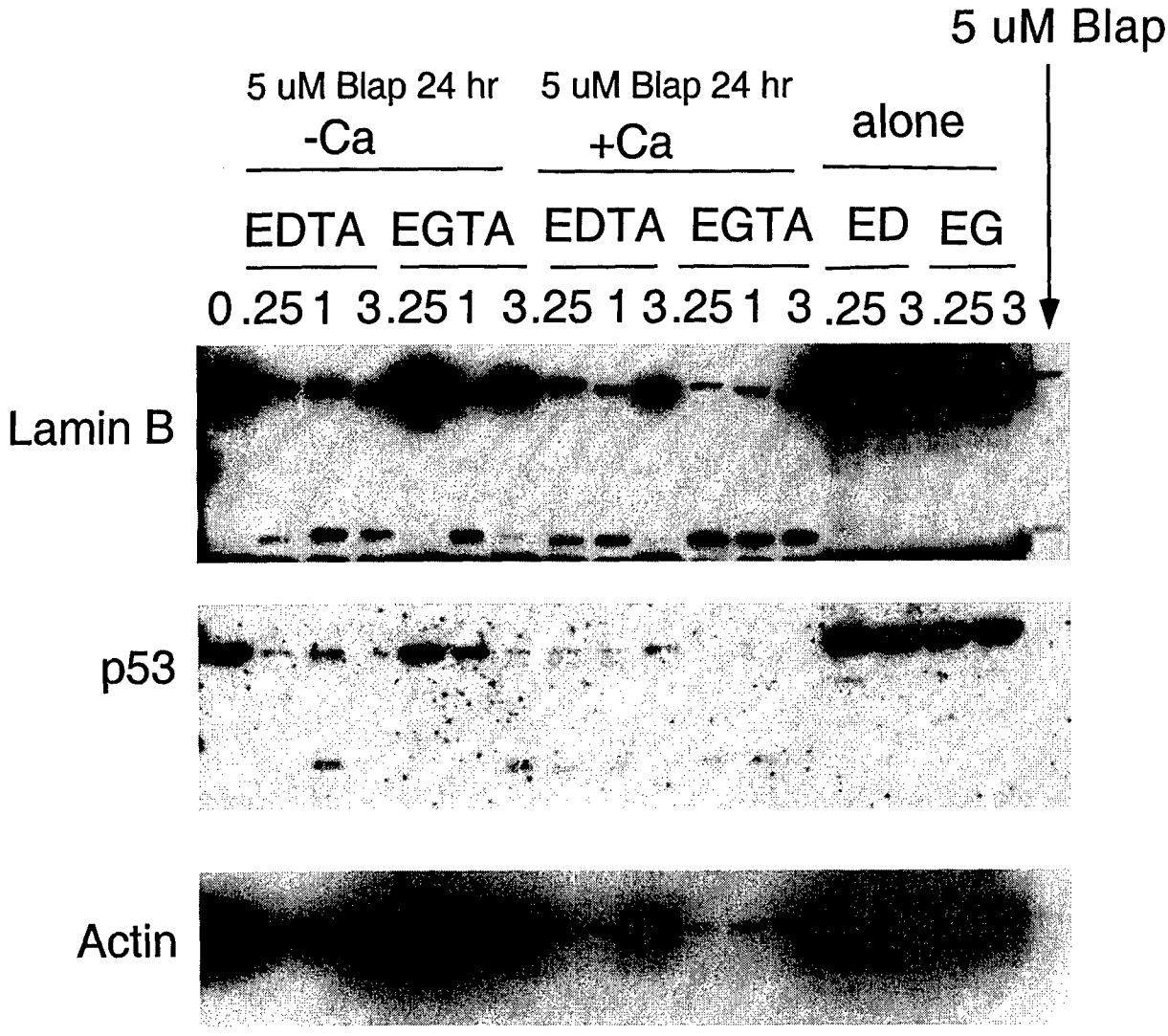

blap12b
3/31/99

Figure 9

Thapsigargin Timecourse and Dose Response in MCF 7 Cells

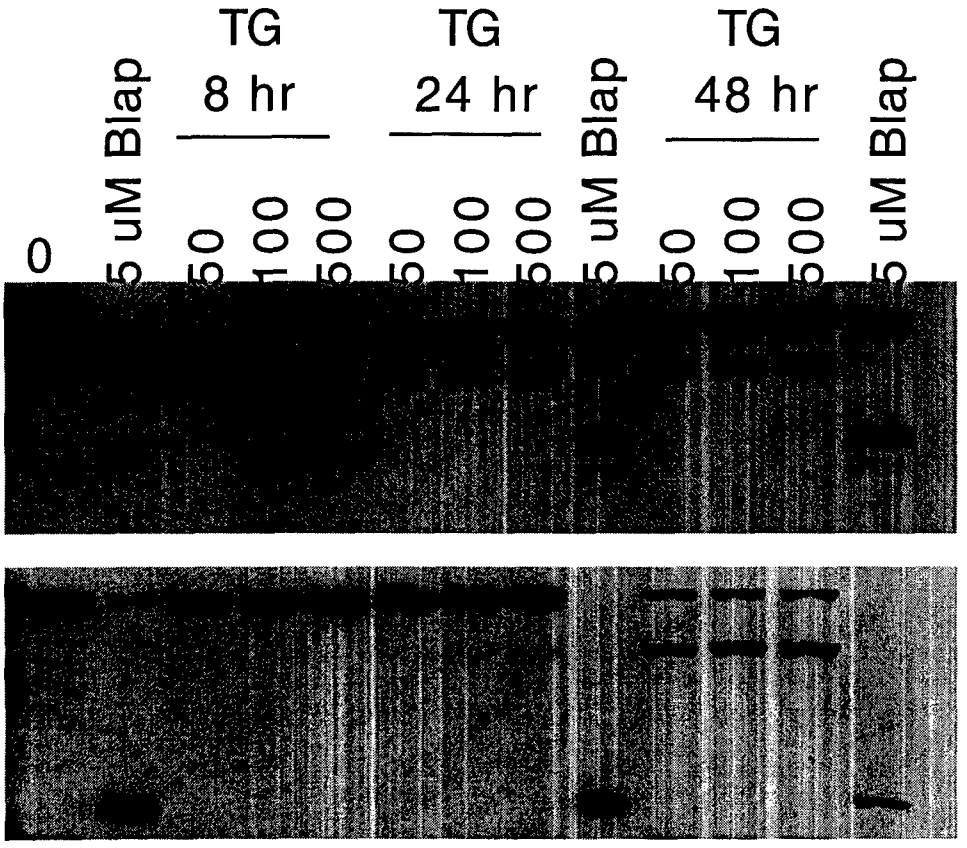

Blap 13
3/11/99

Can BAPTA Block Blap Induced PARP and p53 Cleavage

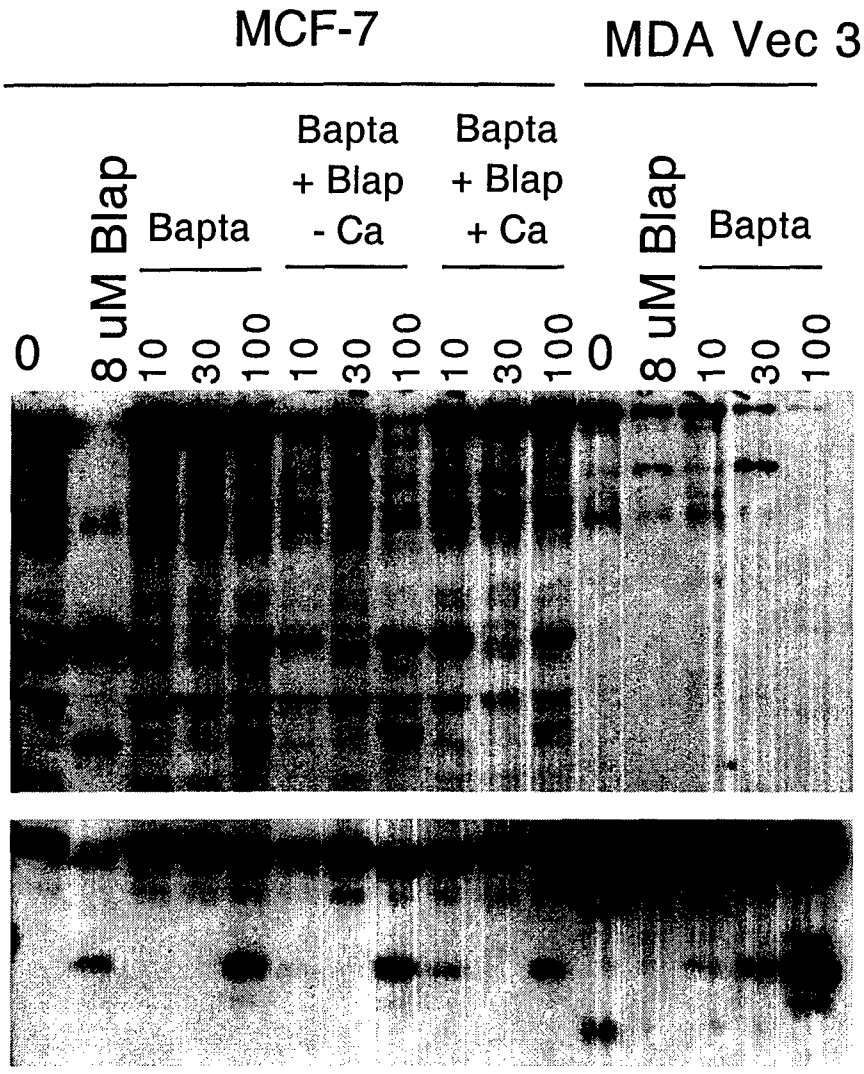

Anti-Parp C2-10

Anti-p53 DO-1

Blap14a
3/11/99

Can BAPTA block Blap Induced PARP and p53 Cleavage

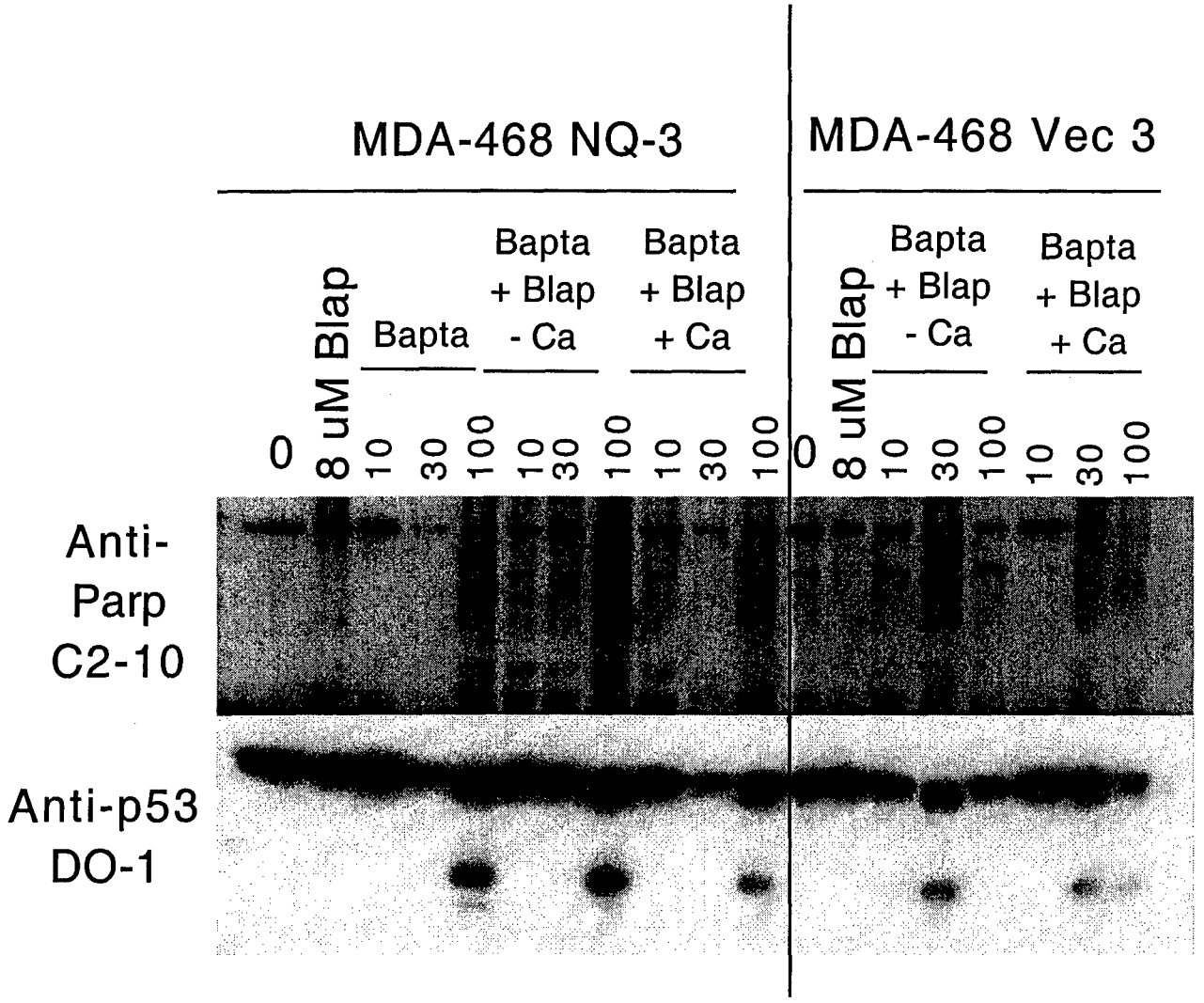

blap14b
3/22/99

MCF 7

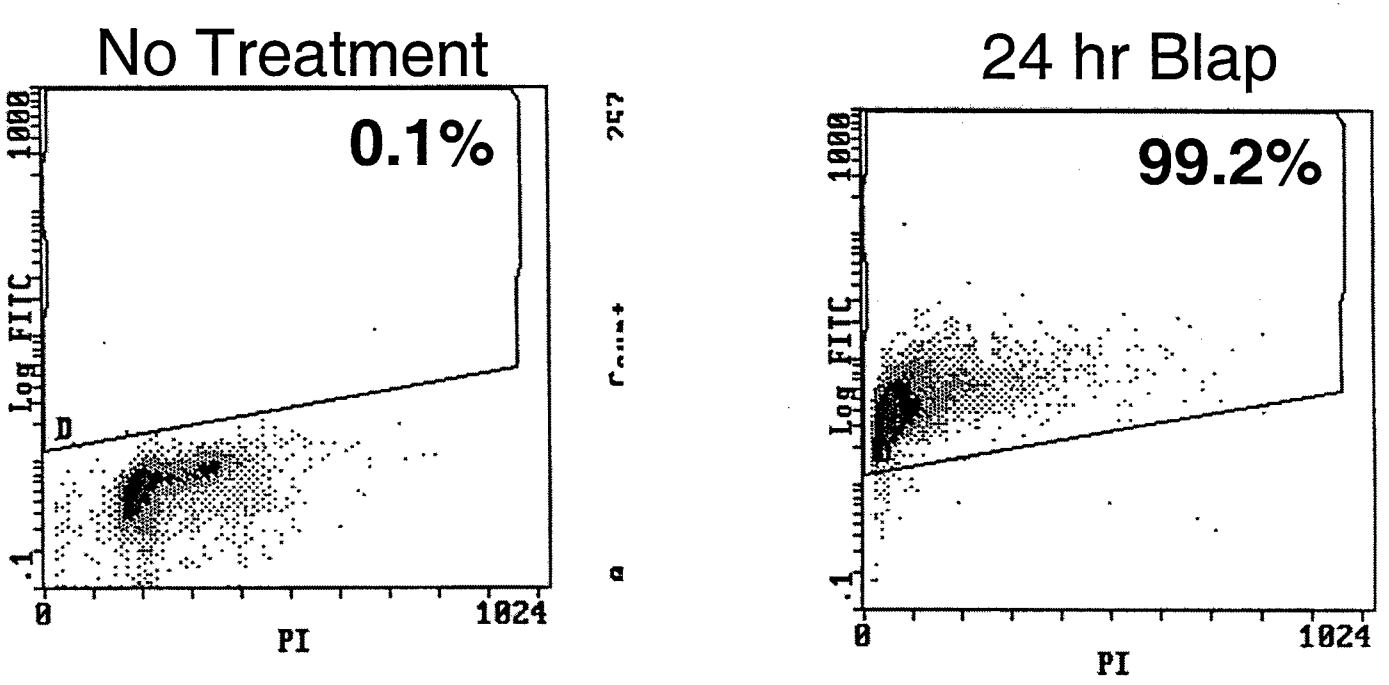

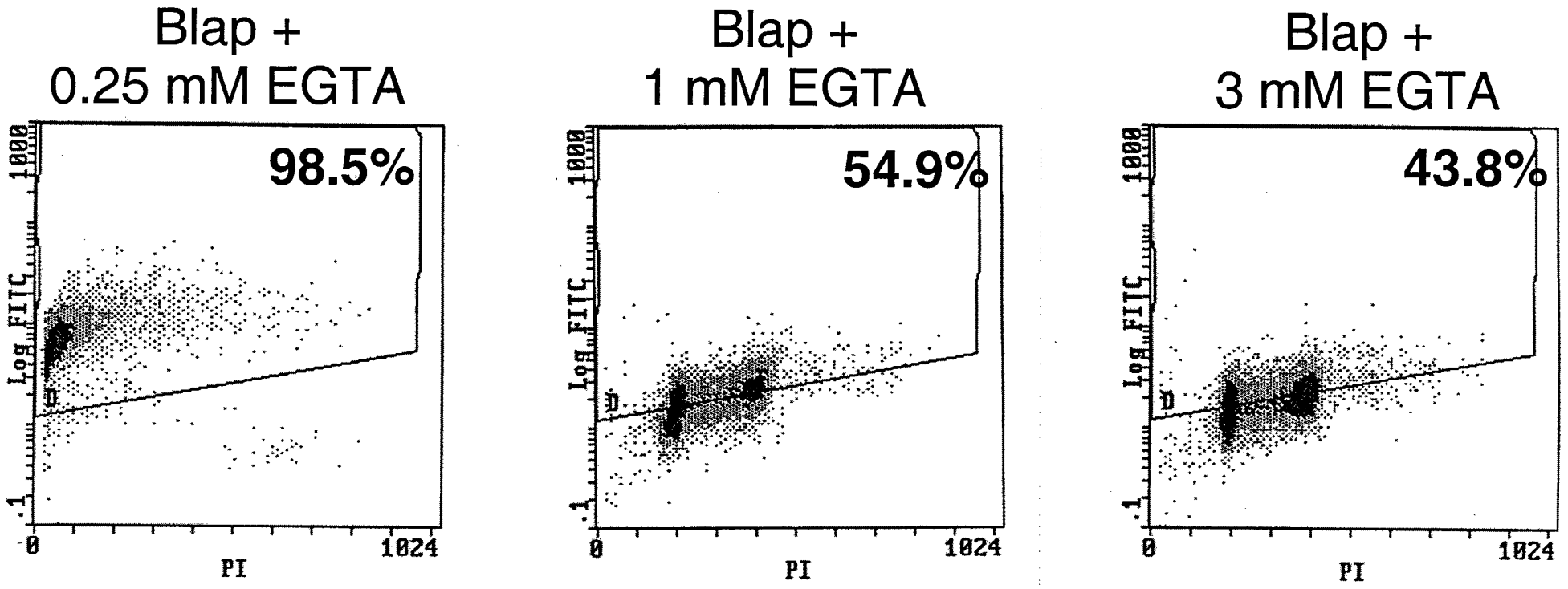

Figure 12

blap 2

Figure 13

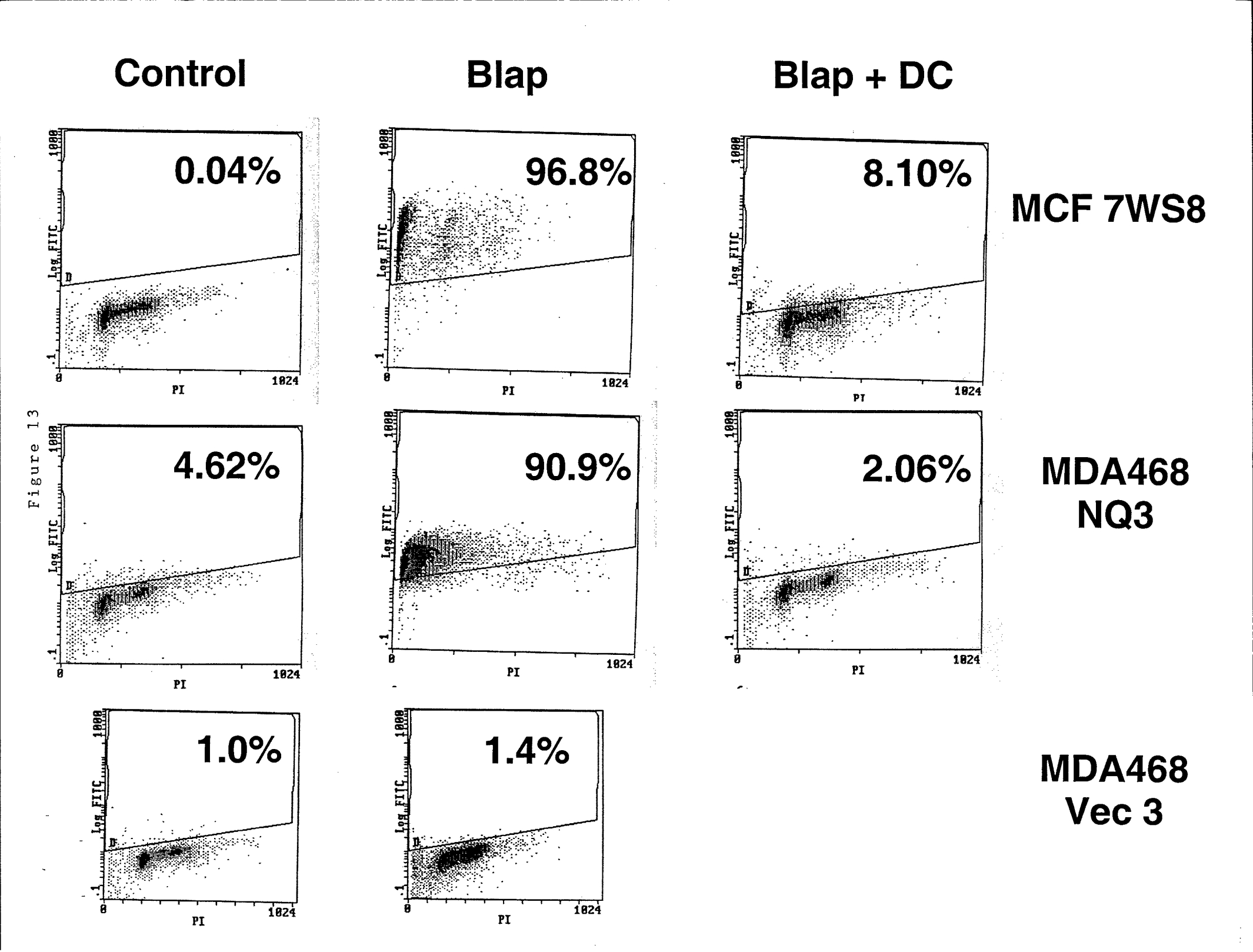
Control
Blap
Blap + DC
0.04%
96.8%
8.10%
MCF 7WS8
4.62%
90.9%
2.06%
MDA468
NQ3
1.0%
1.4%
MDA468
Vec 3
Log FITC
PI
1000
1
0
1024

Figure 14

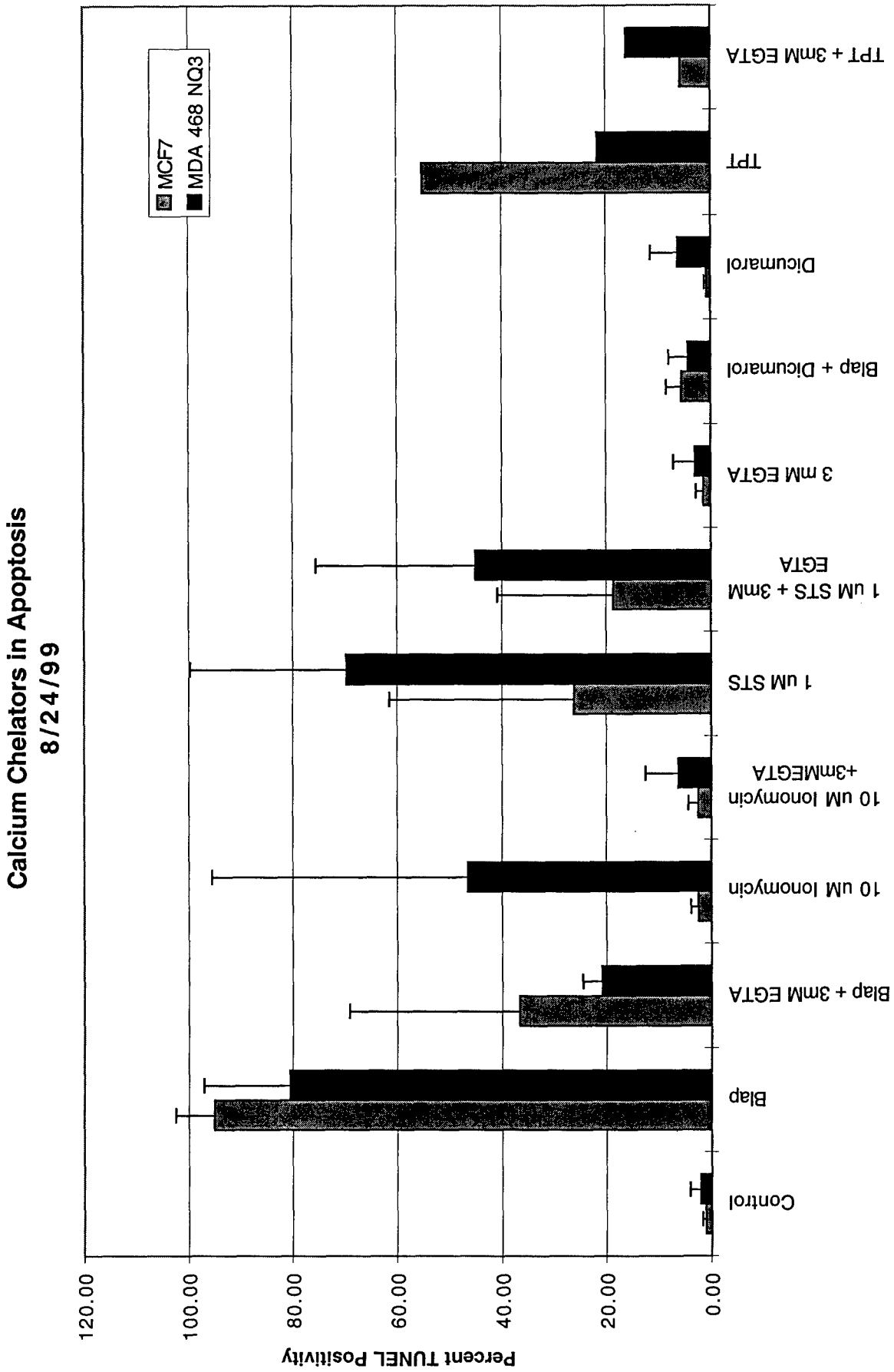

Add Vec 3 ø Blap Blap+DC

Blap 31

Figure 15

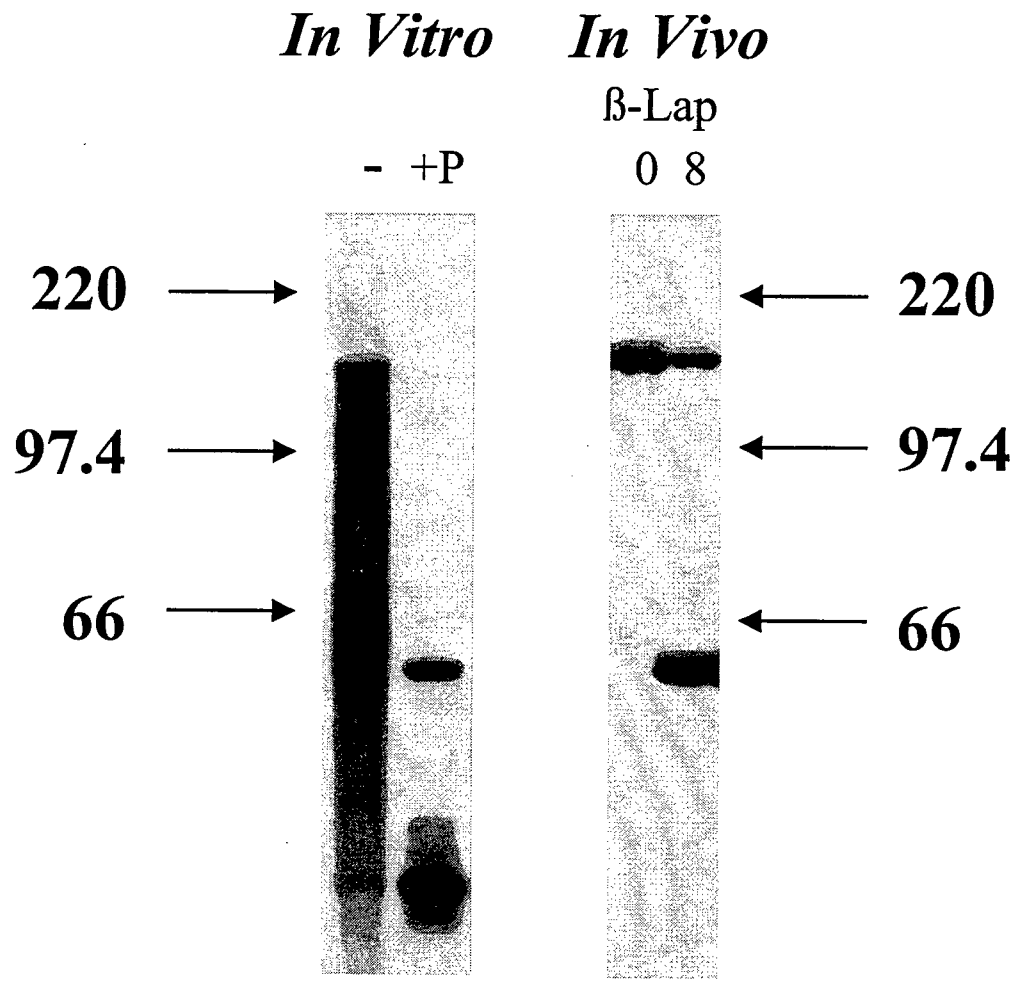

*P=Semi-purified unknown protease

Figure 16

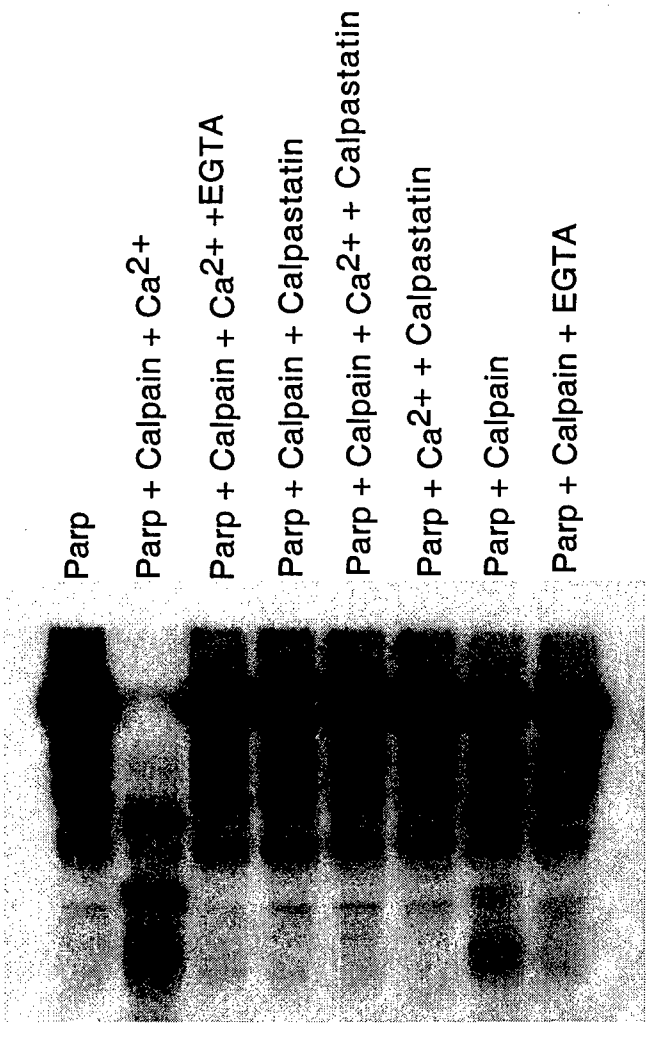
Parp
Parp + Calpain + Ca^{2+}
Parp + Calpain + Ca^{2+} +EGTA
Parp + Calpain + Calpastatin
Parp + Calpain + Ca^{2+} + Calpastatin
Parp + Ca^{2+} + Calpastatin
Parp + Calpain
Parp + Calpain + EGTA

Figure 17

MCF-7:WS8 Cells Transfected with HIS-PARP (Clones)

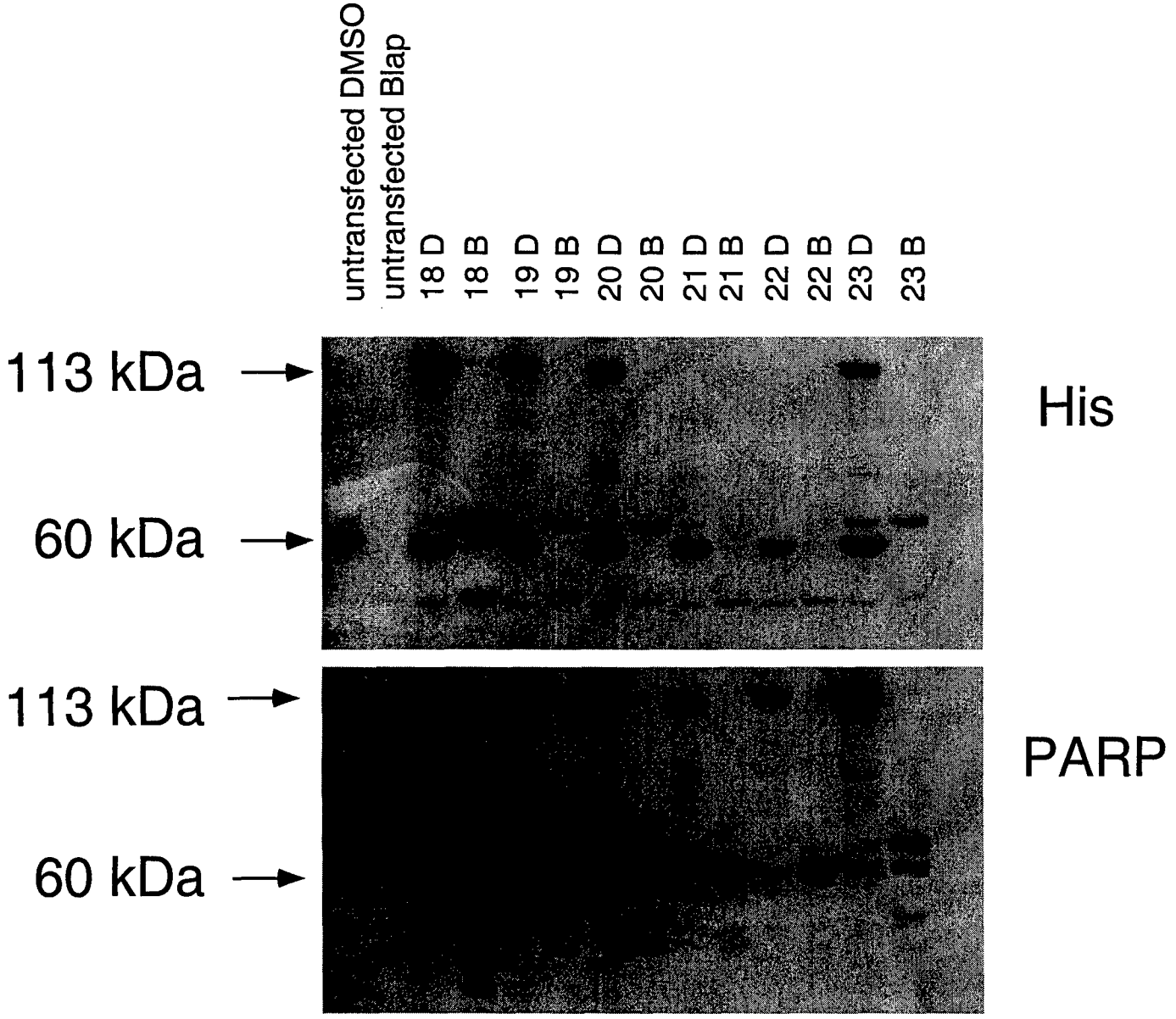

blap 17
5/10/99

Intracellular Calcium Changes in MCF7:WS8 Cells

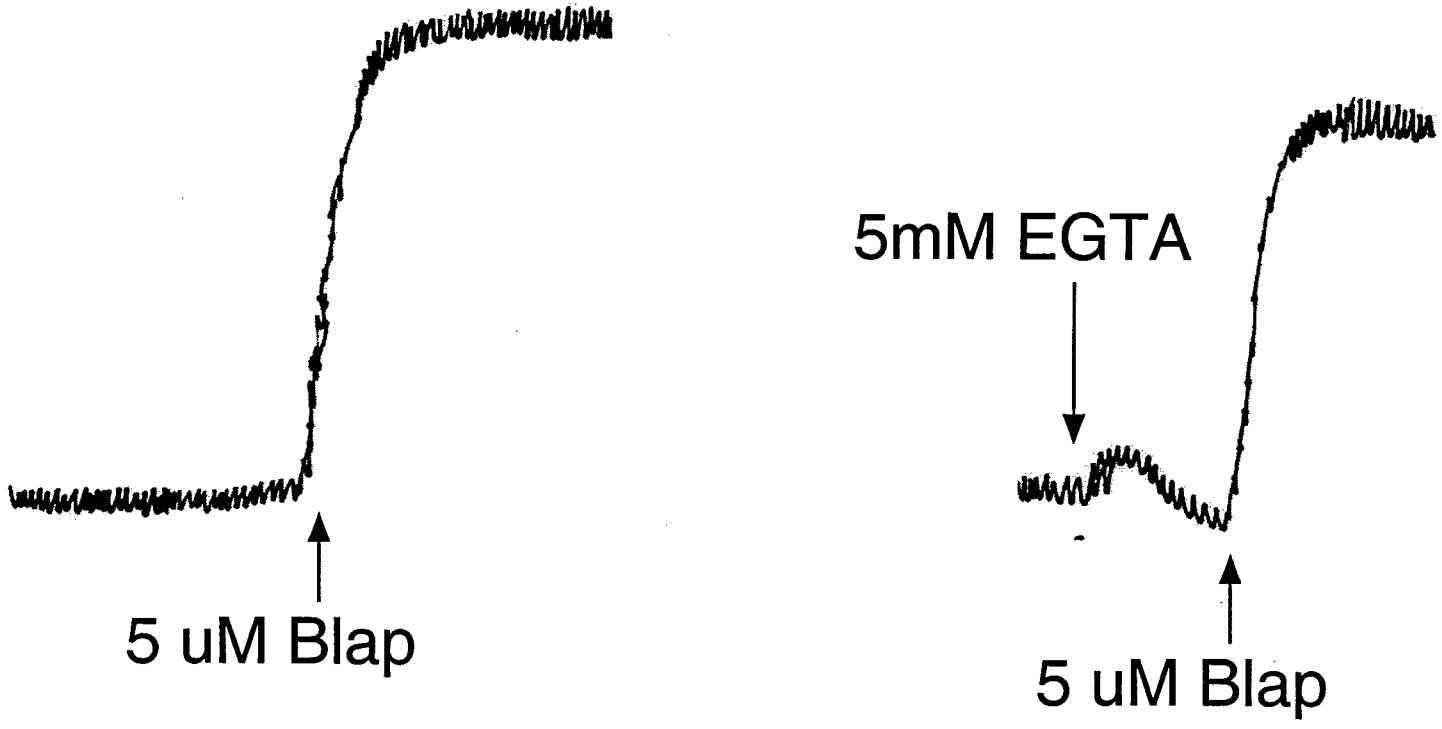

Figure 18

Figure 19

Calcium Release After β-Lapachone Treatment

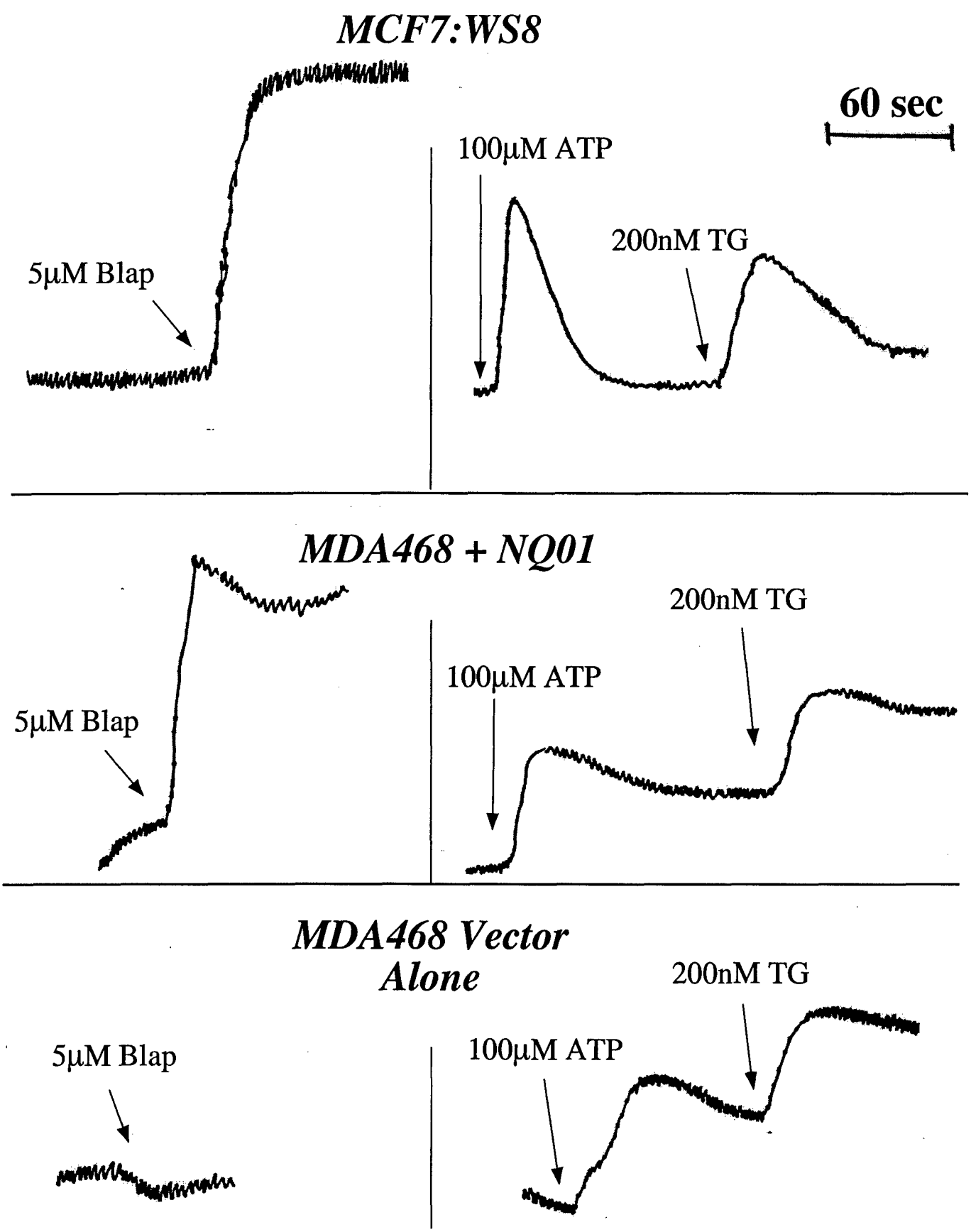

Figure 20

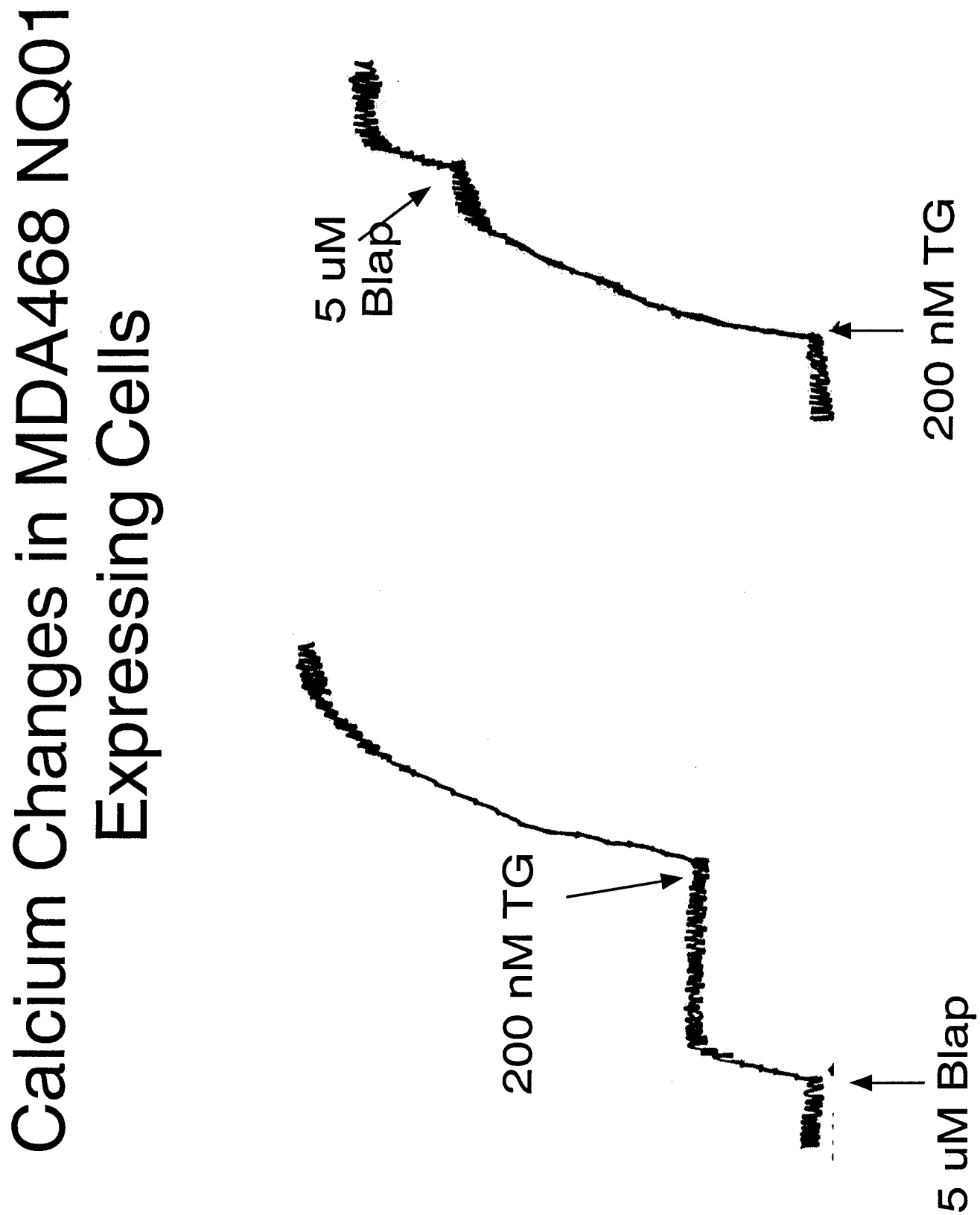
Calcium Changes in MDA468 NQ01 Expressing Cells
5 uM Blap
200 nM TG
200 nM TG
5 uM Blap

Figure 21

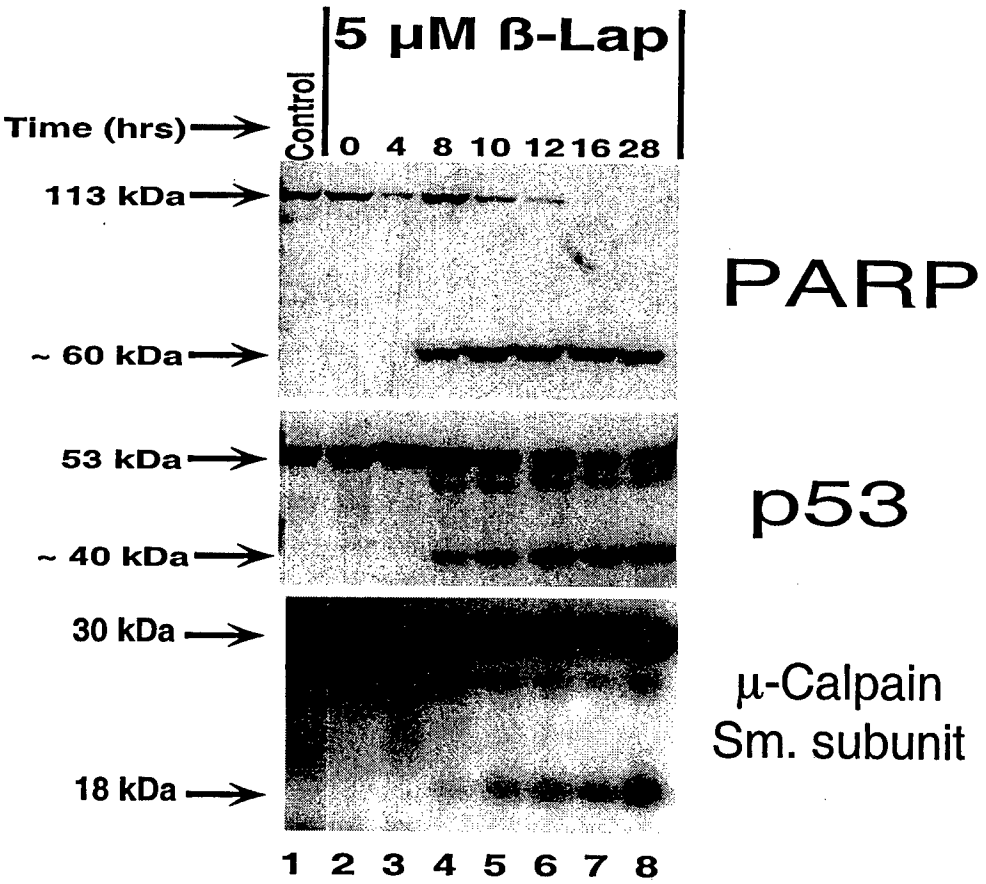
5 µM ß-Lap
Control
Time (hrs)
0 4 8 10 12 16 28
113 kDa
~ 60 kDa
PARP
53 kDa
~ 40 kDa
p53
30 kDa
18 kDa
µ-Calpain
Sm. subunit
1 2 3 4 5 6 7 8

Figure 22

Confocal Microscopy 100x

1^0 Ab:Anti-u-calpain
2^0 Ab: Anti-FITC-mouse

	Control	8 hr after 4hr pulse 8uM Blap
MDA-468 Vec 3	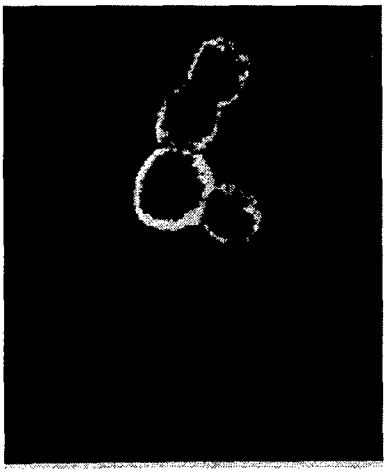	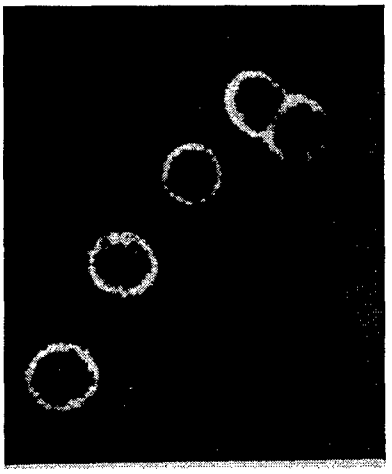
MDA-468 NQ3	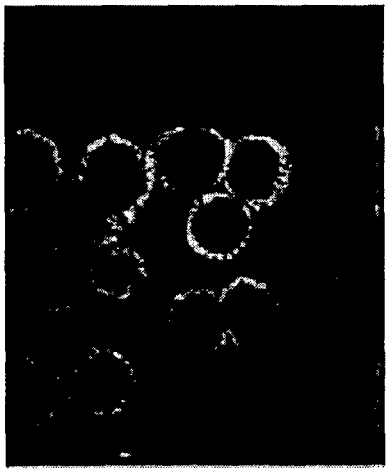	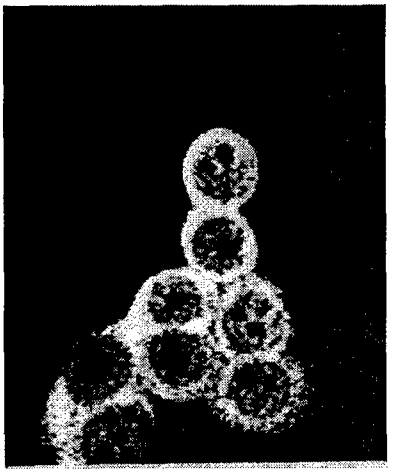

Figure 23

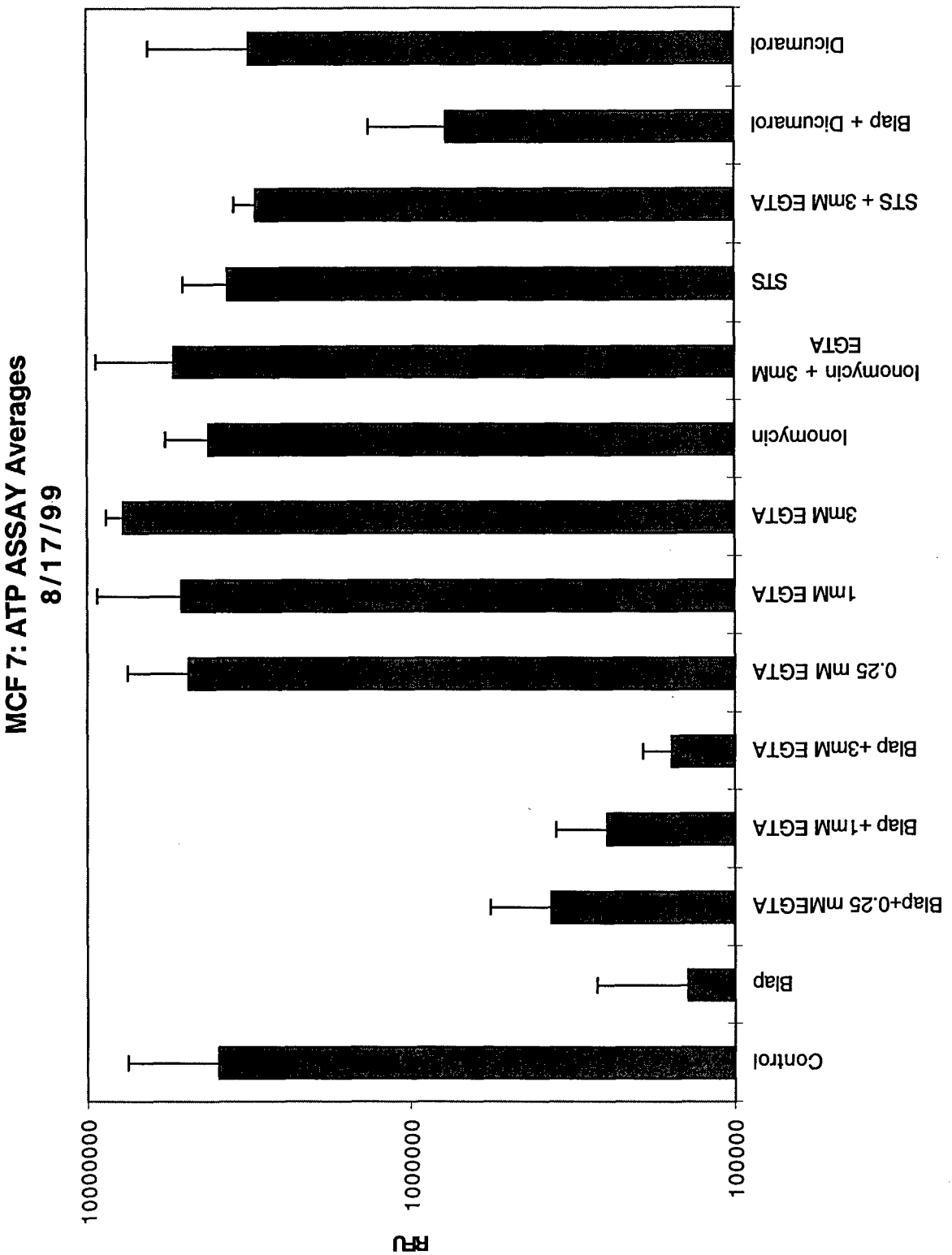
MCF 7: ATP ASSAY Averages
8/17/99
RFU
10000000
1000000
100000
Control
Blap
Blap+0.25 mMEGTA
Blap +1mM EGTA
Blap +3mM EGTA
0.25 mM EGTA
1mM EGTA
3mM EGTA
Ionomycin
Ionomycin + 3mM EGTA
STS
STS + 3mM EGTA
Blap + Dicumarol
Dicumarol

Appendix Items

-Wuerzberger, S.M., Planchon, S.M., Pink, J.J., Bornmann, W. and **Boothman, D.A.** ß-Lapachone-induced apoptosis in MCF-7 human breast cancer cells. 1998; Cancer Res. 58: 1876-1885.

-Pink, J.J., Wuerzberger-Davis, S.M., Tagliarino, C., Planchon, S.M., Yang, X., Froelich, C.J., and Boothman, D.A. A novel noncaspase-mediated proteolytic pathway activated in breast cancer cells during ß-lapachone-mediated apoptosis. 1999; Exp. Cell Res., In Revision.

-Pink, J.J., Planchon, S.M., Tagliarino, C., Varnes, M.E., Siegel, D. and Boothman, D.A. NAD(P)H:quinone oxidoreductase (NQ01) activity is the principal determinant of ß-lapachone cytotoxicity. 1999; J. Biol. Chem., submitted.

-Mendonca, M.S., Howard, K.L., Farrington, D.L., Desmond, L.A., Temples, T.M., Mayhugh, B.M., Pink, J.J. and Boothman, D.A. Delay3ed apoptotic responses associated with radiation-induced neoplastic transformation of human hybrid cells. 1999; Cancer Res. 59: 3972-3979.

-Separovic, D., Pink, J.J., Oleinick, N.L., Kester, M., **Boothman, D.A.,** McLoughlin, M., Pena, L.A., and Haimovitz-Friedman, A. Nieman-Pick human lymphoblasts are resistant to phthalocyanine 4-photodynamic therapy-induced apoptosis. 1999; Biomed Biophys. Res. Commun., 258: 506-512.

[CANCER RESEARCH 58, 1876–1885, May 1, 1998]

Induction of Apoptosis in MCF-7:WS8 Breast Cancer Cells by β-Lapachone[1]

Shelly M. Wuerzberger, John J. Pink, Sarah M. Planchon, Krista L. Byers, William G. Bornmann, and David A. Boothman[2]

Department of Human Oncology and the University of Wisconsin Comprehensive Cancer Center, University of Wisconsin-Madison, Madison, Wisconsin 53792 [S. M. W., J. J. P., S. M. P., K. L. B., D. A. B.]; and Preparative Synthesis Core Facility, Memorial Sloan-Kettering Cancer Center, New York, New York 10021 [W. G. B.]

ABSTRACT

β-Lapachone (β-lap) affects a number of enzymes *in vitro*, including type I topoisomerase (Topo I); however, its exact intracellular target(s) and mechanism of cell killing remain unknown. We compared the cytotoxic responses of MCF-7:WS8 (MCF-7) human breast cancer cells after 4-h pulses of β-lap or camptothecin (CPT), a known Topo I poison. A direct correlation between loss of survival and apoptosis was seen after β-lap treatment (LD_{50} = 2.5 μM). A concentration-dependent, transient sub-2 N preapoptotic cell population was observed at 4–8 h. Estrogen deprivation-induced synchronization and bromodeoxyuridine-labeling studies revealed an apoptotic exit point near the G_1-S border. Apoptosis activated by β-lap was closely correlated with cleavage of lamin B but not with increases in p53/p21 or decreases in bcl-2. Loss of hyperphosphorylated forms of the retinoblastoma protein was observed within 5 h, but cyclins A, B1, and E levels were unaltered for up to 72 h after 5 μM β-lap. Topo I and Topo IIα levels decreased at >24 h. Logarithmic-phase MCF-7 cells were not affected by ≤1 μM β-lap.

In contrast, dramatic and irreversible G_2-M arrest with no apoptosis was observed in MCF-7 cells treated with 1 μM CPT, monitored for 6–10 days posttreatment. MCF-7 cells treated with supralethal doses of CPT (5 μM) resulted in only ~20% apoptosis. No correlation between apoptosis and loss of survival was observed. MCF-7 cells exposed to >5 μM CPT arrested at key cell cycle checkpoints (*i.e.*, G_1, S, and G_2-M), with little or no movement for 6 days. Ten-fold increases in p53/p21 and 2–5-fold decreases in bcl-2, Topo I, Topo IIα, and cyclins A and B1, with no change in cyclin E, were observed. Temporal decreases in bcl-2 and cleavage of lamin B corresponded to the minimal apoptotic response observed.

β-Lap activated apoptosis without inducing p53/p21 or cell cycle arrest responses and killed MCF-7 cells solely by apoptosis. In contrast, concentration-dependent increases in nuclear p53/p21 and various cell cycle checkpoint arrests were seen in MCF-7 cells after CPT. Despite dramatic p53/p21 protein induction responses, CPT-treated MCF-7 cells showed low levels of apoptosis, possibly due to protective cell cycle checkpoints or the lack of specific CPT-activated apoptotic pathways in MCF-7 cells.

INTRODUCTION

β-Lap[3] (3,4-dihydro-2,2-dimethyl-2H-naphtho[1,2-b] pyran-5,6-dione) is a naturally occurring compound that is present in the bark of the Lapacho tree (*Tabebuia avellanedae*), which is native to South America. The compound has a number of concentration-dependent effects *in vivo*, including antitumor, antiviral, and antitrypanosomal activities (1–3). β-Lap has significant antineoplastic activity against a variety of human cancer cells, including prostate cancer and promyelocytic leukemia cells (4, 5), and has reported activity against the S-180 mouse tumor line (6).

β-Lap was the first reported catalytic inhibitor *in vitro* of human DNA Topo I (4, 7, 8), although its exact intracellular target(s) *in vivo* and mechanism of cytotoxicity remain unknown. β-Lap was identified by our laboratory as a radiosensitizer and chemosensitizer of confluence-arrested as well as log-phase human or rodent cancer cells (7, 9, 10). We demonstrated synergistic cytotoxicity in X-irradiated rodent cells, with concomitantly suppressed neoplastic transformation, presumably involving DNA repair inhibition (9). Using enzyme assays *in vitro*, β-lap inhibited Topo I by a distinctly different mechanism from other Topo I poisons, such as CPT and its derivatives (4, 8, 11). Additionally, enzyme assays demonstrated *in vitro* that β-lap could poison the DNA-unwinding enzyme, Topo IIα, resulting in DNA breakage (*i.e.*, DNA DSBs) through DNA-Topo IIα complex formation, similar to other poisons (12). Furthermore, β-lap suppressed the growth of yeast, which lacked Topo I expression, raising doubts about the exact mechanism of action of this compound and suggesting that, in addition to Topo I inhibition, it may have other intracellular targets. However, yeast do not express apoptotic caspases (13) and may not undergo apoptosis, limiting their use as a cytotoxicity model system. Prior data *in vivo* indicated that exposure of human or hamster cells to β-lap did not cause covalent Topo I-DNA or other protein-DNA complexes, as measured by SDS-K^+ precipitation assays (8, 11). In addition, exposure of various human or hamster cells to β-lap did not result in single-strand breaks or DSBs, as measured by alkaline or neutral filter elutions, respectively (9). Because the compound acts on growth-arrested as well as log-phase cells (10), its intracellular target is probably not cell cycle regulated, arguing against Topo IIα as a target *in vivo* (12). These contradictory *in vitro* and *in vivo* data underscore the need to determine the exact intracellular target and mechanism of cell killing for β-lap. To date, few studies have directly examined the cytotoxic responses of human cancer cells after β-lap without prior treatment with ionizing radiation. A better understanding of the mechanism of action of β-lap is warranted due to its anticarcinogenic activity and its ability to radiosensitize cells. Because it is possible that the cytotoxic (antitumor, antiviral, and antitrypanosomal) and anticarcinogenic properties of β-lap are a direct result of apoptosis (4, 5), defining the apoptotic mechanisms induced by this drug may allow us to manipulate cell death pathways for improved chemotherapy or radiotherapy against breast cancer, while protecting normal cells.

Topo poisons have not been adequately explored as antitumor agents for the treatment of breast cancer for multiple reasons, including (but not limited to) a lack of understanding of the molecular biology and cell cycle regulation underlying CPT-induced stress responses. Topo I carries out a single-strand DNA breakage, passage, and rejoining reaction that unwinds DNA. The enzyme is involved in transcription, replication, and recombination (14, 15) and is constitutively expressed during the cell cycle (16). The enzyme is elevated in many human cancers, such as prostate and colon (17), and is an important chemotherapeutic target for the specific elimination of tumor cells, irrespective of cell cycle status. Topo I poisons, such as

Received 9/26/97; accepted 3/4/98.

The costs of publication of this article were defrayed in part by the payment of page charges. This article must therefore be hereby marked *advertisement* in accordance with 18 U.S.C. Section 1734 solely to indicate this fact.

[1] Funded by the efforts of Sara Hildebrand through the Breast Cancer Inspiration Fund and the Breast Cancer Research Fund. This work was also funded by United States Army Medical Research and Material Command Breast Cancer Initiative Grant BC971431 (to D. A. B.), by a United States Army postdoctoral fellowship (to J. J. P.), and by a University of Wisconsin-Madison Comprehensive Cancer Center core grant.

[2] To whom requests for reprints should be addressed, at Department of Human Oncology, K4/626 Clinical Science Center, 600 Highland Avenue, University of Wisconsin-Madison, Madison, WI 53792. Phone: (608) 262-4970; Fax: (608) 263-8613; E-mail: boothman@humonc.wisc.edu.

[3] The abbreviations used are: β-lap, β-lapachone; Topo, topoisomerase; log, logarithmic; CPT, camptothecin; DSB, double-strand break; caspase, cysteine-aspartate specific protease; MCF-7, MCF-7:WS8; pRb, retinoblastoma protein; BrdUrd, bromodeoxyuridine; PI, propidium iodide; PBS-TB, PBS, 0.5% (v/v) Tween 20, and 0.1% BSA.

CPT, cause damage to cells by creating Topo I-mediated DNA lesions. Once damaged, CPT-treated, wild type-expressing human cancer cells exhibit alterations in cell cycle distribution and induction of both p53 and p21 protein levels and can activate apoptosis (18, 19). Although there are few assessments of Topo I levels in human breast cancer compared to normal tissue, there are reports of efficacious antitumor activity of Topo I poisons against human breast cancers (20–22).

β-Lap-activated apoptosis in human myeloid leukemia (HL-60) and prostate cancer cells was independent of p53 status (4, 5). Because agents that induce apoptosis irrespective of p53 status may have potentially great therapeutic value, we investigated the apoptotic responses of MCF-7 human breast cancer cells after transient (4 h) β-lap or CPT treatments. β-Lap killed quiescent or log-phase MCF-7 cells primarily through apoptosis, causing the rapid loss of hyperphosphorylated forms of pRb (within 3–5 h), with no apparent p53/p21 induction responses. In contrast, CPT-treated MCF-7 cells showed dramatic p53/p21 responses and concentration-dependent cell cycle checkpoint arrests but induced low levels of apoptosis, with little change in the phosphorylation status of pRb within 24 h posttreatment, even at supralethal doses.

MATERIALS AND METHODS

Chemicals and Antibodies. β-Lap (M_r 242) and various naphthoquinone derivatives were either made by us or supplied by Drs. Donald T. Witiak (University of Wisconsin-Madison) or A. V. Pinto (Universidade Federal de Rio de Janeiro, Rio De Janeiro, Brazil). CPT (M_r 348.4) was obtained from Sigma Chemical Co. (St. Louis, MO). All chemicals were dissolved as 10 mM stock solutions in DMSO, and aliquots were stored at −20°C. Stock solution concentrations were confirmed by spectrophotometric analyses using an extinction coefficient (e) of 25,790 for β-lap. β-Lap and CPT treatments were always performed in a final DMSO concentration of 0.1%, the amount of DMSO equal to the highest percentage of solvent used in experimental conditions. DMSO at 0.1% did not affect log-phase MCF-7 cells in terms of doubling time, cell growth kinetics, or apoptosis (as monitored by flow cytometry and Hoescht dye staining).

Goat serum and goat FITC-conjugated antibodies were purchased from Sigma Chemical Co. (St. Louis, MO). Antimouse monoclonal anti-BrdUrd antibodies were obtained from Becton Dickinson (San Jose, CA) and used according to the manufacturer's instructions. Antimouse and antirabbit p53, bcl-2, and cyclins B1, E, and A antibodies were obtained from Santa Cruz Biotechnology, Inc. (Santa Cruz, CA). Antimouse p21 and α-tubulin antibodies were obtained from Oncogene Research Products (Cambridge, MA). Antibodies from scleroderma patient serum, which detect human Topo I protein, were purchased from TopoGEN, Inc. (Columbus, OH). Antihuman Topo IIα antibodies were obtained from Genosys, Inc. (The Woodlands, TX).

Cell Lines and Culture Conditions. The human breast cancer cell line MCF-7 was obtained from Dr. V. Craig Jordan (Northwestern University, Chicago, IL). All cells were grown in DMEM with 10% fetal bovine serum in a humidified 10% CO_2-90% air atmosphere at 37°C. MCF-7 cells were seeded at low density (1.0×10^4 cells/ml), allowed to attach and initiate log-phase growth for 24 h, and were then exposed to β-lap or CPT at concentrations of 0.25, 1.0, 5.0, and 10 μM for 4 h. Additional drug concentrations were examined as required. Drugs were removed after 4 h, fresh DMEM (without drug) was added, and samples were collected at various times for nuclear and whole-cell protein, cell cycle redistribution (via flow cytometry), growth inhibition (using changes in DNA content/well), and colony-forming ability (survival) assays as described below. Control groups were treated with DMSO (0.1%) equal to the highest percentage of solvent used in experimental conditions. Time zero ($t = 0$) was considered the point at which various 4-h drug treatments were removed, and fresh medium was added. All experiments were repeated at least three times, each in duplicate. Graphed data for various parameters represent mean ± SE, and data sets were compared using the Student's t test.

Hoechst Staining for Apoptosis. Four h drug treatments were performed as described above. After 24 h, plates were washed twice with PBS [150 mM NaCl and 50 mM KH_2PO_4 (pH 7.4)] and fixed with methanol:glacial acetic acid (3:1, v/v). The fixative was aspirated, and plates were stained with 10 μg/ml Hoechst dye 33258 (Sigma) diluted in PBS. Plates were then washed four times with PBS to remove nonspecific staining. n-Propyl gallate (1–2 drops) was added, and pictures were taken under UV light using a 4′,6-diamidino-2-phenylindole filter or by phase-contrast using a Leitz Laborlux B microscope under the indicated magnification.

Colony-forming Assays. LD_{50} survival determinations were calculated by clonogenic assays (10). Briefly, cells were seeded at various densities on 35-cm^2 tissue culture dishes and allowed 24 h to initiate log-phase growth. Drugs were added for 4 h at various concentrations, ranging from 0.001 to 15 μM. Colonies from control and treated conditions were allowed to grow for 6 days, the time required for a control colony to reach ~50 normally appearing cells. Individual plates were counted, data were graphed as mean ± SE, and statistical analyses of all data sets were performed using the Student's t test. Drug concentrations required to inhibit growth 50% (*i.e.*, IC_{50}s) were also calculated by graphing various drug concentrations *versus* percentage DNA content/well, as previously described (4). Each experiment was performed twice, each in duplicate.

Flow Cytometry. Cells were treated with or without various concentrations of β-lap or CPT as described above. At various intervals following 4-h drug exposures, cells were washed twice with ice-cold PBS, trypsinized, and washed with a Tris saline solution [10 mM Tris (pH 7.0) and 50 mM NaCl]. Cells were then fixed in 90% ethanol-Tris saline and stored at 4°C for up to 7 days. Cells were then washed once with phosphate-citric acid buffer [0.2 M Na_2HPO_4 and 0.1 M citric acid (pH 7.8)] and stained with a solution containing 0.2% Nonidet P-40, RNase A (7000 units/ml), and 33 μg/ml PI for 10 min. In our hands, the phosphate citric acid wash has been a critical step for the accurate assessment of apoptotic cells (4). Stained nuclei were analyzed for DNA-PI fluorescence using a Becton Dickinson FACScan flow cytometer at a laser setting of 36 mW and an excitation wavelength of 488 nm. Resulting DNA distributions were analyzed for the proportion of cells in apoptosis and in G_0/G_1, S, and G_2-M phases of the cell cycle. Data were analyzed by Modfit (Verity Software House, Inc., Topsham, ME), and all experiments were repeated at least three times, each in duplicate. Graphed data represent mean ± SE.

Estrogen Deprivation-induced Synchronization and BrdUrd-labeling Studies. MCF-7 cells were deprived of estrogen for 1 week to arrest cells in early G_1 (23). Cells were then treated with 5 μM CPT or β-lap in estrogen-free medium for 4 h and subsequently released into estrogen-containing complete DMEM to initiate synchronous growth with or without prior drug treatment. At various posttreatment times, control and drug-treated MCF-7 cells were incubated with medium containing 10 μM BrdUrd (Sigma) for 30 min to label S-phase cells. Cells were then trypsinized, collected (500 × g), washed once with ice-cold PBS, and fixed (60% ethanol and 0.3% Tween 20). Samples were obtained at the indicated times for up to 96 h and stored in the dark at 4°C. Cell suspensions were incubated with 0.04% pepsin in 0.01 N HCl for 30 min at room temperature. Cells were collected as before and resuspended in 2.0 N HCl. Samples were then washed with PBS-TB, and RNA was digested with 10 μg/ml RNase A at 37°C for 1 h. Cells were washed with PBS-TB and incubated overnight with mouse monoclonal anti-BrdUrd antibodies (1:2.5 dilution). Samples were then washed with PBS-TB and incubated with goat antimouse IgG FITC-conjugated antibody (1:50 dilution) in PBS, 0.5% (v/v) Tween 20, and 0.1% goat serum for 20 min at room temperature. Cells were collected (500 × g), washed twice in PBS-TB, labeled in 50 μg/ml PI, and analyzed using flow cytometry.

Western Immunoblot Analyses. Whole-cell or nuclear extracts from control and drug-treated MCF-7 cells were isolated at various times for altered expression of key regulatory proteins. The immediate extraction of MCF-7 cells after 4 h drug incubation was marked "$t = 0$" on all Western immunoblots. Briefly, cells were washed twice with ice-cold PBS, scraped from 10-cm^2 tissue culture dishes (Corning, Cambridge, MA), and collected by centrifugation at 500 × g. For nuclear extracts, cell pellets were washed once with ice-cold PBS, resuspended in ice-cold hypotonic solution [10 mM Tris-HCl (pH 7.5), 25 mM KCl, 2 mM Mg acetate, 1 mM DTT, and 1 mM phenylmethylsulfonyl fluoride] and allowed to incubate on ice for 15 min. Samples were then passed through a 25-gauge needle to break cell membranes. Nuclei were then pelleted at 500 × g at 4°C for 5 min, resuspended in hypertonic solution [10 mM Tris-HCl (pH 7.5), 400 mM KCl, 2 mM Mg acetate, 20% glycerol, 1 mM DTT, and 1 mM phenylmethylsulfonyl fluoride] and

incubated on ice for 10 min. Insoluble nuclear debris was removed by centrifugation at 800 × *g* at 4°C for 10 min, and supernatants were aliquotted and stored at −80°C. For whole-cell extracts, cell pellets were washed twice with ice-cold PBS, lysed in loading buffer [62.5 mM Tris (pH 6.8), 6 M urea, 10% glycerol, 2% SDS, 0.003% bromphenol blue, and 5% β-mercaptoethanol], and sonicated on ice for 20 s. Protein concentrations were determined using a Bradford assay (Bio-Rad, Hercules, CA), and 10-μg protein samples were separated by 9 or 6% SDS-PAGE. Separated proteins were transferred to Immobilon-P membranes (Millipore, Bedford, MA) for 3 h at 150 V in a Bio-Rad Mini Trans-Blot Electrophoretic Transfer cell (Richmond, CA). Blots were blocked with PBS containing 10% calf serum and 0.2% Tween 20, probed with various primary antibodies as indicated (using 1:500 to 1:5000 dilutions) for at least 2 h, and washed in PBS-0.2% Tween 20 for 1 h. Blots were incubated with various secondary antibodies (using 1:500 to 1:1000 dilutions), and specific antibody-labeled proteins were detected using the ECL chemiluminescence detection system (Amersham, Buckinghamshire, England). Western immunoblot images were obtained by autoradiography using Fuji Medical X-ray film (Tokyo, Japan) as described (24). Induction levels were quantified using either densitometry or gel image analyses on a Bio-Rad Gel Doc 1000 System.

RESULTS

β-Lap Elicited Greater Apoptotic Responses but CPT Was More Cytotoxic. Survival after a 4-h pulse of various concentrations of β-lap or CPT was assessed as described in "Materials and Methods." LD_{50}s were 2.5 μM and 55 nM for β-lap and CPT, respectively (Fig. 1). MCF-7 cells treated with 5 μM β-lap showed extensive apoptotic-like nuclear condensation at 24 h posttreatment, whereas CPT-treated cells (up to 10 μM) failed to show significant apoptosis (Fig. 2) for up to 10 days posttreatment (Figs. 3 and 4). A direct correlation between apoptosis (quantified at 48 h by flow cytometry) and loss of survival (measured at 6 days posttreatment; Fig. 1) after β-lap was noted. We observed extensive nuclear condensation in MCF-7 cells treated with β-lap; however, classical nuclear blebbing and DNA laddering, as seen with human prostate cancer cells after β-lap (4, 5), were not observed (Fig. 2).

No correlation between loss of survival and apoptosis (Fig. 1*B*) was noted in MCF-7 cells treated with CPT. MCF-7 cells treated with 5 μM CPT resulted in ~20–25% apoptosis (Fig. 2), as quantified by flow cytometry (see Figs. 2 and 3). Apoptosis was not observed in MCF-7 cells treated with 1 μM CPT at 48 h posttreatment using flow cytometry or Hoescht dye staining, although <1% survival was observed (Fig. 1*B*). Thus, although CPT was dramatically more cytotoxic to MCF-7 cells than β-lap, the lethality caused by CPT did not correlate with apoptosis (compare Fig. 1, *A* and *B*); the amount of apoptosis seen in Fig. 1 correlated with that noted in 6–10-day flow cytometric assays (Figs. 3 and 4).

Kinetics of β-Lap-induced Apoptosis in MCF-7 Cells. Untreated log-phase MCF-7 cells replicated with an average population of 28% S, 18% G_2-M, and <1% apoptosis over 96 h following low cell density seeding, as described in "Materials and Methods" (Fig. 4*A*). Gradual increases in G_0/G_1 from 53% to ~75% were observed within 96 h following initial cell plating (Fig. 3*A*). Log-phase MCF-7 cells treated with <1 μM β-lap progressed through the cell cycle with no apoptosis or cell cycle delays (Fig. 3*A*). MCF-7 cells treated with β-lap for 4 h (at levels ≥ LD_{50}) resulted in the concentration-dependent appearance of preapoptotic, sub-G_0/G_1 (<2 N) cells, which peaked at 8–10 h and disappeared by 24 h after drug removal (Fig. 3*B*). Preapoptotic (<2 N) cells were subsequently replaced by apoptotic cells after 24 h (Fig. 3*B*). At 72 h, >60% of the population was apoptotic. Apoptosis in β-lap-treated MCF-7 cells was confirmed by morphological changes, including classical nuclear condensation (Fig. 2*B*). Typical G_1 and/or G_2-M cell cycle checkpoint accumulation, observed after the addition of DNA-damaging agents (*e.g.*, 1 μM CPT, Fig. 3*C*; Refs. 25 and 26), were not observed in MCF-7 cells treated with any concentration of β-lap (Fig. 3*B*). The changes in cell cycle distribution and apoptosis for β-lap-treated MCF-7 cells discussed above were confirmed using temporal, 20-min BrdUrd pulse-labeling techniques.

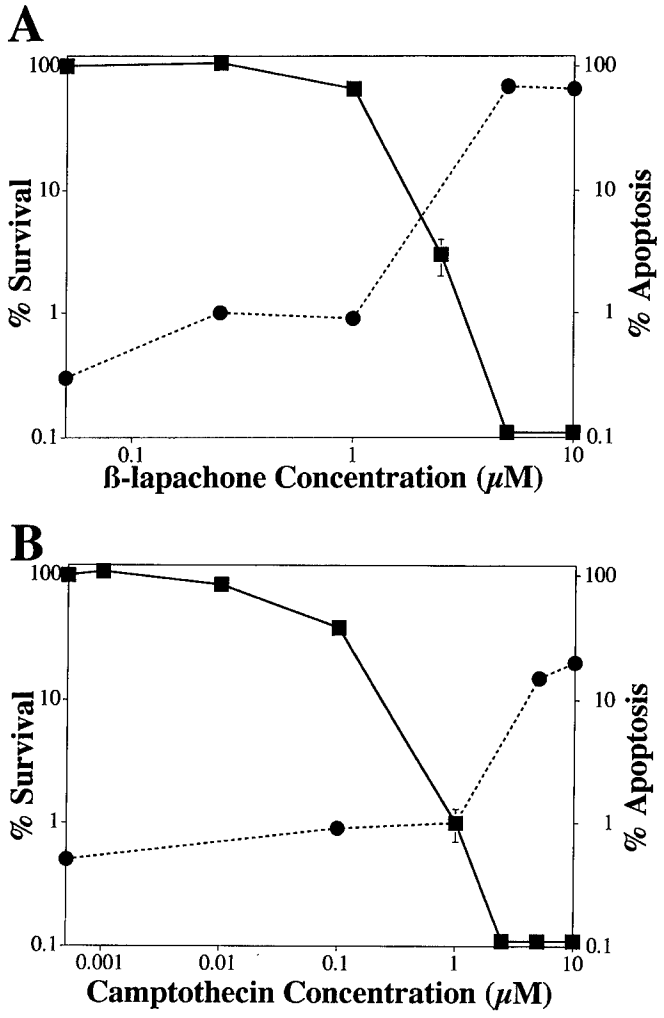

Fig. 1. Survival as a function of apoptosis in MCF-7 cells treated with β-lap or CPT. Log-phase MCF-7 cells were treated with various doses of β-lap (*A*) or CPT (*B*) for 4 h, as described in "Materials and Methods." Cells were assayed for survival by colony-forming ability and induction of apoptosis using flow cytometry or morphological examinations at 48 h, as described in "Materials and Methods." Apoptosis assessed at 48 h using morphological changes and flow cytometric quantitation were identical to measurements taken at 6 days posttreatment (Figs. 3 and 4), the same time survival was assessed. An inverse correlation between survival (■) and apoptosis (●) was noted after β-lap (*A*) but not after CPT (*B*). Data points, means of experiments performed at least three times, each in duplicate (many points were smaller than the symbol); *bars*, SE.

CPT-induced Cell Cycle and Apoptotic Effects in MCF-7 Cells. For comparison, MCF-7 cells were treated with various doses of CPT, a known Topo I poison that causes stabilization of Topo I-DNA cleavable complexes and DNA breaks in human cells, for 4 h (27). A significant and irreversible G_2-M cell cycle arrest, which lasted 144 h (*i.e.*, 6 days), was noted after 1 μM CPT (Fig. 3*C*); other experiments demonstrated that the G_2-M arrest lasted up to 9 days posttreatment (data not shown). G_0/G_1 cells steadily decreased, with little change in S phase, indicating that few cells cycled through the CPT-mediated G_2-M arrest. This was confirmed by BrdUrd pulse labeling, in which little alteration in DNA synthesis was noted in treated cells. Although checkpoint responses after CPT have been described (28), the essentially permanent G_2-M arrest observed in MCF-7 cells following 1 μM CPT has not been reported to our knowledge. Formation of preapoptotic and apoptotic MCF-7 cells noted after β-lap treatment (Fig. 3*B*)

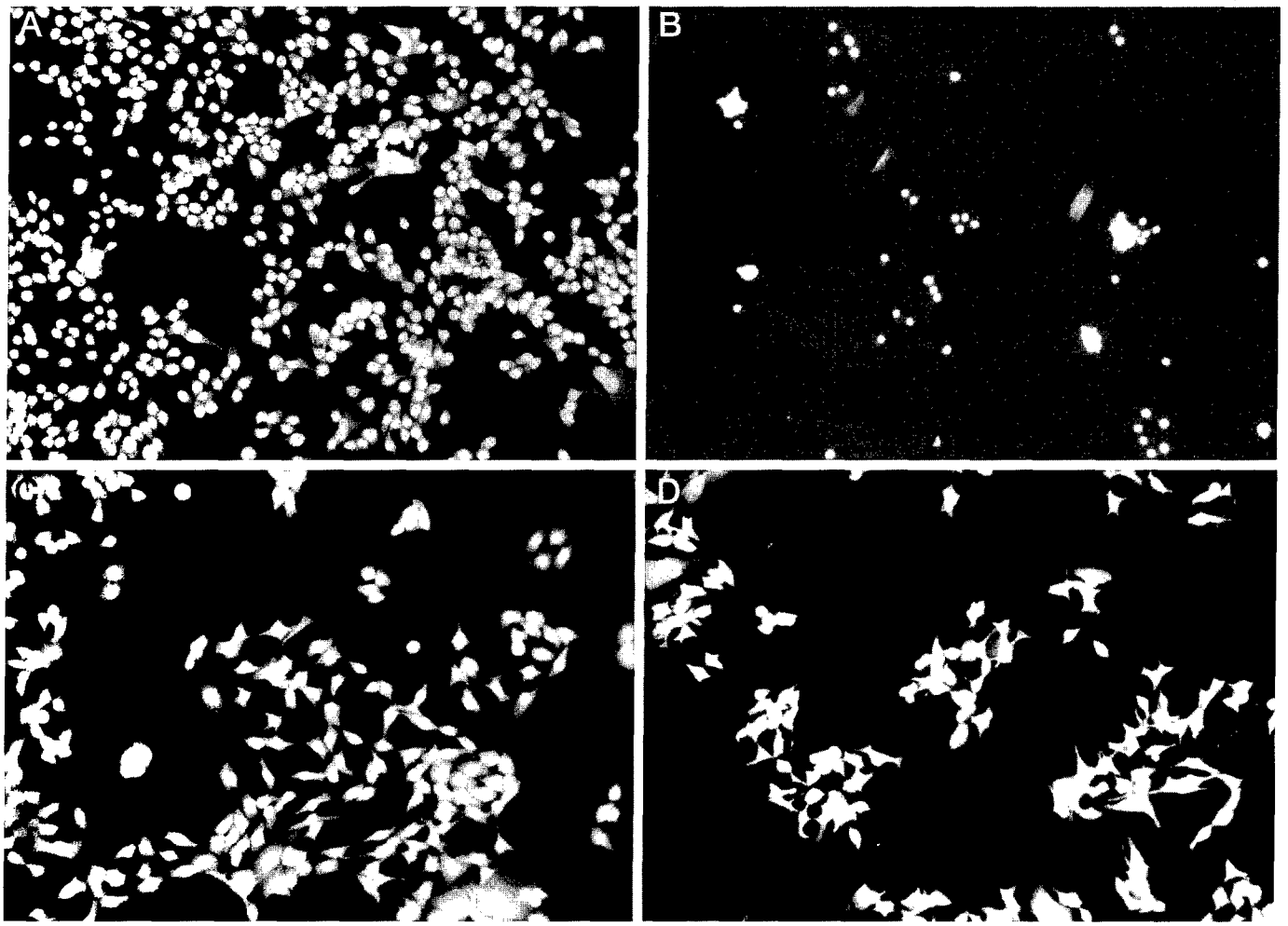

Fig. 2. Visualization of apoptotic responses of MCF-7 cells after β-lap or CPT exposures. Log-phase MCF-7 cells were treated with or without β-lap or CPT and assayed for apoptotic bodies using Hoescht dye staining, as described in "Materials and Methods." Shown are MCF-7 cells treated for 4 h with no drug (*A*), 5 μM β-lap (*B*), 1 μM CPT (*C*), or 5 μM CPT (*D*). Photomicrographs are representative of experiments performed at least five times. Quantitation of apoptosis in MCF-7 cells following various doses of CPT or β-lap using microscopy led to results that were identical to those presented in Fig. 1.

were not observed following doses up to 1 μM CPT for up to 6 days (Figs. 1*B* and 3*C*).

In contrast, MCF-7 cells treated with 5 μM CPT demonstrated rapid and near permanent G_1 and S-phase cell cycle arrests (Fig. 3*D*). Very few MCF-7 cells treated with 5 μM CPT entered G_2, in contrast to the dramatic G_2 block observed with 1 μM CPT. Low-level apoptosis (~10–20%, Fig. 3*D*) was observed for up to 144 h (6 days) in MCF-7 cells treated with 5 μM CPT. A significant amount of apparently nondividing MCF-7 cells were visible on the tissue culture plates after 5 μM CPT treatment. The changes in cell cycle distribution and apoptosis for CPT-treated MCF-7 cells discussed above were confirmed using temporal, 20-min BrdUrd pulse labeling (data not shown).

CPT, but not β-Lap, Repressed Cyclin A and B1 Protein Levels in MCF-7 Cells. We then examined alterations in the steady-state levels of a number of proteins that regulate or are regulated by the cell cycle at various times following β-lap or CPT exposures. Cyclin A is expressed during S and G_2 phases of the cell cycle, and decreased expression of cyclin A may correlate with apoptosis (29). Repression of cyclin A levels in human cells after CPT exposure were noted (30). Steady-state nuclear protein levels of cyclins A, B1, and E were not altered in MCF-7 cells following 5 μM β-lap (Fig. 4), <2 μM β-lap (data not shown), or up to 1.0 μM CPT (data not shown). In contrast, cyclin A and B1 levels dramatically decreased in MCF-7 cells treated with 5 μM CPT, at times (*i.e.*, 24–48 h, Fig. 4) when ~20% apoptosis, significant G_1 delay, and decreases in S-phase were observed (Fig. 3*D*). Decreased steady-state levels of cyclin A [and, presumably, loss of cyclin-dependent kinase activity (30)] after 5 μM CPT correlated well with the delay of treated cells in G_1-S and S phases. In contrast, levels of cyclin E, which is expressed in G_0/G_1 and S phase (31, 32), were unchanged for up to 72 h after 5 μM CPT, consistent with the constant level of G_1 cells (Fig. 3*D*).

Unlike CPT, β-Lap Exposure Did Not Induce p53 or p21 Protein Levels in MCF-7 Cells. Exposure of wild-type p53-expressing rodent or human cells to CPT caused a dramatic increase in nuclear p53 protein levels (25, 33). CPT-mediated p53 induction is thought to be caused by the creation of DSBs and/or single-strand DNA breaks because cells attempt to replicate past Topo I-DNA "cleavable complexes" (25, 33). p53 levels can also be induced by the creation of free radicals (34). Because we previously reported that β-lap catalytically inhibited Topo I *in vitro* (4) and did not induce DNA breaks (9) or stabilize Topo I-DNA complexes (9, 11), we examined changes in p53 and p21 protein levels in MCF-7 cells after β-lap or CPT exposures. MCF-7 cells exposed to 0.1–10 μM β-lap did not induce nuclear or whole-cell p53 or p21 protein levels (Fig. 4 shows p53/p21 expression after 5 μM β-lap). In fact, nuclear levels of p53 actually dropped below basal levels following 10 μM β-lap (data not shown).

In contrast, treatment of MCF-7 cells with CPT (0.1–10 μM, 4 h)

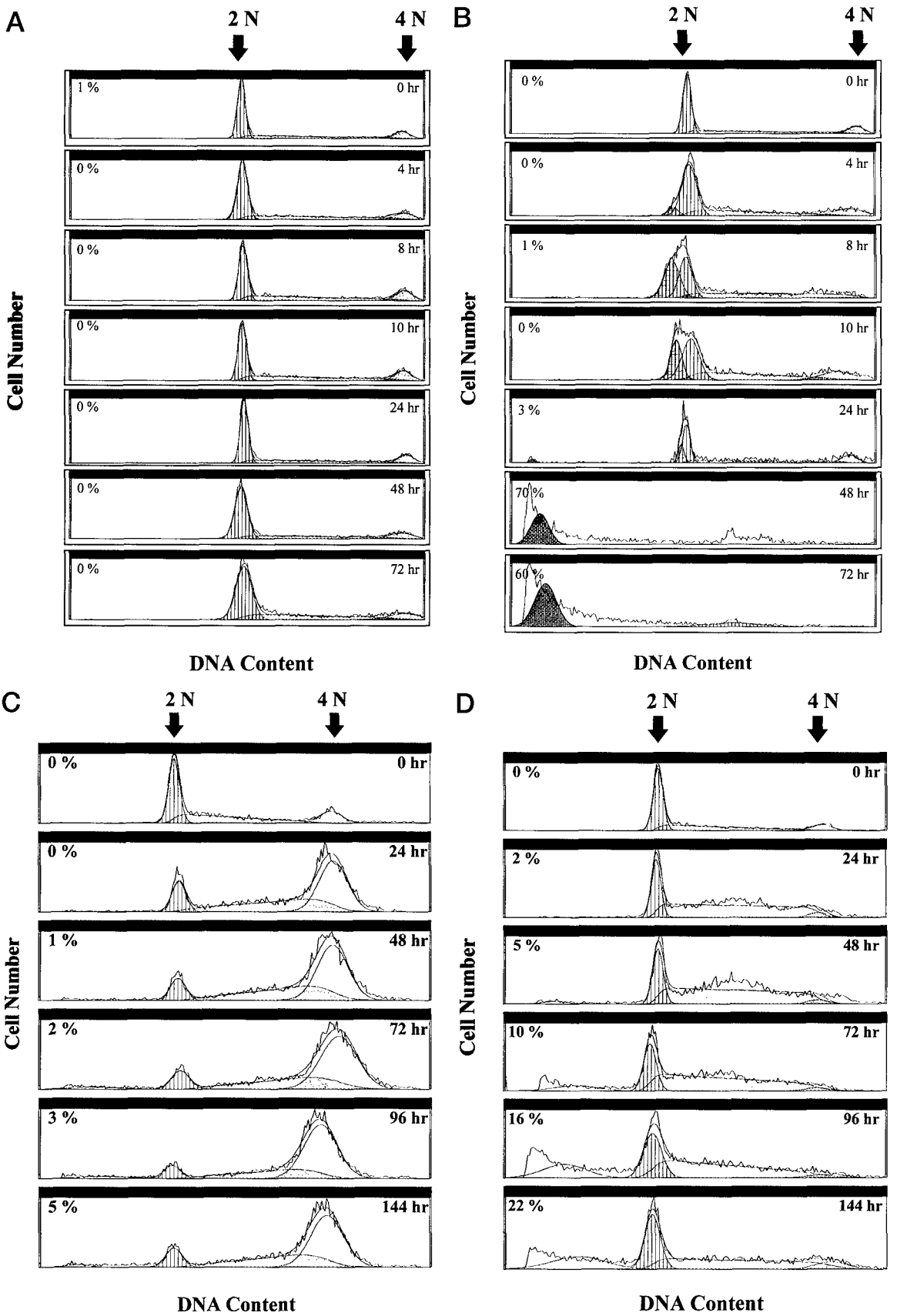

Fig. 3. Cell cycle distribution of log-phase MCF-7 cells after β-lap or CPT exposures. Log-phase MCF-7 cells were treated with DMEM alone (*A*) or with DMEM containing 5 μM β-lap (*B*), 1 μM CPT (*C*), or 5 μM CPT (*D*) for 4 h, after which media were replaced with fresh DMEM. All treatments contained 0.25% DMSO, including DMEM alone. Cells were then monitored for cell cycle changes at various times for 72–144 h (up to 6 days). Preapoptotic cells (*B*) appeared at 4 h only after β-lap treatment and peaked between 8–12 h. *Percentages*, quantifications of DNA amounts. Apoptotic cells (which contained the least amount of DNA) were confirmed by morphological examination (Fig. 2). ▥, G_0/G_1 cells; ▤, S-phase cells; □, G_2-M cells; ▦, preapoptotic cells (only found in β-lap treatment); ▨, apoptotic cells. ——, actual flow cytometric data. Data are representative of cell cycle distribution trends observed in at least six separate experiments.

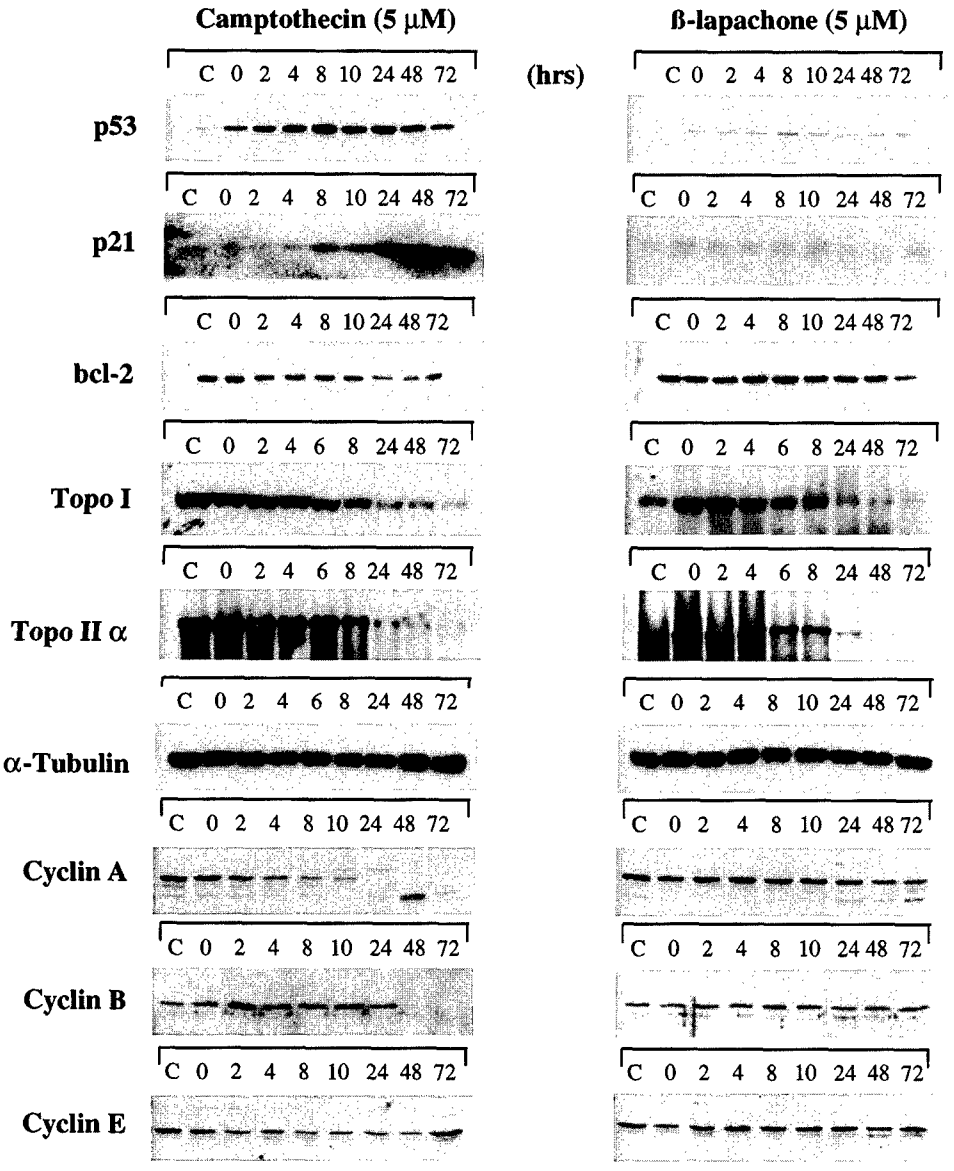

Fig. 4. Changes in protein expression after exposure of MCF-7 cells to β-lap or CPT. Log-phase MCF-7 cells were treated with 5 μM β-lap or CPT (4 h, 37°C) and monitored over time (in h) for the steady-state expression of various proteins. Changes in whole-cell (*i.e.*, p53, p21, Topo I, Topo IIα, bcl-2, and α-tubulin) and nuclear (*i.e.*, cyclins A, B1, and E) protein levels were quantified as described in "Materials and Methods." Fluctuations in protein loading between samples were monitored by α-tubulin levels. Multiple low molecular weight protein bands derived from Topo I or Topo IIα degradation and previously observed after Western immunoblot analyses during apoptosis (39), were observed only in β-lap-treated extracts after extremely long exposures of X-ray film (data not shown). Similar degradation products were not observed after CPT-treated log-phase MCF-7 cells. *Lanes C*, untreated control samples. For the steady state levels of p53, both nuclear (data not shown) and whole-cell (shown) levels demonstrated p53 protein induction by CPT but not by β-lap.

caused 5–10-fold induction of p53 within 4–24 h (Fig. 4). As expected, delayed (with respect to p53) and dramatic increases (peaking at 48 h, Fig. 4) in the steady-state levels of p21 protein were observed in CPT-treated MCF-7 cells, as reported (35, 36).

CPT, but not β-Lap, Repressed bcl-2 Protein Levels in MCF-7 Cells. The mitochondrial protein, bcl-2, plays an important role in protecting cells from apoptosis in various human cells (37). Treatment of MCF-7 cells with 5 μM (or 10 μM) β-lap did not affect the levels of bcl-2 at any time (Fig. 4), although 40–60% apoptosis was noted at 48 h (Fig. 3*B*). In contrast, MCF-7 cells treated with 5 μM CPT demonstrated a decrease in bcl-2 protein levels by 48 h. The Western blot in Fig. 5 used the same protein samples but was loaded differently. Levels of α-tubulin did not change after β-lap or CPT treatments, as shown in Fig. 4. Our results with bcl-2 (*i.e.*, loss of bcl-2 following CPT and no alterations in this protein after β-lap) were consistent with previous data using human leukemia cells (5, 37).

Altered Topo I Levels in MCF-7 Cells after β-Lap or CPT. Decreases in Topo I protein levels were reported in human cells following Topo I poisons (38, 39). Because both CPT and β-lap inhibited Topo I *in vitro* (4, 8, 11) but killed MCF-7 cells by very different mechanisms (Figs. 1–4), we examined changes in cellular Topo I protein levels in MCF-7 cells after 5 μM β-lap or CPT (Fig. 4). Neither drug treatment, given as 4-h pulses, affected total cellular Topo I protein levels for up to 8 h. However, Topo I protein levels decreased ~70% by 24 h (Fig. 4) following 5 μM β-lap or CPT. By 48 h after 5 μM β-lap or CPT, Topo I protein was undetectable. Decreases in cellular Topo I levels in MCF-7 cells treated with β-lap (Fig. 4) coincided with the appearance of apoptosis (compare Fig. 4 to Fig. 3*B*), and apoptotic cleavage fragments, similar to those described previously (39), were observed after longer exposures of Western blots. In contrast, decreased Topo I levels in MCF-7 cells after CPT (Fig. 4) did not coincide with apoptosis because only 10–20% apoptotic cells were noted at 72–144 h (Fig. 3*D*). Topo I-related apoptotic cleavage fragments were not observed after CPT, presumably because low levels of apoptosis were induced.

Repression of Topo IIα Levels in MCF-7 Cells after β-Lap or CPT Treatments. We also examined alterations in total cellular levels of Topo IIα at various times after 5 μM β-lap or CPT (Fig. 4). Topo IIα protein and transcript are expressed in a cell cycle-dependent manner in late S and through G_2-M phases of the cell cycle, with little expression in G_0/G_1 or early S phase (40). Similar decreases in Topo IIα protein levels were observed after β-lap or

border (cells did not enter S phase by BrdUrd incorporation analyses). These results were confirmed using β-lap-treated, estrogen-deprived MCF-7 cells, in which a near synchronous apoptotic loss of G_0/G_1 cells occurred, without G_1 accumulation or S phase-related incorporation of BrdUrd. The lack of β-lap-induced cell cycle checkpoints was also confirmed by unaltered steady-state expression of cyclins A, B1, and E proteins (23, 46–49). Concomitant losses of Topo I and Topo IIα at >24 h posttreatment in β-lap-treated MCF-7 cells (Fig. 4) may have been caused by the apoptotic removal of cells at G_0/G_1 (Fig. 6*B*).

pRb is a tumor suppressor gene that controls transit of cells through the G_1-S border. The pRb protein undergoes a series of phosphorylation events that alter its function to allow cell cycle progression (41). Loss of hyperphosphorylated forms of pRb occurs during apoptosis (42). Treatment of MCF-7 cells with 5 μM β-lap caused the apparent rapid (within 3–5 h posttreatment) dephosphorylation of pRb (Fig. 5). In temporal terms, loss of hyperphosphorylated pRb occurred prior to the apparent activation of a caspase that cleaved lamin B, presumably caspase 6 (39). The loss of hyperphosphorylated pRb and the synchronous loss of G_0/G_1 cells, implicate the G_0/G_1 border as the apoptotic exit point for β-lap-induced apoptosis. Further analyses of the loss of hyperphosphorylated forms of pRb and degradation of this cell cycle control protein is under investigation (44).

MCF-7 cells treated with CPT demonstrated very different cell cycle, protein expression, and apoptotic responses. CPT is a known Topo I poison (27) that results in DNA breaks (25), induction of p53/p21 (18), cell cycle arrests at G_1, S, and G_2-M cell cycle checkpoints (33), and apoptosis (50). Cellular responses to CPT occurred in specific dose-dependent patterns in MCF-7 cells after a 4-h pulse, as well as in a variety of human prostate cancer cells (4). In MCF-7 cells treated with ≤1 μM CPT, significant cell cycle arrest in G_2-M but not in G_1 or S phases was observed (Fig. 3*C*). Increases in p53/p21 nuclear protein levels were observed, presumably as a direct response to DSBs (25), but apoptosis was not noted. DSBs (51), as well as p53/p21 induction (26), may have accounted for the subsequent G_2-M arrest following CPT. In contrast, MCF-7 cells treated with 5 μM CPT stalled primarily in G_1 and S phases, where most cells were at the time of treatment, especially when deprived of estrogen (Fig. 6*C*). Formation of extensive Topo I-DNA complexes after such supralethal doses of CPT probably caused transcriptional interference (14, 15) and subsequent rapid and complete cell cycle arrests, possibly mediated by a rapid and extensive p53 response (Fig. 4). Apoptotic cells (*i.e.*, ~20%) were then observed at 72 h posttreatment with decreases in bcl-2, cyclin B1, and cyclin A, but not cyclin E. Decreases in bcl-2 and cyclin A/cdk2 have been observed after CPT treatment (30, 37, 52). The protein expression data shown in Fig. 4, which demonstrated moderate decreases in bcl-2 in MCF-7 cells after CPT, correlated with the low level of apoptosis observed (37). Although CPT was more cytotoxic than β-lap on a molar ratio basis (Fig. 1), we speculate that the p53/p21 induction and subsequent cell cycle checkpoint arrest responses observed after CPT may have, in fact, promoted repair and prevented apoptosis in MCF-7 cells. Alternatively, but not mutually exclusively, CPT-mediated cell death signals may work through apoptotic pathways (*e.g.*, caspase 3 activation) that are deficient in MCF-7 cells (44). Finally, estrogen-deprived MCF-7 cells treated with CPT appeared resistant to apoptosis, although no differences in survival in quiescent and growing cells were noted. The lack of apoptotic responses after CPT treatment may also participate in the potent carcinogenic properties of this agent (53).

β-Lap Is Not a DNA-damaging Agent. Our data are consistent with the hypothesis that β-lap exposure does not cause DNA breaks in exposed human cells, as reported (9). Exposure of MCF-7 cells to β-lap (up to 10 μM) did not elicit cell cycle checkpoint responses or p53/p21 induction, which can be a very sensitive measure of the appearance of DNA breaks in cells exposed to DNA-damaging agents (25, 33) or agents that generate free radicals (26, 51). In fact, at high doses of β-lap (≥10 μM), we noted decreases in the basal steady-state level of p53 protein. Further research is currently ongoing in our laboratory to examine this p53 degradation. Coordinate cell cycle and p53 responses indicative of DNA damage were observed in MCF-7 cells (which express wild-type p53 protein) after CPT treatment (Figs. 3 and 4). Collectively, our data suggest that β-lap induces a direct apoptotic response in MCF-7 cells, without the formation of DNA breaks, consistent with previous data (9) at a time when Topo I but not Topo IIα protein was expressed. Further research will be required to delineate whether β-lap works through Topo I *in vivo*, because the inhibition of Topo I by β-lap also did not produce DNA breaks or Topo I-DNA complexes (4, 5, 12). We speculate that β-lap may directly activate apoptotic proteases, possibly through a non-nuclear signaling mechanism.

It is interesting that similar and dramatic decreases in Topo I and Topo IIα protein levels occurred after β-lap or CPT (Fig. 4). Alterations in Topo I levels have been reported following poisons that target this enzyme (38, 54). We speculate that decreases in Topo I and/or Topo IIα after β-lap exposure may have resulted from a depletion of cells in G_2-M due to a prior loss of cells at G_1 (Figs. 3*B* and 4) and/or the activation of apoptotic proteases (*e.g.*, caspases), which specifically target these enzymes (39). Consistent with this theory, we observed Topo-related, cleavage fragments that were consistent with previously described apoptotic products following longer exposures of Western blots (39). In contrast, Topo I and Topo IIα protein decreases after 5 μM CPT were not caused solely by apoptotic responses because only 20% apoptosis was observed. Decreases in Topo I may represent irreversible and near complete formation of covalent DNA-Topo I complexes (38, 54), and simultaneous loss of Topo IIα may have resulted from accumulation of exposed cells in G_1 and S phases, with depleted G_2-M cells over time (Figs. 3*D* and 4); Topo IIα is expressed during late S and throughout G_2-M (40).

Manipulation of Apoptotic Pathways for Improved Human Breast Cancer Therapy. Topo I levels are elevated in human prostate and colon cancers (17), but very little data are available for human breast cancers compared to associated normal tissue. The overall levels of Topo I protein or enzyme do not, however, necessarily predict the cytotoxic outcome in many cancer cells (55). Therefore, we believe that it is crucial to better understand how cancer cells, particularly breast cancer cells, are killed following Topo I poisons or following other compounds that mediate apoptotic-dependent cytotoxicity (*e.g.*, β-lap). Equally important are the mechanisms of protection against apoptosis, which may reduce efficacy. Understanding such mechanisms of cell death and cell death protection may allow us to alter apoptotic responses in human breast cancer cells for tumor regression. β-Lap and its derivatives hold great promise for chemotherapeutic approaches that exploit specific apoptotic pathways that are present in tumor cells but absent or weakly activated in normal tissue. We believe that this compound holds promise as a direct chemotherapeutic agent and as a radiosensitizer against human breast cancer, which may also suppress neoplastic transformation and genetic instability induced by damage in normal tissue by apoptotic processes (9). A better understanding of cell stress responses to this agent may lead to the identification of its exact intracellular target.

ACKNOWLEDGMENTS

We thank Drs. Paul C. Carbone (former Director, University of Wisconsin Comprehensive Cancer Center), John D. Neiderhuber (current Director, University of Wisconsin Comprehensive Cancer Center), and Timothy J. Kinsella (Chair, Department of Radiation Oncology, Case Western Reserve University)

for their moral support of our work. We are also very grateful to Drs. V. Craig Jordan and George Wilding for their helpful discussions.

REFERENCES

1. Cruz, F. S., Docampo, R., and de Souza, W. Effect of β-lapachone on hydrogen peroxide production in *Trypanosoma cruzi*. Acta Trop., *35:* 35–40, 1978.
2. Docampo, R., Lopes, J. N., Cruz, F. S., and Souza, W. *Trypanosoma cruzi*: ultrastructural and metabolic alterations of epimastigotes by β-lapachone. Exp. Parasitol., *42:* 142–149, 1977.
3. Schmidt, T. J., Miller-Diener, A., and Litwack, G. β-Lapachone, a specific competitive inhibitor of ligand binding to the glucocorticoid receptor. J. Biol. Chem., *259:* 9536–9543, 1984.
4. Planchon, S. M., Wuerzberger, S. M., Frydman, B., Witiak, D. T., Hutson, P., Church, D. R., Wilding, G., and Boothman, D. A. β-Lapachone-mediated apoptosis in human promyelocytic leukemia (HL-60) and human prostate cancer cells: a p53-independent response. Cancer Res., *55:* 3706–3711, 1995.
5. Li, C. J., Wang, C., and Pardee, A. B. Induction of apoptosis by β-lapachone in human prostate cancer cells. Cancer Res., *55:* 3712–3715, 1995.
6. Docampo, R., Cruz, F. S., Boveris, A., Muniz, R. P., and Esquivel, D. M. β-Lapachone enhancement of lipid peroxidation and superoxide anion and hydrogen peroxide formation by sarcoma 180 ascites tumor cells. Biochem. Pharmacol., *28:* 723–728, 1979.
7. Boothman, D. A., Trask, D. K., and Pardee, A. B. Inhibition of potentially lethal DNA damage repair in human tumor cells by β-lapachone, an activator of topoisomerase I. Cancer Res., *49:* 605–612, 1989.
8. Li, C. J., Averboukh, L., and Pardee, A. B. β-Lapachone, a novel topoisomerase I inhibitor with a mode of action different from camptothecin. J. Biol. Chem., *268:* 22463–22468, 1993.
9. Boothman, D. A., and Pardee, A. B. Inhibition of radiation-induced neoplastic transformation by β-lapachone. Proc. Natl. Acad. Sci. USA, *86:* 4963–4967, 1989.
10. Boothman, D. A., Greer, S., and Pardee, A. B. Potentiation of halogenated pyrimidine radiosensitizers in human carcinoma cells by β-lapachone (3,4-dihydro-2,2-dimethyl-2H-naphtho[1,2-*b*]pyran-5,6-dione), a novel DNA repair inhibitor. Cancer Res., *47:* 5361–5366, 1987.
11. Boothman, D. A., Wang, M., Schea, R. A., Burrows, H. L., Strickfaden, S., and Owens, J. K. Posttreatment exposure to camptothecin enhances the lethal effects of x-rays on radioresistant human malignant melanoma cells. Int. J. Radiat. Oncol. Biol. Phys., *24:* 939–948, 1992.
12. Frydman, B., Marton, L. J., Sun, J. S., Neder, K., Witiak, D. T., Liu, A. A., Wang, H., Mao, Y., Wu, H., Sanders, M. M., and Liu, L. F. Induction of DNA topoisomerase II-mediated DNA cleavage by β-lapachone and related naphthoquinones. Cancer Res., *57:* 620–627, 1997.
13. James, C., Gschmeissner, S., Fraser, A., and Evan, G. I. CED-4 induces chromatin condensation in *Schizosaccharomyces pombe* and is inhibited by direct physical association with CED-9. Curr. Biol., *7:* 246–252, 1997.
14. Sternglaz, R. DNA topoisomerases. Curr. Opin. Cell Biol., *1:* 533–535, 1989.
15. Champoux, J. J. Topoisomerase I is preferentially associated with normal SV40 replicative intermediates, but is associated with both replicating and nonreplicating SV40 DNAs which are deficient in histones. Nucleic Acids Res., *20:* 3347–3352, 1992.
16. Hsiang, Y-H., Wu, H-Y., and Liu, L. F. Proliferation-dependent regulation of DNA topoisomerase II in cultured human cells. Cancer Res., *48:* 3230–3235, 1985.
17. Husain, I., Mohler, J. L., Seigler, H. F., and Besterman, J. M. Elevation of topoisomerase I messenger RNA, protein, and catalytic activity in human tumors: demonstration of tumor-type specificity and implications for cancer chemotherapy. Cancer Res., *54:* 539–546, 1994.
18. El-Deiry, W. S., Harper, J. W., O'Connor, P. M., Velculescu, V. E., Canman, C. E., Jackman, J., Pietenpol, J. A., Burrell, M., Hill, D. E., Wang, Y., Wiman, K. G., Mercer, W. E., Kastan, M. B., Kohn, K. W., Elledge, S. J., Kinzler, K. W., and Vogelstein, B. WAF1/CIP1 is induced in p53-mediated G_1 arrest and apoptosis. Cancer Res., *54:* 1169–1174, 1994.
19. Lowe, S. W., Ruley, H. E., Jacks, T., and Housman, D. E. p53-dependent apoptosis modulates the cytotoxicity of anticancer agents. Cell, *74:* 957–967, 1993.
20. Shimada, Y., Rothenberg, M., Hilsenbeck, S. G., Burris, H. R., Degen, D., and Von, H. D. Activity of CPT-11 (irinotecan hydrochloride), a topoisomerase I inhibitor, against human tumor colony-forming units. Anticancer Drugs, *5:* 202–206, 1994.
21. O'Reilly, S., Kennedy, M. J., Rowinsky, E. K., and Donehower, R. C. Vinorelbine and the topoisomerase 1 inhibitors: current and potential roles in breast cancer chemotherapy. Breast Cancer Res. Treat., *33:* 1–17, 1995.
22. Miller, A. A., Hargis, J. B., Lilenbaum, R. C., Fields, S. Z., Rosner, G. L., and Schilsky, R. L. Phase I study of topotecan and cisplatin in patients with advanced solid tumors: a cancer and leukemia group B study. J. Clin. Oncol., *12:* 2743–2750, 1994.
23. Musgrove, E. A., and Sutherland, R. L. Cell cycle control by steroid hormones. Semin. Cancer Biol., *5:* 381–389, 1994.
24. Boothman, D. A., Fukunaga, N., and Wang, M. Down-regulation of topoisomerase I in mammalian cells following ionizing radiation. Cancer Res., *54:* 4618–4626, 1994.
25. Nelson, W. G., and Kastan, M. B. DNA strand breaks: the DNA template alterations that trigger p53-dependent DNA damage response pathways. Mol. Cell. Biol., *14:* 1815–1823, 1994.
26. Kastan, M. B., and Kuerbitz, S. J. Control of G_1 arrest after DNA damage. Environ. Health Perspect., *5:* 55–58, 1993.
27. Hsiang, Y-H., Hertzberg, R., Hecht, S., and Liu, L. F. Camptothecin induces protein-linked DNA breaks via mammalian DNA topoisomerase I. J. Biol. Chem., *260:* 14873–14878, 1985.
28. Kastan, M. B. p53: a determinant of the cell cycle response to DNA damage. Adv. Exp. Med. Biol., *339:* 291–293, 1993.
29. Meikrantz, W., Gisselbrecht, S., Tam, S. W., and Schlegel, R. Activation of cyclin A-dependent protein kinases during apoptosis. Proc. Natl. Acad. Sci. USA, *91:* 3754–3758, 1994.
30. Shimizu, T., O'Connor, P. M., Kohn, K. W., and Pommier, Y. Unscheduled activation of cyclin B1/Cdc2 kinase in human promyelocytic leukemia cell line HL60 cells undergoing apoptosis induced by DNA damage. Cancer Res., *55:* 228–231, 1995.
31. Prall, O. W. J., Sarcevic, B., Musgrove, E. A., Watts, C. K. W., and Sutherland, R. L. Estrogen-induced activation of Cdk4 and Cdk2 during G_1-S phase progression is accompanied by increased cyclin D1 expression and decreased cyclin-dependent kinase inhibitor association with cyclin E-Cdk2. J. Biol. Chem., *272:* 10882–10894, 1997.
32. Musgrove, E. A., Lee, C. S., Cornish, A. L., Swarbrick, A., and Sutherland, R. L. Antiprogestin inhibition of cell cycle progression in T-47D breast cancer cells is accompanied by induction of the cyclin-dependent kinase inhibitor p21. Mol. Endocrinol., *11:* 54–66, 1997.
33. Kastan, M. B., Onyekwere, O., Sidransky, D., Vogelstein, B., and Craig, R. W. Participation of p53 protein in the cellular response to DNA damage. Cancer Res., *51:* 6304–6311, 1991.
34. Lane, D. P., Midgley, C. A., Hupp, T. R., Lu, X., Vojtesek, B., and Picksley, S. M. On the regulation of the p53 tumour suppressor, and its role in the cellular response to DNA damage. Philos. Trans. R. Soc. Lond. B Biol. Sci. *347:* 83–87, 1995.
35. Elbendary, A., Berchuck, A., Davis, P., Havrilesky, L., Bast, R. C., Jr., Iglehart, J. D., and Marks, J. R. Transforming growth factor β 1 can induce CIP1/WAF1 expression independent of the p53 pathway in ovarian cancer cells. Cell Growth Differ., *5:* 1301–1307, 1994.
36. El-Deiry, W. S., Tokino, T., Waldman, T., Oliner, J. D., Velculescu, V. E., Burrell, M., Hill, D. E., Healy, E., Rees, J. L., Hamilton, S. R., Kinzler, K. W., and Vogelstein, B. Topological control of p21WAF1/CIP1 expression in normal and neoplastic tissues. Cancer Res., *55:* 2910–2919, 1995.
37. Walton, M. I., Whysong, D., O'Connor, P. M., Hockenbery, D., Korsmeyer, S. J., and Kohn, K. W. Constitutive expression of human Bcl-2 modulates nitrogen mustard and camptothecin-induced apoptosis. Cancer Res., *53:* 1853–1861, 1993.
38. Danks, M. K., Garrett, K. E., Marion, R. C., and Whipple, D. O. Subcellular redistribution of DNA topoisomerase I in anaplastic astrocytoma cells treated with topotecan. Cancer Res., *56:* 1664–1673, 1996.
39. Casiano, C. A., Martin, S. J., Green, D. R., and Tan, E. M. Selective cleavage of nuclear autoantigens during CD95 (Fas/APO-1)-mediated T cell apoptosis. J. Exp. Med., *184:* 765–770, 1996.
40. Goswami, P. C., Roti Roti, J. L., and Hunt, C. R. The cell cycle-coupled expression of topoisomerase IIα during S phase is regulated by mRNA stability and is disrupted by heat shock or ionizing radiation. Mol. Cell. Biol., *16:* 1500–1508, 1996.
41. Weinberg, R. A. The retinoblastoma protein and cell cycle control. Cell, *81:* 323–330, 1995.
42. An, B., Johnson, D. E., Jin, J., Antoku, K., and Dou, Q. P. Bcl-2- and CrmA-inhibitable dephosphorylation and cleavage of retinoblastoma protein during etoposide-induced apoptosis. Int. J. Mol. Med., *1:* 131–136, 1998.
43. Oberhammer, F. A., Hochegger, K., Froschl, G., Tiefenbacher, R., and Pavelka, M. Chromatin condensation during apoptosis is accompanied by degradation of lamin A + B, without enhanced activation of cdc2 kinase. J. Cell Biol., *126:* 827–837, 1994.
44. Pink, J., Wuerzberger, S. M., Srinivasan, A., Tomaselli, T., and Boothman, DA. Activation of Ced-3/ICE family proteases in human breast cancer cells undergoing apoptosis in response to topoisomerase I poisons. *In:* Programmed Cell Death Symposium, American Association for Cancer Research Mini-Symposium, October 19–23, 1996.
45. Wang, T. T., and Phang, J. M. Effects of estrogen on apoptotic pathways in human breast cancer cell line MCF-7. Cancer Res., *55:* 2487–2489, 1995.
46. Nurse, P. The Wellcome Lecture, 1992. Cell cycle control. Philos. Trans. R. Soc. Lond. B Biol. Sci., *341:* 449–454, 1993.
47. Musgrove, E. A., Hamilton, J. A., Lee, C. S., Sweeney, K. J., Watts, C. K., and Sutherland, R. L. Growth factor, steroid, and steroid antagonist regulation of cyclin gene expression associated with changes in T-47D human breast cancer cell cycle progression. Mol. Cell. Biol., *13:* 3577–3587, 1993.
48. Sutherland, R. L., Watts, C. K., and Musgrove, E. A. Cyclin gene expression and growth control in normal and neoplastic human breast epithelium. J. Steroid Biochem. Mol. Biol., *47:* 99–106, 1993.
49. Sweeney, K. J., Musgrove, E. A., Watts, C. K., and Sutherland, R. L. Cyclins and breast cancer. Cancer Treat. Res., *83:* 141–170, 1996.
50. Solary, E., Bertrand, R., and Pommier, Y. Apoptosis induced by DNA topoisomerase I and II inhibitors in human leukemic HL-60 cells. Leuk. Lymphoma, *15:* 21–32, 1994.
51. Maity, A., McKenna, W. G., and Muschel, R. J. The molecular basis for cell cycle delays following ionizing radiation: a review. Radiother. Oncol., *31:* 1–13, 1994.
52. Tsao, Y. P., D'Arpa, P., and Liu, L. F. The involvement of active DNA synthesis in camptothecin-induced G_2 arrest: altered regulation of p34cdc2/cyclin B. Cancer Res., *52:* 1823–1829, 1992.
53. Zhang, L. H., and Jenssen, D. Studies on intrachromosomal recombination in SP5/V79 Chinese hamster cells upon exposure to different agents related to carcinogenesis. Carcinogenesis (Lond.), *15:* 2303–2310, 1994.
54. Beidler, D. R., and Cheng, Y. C. Camptothecin induction of a time- and concentration-dependent decrease of topoisomerase I and its implication in camptothecin activity. Mol. Pharmacol., *47:* 907–914, 1995.
55. Pommier, Y., Leteurtre, F., Fesen, M. R., Fujimori, A., Bertrand, R., Solary, E., Kohlhagen, G., and Kohn, K. W. Cellular determinants of sensitivity and resistance to DNA topoisomerase inhibitors. Cancer Invest., *12:* 530–542, 1994.

A Novel Non-Caspase-Mediated Proteolytic Pathway Activated in Breast Cancer Cells During ß-Lapachone-Mediated Apoptosis

John J. Pink ‡, Shelly Wuerzberger-Davis ‡†, Colleen Tagliarino ‡, Sarah M. Planchon ‡, XiaoHe Yang §, Christopher J. Froelich §, and David A. Boothman ‡¶

‡ Department of Radiation Oncology, Laboratory of Molecular Stress Responses, Case Western Reserve University, OH 44106 and § Evanston Northwestern Healthcare Research Institute, Evanston, IL, 60201

RUNNING TITLE: Apoptosis and Atypical PARP Cleavage in Breast Cancer

¶ To whom reprint requests should be directed at: Department of Radiation Oncology, Laboratory of Molecular Stress Responses, BRB-3 East, Case Western Reserve University School of Medicine, 10900 Euclid Avenue, Cleveland, Ohio 44106-4942 Phone 216-368-0840 Fax 216 368-1142
E-mail dab30@po.cwru.edu

† Current address: Department of Human Oncology, University of Wisconsin Comprehensive Cancer Center, Madison, WI 53792

Abstract

ß-Lapachone (ß-lap) effectively killed a variety of breast cancer cell lines via apoptosis, however, the mechanism by which this compound activated downstream proteolytic execution processes remains unknown. Exposure of breast cancer cells to ß-lap (4-10 μM, 4 h) resulted in rapid dephosphorylation of the retinoblastoma protein (pRb) followed by loss of pRb in 24 h. Topotecan (TPT) exposure also led to accumulation of dephosphorylated pRb, albeit to a lesser extent. TPT activated the caspase-mediated protease pathway, similar to ß-lap at low doses and both were prevented by zVAD-fmk. However at higher doses of ß-lap, a novel non-caspase-mediated "atypical" cleavage of PARP (i.e. an ~60 kDa cleavage fragment) was observed in a cell type-dependent manner. Atypical PARP cleavage directly correlated with apoptosis in MCF-7:WS8 cells and was inhibited by the global cysteine protease inhibitors, iodoacetamide and N-ethylmaleimide. This cleavage was insensitive to inhibitors of caspases, granzyme B, cathepsins B and L, trypsin and chymotrypsin-like proteases. The protease responsible appears to be calcium-dependent and the concomitant cleavage of PARP and p53 was consistent with a ß-lap-mediated activation of calpain. ß-Lap exposure also stimulated the cleavage of lamin B, a putative caspase 6 substrate. Re-expression of pro-caspase-3 into caspase-3 null MCF-7:WS8 cells did not affect this proteolytic pathway, while increasing TNF-α sensitivity. This novel apoptotic pathway appears to be a unique response to the cytotoxic effects of ß-lap.

KEY WORDS: Apoptosis, ß-Lapachone, Caspase, Breast Cancer, Poly (ADP)-Ribose Polymerase (PARP), Calpain

Introduction

The execution phase of apoptosis culminates in the activation of a cascade of specific cysteine proteases which cleave following aspartate residues in target proteins. These proteases, named caspases (1), comprise a family of zymogens that are converted to activated proteases by specific cleavage reactions. The activation of these proteases can be indirectly measured by the appearance of relatively long-lived polypeptide cleavage fragments. Substrate cleavage products include the 89 kDa fragment of poly(ADP-ribose) polymerase (PARP), the 46 kDa polypeptide of lamin B, the ~100 kDa C-terminally or ~68 kDa internally cleaved polypeptides of retinoblastoma protein (pRb), and the ~68 kDa fragment derived from Sp1 (2-5). The cleavage sites within some apoptotic death substrates have been precisely mapped and used to design inhibitors of the caspases, such as zVAD-fmk and DEVD-fmk, which were developed using the recognition sites for caspases-1 and -3, respectively (6). In contrast, the global cysteine protease inhibitors, iodoacetamide and N-ethylmaleimide, directly react with active site cysteines and thereby inhibit all cysteine proteases, as well as other enzymes that contain accessible -SH groups (7, 8).

While a great deal of information has been generated regarding the action of caspases during apoptosis, less is known about alternate apoptotic proteolytic pathways that are activated after treatment with various cytotoxic agents. A number of reports have shown that the neutral calcium-dependent protease, calpain, can be activated during apoptosis (9-11); a key *in vivo* target of calpain appears to be p53. Other reports have demonstrated the activation of non-caspase proteases, such as the nuclear scaffold protease (12, 13) and unknown serine proteases during apoptosis (14, 15). The serine

protease(s) described in these studies appeared to be distinct from granzyme B, which induces apoptosis through caspase activation (16).

Distinct changes in pRb appear to be early, as well as late, markers of apoptosis in many human cancer cells treated with chemotherapeutic agents (4, 17, 18). The dramatic accumulation of hypophosphorylated pRb, at the expense of phosphorylated protein, was shown during apoptosis after treatment with a variety of agents (18, 19). The exact mechanism(s) responsible for the accumulation of hypophosphorylated pRb is still unknown, but repression of cell cycle progression has been documented (20). While phosphatase inhibitors prevented the dephosphorylation of pRb, an increase in phosphatase activity was not observed following etoposide-induced apoptosis (17). These data suggested that loss of kinase activity in the presence of constitutive phosphatase levels may account for accumulation of hypophosphorylated pRb.

Cleavage of pRb at later stages of apoptosis has been noted. Two different pRb cleavage events have been reported (4, 5). An et al., (5) have demonstrated the presence of 48 kDa and 68 kDa pRb fragments following treatment of HL-60, U937 or Jurkat cells with Ara-C, VP-16 or the Fas ligand. This cleavage was inhibited by CrmA, bcl-2 or YVAD-cmk, suggesting a caspase-mediated pathway; however, no obvious caspase recognition sites were present at sites in the pRb protein which would give rise to these fragments. A reasonable interpretation of these data could be that caspases were involved upstream, but the protease responsible for cleaving pRb was not a known caspase.

Janicke et al., (4) demonstrated a different *in vivo* cleavage pattern of pRb during apoptosis. This cleavage occurred at a caspase-3 recognition site within the protein, resulting in removal of a small segment (~40 amino

acids) from the C-terminus of pRb and forming an ~100 kDa pRb fragment. Subsequent release of MDM-2 accompanied this proteolysis, however, E2F-1 binding was not affected. Thus, disruption of normal pRb function, through either dephosphorylation or cleavage, is thought to cause a dramatic deregulation of normal cell cycle progression, which thereby stimulates apoptosis by unknown mechanisms.

ß-lapachone (ß-Lap) is a naturally occurring 1,2-naphthoquinone initially isolated from the bark of the Lapacho tree, native to South America. We previously demonstrated that this drug is a radiosensitizing agent against human laryngeal carcinoma and melanoma cell lines (21). Using cell-free assays, ß-lap inhibited Topo I by a mechanism quite different from that of camptothecin (CPT) or the related compounds, TPT, 9-aminocamptothecin or Irinotecan (22). For example, ß-lap administration did not stabilize Topo I-DNA cleavable complexes *in vivo* (23) or *in vitro* (24). In contrast, the CPT family members stabilized cleavable complexes (23), resulting in the formation of DNA single strand nicks (25) and induction of wild-type p53 (26). The fact that ß-lap did not produce DNA single strand nicks in human or hamster cancer cells (25, 27) was indirectly confirmed by the absence of wild-type p53 induction in breast or prostate cancer cells (22, 28). While the *in vitro* assays indirectly suggested that Topo I may be an intracellular target of ß-lap, it seemed likely that it was not the only mechanism through which this compound acted (28, 29). We recently reported that the cytotoxicity caused by ß-lap in MCF-7:WS8 breast cancer cells could be solely accounted for by apoptotic responses (28). Interestingly, ß-lap-mediated apoptosis in MCF-7:WS8 cells was accompanied by a dramatic decrease in p53 steady state levels, prior to the appearance of apoptotic morphologic changes (28). We were, therefore, interested to see if this relationship

between loss of survival and apoptosis held true for other breast cancer cells. We describe a novel, non-caspase, cysteine protease-mediated apoptotic pathway, which was activated independently of cell cycle status, in various breast cancer cells treated with ß-lap. This protease shares some characteristics with the neutral calcium-dependent protease, calpain.

Materials and Methods

Chemicals and Tissue Culture Reagents. Estradiol (E_2), 4-hydroxytamoxifen (4-OHT) (Sigma Chemical Co., St. Louis, MO), or ICI 182,780 (a generous gift from Dr. V. Craig Jordan, Northwestern University) were dissolved in 100% ethanol as 1000X stocks and maintained at -20° C. ß-lap [MW: 242, ε= 25790) generously supplied by Dr. William G. Bornmann (Memorial Sloan Kettering, NY, NY] and topotecan (TPT) (Smith Kline Beecham, Philadelphia, PA) were dissolved in DMSO and concentrations confirmed by spectrophotometric analyses (28, 30). Nocodazole was purchased from Sigma Chemical Co., and a 2 mg/ml stock solution was made in DMSO immediately before use. All tissue culture reagents were purchased from GIBCO Laboratories, Grand Island, NY, unless otherwise stated. Charcoal-stripped serum was prepared by treating fetal bovine serum (FBS) three times with dextran-coated charcoal as described (31).

Antibodies and Protease Inhibitors. The C-2-10 PARP monoclonal antibody was purchased from Enzyme Systems Products (Dublin, CA). An N-terminal PARP (clone N-20), Sp1 polyclonal, p53 monoclonal (clone DO-1) and all horseradish peroxidase-conjugated secondary antibodies were obtained from Santa Cruz Biotechnologies (Santa Cruz, CA). Monoclonal antibodies to pRb (clone G3-245) and underphosphorylated pRb (clone G99-549), were obtained from PharMingen (San Diego, CA). A polyclonal antibody specific to phosphorylated serine 780 of the pRb protein was obtained from Medical and Biological Laboratories Co. Ltd. (Boston, MA). Antibody to caspase-3 was obtained from Transduction Laboratories

(Lexington, KY). Antibody to lamin B was obtained from Matritech, Inc. (Cambridge, MA). zVAD-fmk, DEVD-fmk, zFA-fmk and zAAD-fmk were obtained from Enzyme Systems Products (Dublin, CA), diluted in DMSO and used at 25 μM unless otherwise stated. TPCK, TLCK, iodoacetamide and N-ethylmaleimide were purchased from Sigma Chemical Co. (St. Louis, MO.) and diluted in DMSO (TPCK and TLCK), ethanol (N-ethylmaleimide), or water (iodoacetamide). The pBabe/puro vector was a generous gift from Dr. Todd Sladek.

Tissue Culture and Growth Conditions. MCF-7:WS8, T47D:A18 [clones of the standard MCF-7 and T47D cell lines, selected by limiting dilution cloning of the parental cell lines in whole serum (31-33)] and MDA-MB-231 breast cancer cell lines were obtained from Dr. V. Craig Jordan (Northwestern University, Chicago, IL). MDA-MB-468 cells were obtained from the ATCC. The ER, p53 and pRb status of these cell lines are outlined in Table 1. Cells were grown in RPMI 1640 medium supplemented with 10% FBS, 6 ng/ml bovine insulin, 2 mM L-glutamine, 100 U/ml penicillin and 100 mg/ml streptomycin. For estrogen-free tissue culture medium, phenol red-free RPMI and charcoal-stripped FBS were used as previously described (31). Cells were routinely passed at 1:5 to 1:20 dilutions once per week using 0.1% trypsin. All cells were mycoplasma-free and grown at 37 °C in a humidified incubator with 5% CO_2-95% air atmosphere.

Growth Assays and Estrogen-Deprivation Studies. Forty eight hour or six day growth assays were used to assess the relative sensitivities of breast cancer cells to various drug treatments as previously described (31-33). For estrogen deprivation studies, cells were grown in estrogen-free medium for at least 4 days prior to the start of experiments. Cells were seeded into 96

well plates (1.5 x 10^3 or 1 x 10^4 cells/well) in 0.2 ml of medium on day 0, and allowed to attach for 24 h. On day 1, fresh medium containing the indicated drug(s), was added to the appropriate wells. 17ß-Estradiol (E_2), 4-hydroxytamoxifen (4-OHT), or ICI 182,780 (ICI) were added to cells at 1:1000 dilutions from appropriate stock solutions. Estrogen-deprivation significantly retarded cell growth and dramatically increased the proportion of MCF-7:WS8 and T47D:A18 cells in G_1. For MCF-7:WS8, 83% G_1 cells were observed after 6 days of growth in estrogen-free medium compared to 53% in log-phase cultures. Changes in cell number, measured as DNA content, were then determined in untreated or drug-treated cells by an adaptation of the method of LaBarca and Paigan (34) and analyzed using a Molecular Dynamics Biolumin 960 plate reader with an excitation wavelength of 360 and emission wavelength of 450 nm. Data were expressed as relative growth (T/C) by dividing the DNA content of treated cells (T) by that of untreated cells (C) at identical times. Data points represent the mean ± SEM of at least four replicate wells. All experiments were performed at least three times.

Western Immunoblot Analyses. Whole cell extracts were prepared by direct lysis of PBS washed cells (both floating and attached cells were pooled) in PARP extraction buffer (6 M urea, 2% SDS, 10% glycerol, 62.5 mM Tris-HCl (pH 6.8), 5% ß-mercaptoethanol and 5 mg/ml bromphenol blue). Samples were then sonicated with a fifteen second burst using a Fisher 550 Sonic dismembrator. Equal amounts of protein were heated at 65 °C for 10 min and separated by 10% SDS-PAGE. Separated proteins were transferred to Immobilon-P (Millipore Corp., Bedford, MA) membranes using a Multiphor II semi-dry electroblotting device (Pharmacia Biotech Inc., Piscataway, NJ) according to the manufacturer's instructions. Loading

equivalence and transfer efficiency were monitored by Ponceau S staining of transferred membranes. Standard western immunoblotting techniques were used to probe for various steady state protein levels as indicated and previously described (22, 28). Proteins of interest were visualized with ECL using the Super Signal chemiluminescence reagent (Pierce Chemical Co., Rockford, IL) at 20°C for 5 min. Membranes were exposed to X-ray film and developed. Gels shown represent results of experiments repeated at least three times.

Flow Cytometry. Flow cytometric analyses of breast cancer cell lines before and after ß-lap or TPT treatments were performed as previously described (22, 28).TUNEL assays were performed using the APO-DIRECT™ kit (Phoenix Flow Systems, Inc. San Diego, CA.). The samples were read in a EPICS Elite ESP flow cytometer using an air-cooled argon laser at 488 nm, 15 mW (Beckman Coulter Electronics, Miami, FL). Propidium iodide was read at 640 nm using a long pass optical filter and FITC was read at 525 nm using a band pass filter. Analyses were performed using the Elite acquisition software provided with the instrument.

Retroviral-Mediated Stable Expression of Caspase 3 in MCF-7:WS8 Cells. The pBabe/puro/cpp32 plasmid was constructed by treating the BamHI/PstI cpp32 cDNA insert from pBS/cpp32 plasmid (a generous gift from Dr. Vishva Dixit, Genentech Inc.) with T4 DNA polymerase and then subcloning into the blunt-ended pBabe/puro vector.

MCF-7:WS8 cells ($3x10^5$ cells/plate) were seeded and allowed to grow overnight. The pBabepuro retroviral vector (a generous gift from Dr. T. Sladek, Chicago Medical School) (2 µg/plate) either encoding cpp32 (caspase-3) cDNA, or empty vector were mixed with 10 µl of Lipofectamine

(Life Technologies, Gaithersburg, MD) and transfected into cells according to the manufacturer's instructions. After transfection (24 h), cells were split, diluted and inoculated into 96-well plates. Transfected cells were selected with 2 μg/ml puromycin. Individual clones were screened by immunoblot analysis of caspase 3 expression and positive clones (5 of 12) were pooled for further characterization. A single caspase-3 expressing clone was selected for investigation.

RESULTS

Relative Drug Sensitivities. Log-phase breast cancer cells were exposed to a range of ß-lap or TPT doses for 48 h and cell numbers were compared (using DNA content measurements) to untreated, log-phase growing control cells as described in "Experimental Procedures" (Fig. 1). MCF-7:WS8 cells were the most sensitive (IC_{75} = 3.5 μM) and MDA-MB-231 were the least sensitive (IC_{75} > 10 μM) to ß-lap, with MDA-MB-468 (IC_{75} = 4.0 μM) and T47D:A18 (IC_{75} = 7.0 μM) showing intermediate sensitivities. In contrast, MDA-MB-468 and T47D:A18 cells were the most sensitive to TPT with IC_{75} values of 0.5 μM. MCF-7:WS8 and MDA-MB-231 cells were the most resistant to TPT treatment with IC_{75}s values of 4.0 and 6.0 μM, respectively. Differences in relative sensitivities between breast cancer cells to TPT compared to ß-lap suggested disparate mechanism(s) of growth inhibition or cell death (possibly due to apoptosis).

Cell Cycle-Independent Cytotoxicity. Since Topo I poisons are thought to kill cycling, but not arrested cells (presumably due to DNA synthesis past Topo I-DNA "cleavable complexes"), we assessed the influence of cell cycle progression on ß-lap compared to TPT cytotoxicity using DNA content assays. These studies were restricted to the estrogen-dependent MCF-7:WS8 and T47D:A18 breast cancer cell lines, since their growth in estrogen-deprived, phenol red-free culture medium has been well defined (33). Cells were deprived of estrogen for 6 days, which caused a significant G_1 delay at a predetermined point in the cell cycle (33, 35, 36), prior to addition of either ß-lap or TPT. Cells were then exposed to gradient concentrations of ß-lap or TPT in estrogen deprived (control) medium, control medium containing E_2 (10 nM), medium containing whole serum

alone, or in the presence of inhibitory concentrations of the antiestrogens, 4-hydroxytamoxifen (4-OHT) or ICI 182,780 (ICI) for 48 h (Fig. 2). Both cell lines were stimulated to enter the cell cycle and begin log-phase growth after addition of medium containing 17ß-estradiol or whole serum. Addition of antiestrogens specifically inhibited estrogen-mediated cell growth. Estrogen deprivation and/or antiestrogen administration led to a cytostatic growth inhibition of 75-85% compared with cells grown in medium containing E_2 or whole serum (data not shown and (32, 37)). Additional ß-lap or TPT treatments led to a complete loss of cells, demonstrating a similar cytotoxic response in both log phase ($+E_2$) or arrested ($-E_2$ or plus antiestrogens) cells (Fig. 2).

Apoptotic Protease Activation After ß-Lap or TPT Treatment. To investigate caspase activation pathways in various breast cancer cells following TPT or ß-lap exposures, we examined PARP cleavage using western immunoblot analyses as described in 'Experimental Procedures'. Cells were treated continuously with 5 to 10 μM ß-lap and PARP cleavage was assessed 48 h later. Treatment with 5 μM ß-lap induced classic PARP cleavage, resulting in the appearance of an 89 kDa fragment in all breast cancer cells, except for MDA-MB-231 (Fig. 3). In MCF-7:WS8 cells, a cross-reacting protein of ~80 kDa (indicated by an "* " in Figs. 3, 4 and 5) was present even in untreated cells. The identity of this protein is unknown, however, it does appear to be degraded during apoptosis.

At higher doses of ß-lap we observed an "atypical" ~60 kDa PARP fragment. This "atypical" cleavage of PARP was most apparent in MCF-7:WS8 cells (Fig. 3, lanes 10-12), which were the most sensitive to ß-lap (Figs. 1 and 2). Like MCF-7:WS8, MDA-MB-468 cells demonstrated an

atypical PARP cleavage pattern after 6 μM or greater doses of ß-lap. In general, PARP cleavage reflected the relative sensitivity of each cell line to ß-lap, even though some cells demonstrated primarily the "atypical" cleavage pattern (e.g., MCF-7:WS8), whereas others (e.g. T47D:A18) predominantly showed typical caspase-mediated PARP cleavage. Interestingly, T47D:A18 cells demonstrated atypical PARP cleavage following treatment with 10 μM ß-lap (see lane 24, Fig. 3). A secondary PARP cleavage fragment of ~40 kDa was also observed in cells (e.g., MCF-7:WS8 and MDA-MB-468) which display maximal amounts of the 60 kDa PARP fragment (Fig. 3). It is currently unclear whether this is an unique fragment or the result of further cleavage of the original 60 kDa fragment. However, the steady state levels of the 40 kDa protein were lower than that of the 60 kDa polypeptide and peak levels of the ~40 kDa protein were apparent at times later than the first appearance and peak levels of the 60 kDa fragment. These data suggest that the ~40 kDa fragment is a byproduct of the original cleavage event which resulted in the formation of the 60 kDa PARP protein. Interestingly, the apparent amount of the 60 kDa fragment was much greater than full-length PARP protein. Loading equivalence, as assessed by Ponceau S staining, showed that all lanes contained equal amounts of protein. This apparent incongruity may be the result of either more efficient extraction of the fragment from the nuclear matrix, or increased accessibility of the epitope by antibody, after ß-lap induced cleavage. MDA-MB-231 cells did not show significant PARP cleavage at doses of ß-lap up to 10 μM, in direct correlation with drug sensitivity (Fig. 3).

Breast cancer cell lines were also treated with a range of TPT (10 nM to 10 μM) for 48 h. We also co-administered 25 μM zVAD-fmk, a caspase

inhibitor, to determine if PARP cleavage was caused by caspase activation after three doses of TPT (50, 500 and 5000 nM) (Fig. 4). As observed following ß-lap exposures, the relative sensitivity of breast cancer cells to the growth inhibitory effects of TPT was reflected to some degree in PARP cleavage (Fig. 4). However, the doses of TPT required to elicit PARP cleavage *in vivo* were significantly above the apparent IC_{50} values for each cell line (see Fig. 1); this was not the case for breast cancer cells exposed to ß-lap. These data are consistent with previous data demonstrating that ß-lap is a much more effective inducer of apoptosis than CPT, or its derivatives (20). In agreement with Fig. 1, MDA-MB-468 and T47D:A18 cells were the most sensitive to TPT, in terms of the formation of PARP cleavage fragments. Interestingly, MDA-MB-231 cells showed no PARP cleavage at any TPT dose tested, suggesting that these cells die, or are growth arrested, through a non-apoptotic mechanism. Co-administration of zVAD-fmk inhibited TPT-mediated PARP cleavage in MCF-7:WS8 (lanes 10-12), T47D:A18 (lanes 22 and 23 with 50 and 500 nM, but not 5000 nM TPT) and MDA-MB-468 (lane 22 with 50 nM but not with 500 or 5000 nM TPT) cells. These data suggested that TPT exposure led to the activation of the classic caspase pathway. For each cell line, higher doses of TPT could overcome the inhibition of PARP cleavage caused by co-administration of 25 μM zVAD. Importantly, no dose of TPT gave rise to the atypical PARP cleavage fragment, even when 10 μM TPT was used (lanes 9 and 21, Fig. 4).

Evidence For Two Apoptotic Proteolytic Pathways Activated By ß-Lap. In order to determine whether "atypical" PARP cleavage observed after ß-lap treatment was the result of an activated caspase family member, or another class of cysteine proteases, cells were exposed for 48 h to 8 μM ß-lap in the presence of a battery of known protease inhibitors (Fig. 5).

Included were general chemical inhibitors and more specific cleavage site inhibitors (38). Exposure of MCF-7:WS8 or MDA-MB-468 cells to 8 μM ß-lap caused apoptotic responses (measured by PARP, pRb and Sp1 cleavage) that were insensitive to any of the inhibitors, which were simultaneously administered at previously determined efficacious doses (38). The modest level of 89 kDa PARP cleavage fragment observed in untreated MCF-7:WS8 or MDA-MB-468 cells was due to slight overgrowth of control cells, which activated a basal level of apoptosis and classic PARP cleavage. This basal, caspase-mediated PARP cleavage was completely inhibited by zVAD-fmk in both cell lines (compare the minor 89 kDa PARP cleavage fragment in lane 1 to the absence of this fragment in lane 2 for MCF-7:WS8 in Fig. 5A). zVAD-fmk had similar effects on the low basal levels of apoptosis in MDA-MB-468 cells (Fig. 5B lanes 13 and 14).

As shown in Fig. 3, T47D:A18 cells exposed to 8 μM ß-lap for 48 h showed classic PARP cleavage. As expected, this apoptotic cleavage reaction was completely blocked by co-administration of zVAD-fmk at 25 μM. ß-Lap-treated T47D:A18 cells also showed cleavage of Sp1, giving rise to the previously described 68 kDa fragment (2). In addition, T47D:A18 treated with ß-lap, also resulted in the loss of phosphorylated pRb and the appearance of an ~100 kDa cleavage fragment, which was described by Janicke et al. (4) (compare lanes 13 and 19, Fig. 5A). All cleavage reactions observed in T47D:A18 cells after ß-lap treatment were completely prevented by 25 μM zVAD-fmk. However, accumulation of hypophosphorylated pRb in T47D:A18 cells following ß-lap treatment was unaffected by the administration of 25 μM zVAD (lanes 19 to 20, Fig. 5A). These data are consistent with the activation of a caspase-mediated apoptotic pathway in

T47D:A18 cells after ß-lap treatment, which may be unrelated to changes in pRb phosphorylation state.

MCF-7:WS8 and MDA-MB-468 cell lines, which showed only atypical PARP cleavage after 8 μM ß-lap exposure, also demonstrated an overall decline in Sp1 steady state levels. However, apoptotic cleavage fragments (observed with T47D:A18 cells) were not observed after extended exposures of the Western blots in Fig. 5 (not shown). pRb protein was not expressed in MDA-MB-468 cells due to a homozygous deletion of the pRb gene (39, 40). MCF-7:WS8 cells treated with ß-lap showed an overall loss of pRb, with a modest level of cleavage; a 60 kDa pRb fragment was noted, similar to that described by An and Dou (5). pRb cleavage in MCF-7:WS8 cells caused by ß-lap exposure was not affected by co-administered protease inhibitors (Fig. 5A, lanes 8-12). MDA-MB-231 cells, which were resistant to ß-lap exposure, showed no significant alteration in the steady state levels of PARP, pRb, or Sp1, consistent with their resistance to ß-lap-induced apoptosis and growth inhibition (Fig. 1).

To confirm that ß-lap cytotoxicity was primarily mediated by the induction of apoptosis and not necrosis, we utilized the TUNEL assay, which measures DNA breaks created by apoptotic endonucleases (41). MCF-7:WS8 cells were exposed to a 4 h pulse of 8 μM ß-lap and analyzed for terminal deoxynucleotide transferase-mediated incorporation of FITC-labeled dUTP, 20 h later. Greater than 90% of the ß-lap-treated MCF-7:WS8 cells were TUNEL positive (Fig 6). This finding, in addition to the dramatic nuclear condensation reported previously, (28) confirms that cytotoxicity caused by ß-lap is primarily apoptotic and not due to necrosis.

The global cysteine protease inhibitors, iodoacetamide and N-ethylmaleimide (7, 42, 43), were then used to determine if a cysteine protease

was responsible for the formation of atypical PARP cleavage fragments in MCF-7:WS8 cells (Figs. 3 and 5). MCF-7:WS8 cells were treated with 5 μM ß-lap in medium with or without 10 μM iodoacetamide or 10 μM N-ethylmaleimide (Fig. 7). Cleavage of PARP was prevented by both inhibitors, but was not inhibited by the caspase inhibitors, zVAD-fmk or DEVD-fmk, suggesting that a non-caspase, cysteine protease was primarily responsible for the atypical PARP cleavage observed after ß-lap treatment. Administration of N-ethylmaleimide caused a mobility shift of full length PARP band, possibly due to methylation of cysteine and methionine groups in the protein (42). Neither iodoacetamide nor N-ethylmaleimide prevented ß-lap mediated apoptosis in MCF-7:WS8 cells.

Simultaneous Cleavage of PARP and p53. The inhibition of PARP cleavage by the cysteine alkylating agents suggested that a non-caspase cysteine protease may be responsible for the atypical PARP cleavage observed in cells after treatment with ß-lap. One protease which may fit the data presented in Figs 1-6 could be the neutral calcium-dependent protease, calpain (9). Calpain has a wide substrate specificity and has been shown to specifically cleave p53 during apoptosis (44, 45). We previously noted a loss of basal p53 expression in MCF-7:WS8 cells after ß-lap treatment. We treated MCF-7:WS8 cells with a 4 h pulse of 5 μM ß-lap and isolated whole cell extracts at various times, up to 28 h after drug exposure. Extracts were probed for PARP and subsequently stripped and reprobed for p53 steady state expression. As expected, PARP cleavage was observed by 8 h after drug administration. Importantly, cleavage of p53, giving rise to an ~40 kDa fragment was concomitantly observed with PARP cleavage. This cleavage pattern resembles that observed by Pariat et. al (45) and Kubbutat et. al (44) which was the result of calpain activation.

Since calpain activity is dependent upon changes in Ca^{+2} homeostasis, we utilized the calcium chelators, EDTA and EGTA, to determine if removal of extracellular calcium influenced the appearance of atypical PARP cleavage in MCF-7:WS8 cells after ß-lap treatment. MCF-7:WS8 cells were pretreated with 0.25, 1.0 or 3.0 mM EGTA or EDTA in complete media for 30 minutes. After treatment, medium containing 8 μM ß-lap or DMSO (control medium), including the corresponding concentration of EDTA or EGTA used in the pre-treatment, was added for an additional 4 h. All cells were then treated with medium alone containing EGTA or EDTA for an additional 20 h. Whole cell extracts were then prepared and analyzed for PARP and p53 cleavage fragments. Both EDTA and EGTA showed a dose-dependent inhibition of ß-lap-mediated atypical PARP cleavage in MCF-7:WS8 cells (Fig. 8B). These data suggest that extracellular calcium is a necessary component for ß-lap-mediated atypical PARP cleavage, an attribute consistent with activation of a calcium-dependent, non-caspase cysteine protease, such as calpain.

Loss of Hypophosphorylated pRb and Apoptosis Induced by ß-Lap is Independent of Cell Cycle Status. To investigate the effects of cell cycle position on ß-lap-induced accumulation of hypophosphorylated pRb and apoptosis, estrogen-dependent MCF-7:WS8 cells were cultured in estrogen-free medium for six days as described in 'Experimental Procedures'. To ensure a complete estrogen block, the pure antiestrogen, ICI 182,780 (1 nM) (46, 47), was added to cells growing in estrogen-free medium two days prior to the beginning of each experiment. Increases in G_1 cells (up to 85%) were noted, as described (48). Arrested cells were compared to MCF-7:WS8 cells that were subsequently restimulated to enter the cell cycle by addition of 10 nM E_2 at the time of ß-lap or TPT exposure (i.e., a 4 h pulse of either 8 μM

ß-lap or 5 μM TPT). Drugs were administered as short pulse treatments in order to determine if the rapid accumulation of hypophosphorylated pRb could be reversed after removal of ß-lap or TPT. When used, ICI or E_2 was maintained in the medium.

MCF-7:WS8 cells treated with ß-lap showed a dramatic loss of phosphorylated pRb within 6 h (compare lanes 3 and 4, Fig. 9), followed by general loss of the protein by 18-30 h after treatment (see lanes 10, 13, 16 and 19, Fig. 9); these date are consistent with earlier findings (28). A similar loss of phosphorylated pRb was noted in MCF-7:WS8 cells after 5 μM TPT; however, significant accumulation of hypophosphorylated pRb was not observed until 12 h after treatment (not shown), and complete loss was not noted until 18 h posttreatment (Fig. 9). In control cells, stimulation of arrested cells with estradiol led to an increase in the relative level of hyperphosphorylated pRb [by 6 to 30 h] compared to estrogen-deprived and/or ICI-treated cells (compare hypophosphorylated retinoblastoma protein (pRb) to hyperphosphorylated retinoblastoma protein (pRb-pp) levels in lanes 6, 9 and 12 to lane 3, Fig. 9). The change in phosphorylation status of pRb was accompanied by a dramatic increase in the proportion of cells in S phase by 18 h after E_2 stimulation (43% S phase with E_2, 10% S phase without E_2, compare lanes 12 and 9, Fig. 9). The difference in phosphorylation status of pRb and the proportion of cells in S phase was less pronounced by 30 h, since E_2-stimulated MCF-7:WS8 cells became less synchronous. In both the E_2- and ICI-treated groups, ß-lap exposure led to a complete loss of hyperphosphorylated pRb followed by an overall loss of all forms of pRb. Since estrogen-deprivation can cause an arrest in the cell cycle ~6 h from the restriction point in MCF-7:WS8 cells (49-51), possibly past the first cyclin D1-cdk2-dependent phosphorylation of pRb, the levels

of hyperphosphorylated pRb in estrogen-deprived, antiestrogen-treated MCF-7:WS8 cells were rather high (Fig. 9). Estrogen-independent MDA-MB-231 cells, which showed no change in cell cycle distribution following estradiol or antiestrogen administration, also showed no change in pRb phosphorylation status after ß-lap treatment (data not shown). In MCF-7:WS8 cells treated with either ß-lap or TPT, PARP cleavage (atypical for ß-lap, classic for TPT) was not apparent until 12-18 h after treatment (Fig. 9 for 18 h, and data not shown). Addition of E_2, or maintenance of MCF-7:WS8 cells in estrogen-deprived medium (including ICI), had no effect on the appearance of PARP cleavage (see lanes 10, 13,16 and 19 Fig. 9).

To evaluate the ability of ß-lap to induce apoptosis in cells arrested in mitosis, we utilized the mitotic spindle inhibitor, nocodazole (52). Log-phase MCF-7:WS8 cells were pretreated with 150 ng/ml nocodazole for 18 h, which resulted in accumulation of >85% of cells in G_2/M, as measured by flow cytometry (data not shown). A 4 h pulse of ß-lap (5 μM) was then added to the nocodazole-blocked MCF-7:WS8 cells in fresh medium either with (N) or without nocodazole (N-C), which would allow cells to re-enter the cell cycle. Release of mitotically blocked cells led to a drop from 86% G_2/M to 48% G_2/M within 4 h. An additional group of log-phase cells (C) was also treated with ß-lap. A portion of the cells were harvested immediately (t=0) to establish baseline values for PARP cleavage and cell cycle distribution. Cells were also harvested 4 h posttreatment for Western immunoblot analyses (Fig. 10A, lanes 3-8). The remainder of the cells were fed with fresh medium containing nocodazole alone (lanes 11 &12) or with no drugs (lanes 9,10,13 &14) and harvested 20 h later for Western immunoblot analyses. Cells that were maintained in nocodazole remained arrested in mitosis. By the end of the experiment (20 h posttreatment), >90%

of the nocodazole-treated MCF-7:WS8 cells were arrested at G_2/M (data not shown).

G_2/M Arrested Cells Treated with ß-lap Carry Out Apoptosis and Atypical PARP Cleavage. Atypical PARP cleavage was not observed during the first 4 h after ß-lap treatment. By 24 h posttreatment, however, atypical PARP cleavage was observed in all ß-lap-treated cells, irrespective of nocodazole exposure. These data showed that cells arrested in mitosis were equally sensitive to apoptosis caused by ß-lap exposure, and were as sensitive as cells which were predominantly arrested in G_1 (Fig. 9). As observed with log-phase or G_1-arrested cells, mitotically blocked, ß-lap-treated MCF-7:WS8 cells showed a dramatic accumulation of hypophosphorylated pRb in 4 h after treatment. Loss of all forms of pRb was then noted 24 h posttreatment. Cells arrested in mitosis by nocodazole treatment or released into the cell cycle at the time of ß-lap exposure showed similar ß-lap-mediated accumulation of hypophosphorylated pRb, as demonstrated for log-phase cells treated with this drug (Fig. 9, lanes 3 and 4). Prolonged exposure to nocodazole (24 h) led to a small but measurable amount of apoptosis as indicated by the appearance of 89 kDa PARP and ~100 kDa pRb cleavage fragments (Fig. 10A, compare control cells in lane 9 to nocodazole-treated cells in lane 11). However, this basal level of apoptosis represented a minor proportion of MCF-7:WS8 cells compared to the near complete apoptotic responses and atypical PARP fragmentation seen after ß-lap treatment.

To further investigate the dephosphorylation of pRb after either ß-lap or TPT treatment, we utilized phosphorylation-specific pRb antibodies to probe cell lysates from nocodazole-arrested or log-phase MCF-7:WS8 cells. Cells were pretreated for 18 h with control medium or medium containing

150 ng/ml nocodazole, as above. Media were then replaced with control or nocodazole containing media, including either 5 μM ß-lap or 5 μM TPT for an additional 4 h. We first utilized a polyclonal antibody which reacted only with pRb species that were phosphorylated on serine 780 (53). This site is a substrate for phosphorylation by the cyclin D1/Cdk4 complex, which is activated early in cell cycle progression from G_0 to G_1 (53). Nocodazole treatment alone had little effect on the level of pRb phosphorylated at this site (Fig. 10B). However, ß-lap or TPT treatments alone led to losses of this form of pRb in 4 h, regardless of whether log-phase or mitotically-arrested cells were examined (see Phos pRb signal, Fig. 10B). In order to demonstrate that this result was not simply due to a loss of pRb protein, we utilized a second phosphorylation-specific pRb antibody (clone G99-549), which recognized only hypophosphorylated forms of pRb (54). As shown in Fig. 10B, the signal generated from this antibody (UnPhos pRb) was inversely proportional to the signal generated by the antibody recognizing phosphorylated pRb. These results suggest that during early times (up to 4 h) after ß-lap or TPT exposure there was an accumulation of hypophosphorylated pRb at the expense of hyperphosphorylated pRb.

We (16), as well as others (55), showed that MCF-7:WS8 cells were devoid of caspase-3, due to a deletion in exon 3. To determine whether caspase-3 deficiency was responsible for atypical PARP cleavage, we isolated an MCF-7:WS8 clone that stably expressed full-length pro-form caspase-3 (Casp 3) (see Experimental Procedures). A puromycin resistant clone expressing empty vector (pbabe) was also analyzed. PARP, lamin B and caspase-3 expression were monitored before or 24 h after ß-lap treatment (2-10 μM). Cells were treated for 4 h with 2-10 μM ß-lap and harvested 20 h later. As expected, Casp 3 cells expressed the 32 kDa pro-

form of caspase-3, unlike MCF-7:WS8 cells transfected with the vector alone (compare lanes 1 and 7). Atypical PARP cleavage was noted following ß-lap treatment at similar levels in both transfected cell lines. Classic lamin B cleavage, presumably the result of caspase-6 activation (56, 57), was also observed. These data suggest that expression of caspase-3 had no effect on apoptotic cleavage events in MCF-7:WS8 cells following various doses of ß-lap. Interestingly, loss of pro-caspase-3 protein, in Casp3 cells, mirrored cleavage of both PARP and lamin B. Importantly, the active p12 and p20 fragments of caspase-3 were not observed due to the lower affinity of this antibody to the processed forms of caspase-3. In contrast to ß-lap treatments, Casp 3 cells showed an increased rate of apoptosis after exposure to TNF-α or Granzyme B compared to MCF-7:WS8 cells transfected with pbabe/puro alone (16).

DISCUSSION

We previously showed that ß-lap killed a variety of cells by apoptosis. However, the mechanisms of specific proteolytic execution cascades that were activated by this compound remained unexplored. ß-Lap induced apoptosis independently of p53 status and treated cells showed little changes in cell cycle distribution (22, 28). In MCF-7:WS8 cells, the lethal effects of ß-lap were accounted for solely by apoptosis. In this study, we expanded our investigations to include a battery of breast cancer cell lines which have significant phenotypic and genotypic differences (Table 1). Using this array of cell lines, we demonstrated that ß-lap-mediated apoptosis did not require functional ER or pRb and we confirmed that cell death was not dependent on wild type p53.

Our previous studies could not discern a G_1/S phase-specific apoptotic mechanism which appeared to be induced following ß-lap exposure. We utilized the estrogen-dependent G_1 arrest characteristics of MCF-7:WS8 and T47D:A18 cells (~80% growth inhibition in E_2-deprived, compared to log-phase cells) to show that both cell lines were equally sensitive to ß-lap or TPT, irrespective of their progression through the cell cycle (Fig. 2). When arrested cells were treated with either ß-lap or TPT, the relative cytotoxicity was identical to log-phase cells. This result, especially with TPT, is in apparent conflict with the current paradigm for the mechanism of action of Topo I poisons, which suggested that the primary lethal event was the creation of DNA double strand breaks following movement of the replication fork through the "cleavable complex". This mechanism has been used to describe the S-phase specific killing of cancer cells by TPT. Morris

and Geller (58) also showed that CPT could induce apoptosis in postmitotic rat cortical neurons. Our data indicate that DNA synthesis may not be required for lethality or the stimulation of apoptosis in G_1-arrested breast cancer cells by high dose TPT. These data suggest that DNA-Topo I lesions caused by high dose TPT treatment may activate a nuclear signal (possibly originating from inhibited transcription) that triggers pRb dephosphorylation (see below) and downstream apoptotic reactions. Taken together, these results demonstrate that while actively growing cells may be killed more efficiently in some systems, arrested cells may also be sensitive to the toxic (i.e., apoptotic) effects of Topo I poisons. In comparison with ß-lap, CPT was a less effective inducer of apoptosis; stimulating apoptotic reactions only at concentrations 20- to 100-fold over its IC_{50}. ß-Lap killed cells by apoptosis at concentrations near its IC_{50} , as previously reported (28).

TPT-Induced Caspase Pathways- The initiation pathways leading to caspase activation following treatment with cytotoxic agents, such as the Topo I poisons, are not well understood. While certain aspects of the death pathway are common among many agents, such as loss of mitochondrial membrane potential and release of cytochrome c from the mitochondrial membrane, the upstream activators of these processes are not well characterized. Additionally, the relative expression of caspase family members varies in a cell type-dependent manner. For example, MCF-7:WS8 cells do not express measurable caspases-3 or -10a ((59), Fig. 11 and data not shown). The lack of the initiator caspase-10a may not significantly influence apoptosis following Topo I poisons due to redundancy in the initiation pathway within the cell. However, the lack of a key executioner, such as caspase-3, may adversely affect apoptotic proteolysis. Interestingly,

MCF-7:WS8 cells treated with TPT showed a similar level of apoptosis (by morphology changes) and classic PARP cleavage as T47D:A18 and MDA-MB-468 cells (which both express caspase 3). The apoptotic cleavage reactions in all breast cancer cell lines induced by TPT were blocked by addition of caspase inhibitors, zVAD-fmk or DEVD-fmk. These data suggest that TPT treatment leads to the initiation of the well described caspase pathway that culminates in the activation of caspases-3 and/or -7. Since classic PARP cleavage in caspase-3-deficient MCF-7:WS8 cells occurred after TPT treatment, we suggest that caspase-7 was activated. This is also supported by the fact that introduction of caspase-3 into MCF-7:WS8 cells did not influence the lethality or apoptotic responses caused by TPT. Therefore, our data suggest that TPT can stimulate a direct caspase-7 mediated death pathway in breast cancer cells.

ß-Lap Induces a Novel Apoptotic Protease. Exposure to ß-lap gave rise to an unique pattern of proteolysis. At lower doses, ß-lap treatment caused classic PARP cleavage in all cell lines, except MDA-MB-231. At higher doses, an ~60 kDa "atypical" PARP fragment was observed. The dose range over which this novel fragment appeared was quite sharp and correlated well with the notably sharp growth inhibition responses noted in Figs. 1 and 2 and previously described cytotoxicity (28). Atypical PARP fragmentation was not simply the result of supralethal drug exposure, since cells treated with TPT at doses 200-fold greater than the IC_{50} of the drug did not show the same atypical cleavage pattern. Doses of ß-lap necessary to induce atypical PARP cleavage were generally less than 5-fold over the IC_{50} for ß-lap, depending upon the cell line examined and the method of treatment (i.e. continuous exposure or 4 h pulse). The lack of observable atypical PARP

cleavage at the IC_{50} dose is likely due to a relatively modest, but constant loss of cells through apoptosis that does not result in the accumulation of enough cells containing cleaved PARP to be observed in Western analyses.

Previous reports have shown cleavage of PARP during necrosis, giving rise to a 50 kDa fragment (60). However, the atypical PARP fragment observed in ß-lap treated cells was ~60 kDa (Fig. 4). The demonstration of nuclear condensation, appearance of sub-G_0/G_1 cells (28), >90% TUNEL positive cells (Fig. 6) and inhibition of apoptosis by EDTA and EGTA (Fig. 8B) leaves little doubt that this response was apoptotic. Interestingly, in ß-lap-treated cells, we have noted some unique characteristics that do not fit the "classic" definition of apoptosis. Further study of the action of this novel apoptosis-inducing agent may allow for elucidation of cell death processes which contain characteristics of apoptotic as well as necrotic proteolytic cascades. This agent may induce a heretofore uncharacterized apoptotic pathway that may be exploited for improved treatment of breast cancer. For example, this agent may be useful for treatment of breast cancer which has lost classic caspase-mediated apoptotic responses.

Atypical PARP cleavage observed in MCF-7:WS8 and MDA-MB-468 cells was not likely the result of caspase, Granzyme B, Cathepsins B or L, trypsin or chymotrypsin-like proteases, (see Fig. 5) (38). However, the classic cleavage pattern observed in T47D:A18 cells after low level ß-lap exposures was prevented by 25 µM zVAD-fmk, a general caspase inhibitor. Classic PARP cleavage induced by low dose ß-lap exposure was unaffected by other protease inhibitors, suggesting that a member of the caspase family (probably caspase 7) was responsible for apoptotic proteolysis in T47D:A18 cells. At higher doses of ß-lap, T47D:A18 cells responded like MCF-7:WS8 cells, undergoing apoptosis and atypical PARP cleavage. Lack of inhibition

of atypical PARP cleavage by zVAD-fmk in MCF-7:WS8 cells treated with ß-lap, strongly suggests that activation of the caspase pathway was not necessary for atypical PARP cleavage.

In ß-lap-treated MCF-7:WS8 cells, atypical PARP fragmentation was blocked by iodoacetamide or N-ethylmaleimide, both cysteine alkylating agents (Fig. 7). Additionally, atypical PARP cleavage was not inhibited by a battery of inhibitors (Fig. 5), each used at previously determined effective doses. These data suggest that atypical fragmentation of PARP *in vivo* was due to the activation of a cysteine protease which is apparently not a member of the caspase family of proteases. However, the non-specific reactivity of iodoacetamide and N-ethylmaleimide does allow the possibility that the unknown protease may be indirectly activated after ß-lap treatment by a factor which contains critical –SH groups. One protease which fits the available data could be the neutral calcium-dependent protease, calpain. This possibility is further supported by the fact that p53 was cleaved in ß-lap-treated MCF-7:WS8 cells, giving rise to fragments (Fig. 8A) which match those previously described as being the result of calpain activity (44, 45). Furthermore, the time course of p53 cleavage was concomitant with the appearance of atypically cleaved PARP. Additionally, we provide evidence showing that the apparent cysteine protease is Ca^{+2} dependent, since it's activity (as measured by atypical PARP or p53 cleavage) was prevented by co-administration of EDTA or EGTA (Fig 8B and data not shown). While these findings do not conclusively prove that calpain is responsible for this cleavage, they are suggestive. Our laboratory is currently in the process of definitively identifying the protease responsible for this cleavage of PARP.

Cleavage of Sp1 and pRb by the Novel Apoptotic Protease. ß-Lap treatment led to an overall decrease in Sp1 protein level in MCF-7:WS8

and MDA-MB-468 cells, however, no distinct cleavage fragments were observed. In contrast, ß-lap-treated T47D:A18 cells clearly showed a ~68 kDa Sp1 cleavage fragment as described (2) This Sp1 cleavage which was prevented by zVAD-fmk, suggesting caspase activation. These data suggest that the protease activated in ß-lap-treated MCF-7:WS8 or MDA-MB-468 cells caused a novel form of Sp1 proteolysis that does not result in the accumulation of fragments (such as the ~68 kDa fragment observed in the T47D:A18 cell lysate) recognized by the Sp1 antibody. Chronic low-dose ß-lap exposure can activate a novel caspase-independent apoptotic proteolytic cascade in MCF-7:WS8 and MDA-MB-468 cells. The same pathway can be activated in T47D:A18 cells at higher doses of ß-lap. This protease is present in many breast cancer cells, with the possible exception of the MDA-MB-231 cells, which showed no atypical PARP cleavage at any dose of ß-lap. It is important to note that the caspase-mediated apoptotic pathway can also be activated following ß-lap exposure in a cell line and dose-dependent manner.

The loss of hyperphosphorylated pRb was one of the earliest detectable *in vivo* changes after ß-lap exposure (Figs 9 & 10, ref (22, 28)). pRb is a critical cell cycle regulator whose activity is primarily controlled by specific phosphorylation events (20). Using phosphorylation-specific antibodies, we demonstrated a complete loss of phosphorylated forms of pRb by 4 h in ß-lap-treated MCF-7:WS8 cells (see Fig. 10B). Accumulation of hypophosphorylated pRb after ß-lap treatment was observed regardless of cell cycle status (i.e. estrogen-deprived G_1 arrest, or nocodazole-mediated G_2/M arrest) at the time of drug exposure and accumulation of cells in G_1 was not observed (28). Rather, the dramatic alteration in pRb status after ß-lap exposure appears to explain how this drug can halt cells in any phase of

the cell cycle and elicits an apoptotic response, a mechanism previously proposed by our laboratory (28).

The loss of pRb in MCF-7:WS8 cells at >10 h following ß-lap exposure was very dramatic and differed greatly from the pattern observed in T47D:A18 cells. Dephosphorylation of pRb in ß-lap-treated T47D:A18 cells was unaffected by administration of the caspase inhibitor, zVAD-fmk. However, caspase-mediated c-terminal cleavage of pRb (4) was observed and was blocked by zVAD-fmk. In MCF-7:WS8 cells, protease inhibitors had no effect on the loss of pRb, consistent with the lack of inhibition of atypical PARP cleavage. Extended exposure of the blots shown in Fig. 5 revealed minor ~40 and 60 kDa cleavage fragments (data not shown), which were consistent with those described by An et al. (5).

Neither ß-lap nor TPT appeared to kill breast cancer cells in a cell cycle regulated fashion, as suggested by studies using nocodazole, a microtubule poison. Atypical PARP cleavage occurred simultaneously with the overall loss of pRb, in nocodazole-treated cells. Experiments with TPT showed a more modest dephosphorylation of pRb which was followed by the activation of the classic caspase-mediated pathway.

The use of caspase-3 expressing MCF-7:WS8 cells demonstrated that re-expression of caspase-3 did not lead to enhanced apoptosis or appearance of the caspase-mediated 89 kDa PARP fragmentation after ß-lap exposure. In contrast, other studies have demonstrated enhanced apoptotic reactions in caspase-3 expressing MCF-7:WS8 cells after Granzyme B or TNF-α treatments, compared to cells infected with the empty vector (16).

While ß-lap treatment of MCF-7:WS8 cells appeared to activate a novel apoptotic pathway, classic lamin B cleavage, (primarily due to the activation of caspase-6) was also observed ((28, 56) & Fig. 11). While

caspase-6 is thought to be activated directly by caspase-3 (61, 62), our data suggest that either a distinct upstream protease can activate caspase-6 after ß-lap treatment, or that an unknown, ß-lap activated protease can directly cleave lamin B, giving rise to fragments of similar size to those observed after caspase 6 cleavage. Our data suggest that once the apoptotic protease is activated, it dominates proteolysis in ß-lap-treated MCF-7:WS8 cells, since visible classic PARP cleavage fragments were not observed. Interestingly, overexpression of caspase-3 in MCF-7:WS8 cells did not affect ß-lap cytotoxicity, while increasing sensitivity to granzyme B or TNF-α (16).

Our studies demonstrate that ß-lap can induce at least two independent apoptotic pathways in breast cancer cells. The apoptotic response seems to be independent of the reported *in vitro* poisoning of Topo IIα by ß-lap (29), since G_1 arrested cells (which contain very low Topo IIα enzyme activity) were as effectively killed by ß-lap as log-phase or G_2/M arrested cells (which express high levels of Topo IIα enzyme activity). Furthermore, the *in vivo* pathway activated by ß-lap leading to apoptosis may also be independent of the Topo I inhibition observed *in vitro*. In some cells, ß-lap mediates typical caspase activation, leading to the formation of the classic 89 kDa PARP cleavage fragment *in vivo* (63). In other cells (specifically, MCF-7:WS8), ß-lap activates a novel calcium-dependent, non-caspase cysteine protease. Interestingly, activation of this novel pathway of apoptosis (which may also result in mid-protein cleavage of pRb) eventually occurred in all breast cancer cells, except the inherently resistant MDA-MB-231 cells. Our data suggest that activation of this protease may explain the two pRb cleavage fragments previously described. In T47D:A18 cells, low dose ß-lap can induce C-terminal pRb cleavage, but at higher doses ß-lap causes the

activation of calpain, which appears to cleave pRb resulting in the generation of an unstable polypeptide. An interesting profile of sensitivity of breast cancer cells to ß-lap was observed. Sensitivity to this agent was very different from the cytotoxic responses observed following TPT treatment. The reasons for the resistance of MDA-MB-231 cells to most apoptotic inducing agents remain unknown, but are being explored by our laboratory. In MCF-7:WS8 cells, the primary proteolytic events, which correlate directly with apoptosis induction and loss of survival, appear to be the result of this novel calcium-dependent non-caspase protease. Activation of this protease was not affected by inhibitors of a variety of proteases, most importantly the caspase inhibitors zVAD-fmk and DEVD-fmk. We hypothesize that this calcium-dependent, non-caspase cysteine protease is calpain. When this protease is activated, its novel apoptotic pathway may be a specific target for manipulation in the clinical treatment of breast cancer.

References:

1. Alnemri, E. S., Livingston, D. J., Nicholson, D. W., Salvesen, G., Thornberry, N. A., Wong, W. W., and Yuan, J. Y. (1996). Human Ice/Ced-3 Protease Nomenclature. *Cell*, **87:** 171

2. Piedrafita, F. J., and Pfahl, M. (1997). Retinoid-induced apoptosis and Sp1 cleavage occur independently of transcription and require caspase activation. *Mol. Cell. Biol.*, **17:** 6348-58

3. Patel, T., Gores, G. J., and Kaufmann, S. H. (1996). The role of proteases during apoptosis. *FASEB J.* , **10:** 587-597

4. Janicke, R. U., Walker, P. A., Lin, X. Y., and Porter, A. G. (1996). Specific cleavage of the retinoblastoma protein by an ICE-like protease in apoptosis. *EMBO J.* , **15:** 6969-78

5. An, B., and Dou, Q. P. (1996). Cleavage of retinoblastoma protein during apoptosis: an interleukin 1 beta-converting enzyme-like protease as candidate. *Cancer Res.*, **56:** 438-42

6. Talanian, R. V., Quinlan, C., Trautz, S., Hackett, M. C., Mankovich, J. A., Banach, D., Ghayur, T., Brady, K. D., and Wong, W. W. (1997). Substrate specificities of caspase family proteases. *J. Biol. Chem.*, **272:** 9677-82

7. Kaufmann, S. H., Desnoyers, S., Ottaviano, Y., Davidson, N. E., and Poirier, G. G. (1993). Specific proteolytic cleavage of poly(ADP-ribose) polymerase: an early marker of chemotherapy-induced apoptosis. *Cancer Res.*, **53:** 3976-85

8. Wang, X., Pai, J. T., Wiedenfeld, E. A., Medina, J. C., Slaughter, C. A., Goldstein, J. L., and Brown, M. S. (1995). Purification of an interleukin-1 beta converting enzyme-related cysteine protease that cleaves sterol regulatory element-binding proteins between the leucine zipper and transmembrane domains. *J. Biol. Chem.*, **270:** 18044-50

9. Squier, M. K., Miller, A. C., Malkinson, A. M., and Cohen, J. J. (1994). Calpain activation in apoptosis. *J Cell Physiol*, **159:** 229-37

10. Wood, D. E., Thomas, A., Devi, L. A., Berman, Y., Beavis, R. C., Reed, J. C., and Newcomb, E. W. (1998). Bax cleavage is mediated by calpain during drug-induced apoptosis. *Oncogene*, **17:** 1069-78

11. Porn-Ares, M. I., Samali, A., and Orrenius, S. (1998). Cleavage of the calpain inhibitor, calpastatin, during apoptosis. *Cell Death. Differ.*, **5:** 1028-33

12. Chandra, J., Niemer, I., Gilbreath, J., Kliche, K. O., Andreeff, M., Freireich, E. J., Keating, M., and McConkey, D. J. (1998). Proteasome inhibitors induce apoptosis in glucocorticoid-resistant chronic lymphocytic leukemic lymphocytes. *Blood*, **92:** 4220-9

13. McConkey, D. J. (1996). Calcium-dependent, interleukin 1-converting enzyme inhibitor- insensitive degradation of lamin B1 and DNA fragmentation in isolated thymocyte nuclei. *J. Biol. Chem.*, **271:** 22398-406

14. Shimizu, T., and Pommier, Y. (1997). Camptothecin-induced apoptosis in p53-null human leukemia HL60 cells and their isolated nuclei: effects of the protease inhibitors Z-VAD-fmk and dichloroisocoumarin suggest an involvement of both caspases and serine proteases. *Leukemia*, **11:** 1238-44

15. Marthinuss, J., Andrade-Gordon, P., and Seiberg, M. (1995). A secreted serine protease can induce apoptosis in Pam212 keratinocytes. *Cell Growth Differ.*, **6:** 807-16

16. Yang, X., Stennicke, H. R., Wang, B., Green, D. R., Janicke, R. U., Srinivasan, A., Seth, P., Salvesen, G. S., and Froelich, C. J. (1998). Granzyme B mimics apical caspases. Description of a unified pathway for trans-activation of executioner caspase-3 and -7. *J. Biol. Chem.*, **273:** 34278-83

17. Morana, S. J., Wolf, C. M., Li, J., Reynolds, J. E., Brown, M. K., and Eastman, A. (1996). The involvement of protein phosphatases in the activation of ICE/CED-3 protease, intracellular acidification, DNA digestion, and apoptosis. *J. Biol. Chem.*, **271:** 18263-71

18. Wolf, C. M., Reynolds, J. E., Morana, S. J., and Eastman, A. (1997). The temporal relationship between protein phosphatase, ICE/CED-3 proteases, intracellular acidification, and DNA fragmentation in apoptosis. *Exp. Cell Res.* , **230:** 22-7

19. An, B., Dineley, K. E., Zhang, L. L., Termin, T. A., Meijer, L., and Dou, Q. P. (1997). Involvement of Rb kinases and phosphatases in life and death decisions. *Oncol. Rep.*, **4:** 1129-1134

20. Weinberg, R. A. (1995). The retinoblastoma protein and cell cycle control. *Cell*, **81:** 323-30

21. Boothman, D. A., Trask, D. K., and Pardee, A. B. (1989). Inhibition of potentially lethal DNA damage repair in human tumor cells by beta-lapachone, an activator of topoisomerase I. *Cancer Res.*, **49:** 605-12

22. Planchon, S. M., Wuerzberger, S., Frydman, B., Witiak, D. T., Hutson, P., Church, D. R., Wilding, G., and Boothman, D. A. (1995). Beta-lapachone-

mediated apoptosis in human promyelocytic leukemia (HL-60) and human prostate cancer cells: a p53-independent response. *Cancer Res.*, **55:** 3706-11

23. Boothman, D. A., Wang, M., Schea, R. A., Burrows, H. L., Strickfaden, S., and Owens, J. K. (1992). Posttreatment exposure to camptothecin enhances the lethal effects of x-rays on radioresistant human malignant melanoma cells. *Int. J. Radiat. Oncol. Biol. Phys.*, **24:** 939-48

24. Li, C. J., Averboukh, L., and Pardee, A. B. (1993). beta-Lapachone, a novel DNA topoisomerase I inhibitor with a mode of action different from camptothecin. *J. Biol. Chem.*, **268:** 22463-8

25. Boothman, D. A., and Pardee, A. B. (1989). Inhibition of radiation-induced neoplastic transformation by beta-lapachone. *Proc. Natl. Acad. Sci. USA*, **86:** 4963-7

26. Nelson, W. G., and Kastan, M. B. (1994). DNA strand breaks: the DNA template alterations that trigger p53-dependent DNA damage response pathways. *Mol. Cell. Biol.*, **14:** 1815-23

27. Boothman, D. A. (1994). Enhanced malignant transformation is accompanied by increased survival recovery after ionizing radiation in Chinese hamster embryo fibroblasts. *Radiat. Res.*, **138:** S121-5

28. Wuerzberger, S. M., Pink, J. J., Planchon, S. M., Byers, K. L., Bornmann, W. G., and Boothman, D. A. (1998). Induction of apoptosis in MCF-7:WS8 breast cancer cells by beta- lapachone. *Cancer Res*, **58:** 1876-85

29. Frydman, B., Marton, L. J., Sun, J. S., Neder, K., Witiak, D. T., Liu, A. A., Wang, H. M., Mao, Y., Wu, H. Y., Sanders, M. M., and Liu, L. F. (1997). Induction of DNA topoisomerase II-mediated DNA cleavage by beta- lapachone and related naphthoquinones. *Cancer Res*, **57:** 620-7

30. Lamond, J. P., Wang, M., Kinsella, T. J., and Boothman, D. A. (1996). Radiation lethality enhancement with 9-aminocamptothecin: comparison to other topoisomerase I inhibitors. *Int. J. Radiat. Oncol. Biol. Phys.*, **36:** 369-76

31. Pink, J. J., Bilimoria, M. M., Assikis, J., and Jordan, V. C. (1996). Irreversible loss of the oestrogen receptor in T47D breast cancer cells following prolonged oestrogen deprivation. *Br. J. Cancer*, **74:** 1227-36

32. Pink, J. J., Jiang, S. Y., Fritsch, M., and Jordan, V. C. (1995). An estrogen-independent MCF-7 breast cancer cell line which contains a novel 80-kilodalton estrogen receptor-related protein. *Cancer Res.*, **55:** 2583-90

33. Pink, J. J., and Jordan, V. C. (1996). Models of estrogen receptor regulation by estrogens and antiestrogens in breast cancer cell lines. *Cancer Res.*, **56:** 2321-30

34. Labarca, C., and Paigen, K. (1980). A simple, rapid, and sensitive DNA assay procedure. *Anal. Biochem.*, **102:** 344-52

35. Musgrove, E. A., and Sutherland, R. L. (1993). Acute effects of growth factors on T-47D breast cancer cell cycle progression. *Eur. J. Cancer* , **29A:** 2273-9

36. Musgrove, E. A., and Sutherland, R. L. (1991). Steroids, growth factors, and cell cycle controls in breast cancer. *Cancer Treat. Res.*, **53:** 305-31

37. Pink, J. J., Fritsch, M., Bilimoria, M. M., Assikis, V. J., and Jordan, V. C. (1997). Cloning and characterization of a 77-kDa oestrogen receptor isolated from a human breast cancer cell line. *Br. J. Cancer*, **75:** 17-27

38. Lotem, J., and Sachs, L. (1996). Differential suppression by protease inhibitors and cytokines of apoptosis induced by wild-type p53 and cytotoxic agents. *Proc. Natl. Acad. Sci. USA*, **93:** 12507-12512

39. T'Ang, A., Varley, J. M., Chakraborty, S., Murphree, A. L., and Fung, Y. K. (1988). Structural rearrangement of the retinoblastoma gene in human breast carcinoma. *Science*, **242:** 263-6

40. Lee, E. Y., To, H., Shew, J. Y., Bookstein, R., Scully, P., and Lee, W. H. (1988). Inactivation of the retinoblastoma susceptibility gene in human breast cancers. *Science*, **241:** 218-21

41. Li, X., Traganos, F., Melamed, M. R., and Darzynkiewicz, Z. (1995). Single-step procedure for labeling DNA strand breaks with fluorescein- or BODIPY-conjugated deoxynucleotides: detection of apoptosis and bromodeoxyuridine incorporation. *Cytometry*, **20:** 172-80

42. Zollner, H. (1993). Handbook of enzyme inhibitors. , pp. 728-730: VCH Publishers,

43. Waxman, L. (1981). Calcium-activated proteases in mammalian tissues. *Methods Enzymol.*, **80:** 664-80

44. Kubbutat, M. H., and Vousden, K. H. (1997). Proteolytic cleavage of human p53 by calpain: a potential regulator of protein stability. *Mol. Cell. Biol.*, **17:** 460-8

45. Pariat, M., Carillo, S., Molinari, M., Salvat, C., Debussche, L., Bracco, L., Milner, J., and Piechaczyk, M. (1997). Proteolysis by calpains: a possible contribution to degradation of p53. *Mol. Cell. Biol.*, **17:** 2806-15

46. Wakeling, A. E., and Bowler, J. (1992). ICI 182,780, a new antioestrogen with clinical potential. [Review]. *J. Steroid Biochem. Mol. Biol.* , **43:** 173-7

47. Pink, J. J., and Jordan, V. C. (1995). Molecular mechanisms of antiestrogen resistance. *In:* R. B. Dickson and M. E. Lippman (eds.), Drug and Hormonal Resistance in Breast Cancer: Cellular and Molecular Mechanisms. Hemel Hempstead, Great Britain: Ellis Horwood,

48. Musgrove, E. A., Sarcevic, B., and Sutherland, R. L. (1996). Inducible expression of cyclin D1 in T-47D human breast cancer cells is sufficient for Cdk2 activation and pRB hyperphosphorylation. *J. Cell. Biochem.*, **60:** 363-78

49. Musgrove, E. A., and Sutherland, R. L. (1994). Cell cycle control by steroid hormones. *Semin. Cancer Biol.*, **5:** 381-9

50. Musgrove, E. A., Wakeling, A. E., and Sutherland, R. L. (1989). Points of action of estrogen antagonists and a calmodulin antagonist within the MCF-7 human breast cancer cell cycle. *Cancer Res.*, **49:** 2398-404

51. Foster, J. S., and Wimalasena, J. (1996). Estrogen regulates activity of cyclin-dependent kinases and retinoblastoma protein phosphorylation in breast cancer cells. *Mol. Endocrinol.*, **10:** 488-98

52. Gorbsky, G. J. (1997). Cell cycle checkpoints: arresting progress in mitosis. *Bioessays*, **19:** 193-7

53. Kitagawa, M., Higashi, H., Jung, H. K., Suzuki-Takahashi, I., Ikeda, M., Tamai, K., Kato, J., Segawa, K., Yoshida, E., Nishimura, S., and Taya, Y. (1996). The consensus motif for phosphorylation by cyclin D1-Cdk4 is different from that for phosphorylation by cyclin A/E-Cdk2. *EMBO J.* , **15:** 7060-9

54. Dunaief, J. L., Strober, B. E., Guha, S., Khavari, P. A., Alin, K., Luban, J., Begemann, M., Crabtree, G. R., and Goff, S. P. (1994). The retinoblastoma protein and BRG1 form a complex and cooperate to induce cell cycle arrest. *Cell*, **79:** 119-30

55. Li, F., Srinivasan, A., Wang, Y., Armstrong, R. C., Tomaselli, K. J., and Fritz, L. C. (1997). Cell-specific induction of apoptosis by microinjection of cytochrome c. Bcl-xL has activity independent of cytochrome c release. *J. Biol. Chem.*, **272:** 30299-305

56. Orth, K., Chinnaiyan, A. M., Garg, M., Froelich, C. J., and Dixit, V. M. (1996). The CED-3/ICE-like protease Mch2 is activated during apoptosis and cleaves the death substrate lamin A. *J. Biol. Chem.*, **271:** 16443-6

57. Takahashi, A., Alnemri, E. S., Lazebnik, Y. A., Fernandes-Alnemri, T., Litwack, G., Moir, R. D., Goldman, R. D., Poirier, G. G., Kaufmann, S. H., and Earnshaw, W. C. (1996). Cleavage of lamin A by Mch2 alpha but not CPP32: multiple interleukin 1 beta-converting enzyme-related proteases with distinct substrate recognition properties are active in apoptosis. *Proc. Natl. Acad. Sci. USA*, **93:** 8395-400

58. Morris, E. J., and Geller, H. M. (1996). Induction of neuronal apoptosis by camptothecin, an inhibitor of DNA topoisomerase-I: evidence for cell cycle-independent toxicity. *J. Cell Biol.*, **134:** 757-70

59. Janicke, R. U., Ng, P., Sprengart, M. L., and Porter, A. G. (1998). Caspase-3 is required for alpha-fodrin cleavage but dispensable for cleavage of other death substrates in apoptosis. *J. Biol. Chem.*, **273:** 15540-5

60. Shah, G. M., Shah, R. G., and Poirier, G. G. (1996). Different cleavage pattern for poly(ADP-ribose) polymerase during necrosis and apoptosis in HL-60 cells. *Biochem Biophys Res Commun*, **229:** 838-44

61. Faleiro, L., Kobayashi, R., Fearnhead, H., and Lazebnik, Y. (1997). Multiple species of CPP32 and Mch2 are the major active caspases present in apoptotic cells. *EMBO J.* , **16:** 2271-81

62. Hirata, H., Takahashi, A., Kobayashi, S., Yonehara, S., Sawai, H., Okazaki, T., Yamamoto, K., and Sasada, M. (1998). Caspases are activated in a branched protease cascade and control distinct downstream processes in Fas-induced apoptosis. *J. Exp. Med.*, **187:** 587-600

63. Planchon, S. M., Wuerzberger-Davis, S. M., Pink, J. J., Robertson, K. A., Bornmann, W. G., and Boothman, D. A. (1999). Bcl-2 protects against ß-lapachone-mediated caspase 3 activation and apoptosis in human myeloid leukemia (HL-60) cells. *Oncol Rep*, **6:** 485-492

ACKNOWLEDGMENTS

Funding for this work was provided to us by a grant from the United States Army Medical Research and Materiel Command Breast Cancer Initiative (#DAMD17-98-1-8260 to D.A.B.) and by a Post-doctoral fellowship from the US Army (# DAMD17-97-1-7221 to J.J.P.). We thank Dr. V. Craig Jordan for supplying us with the breast cancer cell lines and the antiestrogen ICI 182,780 and Dr. Vishva Dixit for the caspase 3 cDNA. We thank Dr. William Bornmann for supplying us with ß-lap and Dr. Nancy Oleinick for critical review of the manuscript. We are also grateful for support through the efforts of Mrs. Sara Hildebrand through the Breast Cancer Inspiration Fund and the Breast Cancer Research Fund. This work was also supported by the Arthritis Foundation-Illinois chapter (to C.J.F.). Finally, we are grateful to our many colleagues at the University of Wisconsin Comprehensive Cancer Center for their help in initiating these studies.

Table I

Characteristics of Breast Cancer Cell Lines

CELL LINE	ER	p53	pRb
MCF-7:WS8	**++++**	**WT**	**+**
T47D:A18	**++**	**MUTANT**	**+**
MDA-MB-231	**-**	**MUTANT**	**+**
MDA-MB-468	**-**	**MUTANT**	**-**

Figure Legends

FIG. 1. **Sensitivities of breast cancer cells to ß-lap or TPT.** Cells were seeded into 96-well tissue culture plates (1.5 X 10^3 cells/well) and allowed to attach overnight. Drugs were then added and cells were allowed to grow for an additional 48 h, as described in Experimental Procedures. Cell number was assessed using Hoechst 33258 fluorescence and relative growth inhibition (Relative Growth T/C) was calculated. Shown are toxicities for MCF-7:WS8 (—■—), MDA-MB-231 (···○···), T47D:A18 (—●—), and MDA-MB-468 (···△···) cell lines exposed to various concentrations of ß-lap (ß-Lap) or topotecan (TPT). Data shown is representative of at least two experiments expressed as mean ± SEM of at least four replicate wells.

FIG. 2. **ß-Lap- or TPT-mediated cytotoxicity of G_1 arrested cells.** MCF-7:WS8 and T47D:A18 estrogen-dependent cell lines were grown for six days in estrogen-depleted, phenol red-free medium and exposed to varying concentrations of ß-lap or TPT for 6 days, as indicated. Drugs were included in RPMI 1640 medium containing estrogen-deprived calf serum (Control, —■—), estrogen-replenished, stripped calf serum (10 nM 17ß-estradiol, E_2, —◆—), whole serum alone (···▽···) or whole serum treated with the antiestrogens, 4-hydroxytamoxifen (100 nM 4-OHT, ···⊕···) or ICI 182,780 (100 nM ICI 182,780, ···⊕···). Cell number was then assessed after 6 days using DNA content as in Fig. 1. Relative cell growth of treatment was determined using the DNA content of cells grown in comparable medium without ß-lap or TPT. Data shown are representative of at least two experiments expressed as mean ± SEM of at least four replicate wells.

FIG. 3. **Atypical and classic PARP cleavage in breast cancer cells following ß-lap exposure.** Breast cancer cell lines were treated with ß-lap (5-10 μM) for 48 h and whole cell lysates prepared at various times posttreatment from pooled (attached and floating) cells and assessed for cleavage of PARP using standard Western immunoblot procedures and the C-2-10 monoclonal PARP antibody, described in "Experimental Procedures". An unknown ~80 kDa cross-reacting protein was present in MCF-7:WS8 lysates as indicated by an (∗). The Western blot shown is representative of at least three separate experiments.

FIG. 4. **Caspase-mediated, classical PARP cleavage in breast cancer cells following TPT treatment.** Log-phase breast cancer cells were treated with 10 nM to 10 μM TPT for 48 h. Three doses of TPT (50, 500 and 5,000 nM, lanes 10-12 and 22-24 top and bottom) also included the caspase inhibitor, zVAD-fmk (25 μM). An unknown ~80 kDa cross-reacting protein is present in MCF-7:WS8 lysates as indicated by an (∗). Cells were then harvested and analyzed by Western immunoblotting using the C-2-10 monoclonal PARP antibody as described in Fig. 3.

FIG 5. **Effect of global or specific cleavage site protease inhibitors on ß-lap-mediated atypical PARP cleavage.** Log-phase breast cancer cells were grown for 48 h in RPMI medium alone or in medium containing 8 μM ß-lap. Protease inhibitors were co-administered with ß-lap. The protease inhibitors

used were: 25 μM zVAD-fmk (a caspase family inhibitor), 25 μM zAAD-fmk (an inhibitor of Granzyme B), 25 μM zFA-fmk (an inhibitor of Cathepsins B and L), 1.0 μM TPCK (a trypsin inhibitor) or 10 μM TLCK (a chymotrypsin inhibitor). Control cells received RPMI medium alone (lanes 1 and 13) or RPMI medium containing 8 μM ß-lap (lanes 7 and 19). Whole cell extracts were then analyzed by western immunoblotting as described in 'Experimental Procedures' for PARP cleavage, pRb dephosphorylation and cleavage, and cleavage of the Sp1 transcription factor by repeated probing of the same blots. The Western blot shown is representative of at least three separate experiments.

FIG 6. **ß-Lapachone induced DNA fragmentation.** MCF-7:WS8 cells were treated with 8 μM ß-lap for 4 h and harvested 20 h later. Cells were analyzed for DNA fragmentation using the TUNEL assay. Cells which have significant DNA fragmentation incorporate FITC-dUTP and are shown above the line in both panels. Shown is a representative example of experiments repeated at least three times.

FIG 7. **ß-Lap-induced atypical PARP cleavage was inhibited by the global cysteine protease inhibitors, iodoacetamide and N-ethylmaleimide.** Cells were seeded into 10 cm dishes and allowed to attach overnight. The following day, media ± ß-lap were added to each dish. Duplicate plates also contained either 10 mM Iodoacetamide (I) or 10 mM N-ethylmaleimide (N). Four hours after drug addition, drug-containing media were removed and fresh media without ß-lap were added. At the time of ß-lap removal, Iodoacetamide or N-ethylmaleimide were included in the media for the remainder of the experiment. Cells were grown for an

additional 20 h at which time whole cell lysates were prepared and analyzed in a western immunoblot with anti-PARP antibody.

FIG 8. **Implication of calpain in atypical PARP cleavage.** A: MCF-7:WS8 cells were treated with 5 μM ß-lap for 4 h and whole cell extracts were prepared 20 h later. Western blots were probed with anti-PARP antibody, then stripped and reprobed with anti-p53 antibody. B: MCF-7:WS8 cells were pretreated for 30 min with the designated concentrations of EDTA or EGTA in complete medium. Medium containing 8 μM ß-lap was then added for 4 h in the continued presence of EDTA or EGTA. After ß-lap exposure cells were treated with medium containing only the designated concentrations of EDTA or EGTA for an additional 20 h. Whole cell extracts were prepared and probed for PARP as described above. The blots shown are representative of at least two independent experiments.

FIG 9. **Effect of ß-lap or TPT on logarithmically growing or antiestrogen-arrested MCF-7:WS8 cells.** MCF-7:WS8 cells were estrogen-deprived for six days prior to seeding in estrogen-deprived medium containing 10 nM ICI 182,780 to assure complete blockage of estrogen-stimulated growth. Cells were then treated with: no drug (C); 5 μM ß-lap (ß); or 5 μM TPT (T); in estrogen-free RPMI media supplemented with either 100 nM ICI (I) or 10 nM E_2 (E_2). Whole cell extracts were prepared 24 h later, as described above and changes in cell cycle distribution monitored by flow cytometry as described in 'Experimental Procedures'. For Western analyses, immunoblots were first probed with the C-2-10 anti-PARP monoclonal antibody, then stripped and reprobed with an anti-pRb monoclonal antibody which detected all forms of pRb. For controls, log-

phase MCF-7:WS8 cells were grown continuously in medium containing whole serum (WS) or in medium containing estrogen-deprived serum (SS, for stripped serum) as described in 'Experimental Procedures'. Shown are three separate forms of the pRb protein: (a) pRb-pp = hyperphosphorylated pRb; (b) pRb = hypophosphorylated (nonphosphorylated) pRb; and (c) the cleaved form of pRb, in which 4 kDa of the C-terminus has been removed (Cleaved pRb). PARP protein forms included (a) the full-length PARP polypeptide of 113 kDa; (b) a caspase-mediated 89 kDa PARP fragment; and (c) an ~60 kDa atypical PARP cleavage polypeptide, which sometimes appears as a doublet at ~60 kDa. The western blot shown was representative of at least three separate experiments.

FIG 10. **ß-Lap-induced apoptosis and PARP cleavage in MCF-7:WS8 cells arrested in M phase of the cell cycle.** Cells were seeded into 10 cm tissue culture dishes and allowed to attach overnight. The following day, cells were treated for 16 h with RPMI medium alone (C) or medium containing 50 nM (150 ng/ml) Nocodazole (N). Cells were then treated with RPMI medium containing 5 μM ß-lap or 5 μM TPT in the presence of 50 nM nocodazole or nocodazole-free medium (N-C). The remaining dishes were fed with fresh media without ß-lap or TPT, ± Nocodazole and harvested 20 h later. In A, ß-lap treated cell extracts were examined in a Western immunoblot probed with C-2-10 anti-PARP antibody or the G3-245 anti-pRb antibody. In B, extracts from the same experiment were probed with phosphorylation-specific anti-pRb antibodies. "Phos pRb" indicates the location of phosphorylated pRb, as detected by a polyclonal antibody which recognizes only pRb which has been phosphorylated on serine 780, a Cyclin

D1/cdk4 specific site (41). "UnPhos pRb" indicates the location of fully hypophosphorylated pRb as detected by a monoclonal antibody which recognizes only hypophosphorylated pRb protein . The western blot shown is representative of at least three separate experiments.

FIG. 11. **Effect of caspase-3 expression on ß-lap-mediated proteolysis.** Caspase-3-negative MCF-7:WS8 cells were infected with a retroviral construct expressing full-length pro-caspase-3 (Casp 3) or vector alone (pbabe). Caspase 3 (full length = 32 kDa) expression is shown in the lower panel. Cells were then treated with the designated concentrations of ß-lap for 4 h, fresh medium was added and whole cell extracts were prepared 20 h later. Western immunoblots were then probed with the C-2-10 anti-PARP antibody, stripped and reprobed with Lamin B and later with caspase-3 antibodies. The western blot shown is representative of at least three separate experiments.

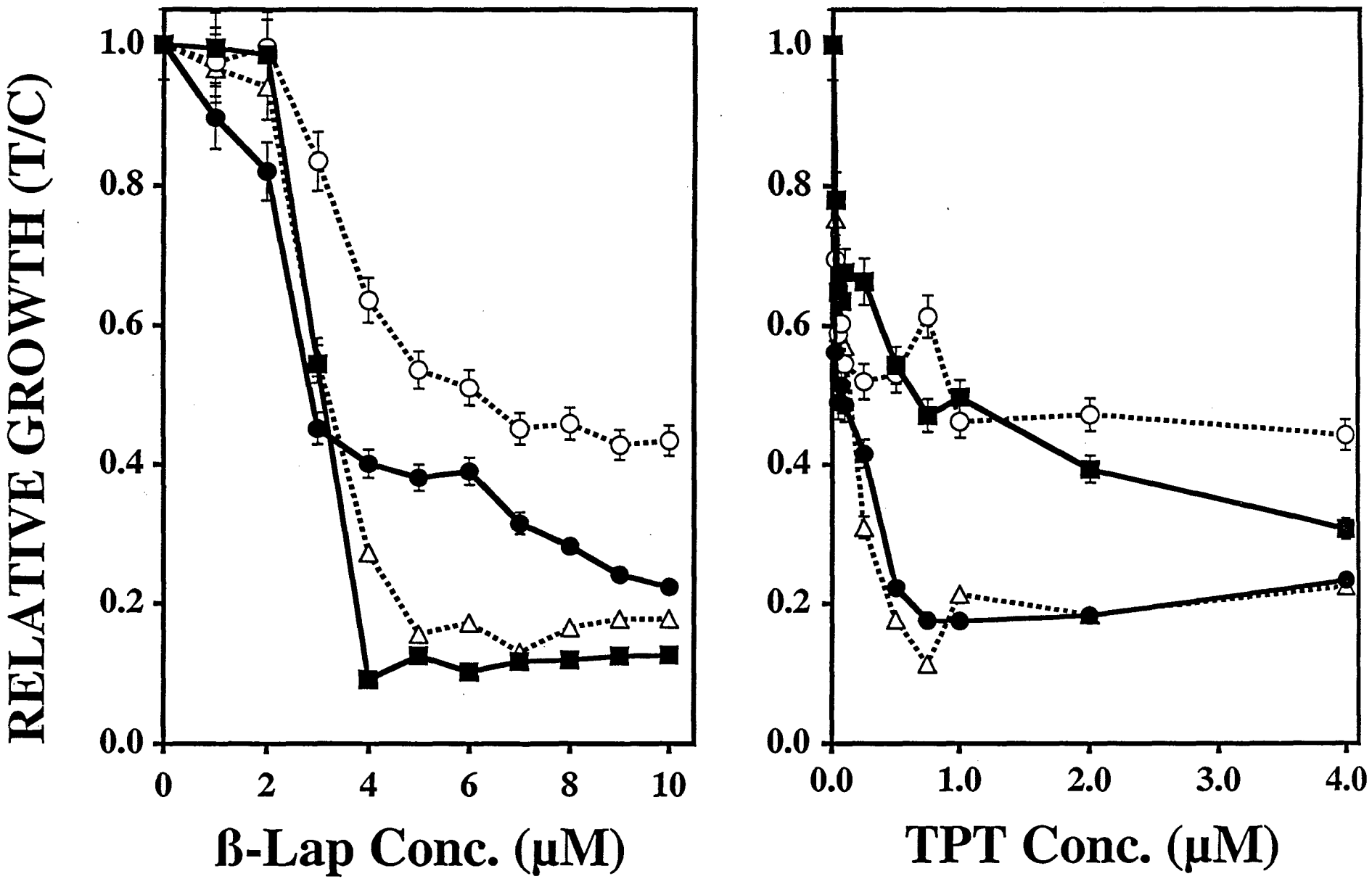
RELATIVE GROWTH (T/C)
1.0
0.8
0.6
0.4
0.2
0.0
0
2
4
6
8
10
ß-Lap Conc. (µM)
1.0
0.8
0.6
0.4
0.2
0.0
0.0
1.0
2.0
3.0
4.0
TPT Conc. (µM)

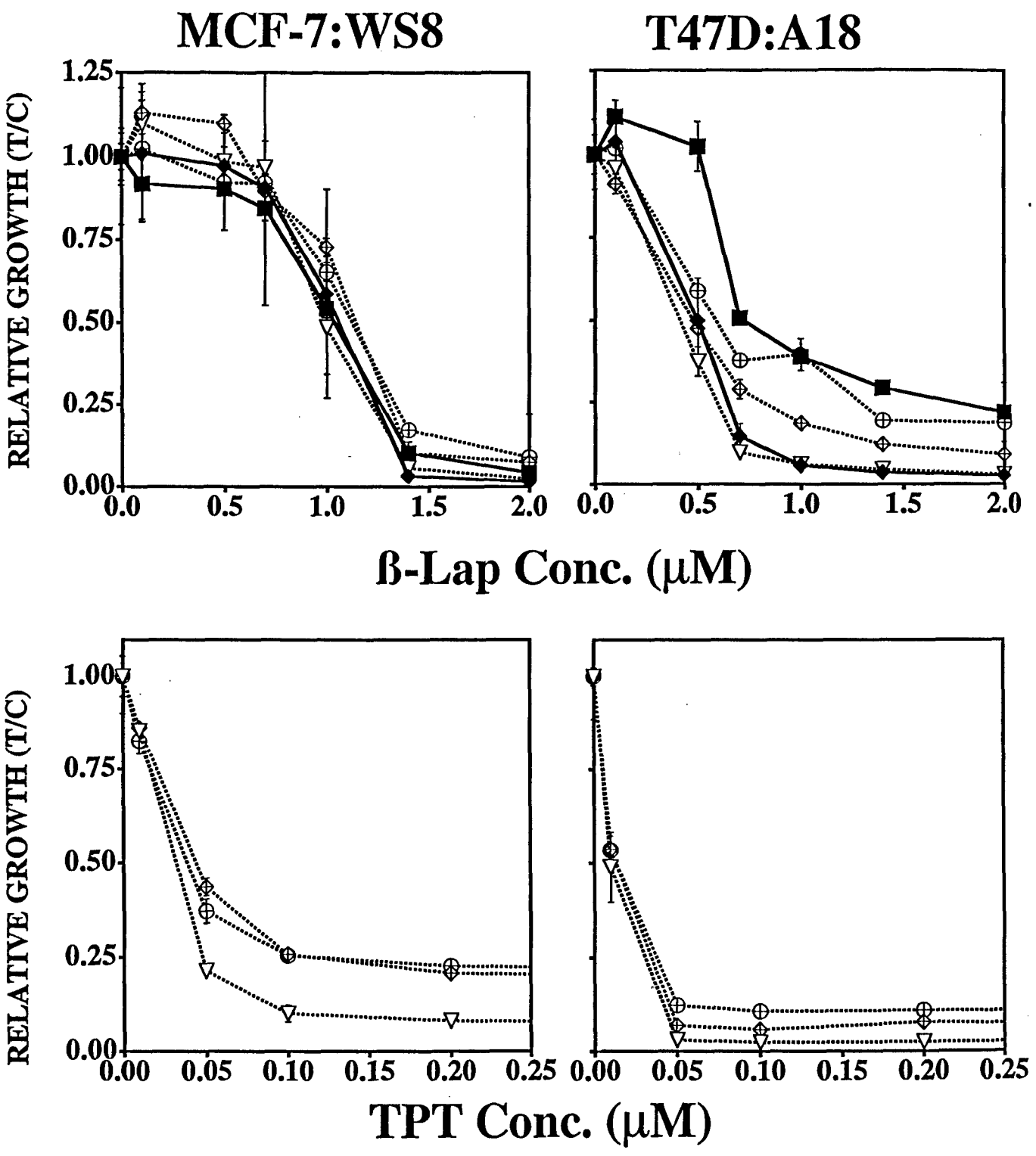
MCF-7:WS8
T47D:A18
RELATIVE GROWTH (T/C)
1.25
1.00
0.75
0.50
0.25
0.00
0.0
0.5
1.0
1.5
2.0
ß-Lap Conc. (μM)
RELATIVE GROWTH (T/C)
1.00
0.75
0.50
0.25
0.00
0.00
0.05
0.10
0.15
0.20
0.25
TPT Conc. (μM)

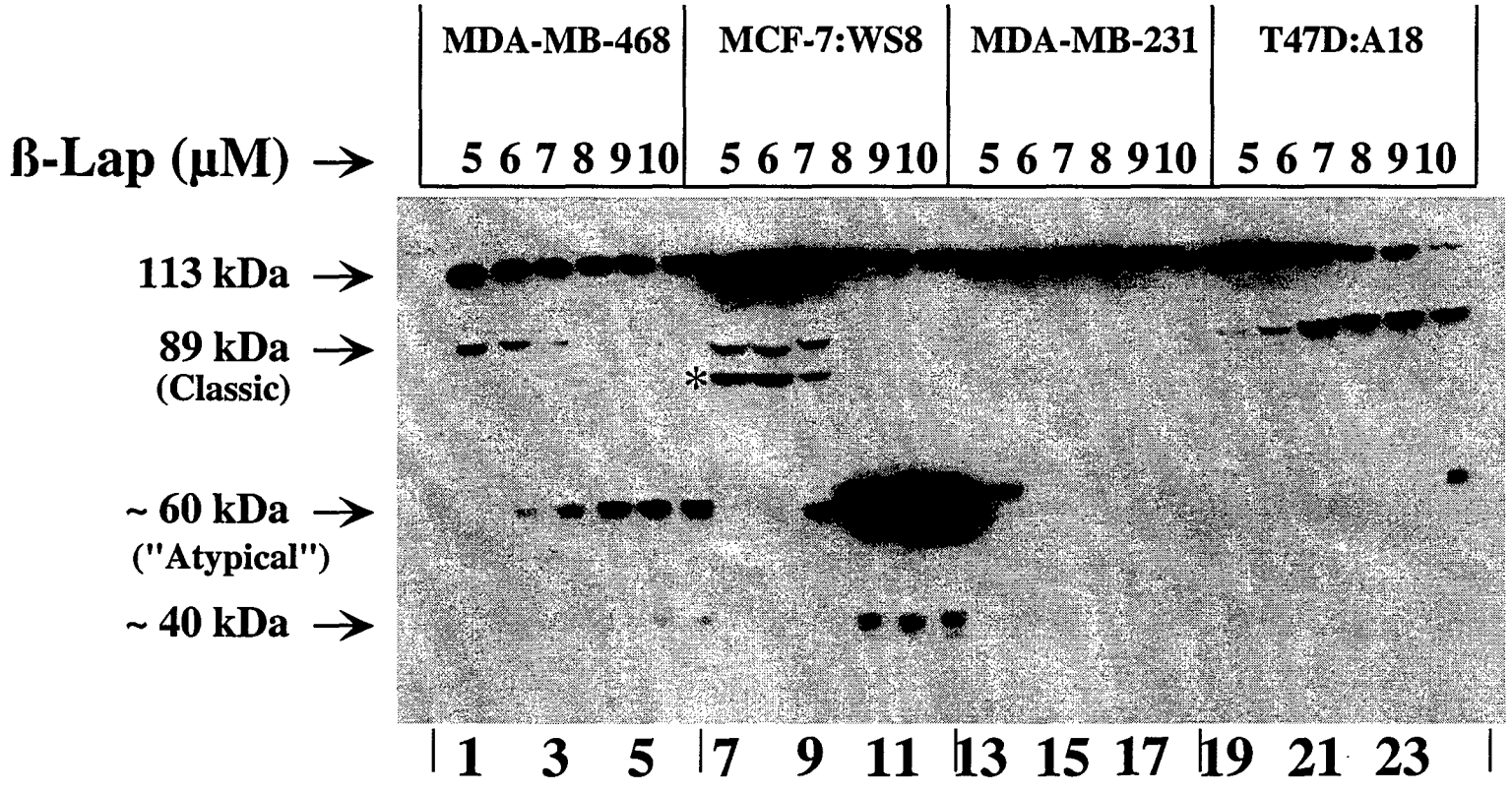
MDA-MB-468
MCF-7:WS8
MDA-MB-231
T47D:A18
ß-Lap (µM) →
5 6 7 8 9 10
5 6 7 8 9 10
5 6 7 8 9 10
5 6 7 8 9 10
113 kDa →
89 kDa →
(Classic)
~ 60 kDa →
("Atypical")
~ 40 kDa →
*
1 3 5 7 9 11 13 15 17 19 21 23

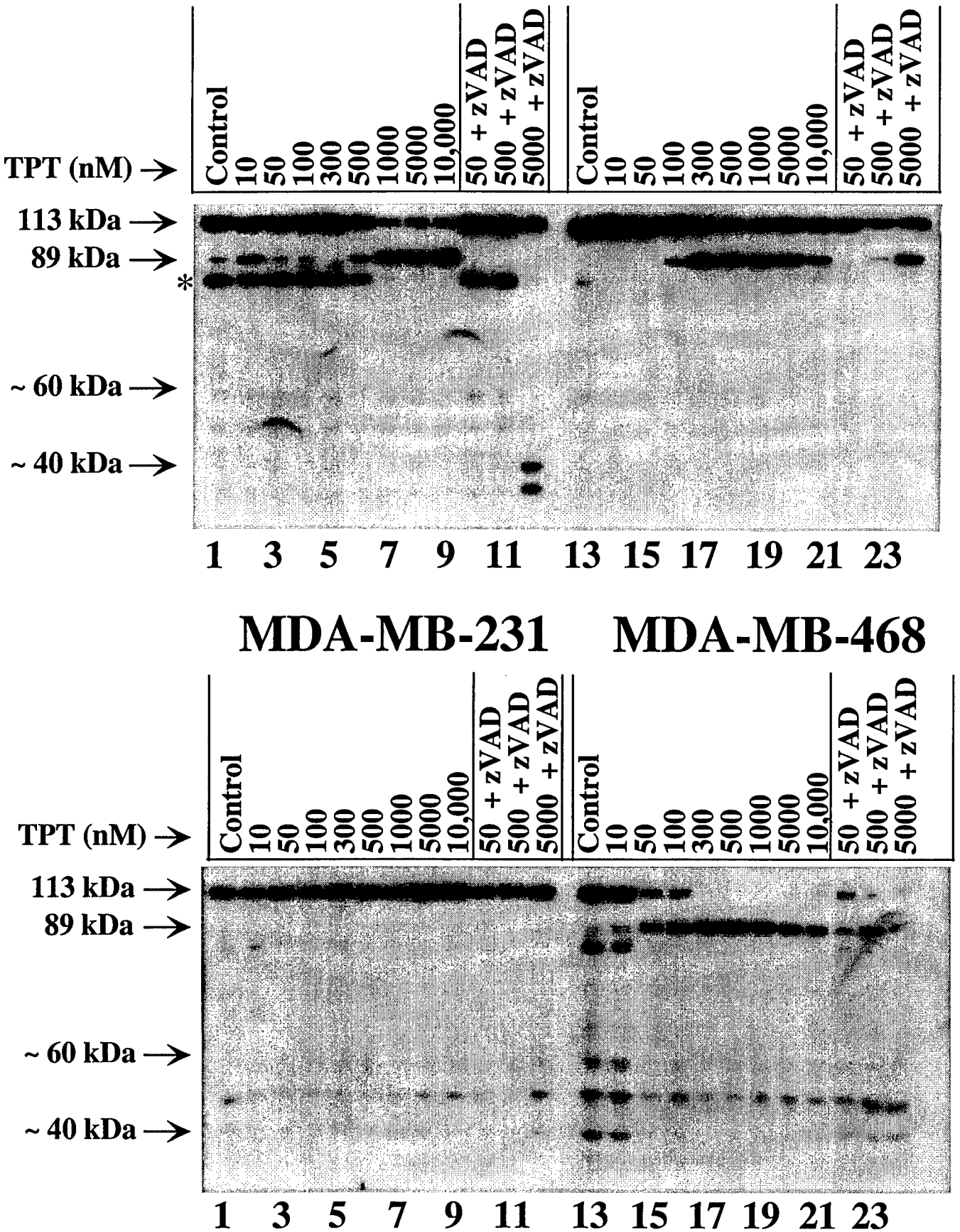
MCF-7:WS8
T47D:A18
TPT (nM)
Control
10
50
100
300
500
1000
5000
10,000
50 + zVAD
500 + zVAD
5000 + zVAD
Control
10
50
100
300
500
1000
5000
10,000
50 + zVAD
500 + zVAD
5000 + zVAD
113 kDa
89 kDa
*
~ 60 kDa
~ 40 kDa
1 3 5 7 9 11 13 15 17 19 21 23
MDA-MB-231
MDA-MB-468
TPT (nM)
Control
10
50
100
300
500
1000
5000
10,000
50 + zVAD
500 + zVAD
5000 + zVAD
Control
10
50
100
300
500
1000
5000
10,000
50 + zVAD
500 + zVAD
5000 + zVAD
113 kDa
89 kDa
~ 60 kDa
~ 40 kDa
1 3 5 7 9 11 13 15 17 19 21 23

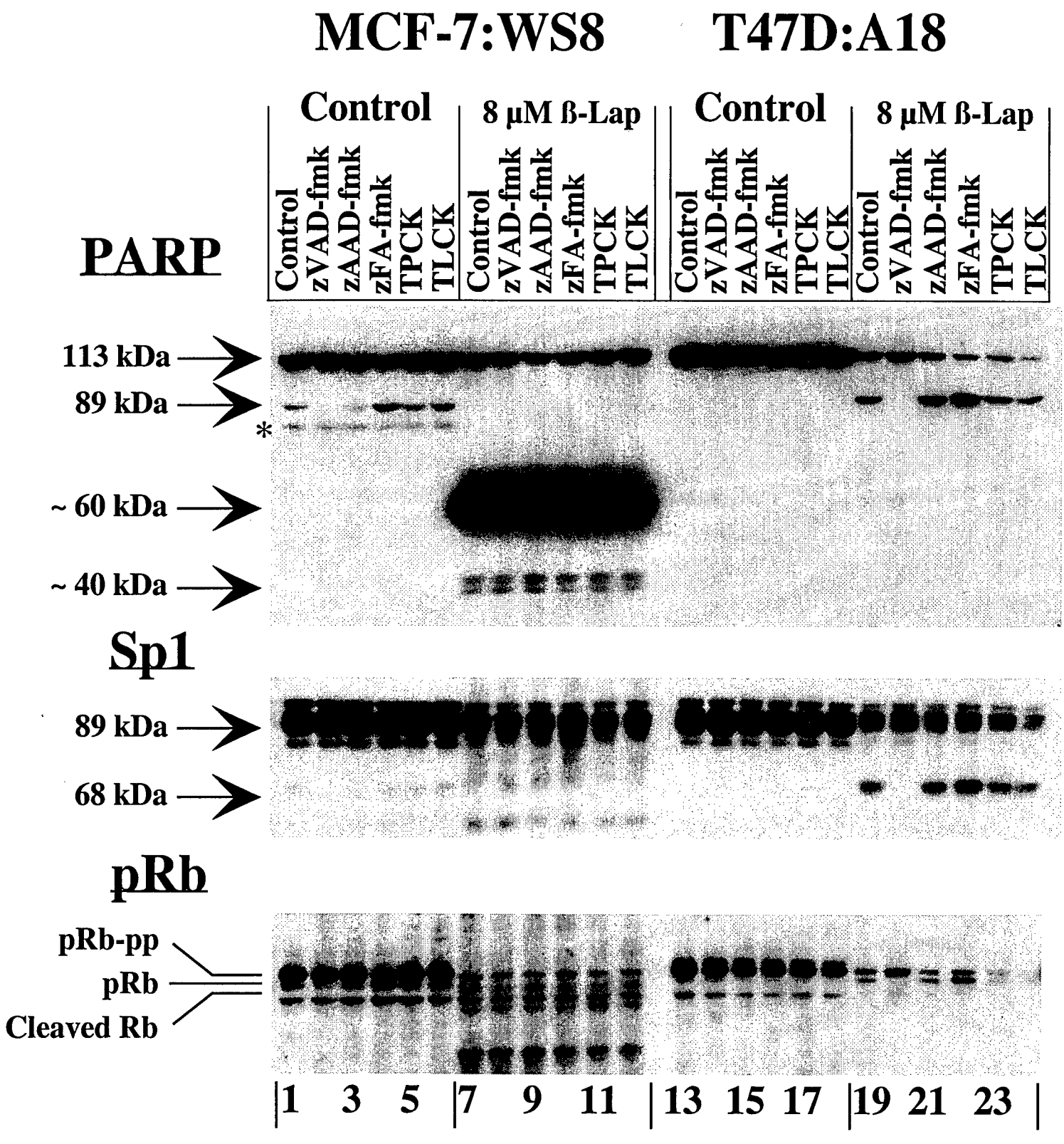
MCF-7:WS8
T47D:A18
Control
8 µM ß-Lap
Control
8 µM ß-Lap
Control
zVAD-fmk
zAAD-fmk
zFA-fmk
TPCK
TLCK
PARP
113 kDa
89 kDa
*
~ 60 kDa
~ 40 kDa
Sp1
89 kDa
68 kDa
pRb
pRb-pp
pRb
Cleaved Rb
1 3 5 7 9 11 13 15 17 19 21 23

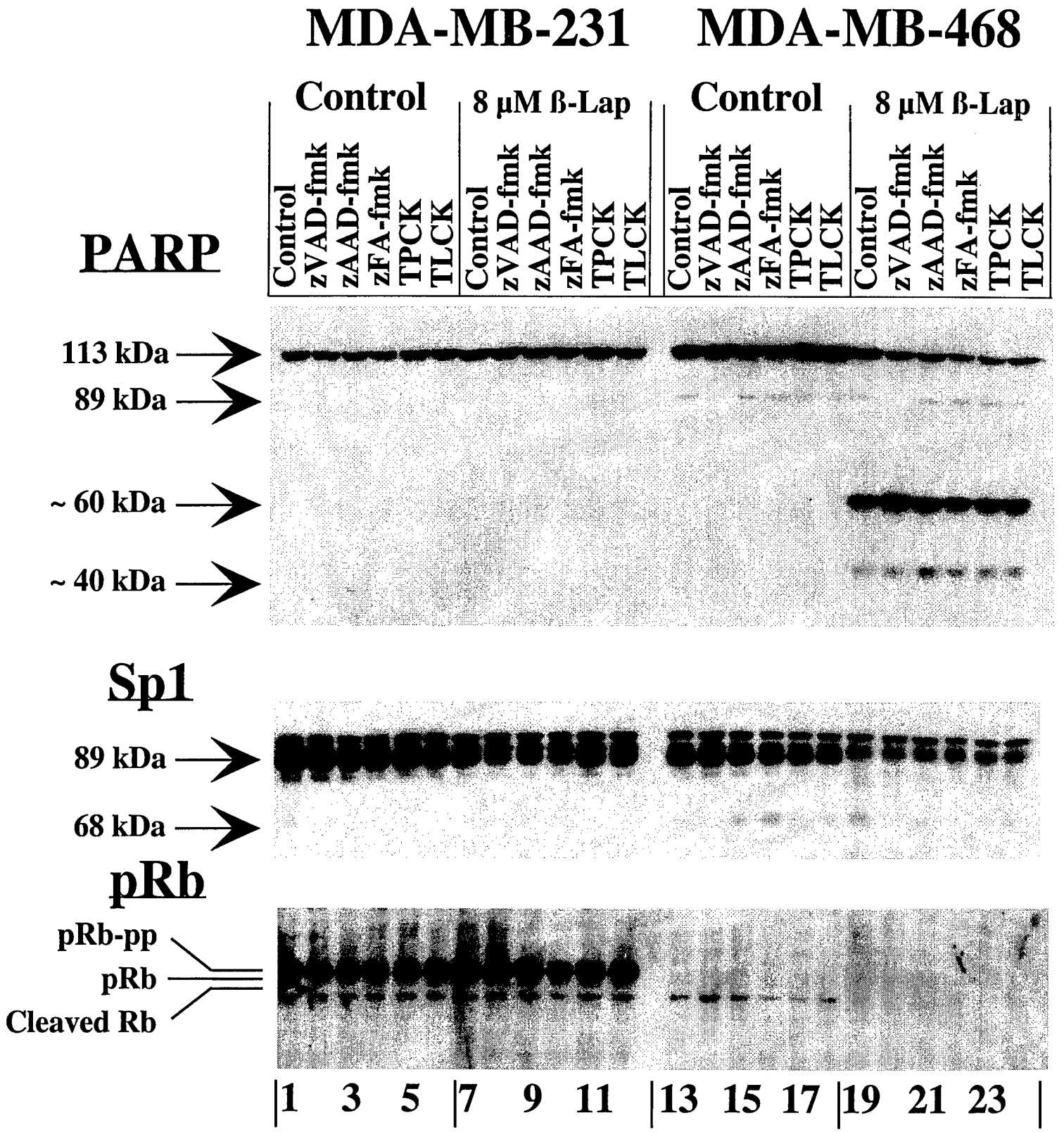
MDA-MB-231
MDA-MB-468
Control
8 μM ß-Lap
Control
8 μM ß-Lap
Control
zVAD-fmk
zAAD-fmk
zFA-fmk
TPCK
TLCK
PARP
113 kDa
89 kDa
~ 60 kDa
~ 40 kDa
Sp1
89 kDa
68 kDa
pRb
pRb-pp
pRb
Cleaved Rb
1 3 5 7 9 11 13 15 17 19 21 23

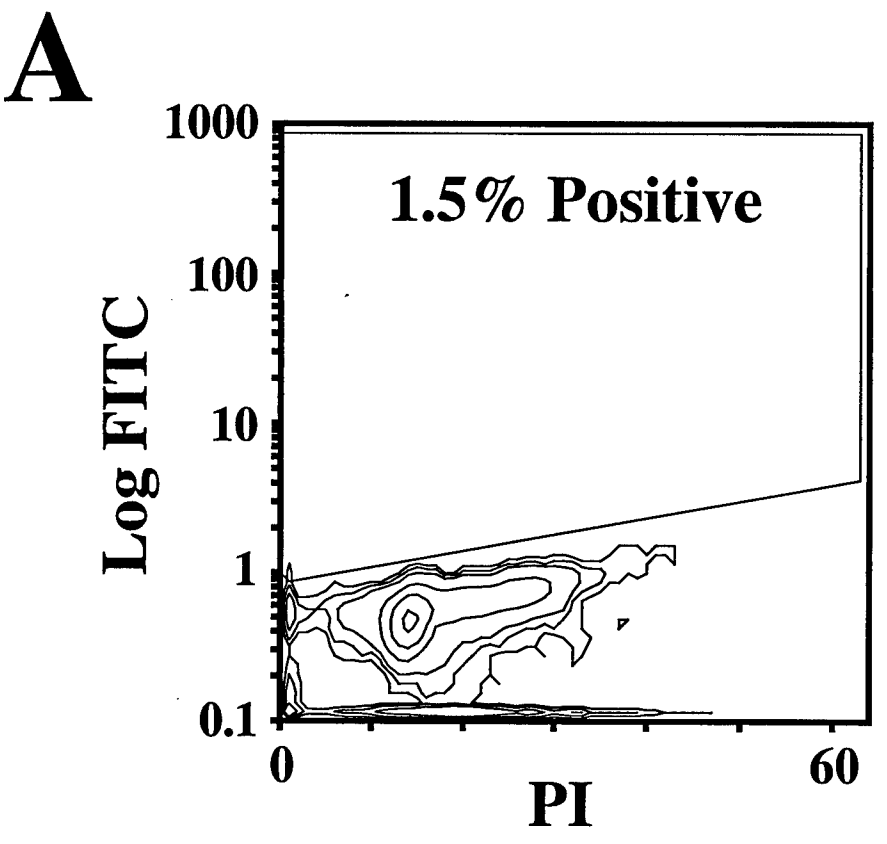
A
1000
100
10
1
0.1
Log FITC
1.5% Positive
0
60
PI

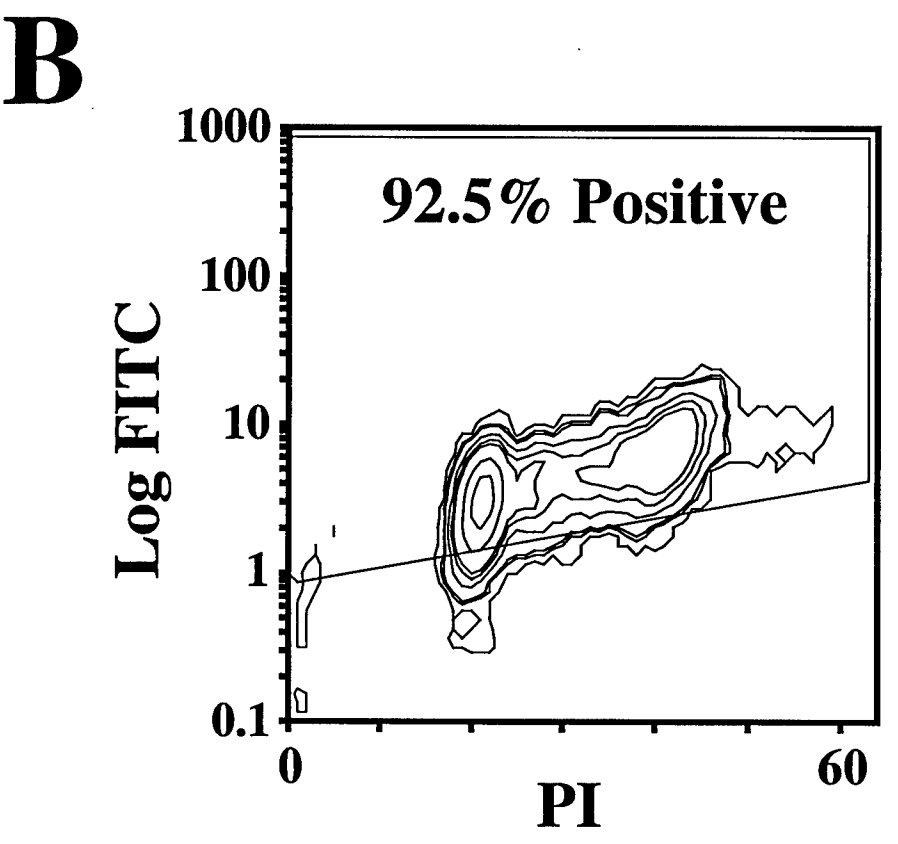
B
1000
100
10
1
0.1
Log FITC
92.5% Positive
0
60
PI

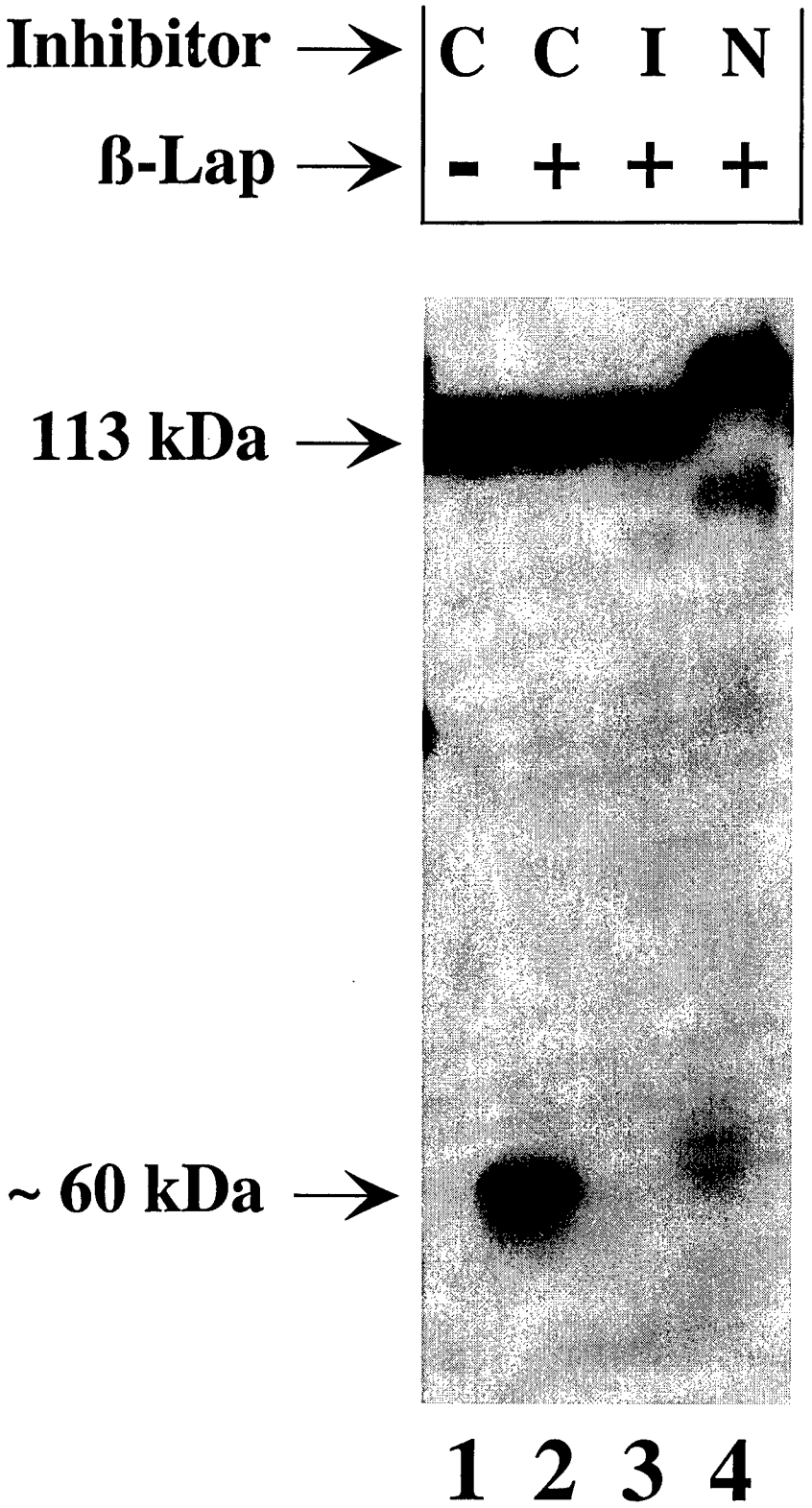
Inhibitor →
C C I N
ß-Lap →
- + + +
113 kDa →
~ 60 kDa →
1 2 3 4

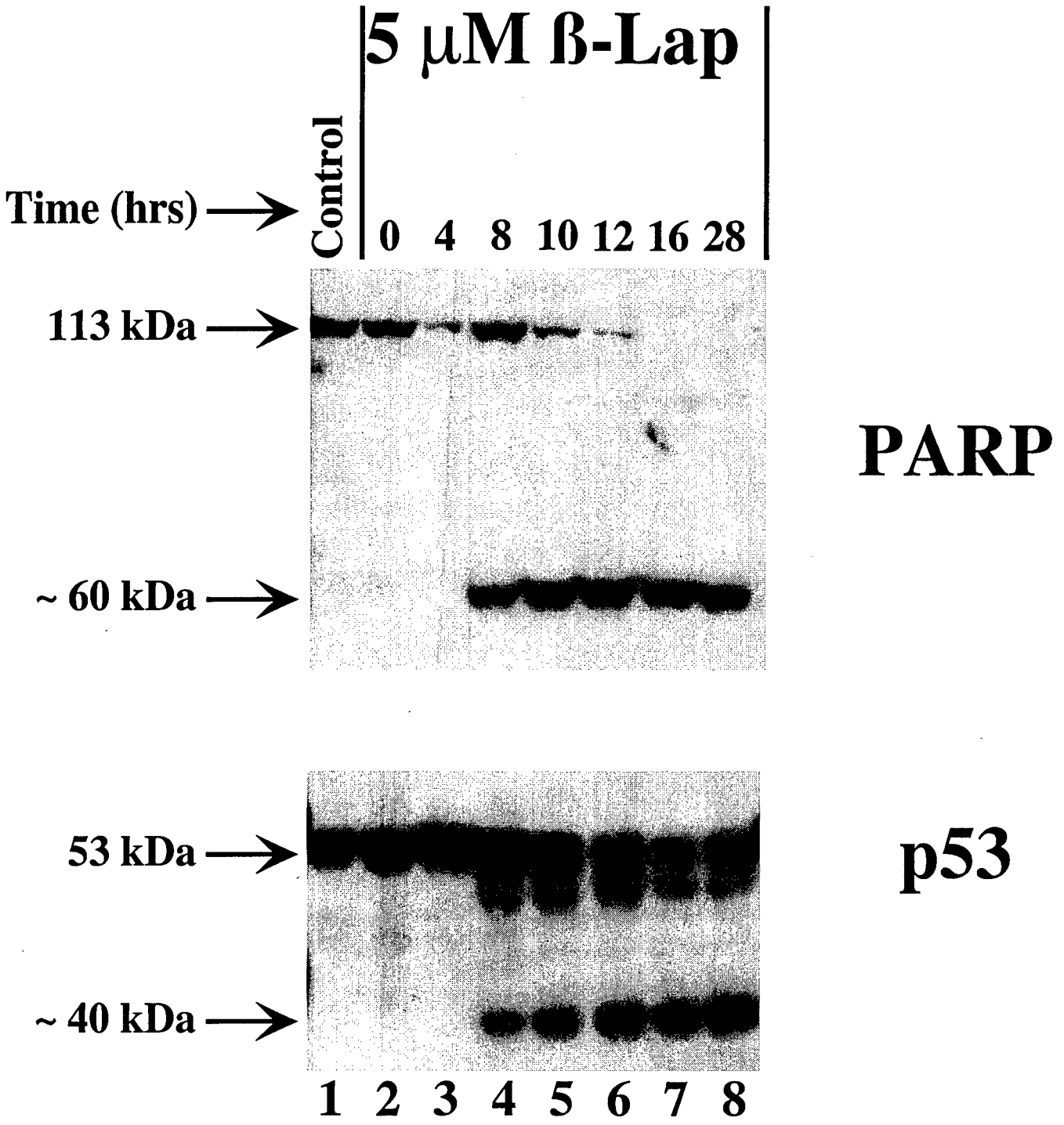
5 μM ß-Lap
Control
Time (hrs)
0 4 8 10 12 16 28
113 kDa
~ 60 kDa
PARP
53 kDa
~ 40 kDa
p53
1 2 3 4 5 6 7 8

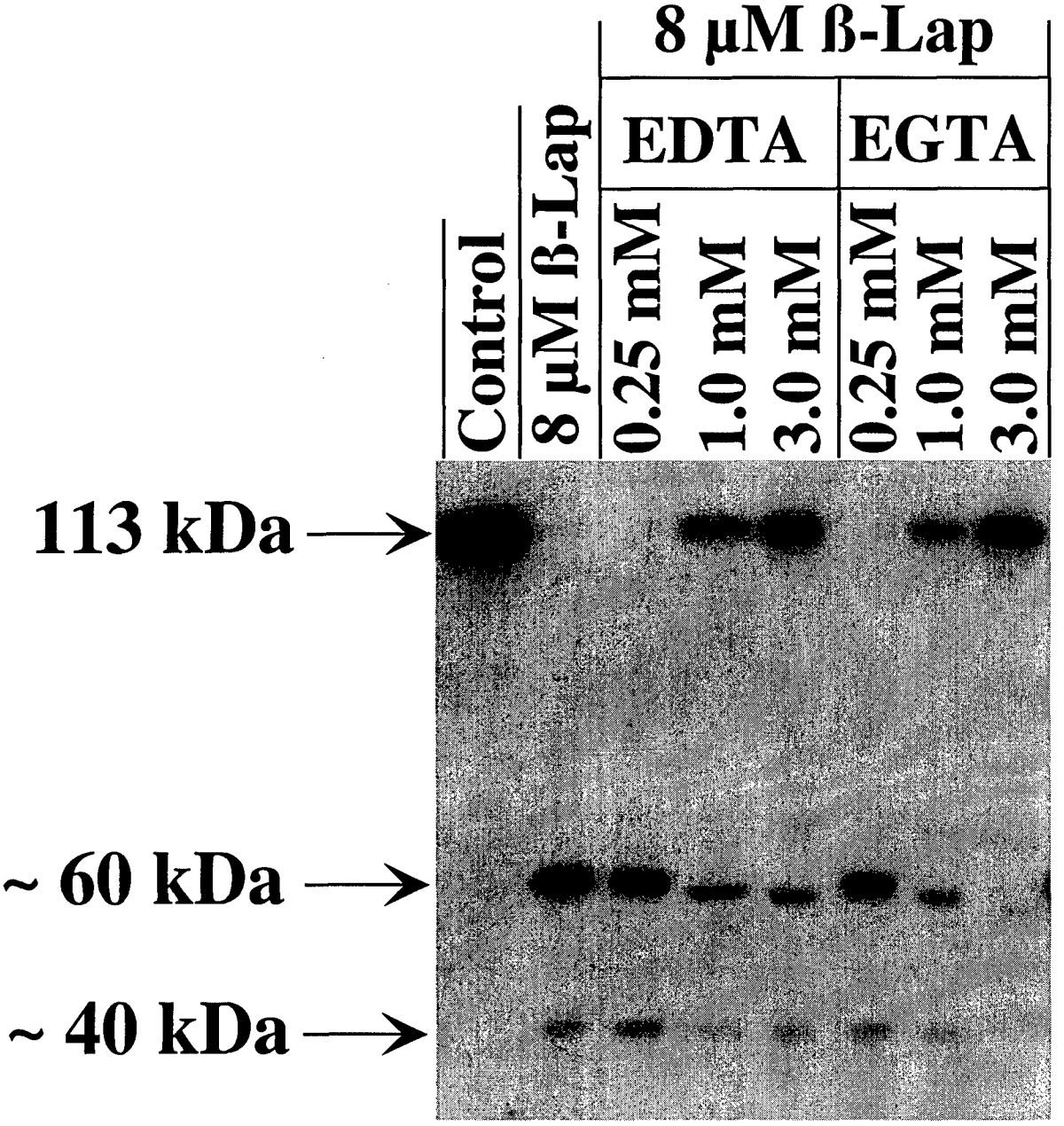
8 µM ß-Lap
EDTA
EGTA
Control
8 µM ß-Lap
0.25 mM
1.0 mM
3.0 mM
0.25 mM
1.0 mM
3.0 mM
113 kDa
~ 60 kDa
~ 40 kDa

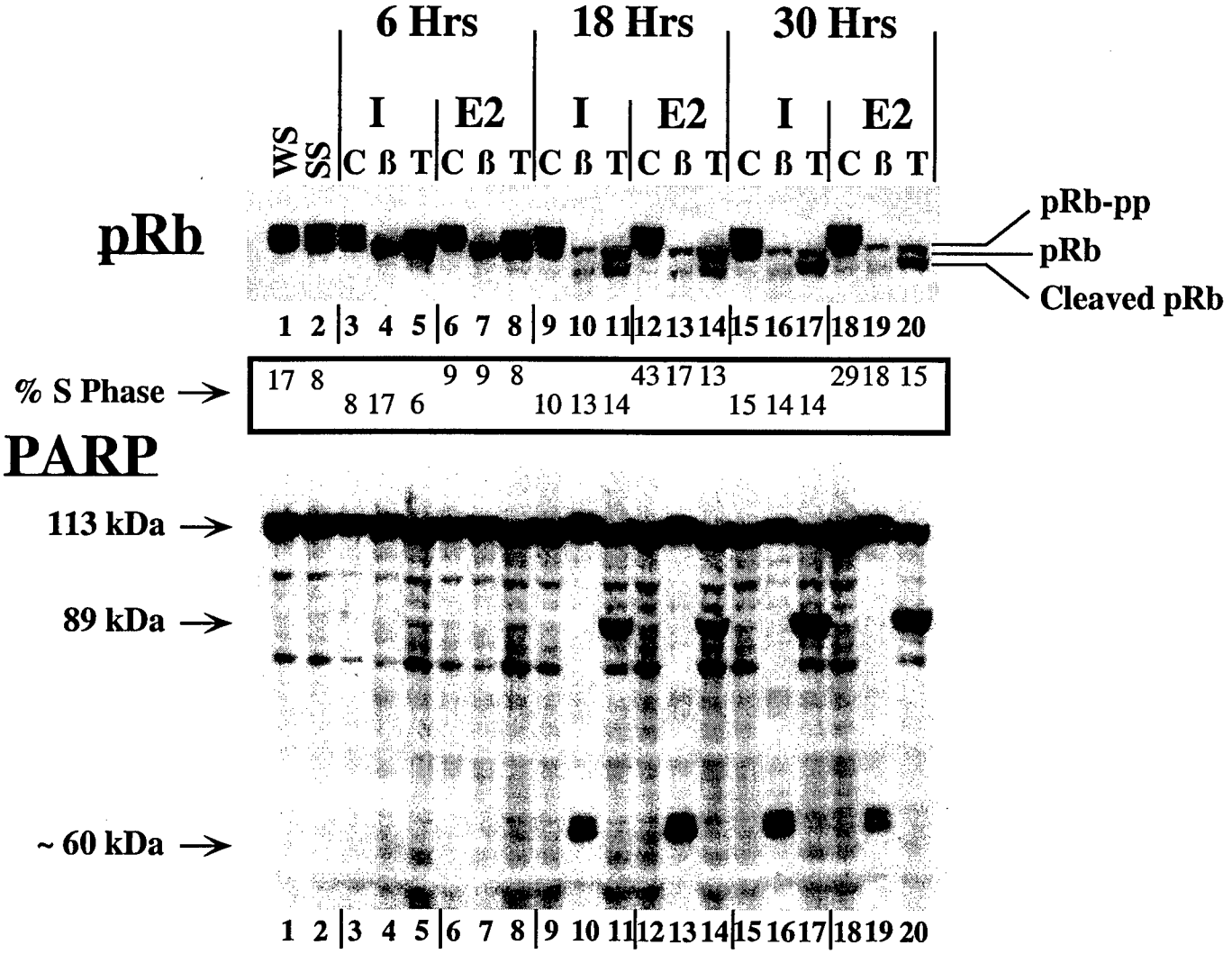
6 Hrs
18 Hrs
30 Hrs
I
E2
I
E2
I
E2
WS
SS
C ß T C ß T C ß T C ß T C ß T C ß T
pRb
pRb-pp
pRb
Cleaved pRb
1 2 3 4 5 6 7 8 9 10 11 12 13 14 15 16 17 18 19 20
% S Phase →
17 8 9 9 8 43 17 13 29 18 15
8 17 6 10 13 14 15 14 14
PARP
113 kDa →
89 kDa →
~ 60 kDa →
1 2 3 4 5 6 7 8 9 10 11 12 13 14 15 16 17 18 19 20

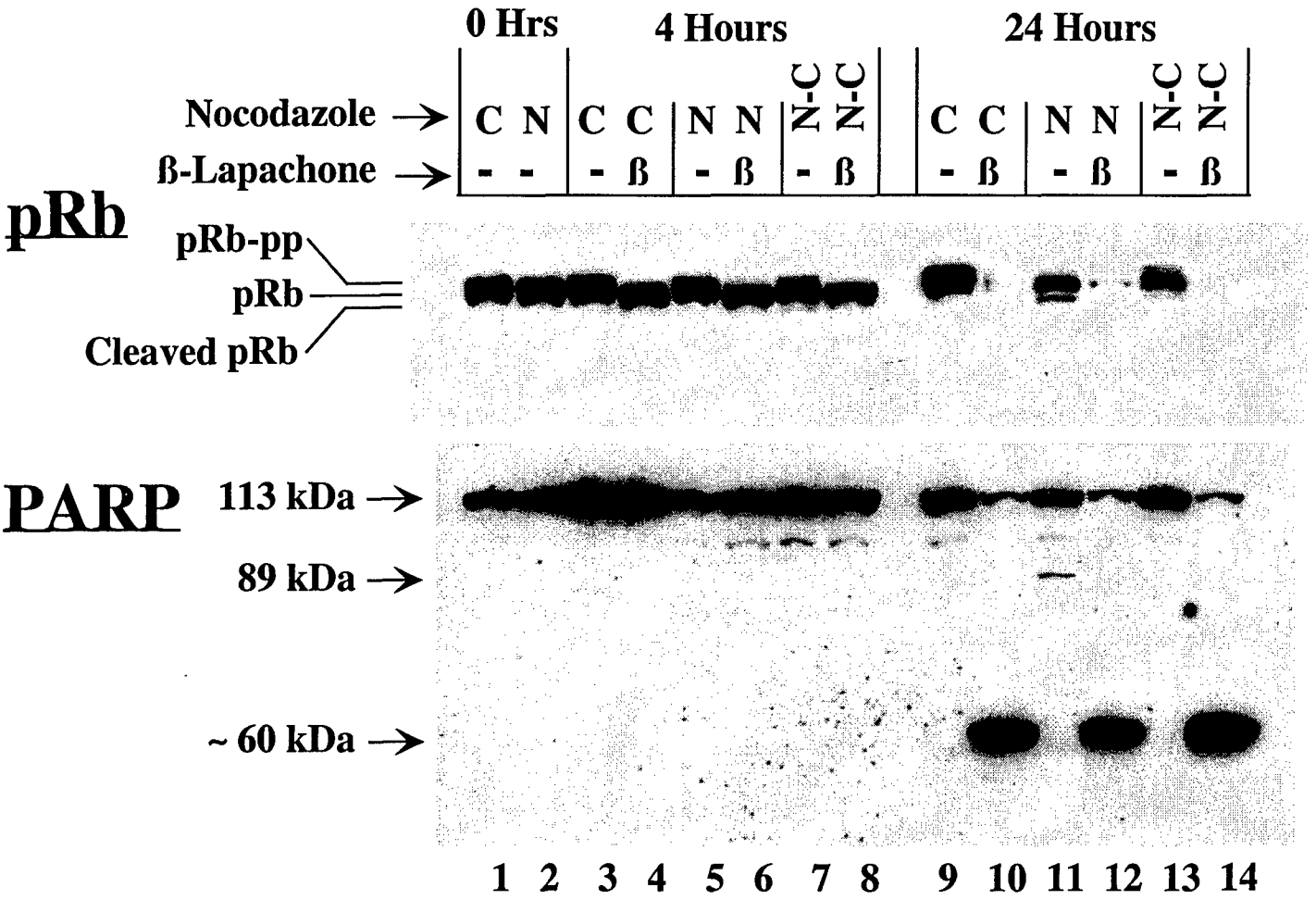
0 Hrs
4 Hours
24 Hours
Nocodazole →
ß-Lapachone →
C N C C N N N-C N-C C C N N N-C N-C
- - - ß - ß - ß - ß - ß - ß - ß
pRb
pRb-pp
pRb
Cleaved pRb
PARP
113 kDa →
89 kDa →
~ 60 kDa →
1 2 3 4 5 6 7 8 9 10 11 12 13 14

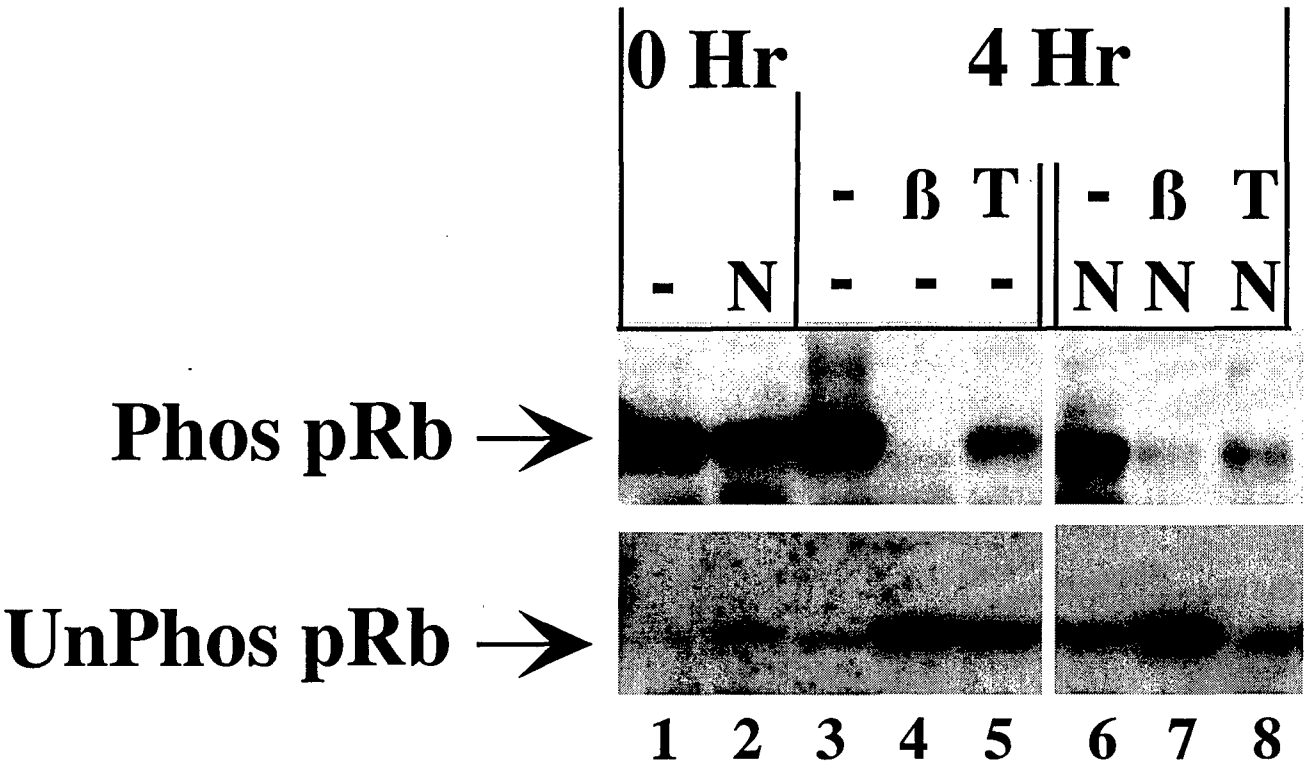
0 Hr
4 Hr
- ß T - ß T
- N - - - N N N
Phos pRb
UnPhos pRb
1 2 3 4 5 6 7 8

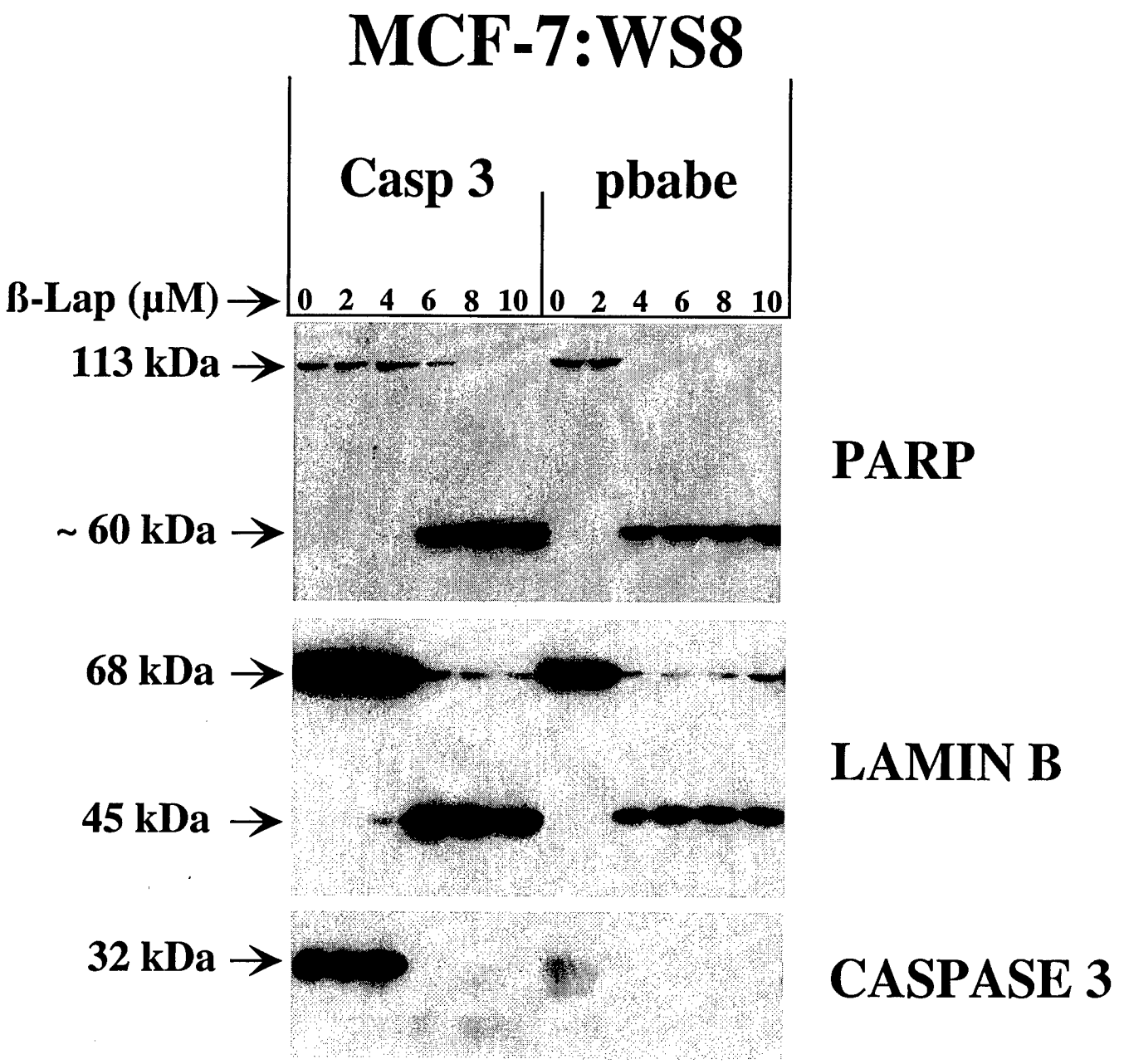
MCF-7:WS8
Casp 3
pbabe
ß-Lap (µM)
0 2 4 6 8 10 0 2 4 6 8 10
113 kDa
~ 60 kDa
PARP
68 kDa
45 kDa
LAMIN B
32 kDa
CASPASE 3

NAD(P)H:Quinone Oxidoreductase (NQO1) Activity is the Principal Determinant of ß-Lapachone Cytotoxicity

John J. Pink‡, Sarah M. Planchon‡, Colleen Tagliarino‡, Marie E. Varnes‡, David Siegel§, and David A. Boothman‡¶

‡ From the Department of Radiation Oncology, Laboratory of Molecular Stress Responses, Ireland Comprehensive Cancer Center, Case Western Reserve University, Cleveland, OH. 44106-4942; § Department of Pharmaceutical Sciences, School of Pharmacy and Cancer Center, University of Colorado Health Sciences Center, Denver, Colorado 80262

* Support for this research was provided the United States Army Medical Research and Materiel Command Breast Cancer Initiative, Grant #DAMD17-98-1-8260 to D.A.B, a post-doctoral fellowship, DAMD17-97-1-7221 to J.J.P. and NIH grant #CA51210 to D.S.

¶ To whom correspondence should be addressed. Tel 216-368-0840; Fax 216-368-1142; E-mail dab30@po.cwru.edu

[1] The abbreviations used are: ß-lap, ß-lapachone, (3,4-dihydro-2,2-dimethyl-2H-naphtho[1,2-*b*] pyran-5,6-dione); NQO1, NAD(P)H:quinone oxidoreductase, DT-diaphorase, xip-3, (E.C. 1.6.99.2); PARP, poly (ADP)-ribose polymerase, MMC mitomycin C; CMV, cytomegalovirus

[2]Footnote: "A Novel Non-Caspase-Mediated Proteolytic Pathway Activated in Breast Cancer Cells During ß-Lapachone-Mediated Apoptosis" Pink, J. J., Wuerzberger-Davis, S., Tagliarino, C., Planchon, S. M., Yang, X., Froelich, C. J., and Boothman, D.A.; submitted

Abstract

ß-Lapachone activates a novel apoptotic response in a number of cell lines. We demonstrate that the enzyme, NAD(P)H:quinone oxidoreductase (NQO1), is a key determinant of ß-lapachone toxicity. NQO1 expression directly correlated with sensitivity to a 4 h pulse of ß-lapachone in a panel of breast cancer cell lines and the NQO1 inhibitor, dicoumarol, significantly protected NQO1 expressing cells from all aspects of ß-lapachone toxicity. Stable transfection of the NQO1-deficient cell line, MDA-MB-468, with an NQO1 expression plasmid increased apoptotic responses and lethality after ß-lapachone exposure. Dicoumarol blocked both the apoptotic responses and lethality. Biochemical studies suggest that reduction of ß-lapachone by NQO1 leads to a futile cycling between the quinone and hydroquinone forms, with a concomitant loss of reduced NAD(P)H. Loss of reduced NAD(P)H is speculated to cause the activation of a novel cysteine protease, which has characteristics consistent with the neutral calcium-dependent protease, calpain. This is the first definitive elucidation of an intracellular target for ß-lapachone in tumor cells. NQO1 could be exploited for gene therapy, radiotherapy and/or chemopreventive interventions, since the enzyme is elevated in a number of tumor types (i.e. breast and lung) and during neoplastic transformation.

Introduction

ß-lap[1], a novel 1,2 naphthoquinone, is a potent cytotoxic agent which demonstrates activity against various cancer cell lines (1-3). At lower doses it is a radiosensitizer of a number of human cancer cell lines (4). We previously demonstrated that the primary mode of ß-lap cytotoxicity is through the induction of apoptosis (1,2). However, the clinical efficacy of this drug remains to be explored and such studies await elucidation of its mechanism of action.

While a number of *in vitro* effects of ß-lap have been described, the key intracellular target of ß-lap remains unknown. ß-Lap has many diverse effects *in vitro*, including a) inhibition of DNA polymerase α (5); b) enhanced lipid peroxidation and free radical accumulation (6); c) inhibition of DNA replication and thymidylate synthase activity (7); d) inhibition of DNA repair (4,8); e) inhibition or activation of DNA topoisomerase I (1,3); f) oxidation of dihydrolipoamide (9); g) induction of Topoisomerase IIα-mediated DNA breaks (10); h) inhibition of poly (ADP-ribose) polymerase (11); and i) inhibition of NF-κB activity (12). While these effects could be hypothetically linked to the cytotoxicity caused by ß-lap administration, most have not been demonstrated *in vivo* and none have led to elucidation of the drug's intracellular target.

Structural similarities between ß-lap and other members of the naphthoquinone family, such as menadione (Vitamin K3, 2-methyl-1,4 naphthoquinone), suggested that the enzyme, NQO1 (DT-diaphorase, quinone

oxidoreductase, E.C. 1.6.99.2), may be involved in the activation or detoxification of ß-lap (13-17). The x-ray-inducible nature of NQO1 (i.e., it was cloned by our laboratory as x-ray inducible transcript–3 , xip-3) was also consistent with this compound's ability to sensitize irradiated cells (18).

NQO1 is a ubiquitous flavoprotein found in most eukaryotes. The human NQO1 gene encodes a 30 kDa protein which is expressed in most tissues, but does show variable tissue-dependent expression. NQO1 is abundant in the livers of most mammals, except humans where it is less abundant than in most other tissues (16,19,20). NQO1 knock-out mice show no detectable phenotype, other than an enhanced sensitivity to menadione, suggesting that the principal function of NQO1 is the detoxification of quinone xenobiotics (21). Importantly, NQO1 is overexpressed in a number of tumors, including breast, colon and lung cancers, compared with surrounding normal tissue (22-25). This observation, more than any other, suggests that drugs which are activated by NQO1, (e.g., MMC, streptonigrin and EO9, see below) should show significant tumor-specific activity.

NQO1 catalyzes a two electron reduction of various quinones (e.g., menadione), utilizing either NADH or NADPH as electron donors. Unlike most other cellular reductases, NQO1 reduces quinones directly to the hydroquinone, bypassing the unstable and highly reactive semiquinone intermediate. Semiquinones are excellent free radical generators, initiating a redox cycle which results in the generation of superoxide. Superoxide can dismutate to hydrogen peroxide and hydroxyl radicals can then be formed by the iron-catalyzed reduction

of peroxide via the Fenton reaction (26). All of these highly reactive species may directly react with DNA or other cellular macromolecules, such as lipids and proteins, causing damage. NQO1-mediated production of the hydroquinone, which can be readily conjugated and excreted from the cell, constitutes a protective mechanism against these types of damage (27). It is thought that this reducing activity of NQO1 protects cells from the toxicity of naturally occurring xenobiotics containing quinone moieties (14).

In addition to its protective effects, NQO1 can also reduce certain quinones to more reactive forms. The most well described of these compounds is MMC. It is through a two electron reduction by NQO1, or through two separate one electron reductions by other reductases (such as NADH:cytochrome-b_5 reductase and NADPH:cytochrome P450 reductase), that the alkylating activity of MMC is revealed (28-30). A correlation was observed between MMC sensitivity and NQO1 activity in a study using sixty-nine cell lines from the National Cancer Institute human tumor cell panel. These data suggested that NQO1 was a critical activator of mitomycin C and likely other quinone-containing antitumor agents (31). Similarly, streptonigrin and EO9, can be activated by NQO1-catalyzed reduction (32).

Dicoumarol [3-3'-methylene-bis(4hydroxycoumarin)], is a commonly used inhibitor of NQO1, which competes with NADH or NADPH for binding to the oxidized form of NQO1. Dicoumarol thereby prevents reduction of various target quinones (33,34). Co-administration of dicoumarol significantly enhances the

toxicity of a number of quinones, including menadione, presumably by increasing oxidative stress in the cell (35-37).

We demonstrate that NQO1 is the principal activating enzyme for ß-lap in breast cancer cells. ß-Lap cytotoxicity was significantly enhanced in breast cancer cells expressing NQO1. Conversely, cells which lacked this enzyme were more resistant to a short term exposure to the drug. Co-administration of dicoumarol protected NQO1-expressing cells from all downstream apoptotic responses and greatly enhanced survival. Stable transfection of NQO1-deficient, MDA-MB-468 cells, homozygous for a proline to serine substitution at amino acid 187 which leads to the synthesis of unstable protein (38), with human NQO1 cDNA sensitized these otherwise resistant cells and re-established apoptotic responses. As seen in other cells expressing endogenous NQO1, cytotoxicity was prevented by dicoumarol. Our data establish that NQO1 activity is the principal determinant of ß-lap cytotoxicity in breast cancer cells. A novel downstream apoptotic pathway induced by ß-lapachone is also discussed.

Experimental Procedures

Cell Culture MCF-7:WS8 and T47D:A18 cells were obtained from V. Craig Jordan (Northwestern University, Chicago, IL). MDA-MB-468 cells were obtained from American Type Culture Collection. All tissue culture components were purchased from GIBCO Laboratories, Grand Island, NY unless otherwise stated. Cells were grown in RPMI 1640 supplemented with 10% calf serum, 2 mM L-glutamine, 100 U/ml penicillin and 100 mg/ml streptomycin. Cells were routinely passed at 1:5-1:20 dilutions once per week using 0.1% trypsin. All cells were grown in a 37°C humidified incubator with 5% CO_2-95% air atmosphere. Tests for mycoplasma, using the Gen-Probe™ Rapid Detection Kit (Fisher Scientific, Pittsburgh, Pa.), were performed quarterly and all cell lines were found to be negative.

Stable Transfection Cells were seeded into 6 well dishes at 2 x 10^5 cells/well and allowed to attach overnight. The following day 1.0 μg of BE8 plasmid DNA containing the human NQO1 cDNA in the pCDNA3 constitutive expression vector (39) was transfected into each of 3 wells using standard calcium phosphate methodology (40). After 2 days, cells were selected for growth in 350 μg/ml Geneticin® (G418, Gibco BRL, Gaithersburg, Md). A stable, pooled population

was established after approximately 3 weeks and subsequently clones were isolated by limiting dilution cloning, as described (41).

Cell Growth Assays Cells were seeded into each well of a 96 well plate (1500 cells/well) in 0.2 ml of media on day 0. The following day (day 1) media were removed and 0.2 ml of medium containing the appropriate compound(s) was added for 4 h. Drugs were then removed, control growth medium was added and cells were allowed to grow for an additional 7 days. Stock solutions of ß-lap (a generous gift from William Bornman, Sloan-Kettering Cancer Center, New York, NY) and menadione (Sigma Chemical Co, St. Louis, MO) were dissolved in DMSO and stored at –80° C. Drugs were added to medium at a 1:1000 dilution immediately before administration to cells. Dicoumarol (Sigma Chemical Co, St. Louis, MO) was suspended in water and solubilized using a minimal amount of NaOH. Dicoumarol was added at a 1:100 dilution to the appropriate medium. DNA content (a measure of cell growth) was determined by fluorescence of the DNA dye Hoescht 33258 (Sigma Chemical Co., St. Louis, Mo.), using an adaptation of the method of LaBarca and Paigan (42) and read in a Cytofluor fluorescence plate reader. Data was expressed as relative growth T/C (treated /control) from 3 or more wells per treatment. Each experiment was repeated at least three times and data were expressed as mean ± SEM. Comparisons were performed using a two-tailed student's t-test for paired samples.

Colony-forming Assays LD_{50} survival determinations were calculated by clonogenic assays (4). Briefly, cells were seeded at various densities on 35-cm^2 tissue culture dishes and allowed 48 h to attach and initiate log-phase growth. Drugs were added for 4 h at various concentrations and removed, as described above. Colonies from control or treated conditions were allowed to grow for 10 days. Colonies with 50 or more normal appearing cells were counted and data were graphed as mean $\pm$ SEM. Shown is a compilation of two independent experiments. Comparisons were performed using a two-tailed student's t-test for paired samples.

Western Blot Analyses Whole cell extracts were prepared by direct lysis of scraped, PBS washed cells (both floating and attached cells were pooled) in buffer comprised of 6 M urea, 2% SDS, 10% glycerol, 62.5 mM Tris-HCl pH 6.8, 5% ß-mercaptoethanol and 5 mg/ml bromphenol blue followed by sonication. Equal amounts of protein were heated at 65° C for 10 min and loaded into each lane of a 10% polyacrylamide gel with a 3% stacking gel. Following electrophoresis, proteins were transferred to Immobilon-P (Millipore Corp., Bedford, MA) using Multiphor II semi-dry electroblotting (Pharmacia Biotech Inc., Piscataway, NJ) according to the manufacturer's directions. Loading equivalence and transfer efficiency were monitored by Ponceau S staining of the membrane. Standard western blotting techniques were used and the proteins of interest were visualized by incubation with Super Signal (Pierce Chemical Co., Rockford, IL) at 20°C for 5 minutes. Membranes were then exposed to x-ray film for an appropriate time and

developed. The C-2-10 anti-PARP antibody was purchased from Enzyme Systems Products (Dublin, CA). The anti-p53 antibody (DO-1) was purchased from Santa Cruz Biotechnology Inc. (Santa Cruz, CA). NQO1 antibody was contained in medium from a mouse hybridoma Clone A180 (43) and was used at a 1:4 dilution in 10% serum, 1x PBS + 0.2% Tween-20 for Western blot analysis.

Preparation of S9 supernatants Cellular extracts for enzyme assays were prepared from cells in mid- to late-log phase growth. Cells were harvested by trypsinization (0.25% trypsin and 1 mM EDTA), washed twice in ice-cold, phenol red-free Hank's balanced salt solution, then resuspended in a small volume of PBS, pH 7.2, containing 10 μg/μl aprotinin. The cell suspensions were sonicated on ice, four times, using 10-second pulses, then centrifuged at 14000*g* for 20 min. The S9 supernatants were aliquoted into microfuge tubes and stored at -80 °C until used.

Enzyme assays: Three enzymes were assayed as described by Fitzsimmons *et al.* (31) and Gustafson *et al* (39). Reaction medium contained 77 μM cytochrome c (practical grade, Sigma Chemical Co., St. Louis, MO) and 0.14% bovine serum albumin in Tris-HCl buffer (50 mM, pH 7.5). NQO1 activity was measured using NADH (200 μM) as the immediate electron donor and menadione (10 μM) as the intermediate electron acceptor. Each assay was repeated in the presence of 10 μM dicoumarol, and activity attributed to NQO1 was that inhibited by dicoumarol (44). NADH:cytochrome b_5 reductase was measured using NADH (200 μM) as the

electron donor, and NADH:cytochrome P-450 reductase was measured using NADPH (200 μM) as electron donor (45) in a Beckman DU 640 spectrophotometer (Beckman Coulter, Fullerton, CA). Reactions were carried out at 37 °C, and were initiated by addition of the S9 supernatants. Varying amounts of supernatants, from 10 to 40 μl, were used to insure linearity of rates with protein concentration. Enzyme activities were calculated as nmoles cytochrome c reduced/min/mg protein, based on the initial rate of change in OD at 550 nm and an extinction coefficient for cytochrome c of 21.1 mM/cm. Results represent average levels of enzyme activity for three separate cell extractions, ± SD.

NADH recycling Assays Assays were performed with either purified NQO1 (46) or S9 extracts from MCF-7:WS8 cells. For assay using purified NQO1, 1.5 μg of recombinant human NQO1 was mixed with 200-500 μM NADH in 50 mM potassium phosphate buffer pH 7.0. Reactions were initiated by addition of 2-20 μM ß-lap or menadione and the change in absorbance at 340 nM was measured over time. For assays using MCF-7:WS8 S9 extracts, 5 μl of extracts containing approximately 2000 units NQO1 per mg protein were mixed with 200 –500 μM NADH in 50 mM Tris-HCl pH 7.5 containing 0.14% BSA. Reactions were initiated by addition of 5-200 μM ß-lap or menadione and change in absorbance at 340 nM was measured for 10 min. All reactions were also performed in the presence of 10 μM dicoumarol, which inhibited all measurable NQO1 activity.

Flow Cytometry and Apoptotic Measurements Flow cytometric analyses were performed as described (1,2). TUNEL assays, to measure DNA fragmentation during apoptosis, were performed using APO-DIRECT™ as described by the manufacturer (Phoenix Flow Systems, Inc. San Diego, CA.). Samples were read in a EPICS Elite ESP flow cytometer using an air-cooled argon laser at 488 nm, 15 mW (Beckman Coulter Electronics, Miami, FL). Propidium iodide was read at 640 nm using a long pass optical filter and FITC was read at 525nm using a band pass filter. Analysis was performed using the Elite acquisition software provided with the instrument. All experiments were performed a minimum of three times.

Results

We previously showed that the naturally occurring 1,2 naphthoquinone, ß-lap, induced apoptosis in a number of breast cancer cell lines (1,2). As a member of the naphthoquinone family, we hypothesized that ß-lap may be a substrate for NQO1 and its toxicity may be influenced by NQO1 expression. We, therefore, tested the effects of dicoumarol on ß-lap-mediated cytotoxicity in MCF-7:WS8 or MDA-MB-468 breast cancer cell lines after a 4 hour pulse of drug. Co-administration of 50 μM dicoumarol during a 4 h pulse of ß-lap caused a significant survival enhancement in MCF-7:WS8 cells (Fig.1). While this protection was dramatic at ß-lap doses of 4-12 μM, the protective effects of dicoumarol were overcome by >14 μM ß-lap. In contrast, MDA-MB-468 cells were relatively resistant (LD_{50} ~ 8 μM, compared with MCF-7:WS8, LD_{50} ~ 4 μM) to ß-lap alone and were not significantly protected by dicoumarol (Fig. 1). Since MDA-MB-468 cells do not express NQO1 (Table I and Fig. 3) and dicoumarol significantly protected NQO1-expressing MCF-7:WS8 cells (Table I and Fig. 3), these data suggested that NQO1 expression was a critical determining factor in ß-lap-mediated cytotoxicity.

We then extended these studies to compare the relative toxicity of menadione (2-methyl-1,4-naphthoquinone) to ß-lap, either alone or in the presence of dicoumarol. Three breast cancer cell lines (T47D:A18, MDA-MB-468 and MCF-7:WS8) were treated with a 4 h pulse of drugs and relative growth was

measured 7 days later (Fig. 2). Dicoumarol significantly inhibited ß-lap toxicity in MCF-7:WS8 and T47D:A18 cells. In contrast, dicoumarol showed little or no protective effect in MDA-MB-468 cells (Compare graphs A,C & E in Fig. 2).

In a parallel experiment using menadione, alone or with dicoumarol, the relative sensitivities of the cell lines to menadione were opposite those found with ß-lap, MCF-7:WS8 cells were the most resistant to menadione and MDA-MB-468 cells were the most sensitive. Co-administration of dicoumarol caused a significant sensitization of MCF-7:WS8 cells to menadione toxicity, with a decrease in the relative IC_{50} from 12 to 3 μM. MDA-MB-468 cells, which were inherently more sensitive to menadione, were unaffected by dicoumarol co-administration. T47D:A18 cells were only minimally sensitized to menadione exposure when dicoumarol was co-administered (compare graphs B, D & F, Fig. 2). These data were consistent with NQO1 expression (Fig. 3), where NQO1 protein levels were high in MCF-7:WS8 cells, moderate in T47D:A18 cells and undetectable in MDA-MB-468 cells. NQO1 enzyme activities were consistent with protein levels (Compare Fig. 3 and Table I). Using these cell extracts we showed that ß-lap could substitute for menadione in this *in vitro* assay demonstrating that the compound was a suitable NQO1 substrate in intact cells (Fig.9 and data not shown). These data demonstrated that both menadione and ß-lap could serve as substrates for NQO1-mediated reduction and suggested that the end results of these reductions were opposite (i.e., menadione was inactivated by reduction and ß-lap was activated by reduction).

We previously showed that apoptosis in various human breast cancer cell lines induced by ß-lap administration was unique, in that it caused a pattern of PARP and p53 cleavages distinct from that induced by other caspase-activating agents. After ß-lap treatment, we observed a 60 kDa PARP fragment, which was likely due to the activation of the neutral, calcium-dependent protease, calpain[2]. To investigate the effect of dicoumarol on this cleavage pattern in MCF-7:WS8 cells, we treated cells with a 4 h pulse of 8 μM ß-lap alone, or in the presence of 50 μM dicoumarol. Cells were lysed 20 h later and PARP cleavage monitored. We also investigated the effects of 1 μM staurosporine treatment, in order to determine if dicoumarol could block classic apoptotic proteolysis, or if it was specific for ß-lap-induced apoptosis. As seen in Fig. 4, dicoumarol completely abrogated atypical PARP cleavage after ß-lap exposure, but had no effect on staurosporine-induced classic PARP cleavage (i.e., formation of an 89 kDa PARP fragment (47)) in MCF-7:WS8 cells. The fact that dicoumarol significantly protected NQO1-expressing cells from ß-lap-mediated apoptosis strongly suggested a role for NQO1 in ß-lap toxicity. However, previous studies indicated that dicoumarol may also inhibit other cellular enzymes (48).

In order to definitively demonstrate the role of NQO1 in ß-lap toxicity, we utilized the NQO1-negative, ß-lap-resistant, MDA-MB-468 cell line to determine if exogenous expression of NQO1 could sensitize these cells to ß-lap. We stably transfected MDA-MB-468 cells with a constitutive NQO1 expression vector under the control of a CMV promoter. We also performed a parallel transfection using

the empty vector, pcDNA3. Following selection of a pooled population of G418 resistant cells, we isolated a number of clones by limiting dilution subcloning, as described in Experimental Procedures. NQO1 expression in isolated clones was then determined by Western blot analyses (Fig. 5) and enzyme assays (Table II). In all cases, enzyme activity correlated with protein expression. As shown in Fig. 5 and Table II, the empty vector-containing clones did not demonstrate measurable NQO1 expression, as observed with parental, non-transfected cells (see lanes 2, 3 & 4). Of the ten clones isolated from the NQO1 transfections, nine exhibited NQO1 expression. Clone NQ-2 (lane 6) showed no measurable NQO1 expression.

We tested a number of the clones for ß-lap and menadione sensitivity. Growth inhibition was measured after a 4 h pulse of drugs, either alone or in the presence of 50 μM dicoumarol. Relative growth of ß-lap-treated, compared to control, (T/C) cells was determined seven days after drug exposures, using DNA amount per well as an indicator of cell growth. In all cases, expression of NQO1 led to a marked increase in sensitivity to ß-lap (see Fig 6A). Co-administration of 50 μM dicoumarol selectively inhibited ß-lap toxicity in all clones which expressed NQO1. Dicoumarol did not affect the relatively more ß-lap-resistant Vec-3 or NQ-2 clones, which did not express NQO1.

Opposite results were observed after menadione treatments. Cells expressing NQO1 were more resistant to menadione than NQO1-negative clones and resistance could be ameliorated by dicoumarol co-administration (data not shown). To demonstrate that this effect was not due simply to transient growth inhibition,

we also measured clonogenic survival of the Vec-3, NQ-3 and NQ-7 clones after 4 h treatment with ß-lap alone, or in the presence of 50 μM dicoumarol (Fig. 6B). Relative survival closely mimicked growth inhibition, demonstrating the sensitizing effect of NQO1 expression on ß-lap cytotoxicity. These data clearly established that NQO1 activity was critical for the acute toxicity of ß-lap.

To confirm that cell death occurred due to the induction of apoptosis in the NQO1 transfectants, we used TUNEL assays to measure DNA fragmentation due to apoptosis after ß-lap treatment. Cells were treated with a 4 h pulse of 8 μM ß-lap alone, or in combination with 50 μM dicoumarol, harvested 48 h later, and monitored for apoptosis using TUNEL assays, where terminal deoxynucleotide transferase-mediated FITC-dUTP incorporation was measured. As shown in Figure 7B , Vec-3 cells showed less than 2% TUNEL positive (apoptotic) cells after ß-lap treatment. All NQO1 expressing clones showed between 30% and 70% TUNEL positive cells. Dicoumarol co-administration completely blocked apoptotic-related DNA fragmentation in all the NQO1-expressing MDA-MB-468 clones. These findings further demonstrated that while certain aspects of ß-lap cytotoxicity were unique, (e.g., atypical PARP cleavage), other aspects conform to the classic apoptotic pathway (e.g., DNA fragmentation, as measured by TUNEL assays and the presence of a sub-G_0/G_1 cell population (2)).

We next utilized a number of the NQO1-expressing MDA-MB-468 clones to determine if cytotoxicity equated with corresponding increases in atypical apoptotic proteolysis, as measured by PARP and p53 cleavage. NQO1-expressing

clones were exposed to 4 μM or 8 μM ß-lap for 4 h and cell lysates were prepared 48 h later. As observed in Fig. 8A, clones with NQ01 expression, (i.e., NQ-1, NQ-3, NQ-6 and NQ-7) demonstrated a prevalent 60 kDa PARP cleavage fragment after exposure to 8 μM ß-lap. The NQO1 negative clone, Vec-3, exhibited no PARP cleavage at either ß-lap doses. We noted cleavage of p53 (resulting in an ~ 40 kDa fragment) at the same ß-lap doses which gave rise to the 60 kDa PARP fragment. Cells exposed to 10 μM menadione ± dicoumarol showed an opposite pattern, as monitored by p53 and PARP cleavage (Fig. 8B and data not shown). Dicoumarol enhanced p53 cleavage after menadione exposure. Importantly, NQO1 expression also lead to resistance to menadione-induced p53 cleavage, which could be reversed by co-administration of dicoumarol. Previous studies from our laboratory suggested that both the PARP and p53 cleavage events were the result of activation of the calcium-dependent protease, calpain[2].

To further characterize the nature by which ß-lap could serve as a substrate for NQO1, we measured NADH oxidation using a modified *in vitro* assay. Using purified recombinant human NQO1, or cell extracts containing NQO1, we measured the oxidation of NADH in the presence of either menadione or ß-lap. This assay was different from that used to measure NQO1 activity in cell lysates (described in Tables I & II), in that a terminal electron acceptor (i.e., cytochrome c) was not included in the reaction. If the substrates (menadione or ß-lap) were utilized once in the enzyme reaction, the compounds could not reduce a terminal electron acceptor and would thereby presumably accumulate in their respective

hydroquinone forms. This would result in oxidation of 1 mole of NADH per mole of quinone reduced. As expected, menadione reduction resulted in the oxidation of 1-3 moles of NADH per mole of menadione in 2 min and 3-4 moles of NADH per mole of menadione in 5 min using S9 extracts from MCF-7:WS8 or NQ-3 cells (Fig 9 and data not shown). ß-Lap resulted in the oxidation of 10-20 moles of NADH per mole of ß-lap in 2 min and 50-60 moles of NADH per mole of ß-lap in 5 minutes (Fig. 9). The relative NADH oxidation with ß-lap may be an underestimate of ß-lap-mediated NADH oxidation, due to exhaustion of reduced NADH at later timepoints. Using purified NQO1 this effect was even more pronounced, giving rise to oxidation of 10 moles of NADH per mole of ß-lap in 10 sec and 100 moles of NADH per mole of ß-lap in 10 min (data not shown). These results strongly suggest that the hydroquinone form of ß-lap is unstable and rapidly undergoes auto-oxidation to the parent quinone, which can again serve as substrate for reduction by NQO1.

Discussion

We demonstrated that ß-lap cytotoxicity is dependent upon the expression of the obligate two-electron reductase, NQO1. Dicoumarol, an NQO1 inhibitor, significantly protected NQO1-expressing breast cancer cell lines against all tested aspects of ß-lap toxicity, including cell death. Overall, NQO1 expression correlated well with sensitivity of various breast cancer cell lines to the effects of ß-lap. Use of the redox cycling compound menadione, which is detoxified by NQO1, demonstrated that the protection offered by dicoumarol is not the result of a global apoptotic inhibition, since dicoumarol significantly enhanced the cytotoxicity of menadione, in cells which expressed NQO1 (Fig. 2). Dicoumarol also did not influence staurosporine-induced apoptosis. In addition, the relative sensitivities of the cell lines to menadione were opposite those of ß-lap, demonstrating that the ß-lap-sensitive cells were not merely sensitive to unrelated cytotoxic compounds. Exogenous expression of NQO1, in NQO1-deficient MDA-MB-468 cells, shifted the LD_{99} from >10 μM to less than 4 μM. While this shift may appear modest, the dose-response curves for both growth inhibition and survival after ß-lap treatment were extremely steep. At 4 μM ß-lap, 60% of the NQO1-negative cells survived, whereas less than 0.05% survival was noted in cells transfected with NQO1. A similarly steep curve was noted with growth inhibition, where treatment with 4 μM ß-lap lead to greater than 90% growth in the NQO1-negative cells and undetectable

growth in the NQO1-expressing cells. In both survival and growth measurements, addition of 50 μM dicoumarol protected NQO1-expressing cells completely and resulted in values nearly equal to that observed in untreated cells. While these findings suggest that ß-lap should show considerable activity against NQO1 expressing tumors, the dose-response curves indicate that the overall drug exposure will undoubtedly need to be closely monitored if this drug is to prove clinically useful.

ß-Lap may be activated by NQO1 in a manner analogous to that of MMC or EO9 (49,50). However, unlike MMC (51) there is no indication of direct DNA damage by ß-lap as assessed by p53 induction, alkaline or neutral filter elution, or covalent complex protein-DNA formation (2,52,53). Most specific demonstrations of ß-lap activity have come from *in vitro* assays. For example, topoisomerase IIα-mediated DNA damage has been observed *in vitro* after treatment with either ß-lap or menadione (10). However, the expected downstream effects of this damage (e.g., p53 induction, DNA/topoisomerase IIα complexes, etc.) have not been observed (1,2). In addition, we previously showed that topoisomerase I could be inhibited or activated *in vitro* in a manner distinct from that of the classic topoisomerase I inhibitor, camptothecin (1). Neither "cleavable complex" formation (8), nor increases in the steady state levels of wild-type p53 were observed following ß-lap treatment. In contrast, camptothecin, or Topoisomerase IIα inhibitors, caused a dramatic increase in p53, as previously reported (1,54). The observations reported here suggest that ß-lap must either be activated (reduced) to inhibit topoisomerases

I or IIα, or that topoisomerase inhibition is not a necessary component of ß-lap-mediated cytotoxicity.

One particularly unique aspect of ß-lap toxicity is the apparent activation of a novel protease, which we first discerned by observation of an atypical cleavage pattern of the DNA repair protein and apoptotic substrate, PARP[2]. This pattern (giving rise to an ~ 60 kDa fragment, instead of the classic 89 kDa fragment) was unique to ß-lap-mediated apoptosis and correlated well with lethality. In addition, investigation of p53 proteolysis after ß-lap treatment showed a fragment of ~40 kDa (Fig. 7B), which was similar to that previously attributed to calpain activation (55). Calpain has been implicated in apoptosis in a number of systems (56-58) and we hypothesize that calpain is the primary protease activated in ß-lap-mediated cell death[2]. The data regarding the role of calpain as an inducer of apoptosis or simply a component of the execution phase of apoptosis appears to depend upon the cell type and method of apoptosis induction. The demonstration of menadione-induced p53 cleavage (Fig. 8) suggests that this proteolytic pathway is not unique to ß-lap. Enhancement of menadione-mediated proteolysis by dicoumarol suggests that the hydroquinone form of menadione is a nontoxic species, or is rapidly conjugated and excreted from the cell and does not activate this cell death pathway (59). However, when menadione is reduced to the semiquinone, in the absence of NQO1 activity, it can also undergo a futile cycle, leading to the loss of reduced NAD(P)H (60). This futile cycle is less potent than the ß-lap futile cycling, but can be

activated by high concentrations of menadione in NQO1 expressing cells and lower menadione concentrations in cells lacking NQO1 activity.

While reduction of ß-lap appears to be critical for it's cytotoxic effects against breast cancer cells, the mechanism by which reduction of ß-lap leads to toxicity is still unresolved. Our findings regarding the futile cycling of ß-lap suggest a possible component of the cytotoxic mechanism. ß-Lap-mediated exhaustion of NADH in the *in vitro* studies (Fig. 8) suggests that the hydroquinone form of ß-lap is unstable and auto-oxidizes back to the parent compound. In an intact cell this futile cycle would be expected to continue until one of the critical components of the reaction is exhausted (Fig. 10). Since NQO1 can utilize either NADH or NADPH as electron donors, this futile cycle could lead to a substantial loss of NADH and NADPH with a concomitant rise in NAD+ and NADP+ levels. This would have a dramatic effect on any cellular process requiring NADH or NADPH. It is likely that this exhaustion of reduced enzyme co-factors may be a critical factor for the activation of the apoptotic pathway after ß-lap treatment. The downstream consequences of this futile cycle are currently under investigation in our laboratory.

At higher doses of ß-lap (> 10 μM), NQO1-negative cells and NQO1-expressing cells treated with dicoumarol, were killed by ß-lap. This may be due to the production of oxidative stress, as a result of one electron reduction of ß-lap by other enzymes, such as cytochrome b5 reductase and/or cytochrome P450 reductase (61). One electron reduction of ß-lap to the semiquinone would be

expected to cause extensive redox cycling with the formation of various reactive species and previous studies showed that ß-lap caused oxygen radical formation in trypanosomes (62,63). We speculate that ß-lap-mediated free radical formation can be lethal to NQ01-deficient cells, as we previously reported with HL60 cells. The result in these studies was stimulation of a caspase-mediated death pathway (1). This hypothesis is supported by a recent study which showed that ß-lap can induce apoptosis in HL-60 cells through peroxide production (64). Alternatively, other members of the NQO1 family which are insensitive to dicoumarol, such as NQO2 (65,66), may be present and reduce (i.e., activate) ß-lap when administered at high doses. However, we hypothesize that the production of cytosolic free radicals is not a primary mode of cell death in NQO1-expressing cells, since free radical scavengers (e.g., alpha-tocopherol, N-acetyl-L-cysteine (NAC) or pyrrolidinedithiocarbamate (PDTC)) did not significantly affect lethality caused by ß-lap exposure (data not shown). The free radical driven pathways may predominate in NQO1-negative cells or in cells with inactivated NQO1. We propose that when active NQO1 is present, the pathway described in Fig. 10 is primarily responsible for cell death.

Our data identifying the intracellular target of ß-lap as NQ01 may explain the myriad of *in vitro* and *in vivo* responses reported for this compound. ß-Lap exposure synergizes with MMS, ionizing radiation and ultraviolet light irradiation damage (67). We speculate that the synergy between this compound and these DNA damaging agents is related to the induction of NQ01 (cloned as an X-ray-

inducible protein by our laboratory (18) and that of Fornace et. al., (68)). This is further supported by the fact that only posttreatments of 4-5 hours and not pretreatments, with ß-lap caused synergistic cell killing. Induction of ß-lap's target may have been required for synergy and the induction kinetics of NQ01/XIP3 after ultraviolet light or ionizing radiation exposures (i.e., ~2 h) appear to fit this mechanism (18). ß-Lap exposure also prevented the formation of ionizing radiation-inducible secondary neoplastic transformants in Chinese hamster embryo fibroblasts (52). Since NQ01 expression is thought to increase during early stages of neoplastic initiation (possibly due to the permanent induction of a normal stress response, i.e., induction of NQ01) (69,70), it is possible that ß-lap administration selectively eliminates genetically damaged cells that constitutively overexpress this preneoplasic marker (i.e., NQ01). These data suggest that it may be possible to exploit this IR-inducible NQ01 target protein for improved radio-chemo-therapy, which would also result in a significantly lower level of IR-induced secondary carcinogenesis, as was previously reported (52).

Thus, our data strongly suggest that NQ01 expression is a critical determinant of ß-lap-mediated apoptosis and lethality. The connection between the futile cycle of oxidation and reduction of ß-lap by NQ01 and the activation of calpain-mediated apoptosis (Fig. 10) is currently under investigation in our laboratory. Investigation of this drug should shed light on calpain-mediated cell death processes and yield clinical regimens using ß-lap or more efficient drugs in combination with DNA damaging agents (e.g., radiotherapy). Use of this drug

against tumors which overexpress NQ01, such as breast, colon, or lung cancers is indicated. Identification of NQO1 as the intracellular target of ß-lap also suggests the use of this compound for chemoprevention, since NQO1 is commonly elevated during neoplastic progression (43).

Acknowledgments We thank Dr. Dan Gustafson and Dr. Charles Waldren for the NQO1 cDNA expression vector. We also thank Dr. Jill Kolesar and Peter Allen for helpful discussions and Dr. David Ross for critical reading of the manuscript.

References

1. Planchon, S. M., Wuerzberger, S., Frydman, B., Witiak, D. T., Hutson, P., Church, D. R., Wilding, G., and Boothman, D. A. (1995) *Cancer Res.* **55,** 3706-11
2. Wuerzberger, S. M., Pink, J. J., Planchon, S. M., Byers, K. L., Bornmann, W. G., and Boothman, D. A. (1998) *Cancer Res.* **58,** 1876-85
3. Li, C. J., Averboukh, L., and Pardee, A. B. (1993) *J. Biol. Chem.* **268,** 22463-8
4. Boothman, D. A., Greer, S., and Pardee, A. B. (1987) *Cancer Res.* **47,** 5361-6
5. Schuerch, A. R., and Wehrli, W. (1978) *Eur. J. Biochem.* **84,** 197-205
6. Docampo, R., Cruz, F. S., Boveris, A., Muniz, R. P., and Esquivel, D. M. (1979) *Biochem. Pharmacol.* **28,** 723-8
7. Boorstein, R. J., and Pardee, A. B. (1983) *Biochem. Biophys. Res. Commun.* **117,** 30-6
8. Boothman, D. A., Trask, D. K., and Pardee, A. B. (1989) *Cancer Res.* **49,** 605-12
9. Molina Portela, M. P., and Stoppani, A. O. (1996) *Biochem. Pharmacol.* **51,** 275-83
10. Frydman, B., Marton, L. J., Sun, J. S., Neder, K., Witiak, D. T., Liu, A. A., Wang, H. M., Mao, Y., Wu, H. Y., Sanders, M. M., and Liu, L. F. (1997) *Cancer Res.* **57,** 620-7
11. Vanni, A., Fiore, M., De Salvia, R., Cundari, E., Ricordy, R., Ceccarelli, R., and Degrassi, F. (1998) *Mutat Res* **401,** 55-63
12. Manna, S. K., Gad, Y. P., Mukhopadhyay, A., and Aggarwal, B. B. (1999) *Biochem. Pharmacol.* **57,** 763-74
13. Robertson, N., Haigh, A., Adams, G. E., and Stratford, I. J. (1994) *Eur. J. Cancer* **30A,** 1013-9
14. Cadenas, E. (1995) *Biochem. Pharmacol.* **49,** 127-40

15. Ross, D., Beall, H., Traver, R. D., Siegel, D., Phillips, R. M., and Gibson, N. W. (1994) *Oncol. Res.* **6,** 493-500

16. Rauth, A. M., Goldberg, Z., and Misra, V. (1997) *Oncol. Res.* **9,** 339-49

17. Ross, D., Siegel, D., Beall, H., Prakash, A. S., Mulcahy, R. T., and Gibson, N. W. (1993) *Cancer Met. Rev.* **12,** 83-101

18. Boothman, D. A., Meyers, M., Fukunaga, N., and Lee, S. W. (1993) *Proc. Natl. Acad. Sci. USA* **90,** 7200-4

19. Chen, S., Knox, R., Lewis, A. D., Friedlos, F., Workman, P., Deng, P. S., Fung, M., Ebenstein, D., Wu, K., and Tsai, T. M. (1995) *Mol. Pharmacol.* **47,** 934-9

20. Jaiswal, A. K., McBride, O. W., Adesnik, M., and Nebert, D. W. (1988) *J. Biol. Chem.* **263,** 13572-8

21. Radjendirane, V., Joseph, P., Lee, Y. H., Kimura, S., Klein-Szanto, A. J., Gonzalez, F. J., and Jaiswal, A. K. (1998) *J. Biol. Chem.* **273,** 7382-9

22. Marin, A., Lopez de Cerain, A., Hamilton, E., Lewis, A. D., Martinez-Penuela, J. M., Idoate, M. A., and Bello, J. (1997) *Br. J. Cancer* **76,** 923-9

23. Malkinson, A. M., Siegel, D., Forrest, G. L., Gazdar, A. F., Oie, H. K., Chan, D. C., Bunn, P. A., Mabry, M., Dykes, D. J., Harrison, S. D., and et al. (1992) *Cancer Res.* **52,** 4752-7

24. Belinsky, M., and Jaiswal, A. K. (1993) *Cancer Met. Rev.* **12,** 103-17

25. Joseph, P., Xie, T., Xu, Y., and Jaiswal, A. K. (1994) *Oncol. Res.* **6,** 525-32

26. Buettner, G. R. (1993) *Arch. Biochem. Biophys.* **300,** 535-43

27. Ross, D., Thor, H., Orrenius, S., and Moldeus, P. (1985) *Chemico-Biological Interactions* **55,** 177-84

28. Riley, R. J., and Workman, P. (1992) *Biochem. Pharmacol.* **43,** 1657-69

29. Siegel, D., Beall, H., Senekowitsch, C., Kasai, M., Arai, H., Gibson, N. W., and Ross, D. (1992) *Biochemistry* **31,** 7879-85

30. Prakash, A. S., Beall, H., Ross, D., and Gibson, N. W. (1993) *Biochemistry* **32,** 5518-25

31. Fitzsimmons, S. A., Workman, P., Grever, M., Paull, K., Camalier, R., and Lewis, A. D. (1996) *J. Natl. Cancer Inst.* **88,** 259-69

32. Beall, H. D., Murphy, A. M., Siegel, D., Hargreaves, R. H., Butler, J., and Ross, D. (1995) *Mol. Pharmacol.* **48,** 499-504

33. Hollander, P. M., and Ernster, L. (1975) *Arch. Biochem. Biophys.* **169,** 560-7

34. Hosoda, S., Nakamura, W., and Hayashi, K. (1974) *J. Biol. Chem.* **249,** 6416-23

35. Duthie, S. J., and Grant, M. H. (1989) *Br. J. Cancer* **60,** 566-71

36. Akman, S. A., Doroshow, J. H., Dietrich, M. F., Chlebowski, R. T., and Block, J. S. (1987) *J. Pharmacol. Exp. Ther.* **240,** 486-91

37. Thor, H., Smith, M. T., Hartzell, P., Bellomo, G., Jewell, S. A., and Orrenius, S. (1982) *J. Biol. Chem.* **257,** 12419-25

38. Siegel, D., McGuinness, S. M., Winski, S. L., and Ross, D. (1999) *Pharmacogenetics* **9,** 113-21

39. Gustafson, D. L., Beall, H. D., Bolton, E. M., Ross, D., and Waldren, C. A. (1996) *Mol. Pharmacol.* **50,** 728-35

40. Sambrook, J., Fritsch, E. F., and Maniatis, T. (1989) *Molecular Cloning-A Laboratory Manual*, Cold Spring Harbor Laboratory Press, Cold Spring Harbor

41. Pink, J. J., Bilimoria, M. M., Assikis, J., and Jordan, V. C. (1996) *Br. J. Cancer* **74,** 1227-36

42. Labarca, C., and Paigen, K. (1980) *Anal. Biochem.* **102,** 344-52

43. Siegel, D., Franklin, W. A., and Ross, D. (1998) *Clin Cancer Res* **4,** 2065-70

44. Hollander, P. M., Bartfai, T., and Gatt, S. (1975) *Arch. Biochem. Biophys.* **169,** 568-76

45. Strobel, H. W., and Dignam, J. D. (1978) *Methods Enzymol* **52,** 89-96

46. Beall, H. D., Mulcahy, R. T., Siegel, D., Traver, R. D., Gibson, N. W., and Ross, D. (1994) *Cancer Res.* **54,** 3196-201

47. Kaufmann, S. H., Desnoyers, S., Ottaviano, Y., Davidson, N. E., and Poirier, G. G. (1993) *Cancer Res.* **53,** 3976-85

48. Preusch, P. C., Siegel, D., Gibson, N. W., and Ross, D. (1991) *Free Radic. Biol. Med.* **11,** 77-80

49. Siegel, D., Gibson, N. W., Preusch, P. C., and Ross, D. (1990) *Cancer Res.* **50,** 7483-9

50. Keyes, S. R., Fracasso, P. M., Heimbrook, D. C., Rockwell, S., Sligar, S. G., and Sartorelli, A. C. (1984) *Cancer Res.* **44,** 5638-43

51. Hess, R., Plaumann, B., Lutum, A. S., Haessler, C., Heinz, B., Fritsche, M., and Brandner, G. (1994) *Toxicol. Lett.* **72,** 43-52

52. Boothman, D. A., and Pardee, A. B. (1989) *Proc. Natl. Acad. Sci. USA* **86,** 4963-7

53. Boothman, D. A., Wang, M., Schea, R. A., Burrows, H. L., Strickfaden, S., and Owens, J. K. (1992) *Int. J. Radiat. Oncol. Biol. Phys.* **24,** 939-48

54. Nelson, W. G., and Kastan, M. B. (1994) *Mol. Cell. Biol.* **14,** 1815-23

55. Kubbutat, M. H., and Vousden, K. H. (1997) *Mol. Cell. Biol.* **17,** 460-8

56. Squier, M. K., and Cohen, J. J. (1997) *J. Immunol.* **158,** 3690-7

57. Wood, D. E., and Newcomb, E. W. (1999) *J. Biol. Chem.* **274,** 8309-15

58. Squier, M. K., Sehnert, A. J., Sellins, K. S., Malkinson, A. M., Takano, E., and Cohen, J. J. (1999) *J. Cell. Physiol.* **178,** 311-9

59. Wefers, H., and Sies, H. (1983) *Archives of Biochemistry & Biophysics* **224,** 568-78

60. Bellomo, G., Jewell, S. A., and Orrenius, S. (1982) *J. Biol. Chem.* **257,** 11558-62

61. Iyanagi, T. (1990) *Free Radical Research Communications* **8,** 259-68

62. Molina Portela, M. P., Fernandez Villamil, S. H., Perissinotti, L. J., and Stoppani, A. O. (1996) *Biochem. Pharmacol.* **52,** 1875-82

63. Docampo, R., Cruz, F. S., Boveris, A., Muniz, R. P., and Esquivel, D. M. (1978) *Arch Biochem Biophys* **186,** 292-7

64. Chau, Y. P., Shiah, S. G., Don, M. J., and Kuo, M. L. (1998) *Free Radic Biol Med* **24,** 660-70

65. Zhao, Q., Yang, X. L., Holtzclaw, W. D., and Talalay, P. (1997) *Proc. Natl. Acad. Sci. USA* **94,** 1669-74

66. Jaiswal, A. K. (1994) *J. Biol. Chem.* **269,** 14502-8

67. Boorstein, R. J., and Pardee, A. B. (1984) *Biochem. Biophys. Res. Commun.* **118,** 828-34

68. Fornace, A. J., Jr., Alamo, I., Jr., and Hollander, M. C. (1988) *Proc Natl Acad Sci U S A* **85,** 8800-4

69. Williams, J. B., Wang, R., Lu, A. Y., and Pickett, C. B. (1984) *Arch. Biochem. Biophys.* **232,** 408-13

70. Farber, E. (1984) *Can J Biochem Cell Biol* **62,** 486-94

Table I

	Enzyme Activities (nmol/min/mg)*		
Cell Line	**NQO1**	**NADH:cytochrome b_5 reductase**	**NADPH:cytochrome P-450 reductase**
MCF-7:WS8	2,600 ± 560	81 ± 18	27 ± 5.0
T47D:A18	82 ± 17	131 ± 35	31 ± 1.0
MDA-MB-468	ND**	100 ± 11	301 ± 7.6

* Units are nanomoles of cytochrome c reduced per minute per milligram of protein.
** ND = NQO1 not detected. The difference in the rate of cytochrome c reduction with and without dicoumarol was not statistically significant, based on Student's t-test.
Values represent averages for two or more separate S9 preparations, ± SD

Table II

Clone	NQO1 Activity*
Vec-3	ND**
NQ-1	7400 ± 1200
NQ-2	ND**
NQ-3	9300 ± 500
NQ-6	16,500 ± 2700
NQ-7	12,000 ± 700

* Units are nanomoles of cytochrome c reduced per minute per milligram of protein.
** ND = NQO1 not detected. The difference in the rate of cytochrome c reduction with and without dicoumarol was not statistically significant, based on Student's t-test.
Values represent averages for two or more separate S9 preparations, ± SD.

Figure Legends

FIG. 1. Co-administration of dicoumarol protects MCF-7:WS8, but not MDA-MB-468, cells from ß-lap-mediated cytotoxicity. Cells were seeded into 60 mm dishes (10,000 and 1000 cells/dish, in triplicate) and allowed to attach overnight. Cells were then exposed to a 4 h pulse of ß-lap either alone (—■—) or with 50 µM dicoumarol (▪▪◇▪▪). Media were removed, fresh drug-free media were added and cells were allowed to grow for 10 days. Plates were then washed and stained with crystal violet in 50% methanol. Colonies of greater than 50 normal-appearing cells were then counted and plotted v. ß-lap concentration. Shown is the mean (± SEM) of triplicate plates from two independent experiments .

FIG. 2 Relative growth inhibition of various breast cancer cell lines by ß-lap or menadione . Cells (A,B: MCF-7:WS8 C,D: T47D:A18 and E,F: MDA-MB-468) were seeded into 96 well plates (1500 cells/well) and allowed to attach overnight. Media containing drugs (ß-lap in A,C &E ;menadione in B,D & F), either alone (—●— ß-lap, —■— menadione) or in the presence of 50 µM dicoumarol(··○·· ß-lap, ··□·· menadione) , were then added for 4h. Media were then removed, fresh drug-free media were added and the cells were allowed to grow for an additional 7 days. Relative DNA per well was then determined by

Hoescht 33258 fluorescence and relative growth (treated / control DNA) was plotted. Each point represents the mean of four independent wells ± SEM.

FIG. 3 NQO1 expression in various breast cancer cell lines. Whole cell extracts were prepared from exponentially growing cell lines. Equal protein was loaded into each lane and confirmed by Ponceau S staining. Proteins were separated by standard 10% SDS-PAGE, transferred to Immobilon P and probed with medium from an anti-NQO1 hybridoma followed by HRP conjugated anti-mouse secondary antibody. Signals were visualized using Super Signal reagent as described in Experimental Procedures. Shown is a representative blot from experiments performed at least three times.

FIG. 4 Dicoumarol inhibition of ß-lap-induced atypical PARP cleavage. MCF-7:WS8 cells were treated with a 4 h pulse of 8 μM ß-lap (ß, lanes 3 & 4) or a 24 h pulse of 1 μM staurosporine (S, lanes 5 & 6) either alone or with 50 μM dicoumarol during the time of drug exposure. Untreated cells (C, lane 1) or cells treated only with 50 μM dicoumarol (C + Dic, lane 2) were included as controls. Whole cell extracts were prepared at 24 h and analyzed using standard western blot techniques as described for FIG. 3. The blot was probed with the C-2-10 anti-PARP monoclonal antibody followed by HRP-conjugated anti-mouse secondary antibody and visualized with Super Signal reagent. Shown is a representative blot from experiments performed at least three times.

FIG. 5 NQO1 protein expression in MDA-MB-468 transfectants. Whole cell extracts were prepared from exponentially growing parental MCF-7:WS8 and MDA-MB-468 cells, 2 control vector alone MDA-MB-468 transfectants and 10 NQO1 expression vector MDA-MB-468 transfectants. Equal amounts of protein were analyzed by standard western blot techniques as described above using anti-NQO1 as described for Fig. 4. Shown is a representative blot from experiments performed at least three times.

FIG. 6 NQO1 expression sensitizes cells to acute ß-lap cytotoxicity. In A: Acute ß-lap toxicity was determined using the control vector MDA-MB-468 transfectant, (clone Vec-3) and 5 NQO1 vector-containing MDA-MB-468 transfectants, as described in Fig 2. Note that clone NQ-2 showed no measurable NQO1 expression (Fig. 5 and Table II). Cells were exposed to a 4 h pulse of a range of ß-lap doses either alone (··○··) or with 50 μM dicoumarol (—●—) and then allowed to grow for an additional 7 days, at which time DNA content for treated (T) cells was measured and plotted relative to control (C) cells. In B: Vec-3 (—■— ; ··□··), NQ-1 (—▲— ; ··△··) and NQ-3 (—●— ; ··○··) cells were treated with a 4 h pulse of a range of ß-lap doses alone (—■— ; —▲— ; —●—) or with 50 μM dicoumarol (··□·· ; ··△·· ; ··○··). Overall survival, as assessed by colony forming ability, was measured after 10 days growth in control media.

Shown is a representative graph from experiments performed at least three times with each group consisting of at least triplicate determinations. Differences between treatments were compared using a two-tailed student's t-test for paired samples and groups having $p<0.01$ compared with ß-lap or dicoumarol alone are indicated by an asterisk *.

FIG. 7 Acute ß-lap-mediated apoptosis requires NQO1 activity. DNA fragmentation was assessed using the TUNEL assay, as described in "Experimental Procedures". Cells were exposed to a 4 h pulse of ß-lap alone or in combination with 50 μM dicoumarol and TUNEL assays were performed to monitor apoptosis 44 h later using the APO-DIRECT™ Kit. Data were analyzed using an EPICS Elite ESP flow cytometer. Shown are the results of one experiment representative of at least three independent assays.

FIG. 8 NQO1 expression sensitizes cells to ß-lap-mediated apoptotic proteolysis and inhibits menadione-mediated apoptotic proteolysis. Apoptotic proteolysis was measured in cells exposed to a 4 h pulse of 8 μM ß-lap alone (ß), 8 μM Menadione alone (M) or in combination with 50 μM dicoumarol (ß + D; & M + D). Whole cell extracts were prepared 44 h after drug treatment and analyzed using standard western blot techniques. In A: PARP cleavage was assessed using the C-2-10 monoclonal antibody, the blots were then stripped and reprobed with the anti-NQO1 antibody. In B: cells were treated with either ß-lap or menadione

for 4 h and then probed with a p53 antibody (DO-1). Equal protein loading was assessed by Ponceau S staining as described in Experimental Procedures. Shown is a representative blot from experiments performed at least three times.

FIG. 9 ß-Lap-mediated NADH oxidation and futile cycling by NQO1-containing cell extracts. S9 extracts prepared from MCF-7:WS8 cells served as a source for NQO1 and were mixed with 500 μM NADH in 50 mM Tris-HCl, pH 7.5, as described in Experimental Procedures. Reactions were initiated by adding ß-lap or menadione and changes in absorbance at 340 nm (NADH absorbs at 340, NAD+ does not) were measured over time for 10 min. Total loss of NADH was then calculated and divided by the concentration of ß-lap or menadione used. This ratio was then plotted as a function of ß-lap or menadione concentration. Shown is a representative graph from experiments repeated at least two times.

FIG. 10 Proposed model for ß-lapachone-mediated cytotoxicity in cells expressing NQO1. In cells which express NQO1, the 1,2 naphthoquinone ß-lap(Q) is reduced to the hydroquinone form (ß-lap(HQ)) using 1 molecule of NADH per reaction. The hydroquinone form of ß-lap is presumably unstable and spontaneously autooxidizes to it's original parent form, likely through a semiquinone intermediate (ß-Lap (SQ•), which can cause redox cycling and oxidative stress. The regenerated parent compound can then serve as substrate for

another round of reduction. This *Futile cycle* causes a rapid and severe loss in reduced NAD(P)H, which ultimately activates of calpain by mechanisms which are not completely understood at present.

Table I

	Enzyme Activities (nmol/min/mg)*		
Cell Line	**NQO1**	**NADH:cytochrome b_5 reductase**	**NADPH:cytochromeP-450 rec**
MCF-7:WS8	2,640.9 ± 555.1	80.6 ± 17.8	27.0 ± 5.0
MDA-MB-231	ND**	97.5 ± 30.9	33.3 ± 13.0
T47D:A18	82.1 ± 17.1	131.3 ± 34.5	31.5 ± 1.0
MDA-MB-468	ND	100.5 ± 11.2	30.9 ± 7.6
Vec-3	ND	82.7 ± 11.6	26.6 ± 4.9
NQ-1	7,409.5 ± 1208.2	-------	----------
NQ-2	ND	-------	---------
NQ-3	9,276.1 ± 490.6	62.2 ± 17.6	40.2 ± 8.0
NQ-6	16,597.6 ± 2706.1	--------	--------
NQ-7	11,836.1 ± 700.8	----------	---------

* Units are nanomoles of cytochrome c reduced per minute per milligram of protein.

** ND = NQO1 not detected. The difference in the rate of cytochrome c reduction with and without dicoumarol was not statistically significant, based on Student's t-test.

Values represent averages for two or more separate S9 preparations, ± SD.

Fig. 1

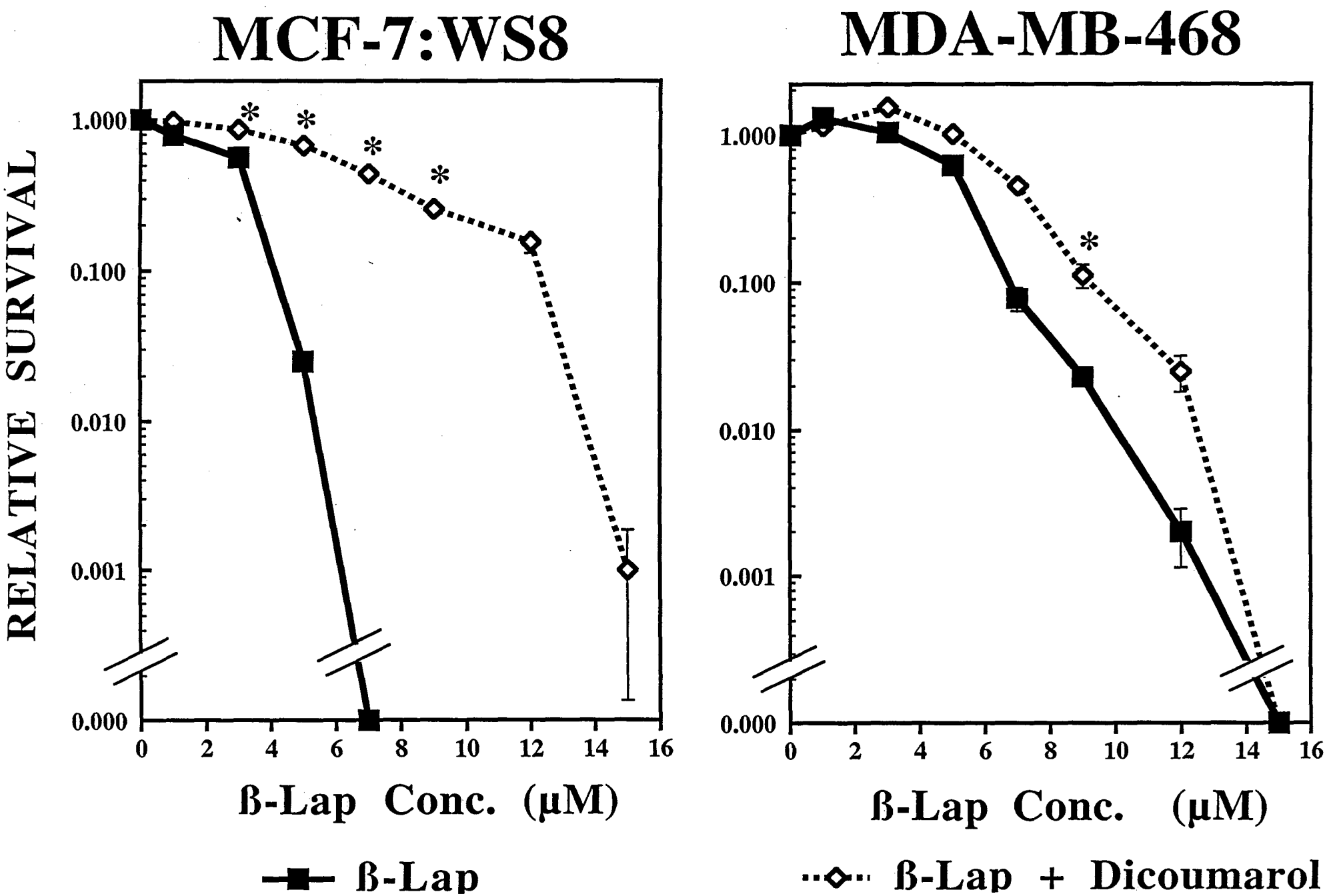
MCF-7:WS8
MDA-MB-468
RELATIVE SURVIVAL
1.000
0.100
0.010
0.001
0.000
0
2
4
6
8
10
12
14
16
ß-Lap Conc. (µM)
ß-Lap
ß-Lap + Dicoumarol

Fig. 2

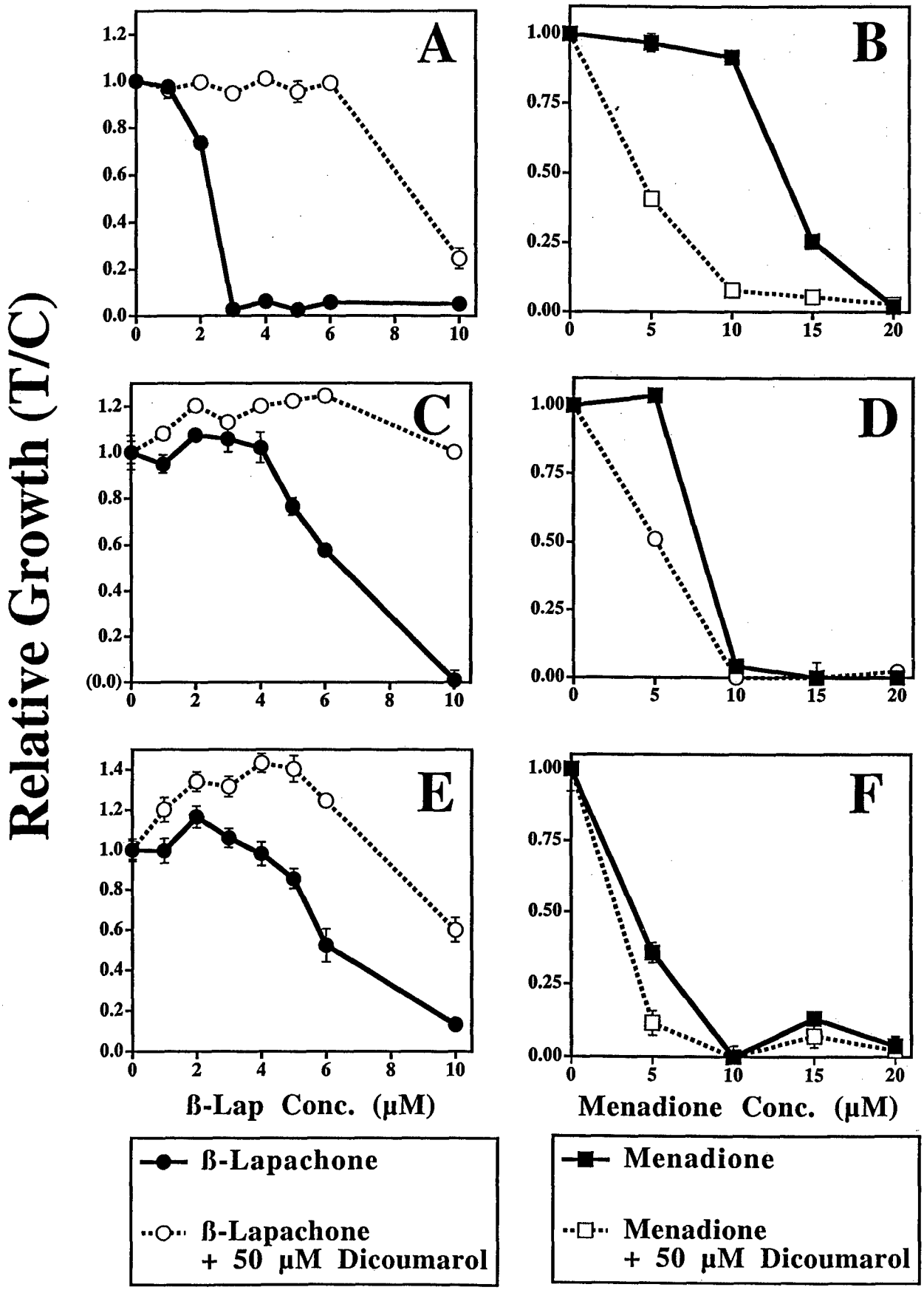
Relative Growth (T/C)
A
B
C
D
E
F
ß-Lap Conc. (µM)
Menadione Conc. (µM)
ß-Lapachone
ß-Lapachone + 50 µM Dicoumarol
Menadione
Menadione + 50 µM Dicoumarol

Fig. 3

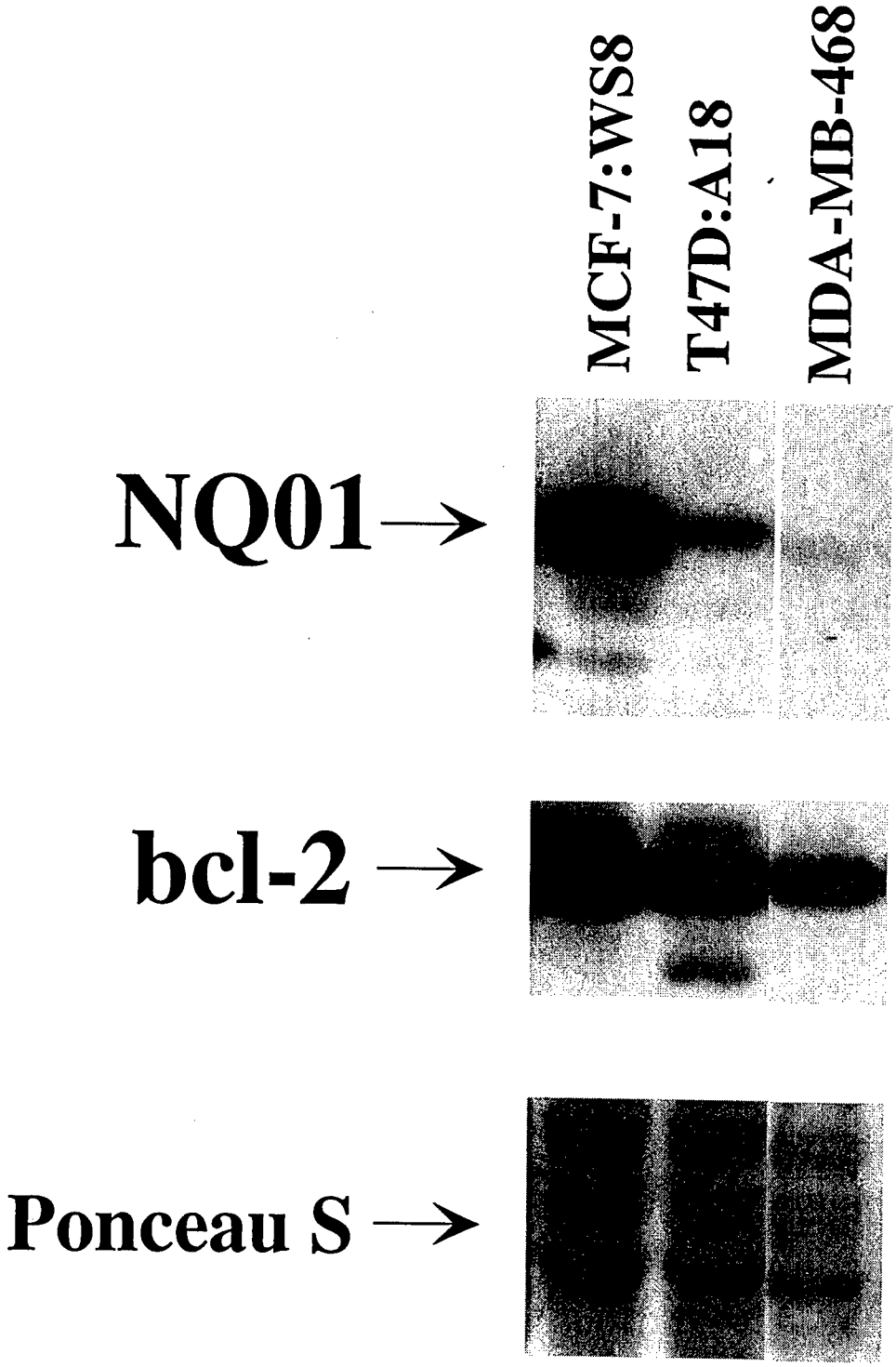

Fig. 4

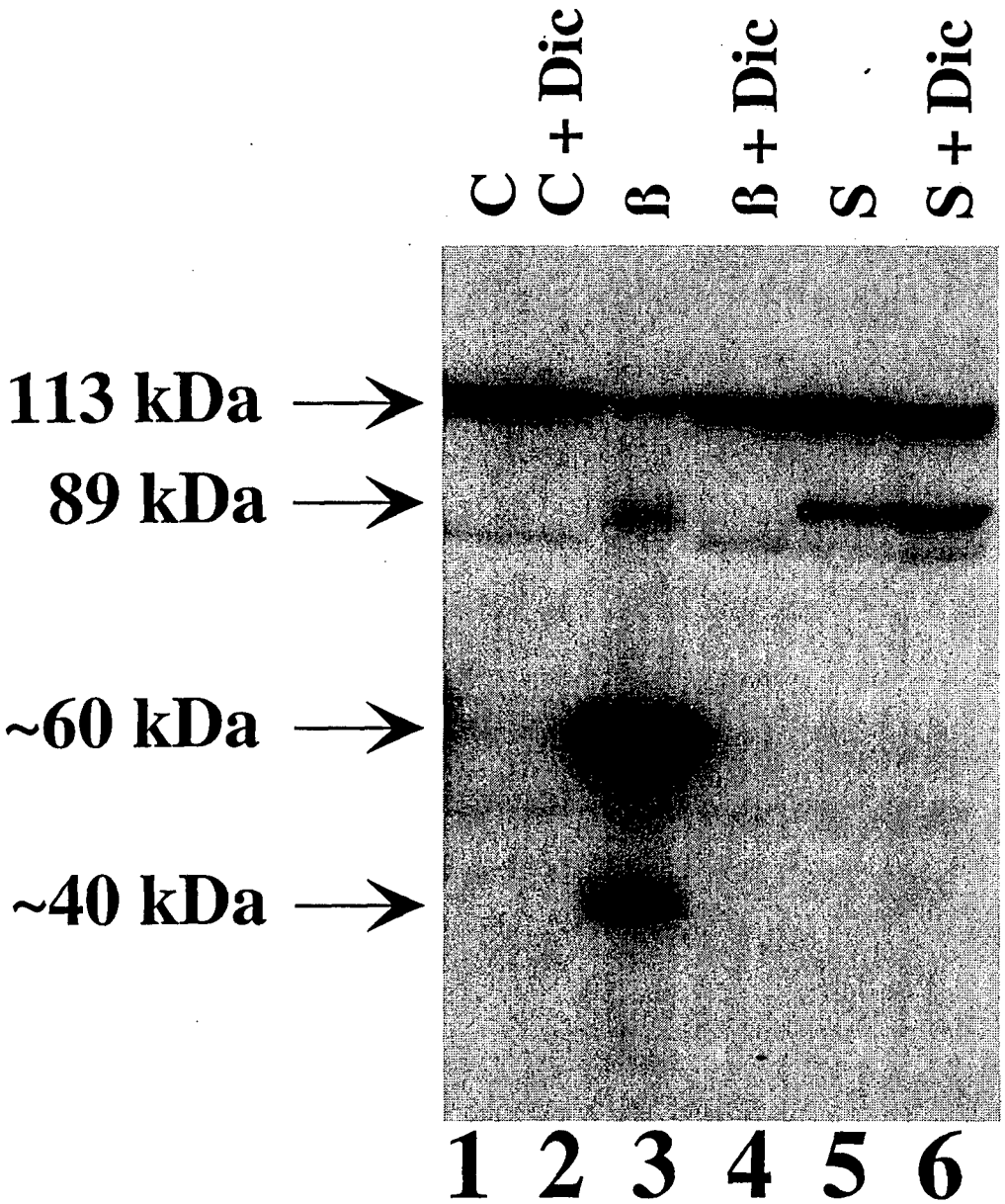

Fig. 5

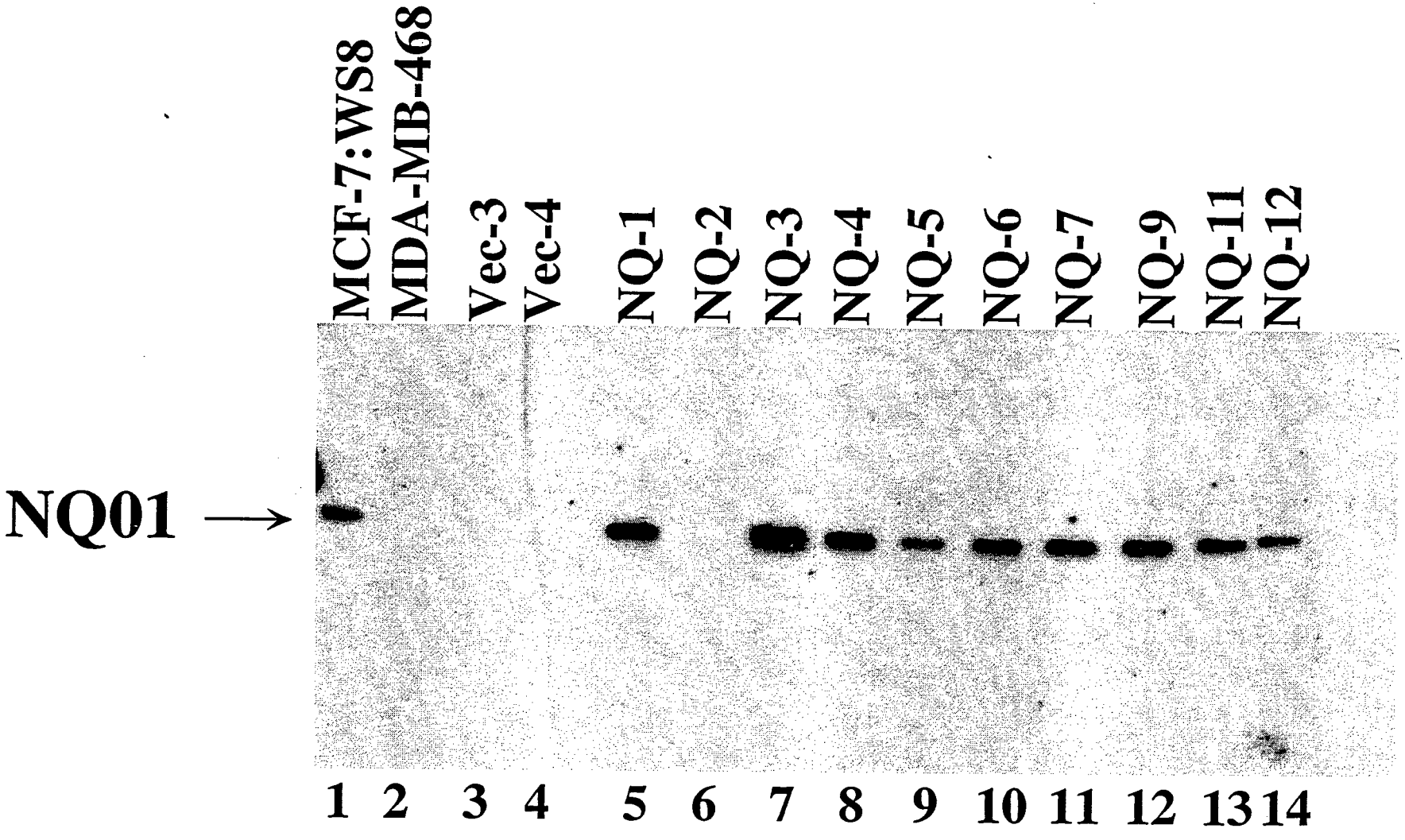
MCF-7:WS8
MDA-MB-468
Vec-3
Vec-4
NQ-1
NQ-2
NQ-3
NQ-4
NQ-5
NQ-6
NQ-7
NQ-9
NQ-11
NQ-12
NQ01
1 2 3 4 5 6 7 8 9 10 11 12 13 14

Fig. 6A

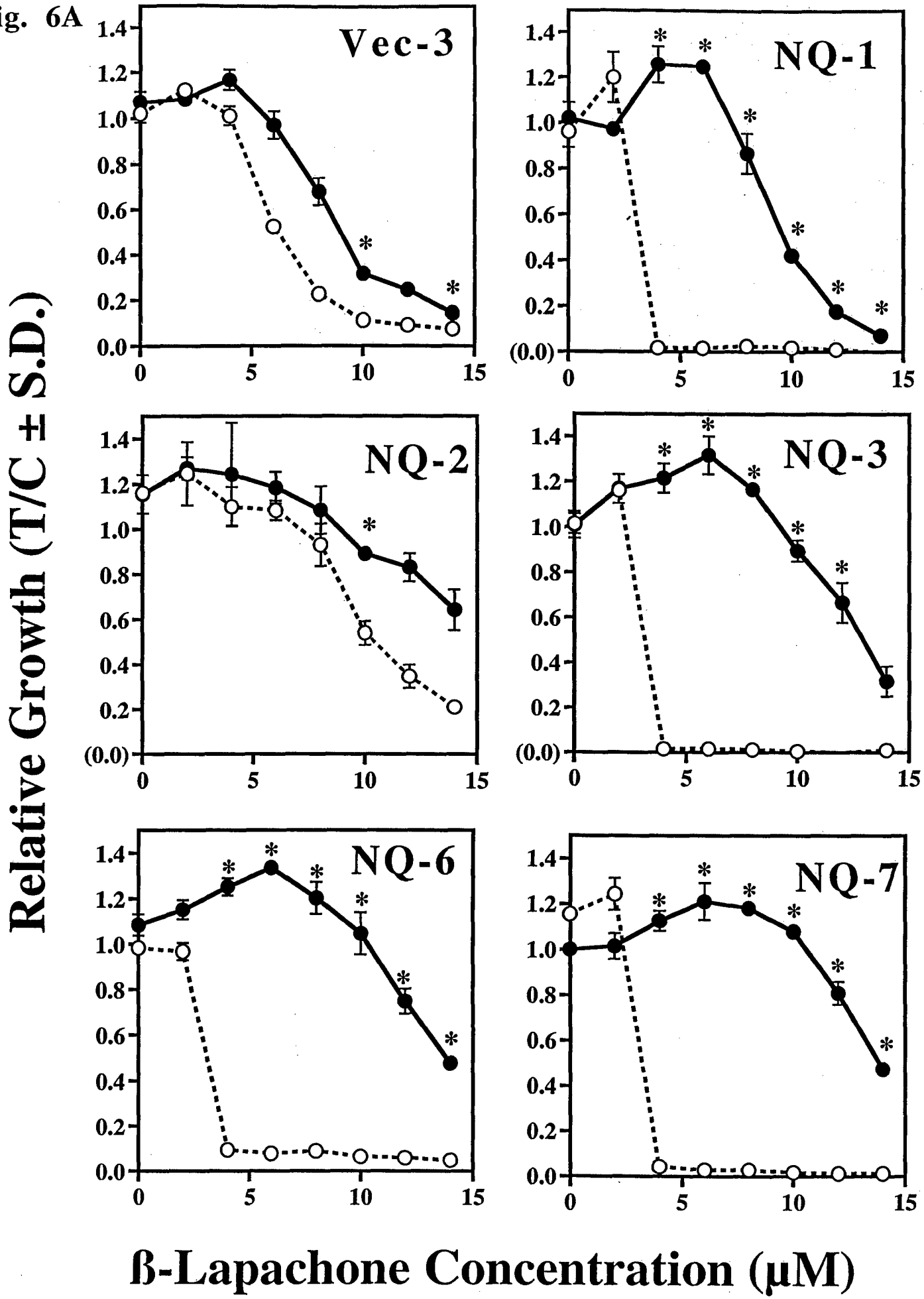
Vec-3
NQ-1
NQ-2
NQ-3
NQ-6
NQ-7
Relative Growth (T/C ± S.D.)
ß-Lapachone Concentration (μM)

FIG. 6B

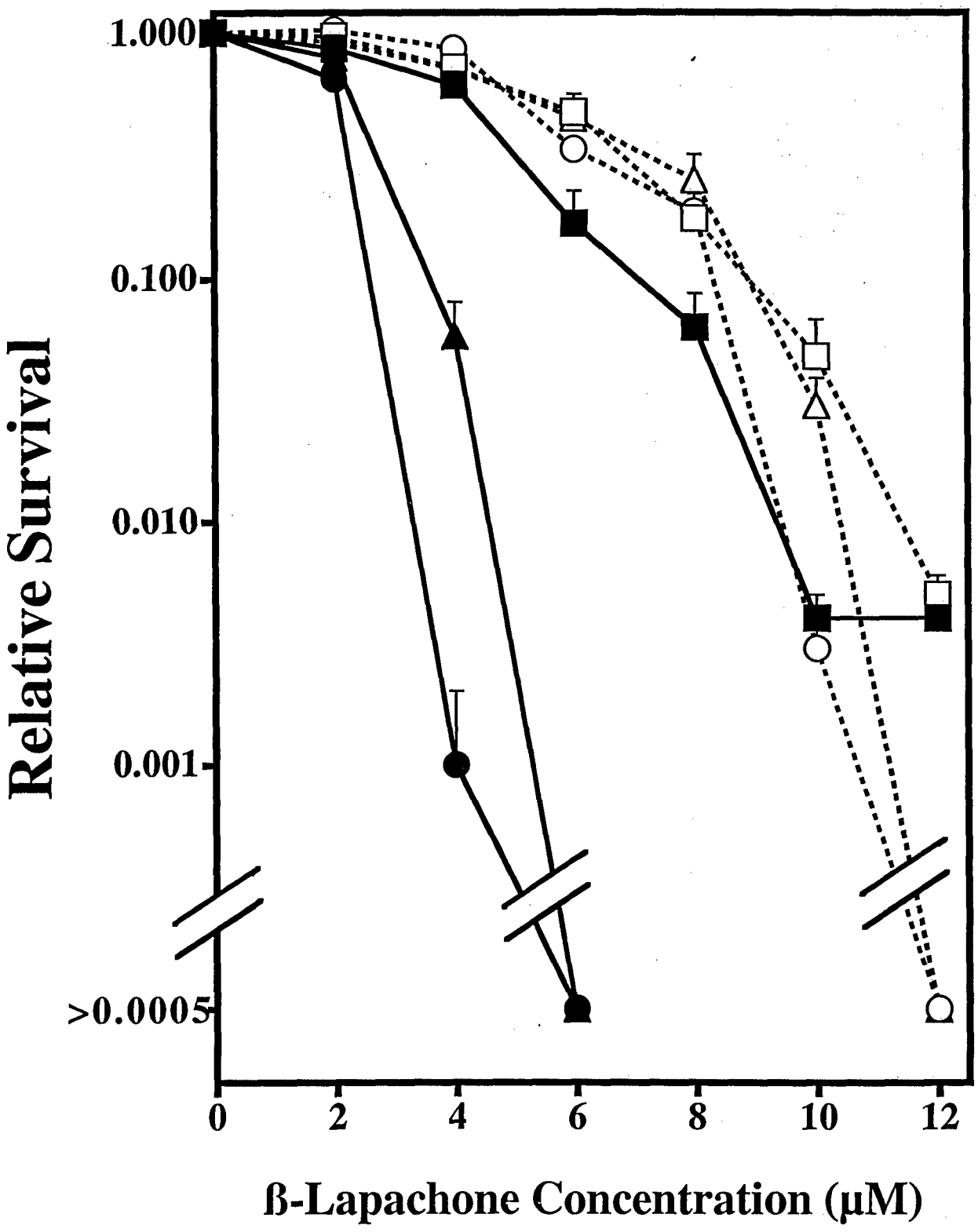
1.000
0.100
0.010
0.001
>0.0005
Relative Survival
0
2
4
6
8
10
12
ß-Lapachone Concentration (μM)

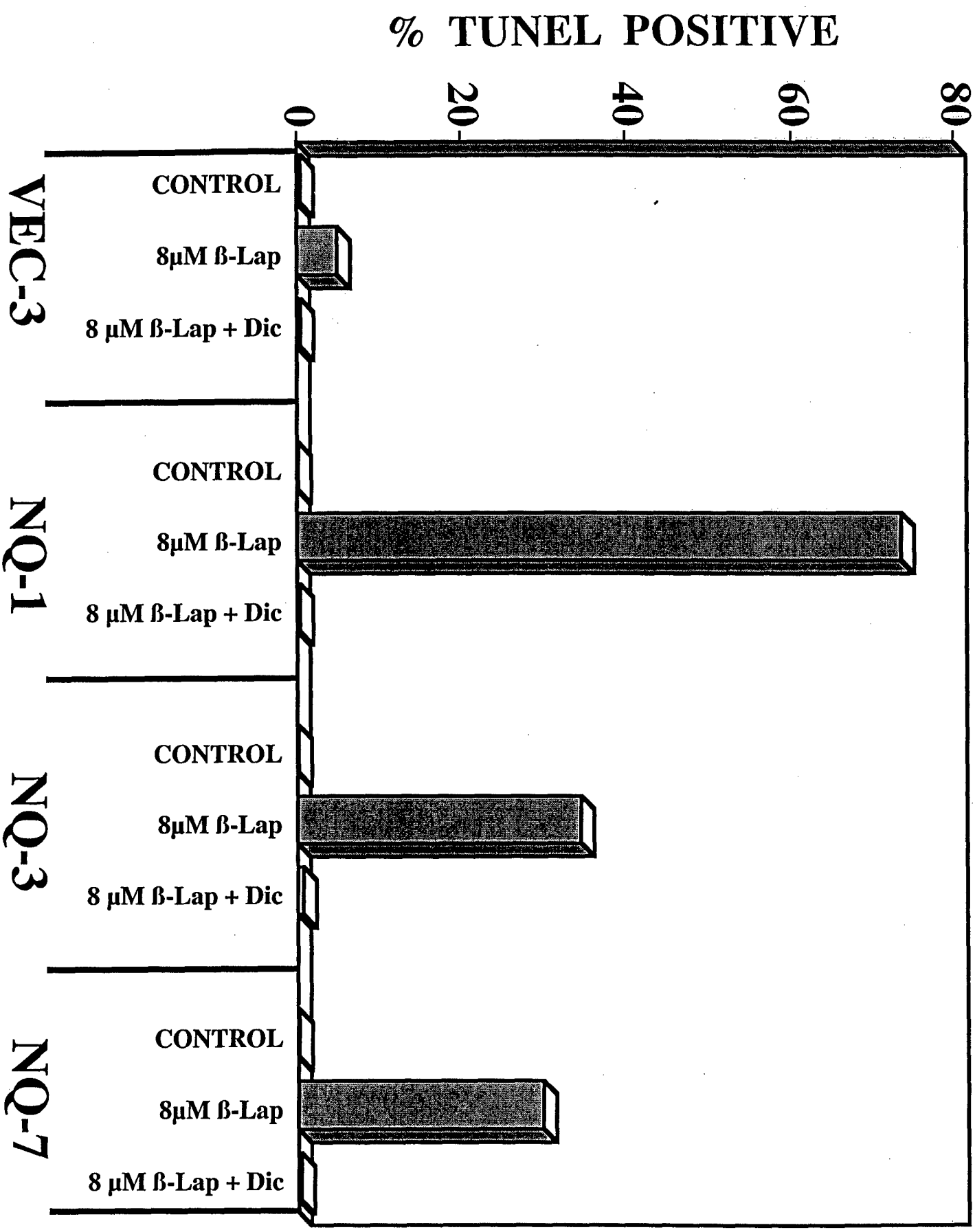
% TUNEL POSITIVE
0
20
40
60
80
VEC-3
CONTROL
8μM ß-Lap
8 μM ß-Lap + Dic
NQ-1
CONTROL
8μM ß-Lap
8 μM ß-Lap + Dic
NQ-3
CONTROL
8μM ß-Lap
8 μM ß-Lap + Dic
NQ-7
CONTROL
8μM ß-Lap
8 μM ß-Lap + Dic

Fig. 8

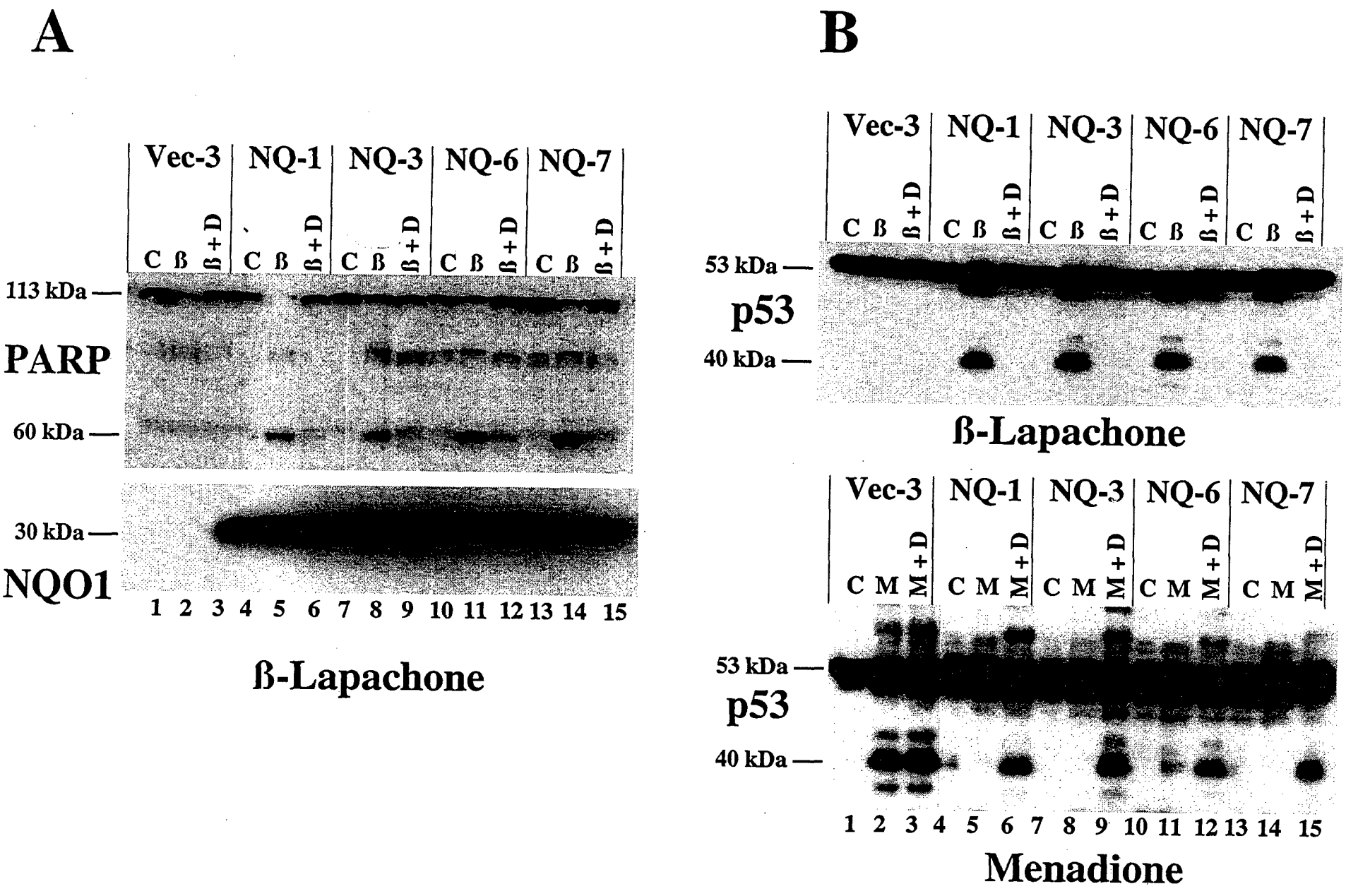
A
Vec-3
NQ-1
NQ-3
NQ-6
NQ-7
C ß ß+D
113 kDa
PARP
60 kDa
30 kDa
NQO1
1 2 3 4 5 6 7 8 9 10 11 12 13 14 15
ß-Lapachone
B
Vec-3
NQ-1
NQ-3
NQ-6
NQ-7
C ß ß+D
53 kDa
p53
40 kDa
ß-Lapachone
C M M+D
53 kDa
p53
40 kDa
1 2 3 4 5 6 7 8 9 10 11 12 13 14 15
Menadione

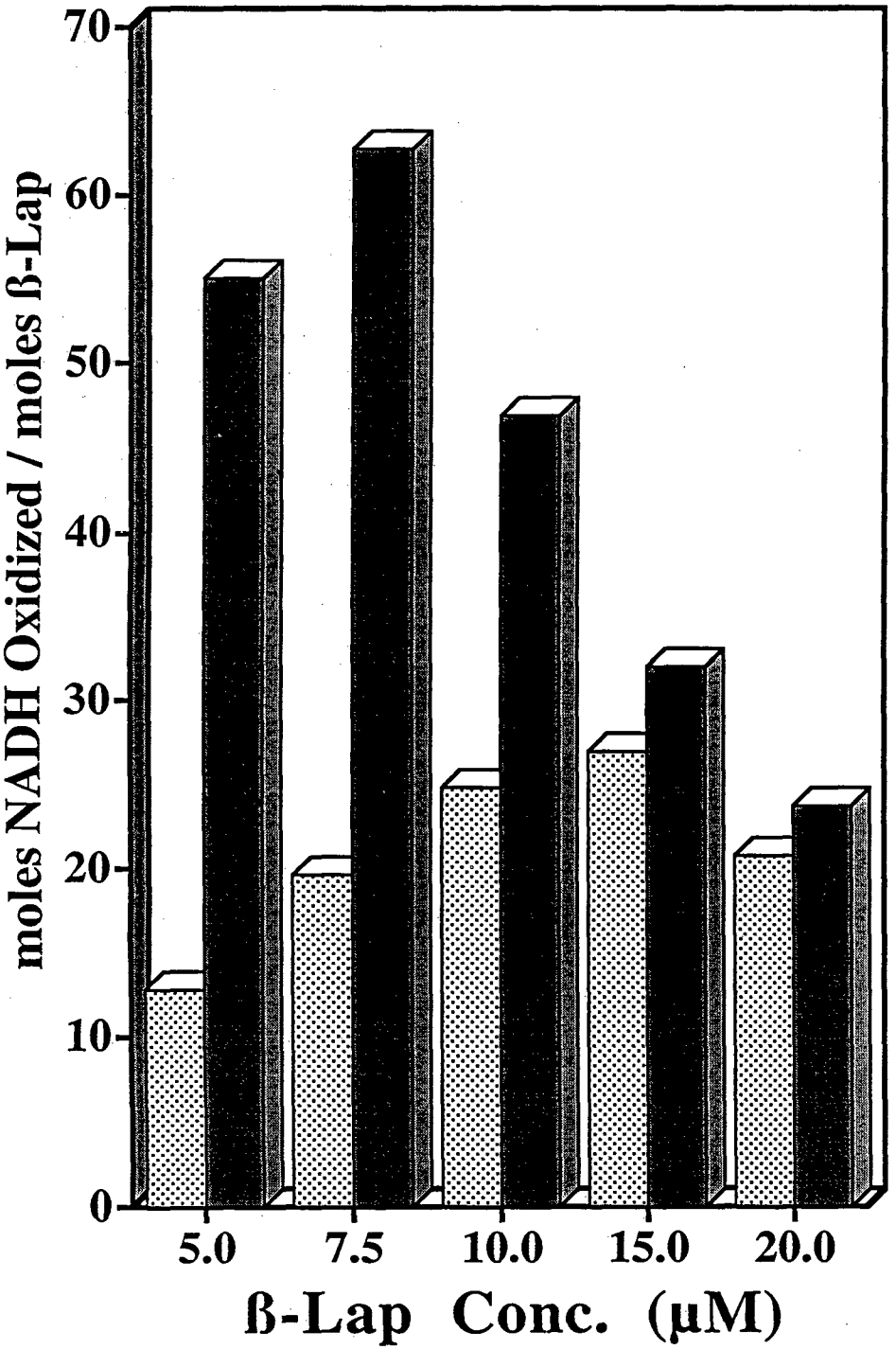
moles NADH Oxidized / moles ß-Lap
70
60
50
40
30
20
10
0
5.0
7.5
10.0
15.0
20.0
ß-Lap Conc. (µM)

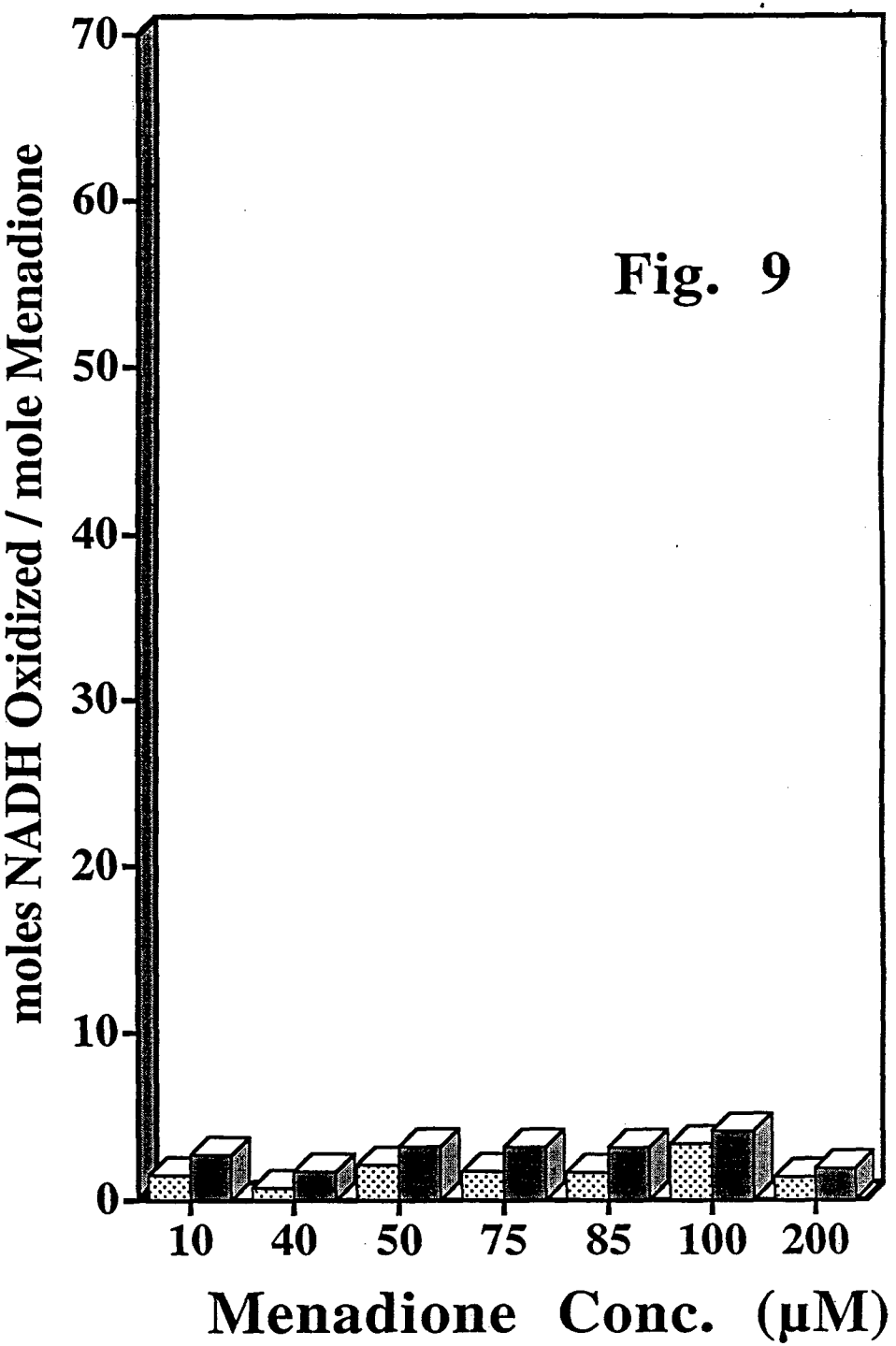
moles NADH Oxidized / mole Menadione
70
60
50
40
30
20
10
0
10
40
50
75
85
100
200
Menadione Conc. (µM)

Fig. 9

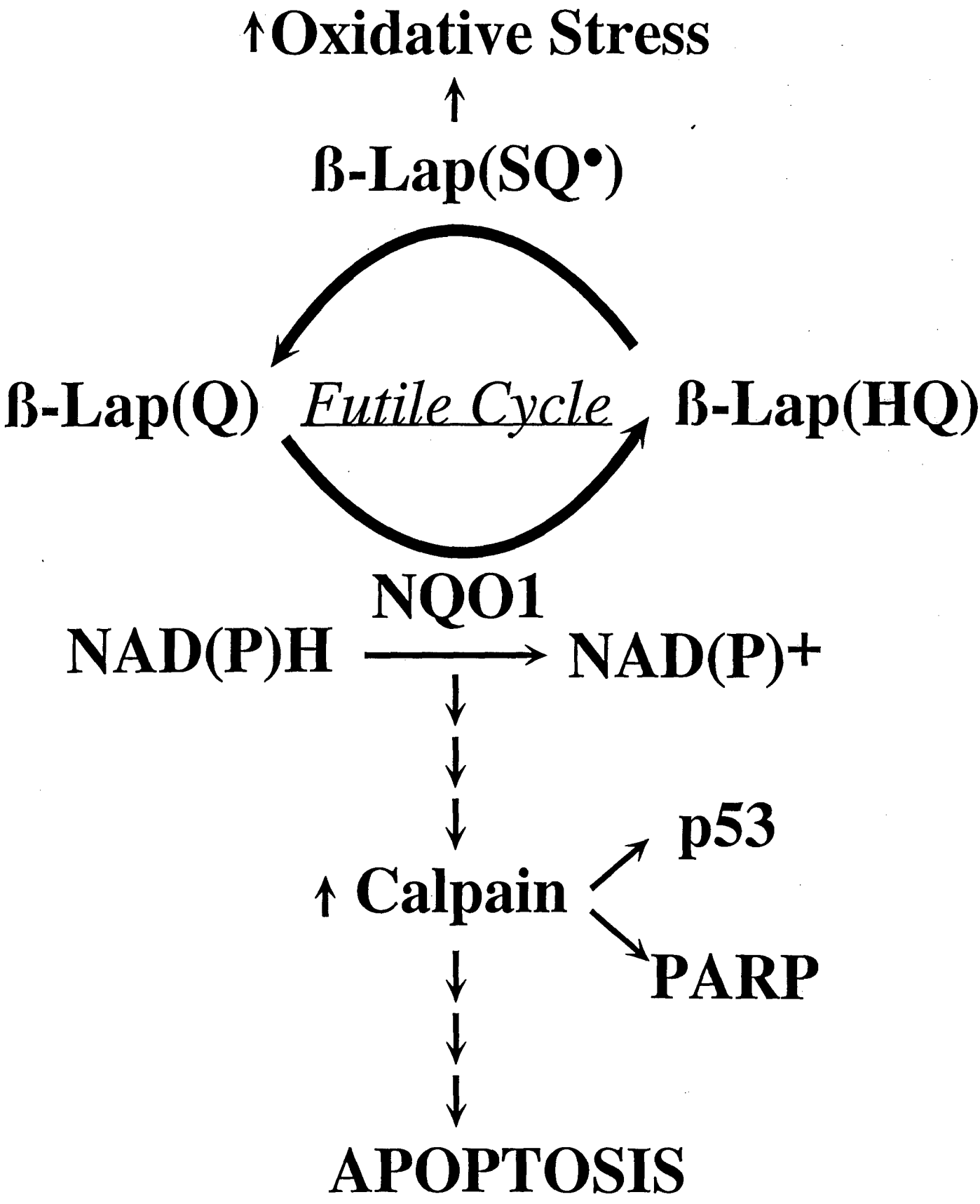
↑Oxidative Stress
↑
ß-Lap(SQ•)
ß-Lap(Q)
Futile Cycle
ß-Lap(HQ)
NQO1
NAD(P)H
NAD(P)+
↑ Calpain
p53
PARP
APOPTOSIS

Biochemical and Biophysical Research Communications 258, 506–512 (1999)
Article ID bbrc.1999.0670, available online at http://www.idealibrary.com on IDEAL®

Niemann–Pick Human Lymphoblasts Are Resistant to Phthalocyanine 4-Photodynamic Therapy-Induced Apoptosis

Duska Separovic,*[,1] John J. Pink,* Nancy A. Oleinick,* Mark Kester,† David A. Boothman,* Maureen McLoughlin,‡ Louis A. Peña,‡ and Adriana Haimovitz-Friedman‡

*Department of Radiation Oncology, Case Western Reserve University School of Medicine, Cleveland, Ohio 44106-4942; †Department of Pharmacology, Pennsylvania State University Milton S. Hershey Medical Center, Hershey, Pennsylvania 17033; and ‡Department of Radiation Oncology, Memorial Sloan-Kettering Cancer Center, New York, New York 10021

Received April 8, 1999

Stress-induced activation of sphingomyelinase (SMase) leading to generation of ceramide, a lipid mediator, has been associated with apoptosis in several malignant and nonmalignant cell lines. Photodynamic therapy (PDT), with the phthalocyanine photosensitizer Pc 4 [HOSiPcOSi(CH$_3$)$_2$(CH$_2$)$_3$N(CH$_3$)$_2$], is an oxidative stress associated with increased ceramide generation and subsequent induction of apoptosis in various cell types. We assessed the role of SMase in photocytotoxicity. Normal human lymphoblasts accumulated ceramide and underwent apoptosis after Pc 4-PDT. In contrast, Niemann–Pick disease (NPD) lymphoblasts, which are deficient in acid sphingomyelinase (ASMase) activity, failed to respond to Pc 4-PDT with ceramide accumulation and apoptosis, suggesting that ASMase may be a Pc 4-PDT target. NPD lymphoblasts were exposed to exogenous bacterial sphingomyelinase (bSMase) to test whether these defects are reversible. Treatment of NPD cells with bSMase itself led to elevated ceramide formation, which did not translate into induction of apoptosis. However, a combination of Pc 4-PDT + bSMase induced a significant apoptotic response. Thus, the combined treatment of Pc 4-PDT + bSMase, rather than bSMase alone, was required to restore apoptosis in NPD cells. These data support the hypothesis that SMase is a proapoptotic factor determining responsiveness of cells to Pc 4-PDT. © 1999 Academic Press

Key Words: **acid sphingomyelinase; apoptosis; ceramide; Pc 4; phthalocyanine.**

Photodynamic therapy is a cancer treatment that uses a photosensitizer, light and oxygen to generate singlet oxygen, as well as other reactive oxygen species (ROS). The formation of ROS in cellular targets results in cell death and tumor ablation (1). PDT, as an oxidative stress, initiates apoptosis *in vitro* (2) and *in vivo* (3). Stress inducers, such as tumor necrosis factor-α, ionizing or UV radiation, heat shock, and H_2O_2, initiate apoptosis via ceramide generation (4–6). We have demonstrated that Pc 4-photodynamic treatment of LY-R mouse lymphoma, U937 human leukemia, or CHO Chinese hamster ovary cells leads to elevated intracellular ceramide levels and subsequent induction of apoptosis. Furthermore, exogenous cell-permeable C2-ceramide mimics the effect of Pc 4-PDT, as evidenced by DNA fragmentation in these cells (7, 8).

Sphingomyelinase (SMase), the enzyme that catalyzes the initial step in the sphingomyelin pathway, can be activated in response to pro-apoptotic stimuli, resulting in the generation of ceramide (9). Several isoforms of SMase have been identified, two of which have been cloned (10, 11). The enzymes are distinguished based upon their pH optima, cellular localization and cation dependence (12). Acid sphingomyelinase (ASMase) requires zinc for its activity and can be found in lysosomes or be secreted, depending on post-translational processing (13, 14). ASMase, as well as

[1] Corresponding author. Department of Radiation Oncology, School of Medicine (BRB-3E), Case Western Reserve University, 10900 Euclid Avenue, Cleveland, Ohio 44106-4942. Fax: 216-368-1142. E-mail: dxs66@po.cwru.edu.

Abbreviations: ASMase, acid sphingomyelinase; bSMase, bacterial sphingomyelinase; C2-ceramide, *N*-acetyl sphingosine; DAG, 1,2-diacyl glycerol; DMF, dimethyl formamide; EBV, Epstein–Barr virus; FBS, heat-inactivated fetal bovine serum; FITC, fluorescein isothiocyanate; LED, light-emitting diode array; LY-R, L5178Y-R mouse lymphoma cells; NSMase, neutral sphingomyelinase; NPD, Niemann–Pick disease; PAGE, polyacrylamide gel electrophoresis; PBS, phosphate-buffered saline; PDT, photodynamic therapy; PI, propidium iodide; ROS, reactive oxygen species; SAPK/JNK, stress-activated protein kinase/c-Jun N-terminal kinase; SDS, sodium dodecyl sulfate; SMase, sphingomyelinase; TdT, terminal deoxynucleotidyl transferase; TLC, thin layer chromatography; TNF-α, tumor necrosis factor-α.

0006-291X/99 $30.00

neutral SMase (NSMase), have been associated with apoptosis in a variety of cells involving various receptors. However, in human lymphoblasts ASMase alone appears to be involved in apoptosis induced by ionizing radiation and Fas (15, 16). To test the role of SMase in Pc 4-PDT-induced apoptosis, cultured Niemann-Pick disease (NPD) human lymphoblasts were used. NPD is an autosomal recessive disorder caused by loss-of-function mutations within the ASMase gene (10). We demonstrate that ASMase deficiency correlates with suppressed ceramide generation and apoptosis after Pc 4-PDT. The defect in apoptotic response is reversed by the combined treatment of Pc 4-PDT and bacterial sphingomyelinase (bSMase).

MATERIALS AND METHODS

Materials. The phthalocyanine photosensitizer Pc 4, HOSiPcOSi-$(CH_3)_2(CH_2)_3N(CH_3)_2$ (17), was supplied by Drs. Ying-syi Li and Malcolm E. Kenney (Department of Chemistry, Case Western Reserve University). *E. coli sn*-1,2-DAG kinase were from Calbiochem (La Jolla, CA), while sphingomyelinase (*S. aureus*) was from Sigma (St. Louis, MO). [γ-^{32}P]ATP (4500 Ci/mmol) was from ICN (Irvine, CA). The cell culture media were supplied by Gibco-BRL (Gaithersburg, MD), while fetal bovine serum was from Intergen (Purchase, NY). The C-2-10 PARP monoclonal antibody was purchased from Enzyme Systems Products (Dublin, CA). The horseradish peroxidase-conjugated secondary antibody was obtained from Santa Cruz Biotechnologies (Santa Cruz, CA). All other chemicals were purchased from Fisher Scientific (Pittsburgh, PA). TLC plates (aluminum sheets of silica gel 60) were from EM Industries (Gibbstown, NJ).

Cell culture and treatments. Both normal and NPD human lymphoblasts (MS1418) were Epstein–Barr virus (EBV)-transformed and were kindly provided by Drs. Edward H. Schuchman and Adriana Haimovitz-Friedman. The cells were cultured in RPMI 1640 supplemented with 5 mM L-glutamine and 15% heat-inactivated fetal bovine serum (FBS). The cells were grown in T-25 flasks maintained upright at 37°C under 5% CO_2 and were subcultured twice weekly at a density of 2×10^5/mL. The lymphoblasts were not maintained in continuous culture for more than two months. For experiments, an aliquot of a stock solution of Pc 4 (0.5 mM in DMF) was added to the cells (5×10^6) in T-25 culture flasks containing 10 mL of a low serum medium (1% FBS + RPMI) to give the desired concentration of 200 nM. After overnight incubation, the cells were irradiated using an LED array (EFOS, Mississauga, Ontario, Canada; λ_{max} ~670-675 nm) and then incubated at 37°C for desired periods of time before harvest. In experiments in which bSMase was used, the enzyme was added to the cells in 0.1% FBS + RPMI medium. Membrane integrity of either of the two cell lines was not significantly affected by the treatments, as assessed by trypan blue dye exclusion.

TUNEL assay (APO-DIRECT) and flow cytometry. The procedures for cell fixation and staining with fluorescein isothiocyanate (FITC)/dUTP, using terminal deoxynucleotidyl transferase (TdT), and propidium iodide (PI), were performed according to the manufacturer's instructions (Phoenix Flow Systems, San Diego, CA). Cells were analyzed by an EPICS ESP flow cytometer (Coulter Corp., Hialeah, FL) in the Flow Cytometry Facility of the Case Western Reserve University/Ireland Comprehensive Cancer Center. Fluorescence measurements were made using the following parameters: 488 nm (excitation), 520 nm (Fluorescein emission) and 623 nm (PI emission). Data analysis was performed using version 4.1 of the instrument software.

Measurement of ceramide level. Ceramide mass was determined by the DAG kinase assay as described previously (8). Following Pc 4-PDT treatment and incubations, cells were extracted with 2 mL chloroform/methanol/1 M HCl (500/500/5, v/v/v). Lipids in the lower phase were dried under nitrogen and subjected to alkaline hydrolysis (0.1 M methanolic KOH for 1 h at 37°C) to remove glycerophospholipids. Samples were reextracted, and lipids from the chloroform-phase extract were quantified by the DAG kinase reaction. Ceramide was resolved by TLC using chloroform/methanol/acetone/glacial acetic acid (50/15/20/10, v/v), and quantified using a PhosphorImager 445 SI (Molecular Dynamics, Sunnyvale, CA) and by comparison to a concomitantly run standard curve comprised of known amounts of ceramide.

Western immunoblot analyses. Whole cell extracts were prepared by direct lysis of PBS-washed cells in lysis buffer [6 M urea, 2% SDS, 10% glycerol, 62.5 mM Tris-HCl (pH 6.8)], sonicated with a fifteen second burst using a Fisher 550 Sonic dismembrator. Equal amounts of protein were heated at 65°C for 10 min and separated by 10% SDS-PAGE. Separated proteins were transferred to Immobilon-P (Millipore, Bedford, MA) membranes using a Multiphor II semi-dry electroblotting device (Pharmacia Biotech, Piscataway, NJ) according to the manufacturer's instructions. Loading equivalence and transfer efficiency were monitored by Ponceau S staining of transferred membranes. Standard western immunoblotting techniques were used to probe for PARP levels as previously described (18). Proteins of interest were visualized with ECL using the Super Signal chemiluminescence reagent (Pierce, Rockford, IL) at 20°C for 5 min. Membranes were exposed to X-ray film and developed.

Cellular uptake of Pc 4. Following a 15-h incubation in 0.1% FBS-RPMI containing [^{14}C] Pc 4 (200 nM; 6.35 μCi/μmol) ± SMase (500 mU/mL), cells (2.5×10^6) were harvested, counted by hemocytometer, and collected on a glass fiber filter (Gelman Scientific, Ann Arbor, MI). The filters were allowed to dry and were placed in scintillation vials. The radioactivity was counted in a L3801 Beckman Liquid Scintillation Counter (Fullerton, CA).

Statistics. Statistical analyses were performed by Student *t*-test and Mann-Whitney test.

RESULTS AND DISCUSSION

The apoptotic response of the two lymphoid cell lines to Pc4-PDT was assessed using the TUNEL assay and flow cytometry. Pc4-PDT induced a dose- and time-dependent increase in apoptosis in normal lymphoblasts (Fig. 1). Apoptosis was not detected before 2 h at the lowest PDT dose (200 nM Pc 4 + 45 mJ/cm^2; data not shown) and was maximal by 6 h at the highest PDT dose (200 nM Pc 4 + 90 mJ/cm^2; data not shown). In contrast, apoptosis was significantly suppressed in the NPD cells after Pc 4-PDT. An increase in the NPD apoptotic cell population was only detected at the highest PDT dose (200 nM Pc 4 + 90 mJ/cm^2) 6 h after treatment. Curiously, the apoptotic response of the normal human lymphoblasts to ionizing radiation (15) and Pc 4-PDT was different, since (i) the peak effect induced by radiation and Pc 4-PDT in these cells was approximately 40 and 90%, respectively, and (ii) the onset of the process was detected by 8 and 2 h, respectively. The data indicate that Pc 4-PDT is a more effective inducer of apoptosis than ionizing radiation. These differences suggest potential underlying mechanistic differences between radiation- and Pc 4-PDT-induced apoptosis.

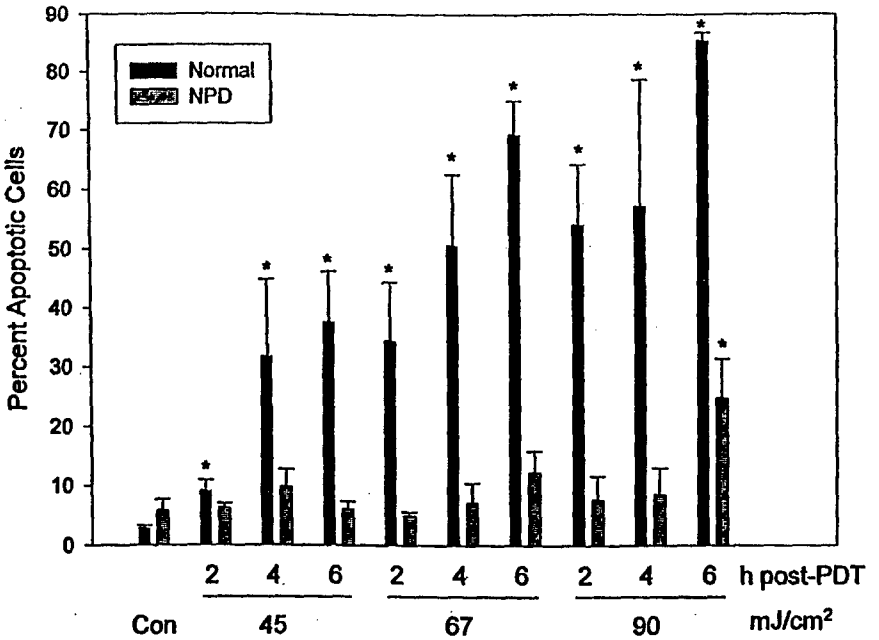

FIG. 1. Pc 4-PDT-induced apoptosis in normal or NPD lymphoblasts. The cells were exposed to red light (45, 67, or 90 mJ/cm²) 15 h after addition of Pc 4, then harvested for assay 2, 4, or 6 h later. Controls consisted of treatment with red light only, Pc 4 only or no treatment. Viability of cells was unaffected by light or Pc 4. Data are shown as the mean ± SE for two to six independent determinations. At the indicated times postirradiation, cells were collected, and analyzed for FITC/dUTP incorporation and PI staining by flow cytometry. Con, untreated control; *, significantly different from corresponding untreated control ($P < 0.03$, Mann-Whitney test).

To assess whether the deficiency in apoptosis in NPD cells correlated with alterations in ceramide formation, the kinetics of ceramide generation in response to Pc 4-PDT were measured in both cell lines. Following exposure of normal lymphoblasts to PDT (200 nM Pc 4 + 67 mJ/cm²), ceramide was elevated above control levels by 66, 67, 39 and 24% at 5, 10, 15, and 30 min, respectively (Fig. 2). However, ceramide accumulation was significantly suppressed in NPD cells after Pc 4-PDT. Since NPD lymphoblasts have a normal level of NSMase activity (15) and express only 2% or less residual ASMase activity (15), our data indicate that abnormalities in apoptosis and ceramide generation in these cells post-Pc 4-PDT correlate with the loss of ASMase function. These results agree with the similar defects observed in NPD cells in response to ionizing radiation (15). By contrast, Boesen-deCock *et al.* (19) showed that ASMase is not required in anti-Fas-induced ceramide formation and apoptosis in NPD cells. Perhaps the difference in the responses to two different stimuli, radiation and anti-Fas, is due to phenotypic changes that can occur upon continuous *in vitro* culture of NPD cells (19).

Treatment of cells with bSMase results in generation of ceramide with a subsequent restoration of the lost ceramide responses, such as apoptosis (20). To test if bSMase can restore apoptosis in NPD lymphoblasts after Pc 4-PDT, the cells were treated with the exogenous enzyme. While bSMase alone (50 mU/mL) did not induce apoptosis, the combined treatment, bSMase + Pc 4-PDT, initiated the process in a PDT dose-dependent fashion in NPD cells (Fig. 3A). Similar results were also obtained in the presence of higher doses of bSMase (300 or 500 mU/mL) ± Pc 4-PDT (data not shown). In normal cells, in contrast to Pc 4-PDT, bSMase itself (50 mU/mL), did not induce apoptosis. In the presence of both treatments the extent of apoptosis was not further increased. The combined treatment was more effective in generating an apoptotic cell population in normal lymphoblasts than in NPD cells. Perhaps ASMase is a critical Pc 4-PDT target for the induction of apoptosis, and the absence of a functional ASMase in NPD cells may account for the observed difference.

We then examined whether the synergistic apoptotic response to the combined treatment of Pc 4-PDT+ bSMase would translate into altered ceramide formation in NPD cells. bSMase alone induced a 7.7-fold increase in ceramide levels (Fig. 3B), without subsequent apoptosis (Fig. 3A). Following combined Pc 4-PDT and bSMase treatments, ceramide levels were elevated to the same extent as with bSMase alone and apoptosis was induced. In normal lymphoblasts bSMase alone increased ceramide levels 7.4-fold above baseline (Fig. 3B). However, exogenous bSMase did not induce apoptosis (Fig. 3A), suggesting that the ceramide effectors and the primary components of the apoptotic machinery are out of reach. The combined treatment with Pc 4-PDT + bSMase did not further increase ceramide accumulation beyond that observed

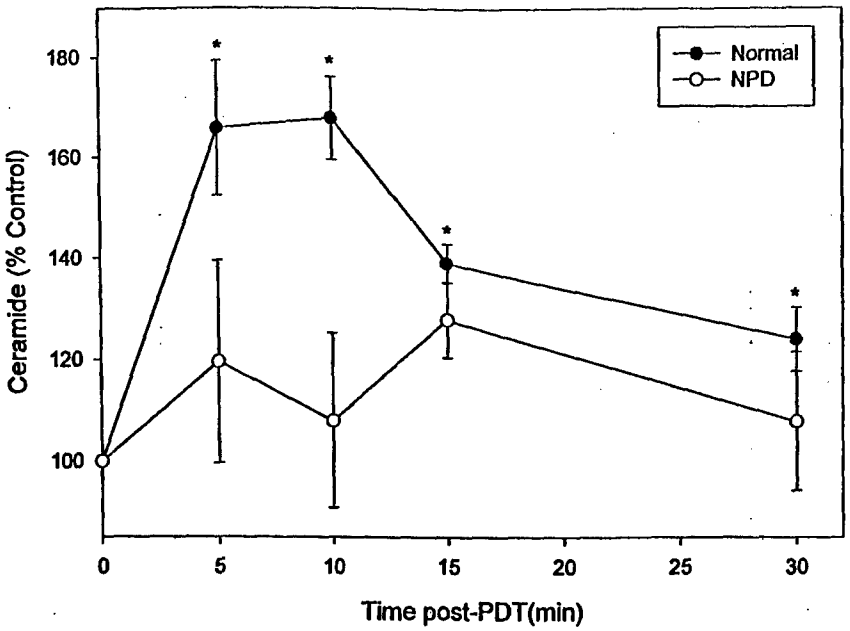

FIG. 2. Time course of ceramide accumulation in response to Pc 4-PDT in normal or NPD lymphoblasts. Following exposure to PDT (200 nM Pc 4 + 67 mJ/cm^2), the cells were incubated for the indicated times. Lipids were extracted, and ceramide was measured using the DAG kinase assay. The control ceramide levels in the normal and NPD lymphoblasts were 64 ± 11 pmol/10^6 cells (mean ± SE; n = 31) and 92 ± 16 pmol/10^6 cells (mean ± SE; n = 29), respectively. Data were calculated as the percentage of time-matched, Pc 4-treated controls analyzed in the same experiment and are shown as the mean ± SE of five to ten separate determinations. *, significantly different from corresponding Pc 4-treated control ($P < 0.03$, paired Student t test).

in the presence of bSMase alone. Curiously, a smaller ceramide increase, ranging from 35% to 82%, correlated with a significant and a dose-dependent induction of apoptosis in normal cells post-Pc 4-PDT. Perhaps ceramide must reach a threshold concentration at a critical Pc 4-PDT target, *e.g.* the ASMase pool, to trigger apoptosis.

To confirm the observed apoptotic changes following treatment, another apoptotic marker was used. Cysteine-aspartate specific proteases (caspases) are central mediators of the late stages of apoptosis (21). PDT (22), as well as ceramide (23), can activate these enzymes. In particular, caspase-3, the protease that cleaves poly(ADP-ribose) polymerase (PARP) into 89 and 24 kDa fragments from the 113 kDa full-length peptide, is activated post-PDT (22). Here we show that after treatment of normal lymphoblasts with Pc 4-PDT ± bSMase, PARP cleavage was induced (Fig. 4). In contrast, only the highest PDT dose (200 nM Pc 4 + 90 mJ/cm^2) induced partial PARP cleavage in NPD cells. In addition, a low level of cleavage product appeared following treatment of NPD cells with Pc 4-PDT + bSMase. However, bSMase itself (50 mU/mL) did not induce PARP cleavage in either of the two cell lines. These results are in agreement with previous observations that treatment with exogenous bSMase did not cause apoptosis when administered without Pc 4-PDT.

To rule out the possibility that bSMase could have affected the uptake of Pc 4, leading to altered photocytotoxicity, both cell lines were treated with [^{14}C] Pc 4 (200 nM) ± bSMase (500 mU/mL) for 15 h, and the level of cell-associated Pc 4 was assessed. Cell uptake was similar in the two cell lines and was not altered by the presence of bSMase (data not shown).

The observations that bSMase-induced ceramide accumulation did not result in apoptosis and that in NPD cells a potentiated apoptotic response to the combined treatment did not lead to altered ceramide generation beyond that induced by bSMase itself suggest that the effect of bSMase alone is insufficient to initiate the death process. The inability of bSMase to induce apoptosis under conditions effectively generating ceramide has been shown (24, 25). Ceramide generated at the plasma membrane by bSMase did not trigger apoptosis probably because: (i) bSMase-generated ceramide is found in a plasma membrane compartment that is distinct from specialized plasma membrane domains (caveolae) where the "signaling" ceramide is formed (26); (ii) ceramide formed by bSMase in the outer leaflet of the cell membrane is unavailable to intracellular apoptotic effectors (24); or (iii) the high levels of ceramide are converted or degraded into non- or anti-apoptotic agents, such as glucosylceramide (27) or sphingosine-1-phosphate (28).

The mechanism(s) underlying the synergistic apoptotic responses in NPD cells following treatment with Pc-4-PDT + bSMase have yet to be determined. Several possibilities are suggested. First, Pc-4-PDT may affect membrane fluidity in such a way that flipping of

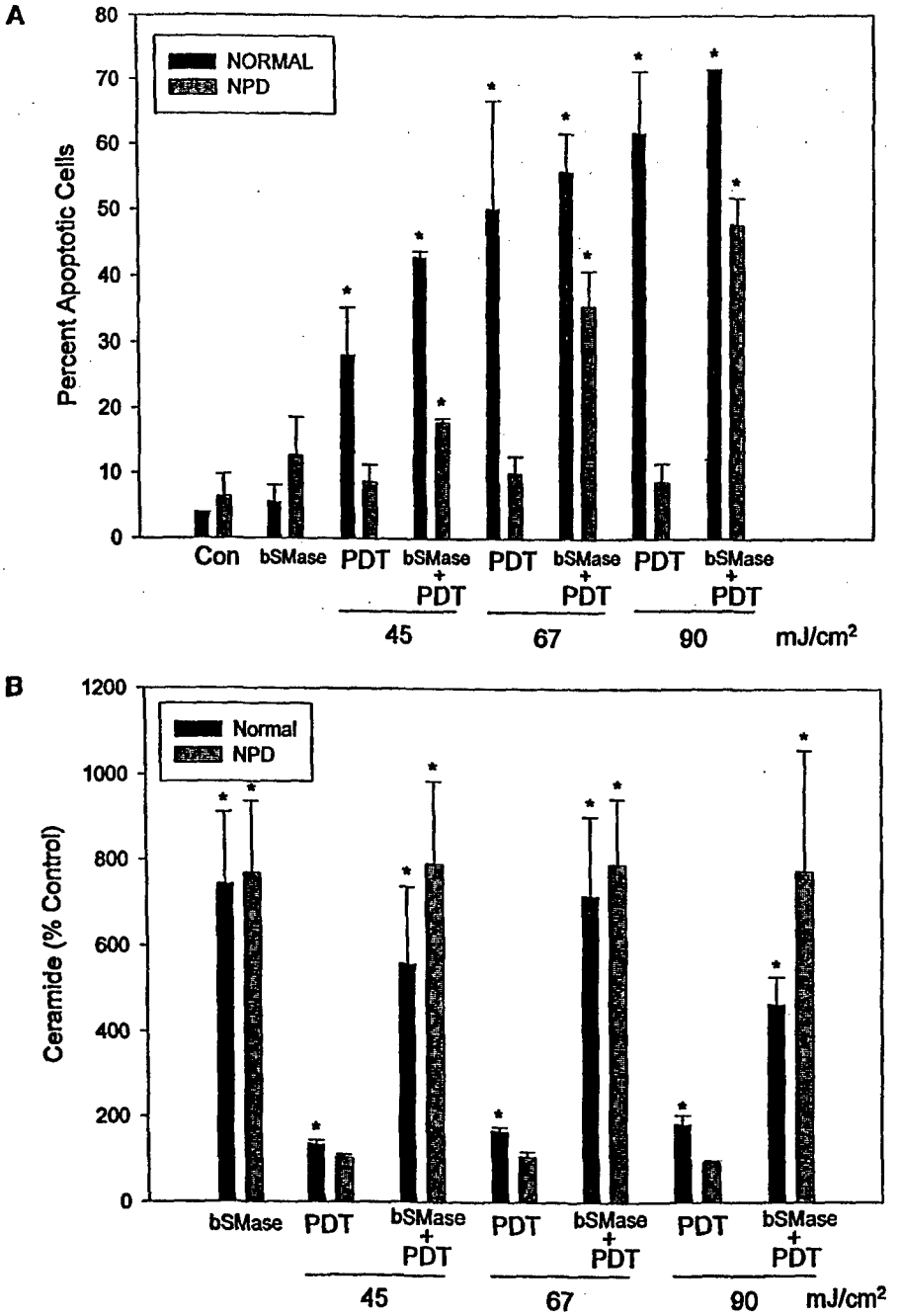

FIG. 3. The effect of Pc 4-PDT ± bacterial sphingomyelinase (bSMase) on the induction of apoptosis (A) or ceramide accumulation (B) in normal or NPD lymphoblasts. Following a 15 h exposure to Pc 4 (200 nM) ± bSMase (50 mU/mL), the cells were irradiated at the indicated fluences, and then incubated for 6 h (A) or 10 min (B). Cells were collected, and then analyzed for FITC/dUTP incorporation and PI staining by flow cytometry (A) or ceramide accumulation by the DAG kinase assay (B). Data are shown as the mean ± SE for three to nine independent determinations. (A) Con, untreated control; *, significantly different from corresponding untreated control ($P < 0.04$, Mann-Whitney test). (B) *, significantly different from corresponding Pc 4-treated control ($P < 0.05$, paired Student t-test).

ceramide from the outer to the inner leaflet is facilitated, allowing the lipid interaction with the downstream targets involved in signaling and/or execution of apoptosis. Second possibility is that ceramide generation does not suffice for triggering apoptosis and that additional signals are needed (*e.g.*, ROS) to induce the death machinery. Conversely, positive feedback loops may have to be activated, i.e. ceramide stimulates ROS production (29), and ROS in turn activates ceramide formation leading ultimately to initiation of apoptosis.

The hypothesis that ceramide signals Pc-4-PDT-induced apoptosis in normal human lymphoblasts is supported by the observation of an early rise (*i.e.*, 5 min after PDT) in ceramide levels that preceded the ap-

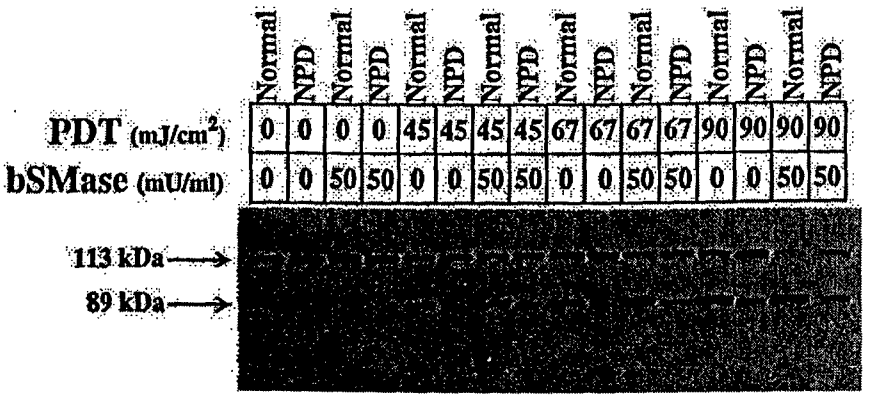

FIG. 4. PARP cleavage in normal or NPD lymphoblasts after Pc 4-PDT ± bacterial sphingomyelinase (bSMase) treatment. Following a 15 h treatment with Pc 4 (200 nM) ± bSMase, the cells were irradiated at the indicated fluences, and then incubated for 6 h. Cells were collected and analyzed for PARP cleavage. Similar data were obtained in two additional experiments.

pearance of apoptotic cells (2 h post-PDT). Similar data were obtained for other cells (7, 8). If ceramide mediates apoptosis in response to Pc-4-PDT, the downstream targets of ceramide need to be identified. PDT, like other stresses (15, 30), stimulates the SAPK/JNK cascade (31). Thus, the SAPK/JNK signaling pathway may play a role in Pc-4-PDT-induced ceramide-mediated apoptosis. In addition, a variety of evidence implicates mitochondrial damage and the release of cytochrome c as key events in PDT-induced apoptosis (22). Ceramide may participate by enhancing the level of oxidative damage to mitochondria (32).

Caspases are potential downstream ceramide targets, since apoptosis is blocked by caspase inhibition, while induced ceramide accumulation is not (20, 33). These findings, however, have been challenged by observations that caspase inhibitors can prevent accumulation of the lipid (34). More direct studies using caspase knockout models, are required to assess the role of ceramide in caspase activation and subsequent apoptosis.

The aim of the present study was to assess the role of SMase in Pc 4 photocytotoxicity. The data suggest that ASMase may be a Pc 4-PDT target, since ceramide formation correlates with Pc-4-PDT-induced apoptosis in normal lymphoblasts, but not in NPD cells. The attempt to reverse the abnormalities in NPD cells using bSMase led to potentiated apoptosis without augmented ceramide generation beyond that induced by bSMase alone. These novel observations are consistent with the notion that SMase is a proapoptotic factor determining responsiveness of cells to Pc4-PDT. More extensive investigations using other photosensitizers are required to test whether ASMase is a general photocytotoxic target. Further and more direct elucidation of the role of SMase in PDT cytotoxicity may suggest methods to improve the therapeutic efficacy of the treatment.

ACKNOWLEDGMENTS

The authors are indebted to Drs. Malcolm E. Kenney and Ying-syi Li (Dept. Chemistry, CWRU) for the generous gift of [^{14}C] Pc 4. This research was supported by U.S. Public Health Service Grants P01 CA48735 to N.L.O., R29CA77475 to D.S., and Cancer Center Support Grant P30 CA43703 from the National Cancer Institute, DHHS. Funding was also supplied by U.S. Army Material Command DOD Grant BC97143 to D.A.B. and a post-doctoral fellowship to J.J.P.

REFERENCES

1. Henderson, B. W., and Dougherty, T. J. (1992) *Photochem. Photobiol.* **55**, 145–157.
2. Agarwal, M. L., Clay, M. E., Harvey, E. J., Evans, H. H., Antunez, A. R., and Oleinick, N. L. (1991) *Cancer Res.* **51**, 5993–5996.
3. Zaidi, S. I. A., Oleinick, N. L., Zaim, M. T., and Mukhtar, H. (1993) *Photochem. Photobiol.* **58**, 771–776.
4. Verheij, M., Bose, R., Lin, X. H., Yao, B., Jarvis, W. D., Grant, S., Birrer, M. J., Szabo, E., Zon, L. I., Kyriakis, J. M., Haimovitz-Friedman, A., Fuks, Z., and Kolesnick, R. (1996) *Nature* **380**, 75–79.
5. Wright, S. C., Zheng, H., and Zhong, J. (1996) *FASEB J.* **10**, 325–332.
6. Monney, L., Olivier, R., Otter, I., Jansen, B., Poirier, G. G., and Borner, C. (1998) *Eur. J. Biochem.* **251**, 295–303.
7. Separovic, D., He, J., and Oleinick, N. L. (1997) *Cancer Res.* **57**, 1717–1721.
8. Separovic, D., Mann, K. J., and Oleinick, N. L. (1998) *Photochem. Photobiol.* **68**, 101–109.
9. Peña, L. A., Fuks, Z., and Kolesnick, R. (1997) *Biochem. Pharmacol.* **53**, 615–621.
10. Schuchman, E. H., Suchi, M., Takahashi, T., Sandhoff, K., and Desnick, R. J. (1991) *J. Biol. Chem.* **266**, 8531–8539.
11. Tomiuk, S., Hofmann, K., Nix, M., Zumbansen, M., and Stoffel, W. (1998) *Proc. Natl. Acad. Sci. USA* **95**, 3638–3643.
12. Perry, D. K., and Hannun, Y. A. (1998) *Biochim. Biophys. Acta* **1436**, 233–243.
13. Schissel, S. L., Schuchman, E. H., Williams, K. J., and Tabas, I. (1996) *J. Biol. Chem.* **271**, 18431–18436.
14. Schissel, S. L., Jiang, X.-c., Tweedie-Hardman, J., Jeong, T.-s., Camejo, E. H., Najib, J., Rapp, J. H., Williams, K. J., and Tabas, I. (1998) *J. Biol. Chem.* **273**, 2738–2746.

15. Santana, P., Peña, L. A., Haimovitz-Friedman, A., Martin, S., Green, D., McLoughlin, M., Cordon-Cardo, C., Schuchman, E. H., Fuks, Z., and Kolesnick, R. (1996) *Cell* **86**, 189–199.
16. De Maria, R., Rippo, M. R., Schuchman, E. H., and Testi, R. (1998) *J. Exp. Med.* **187**, 897–902.
17. Oleinick, N. L., Antunez, A. R., Clay, M. E., Rihter, B. D., and Kenney, M. E. (1993) *Photochem. Photobiol.* **57**, 242–247.
18. Wuerzberger, S. M., Pink, J. J., Planchon, S. M., Byers, K. L., Bornmann, W. G., and Boothman, D. A. (1998) *Cancer Res.* **58**, 1876–1885.
19. Boesen-de Cock, J. G. R., Tepper, A. D., de Vries, E., van Blitterswijk, W. J., and Borst, J. (1998) *J. Biol. Chem.* **273**, 7560–7565.
20. Tepper, A. D., Cock, J. G., de Vries, E., Borst, J., and van Blitterswijk, W. J. (1997) *J. Biol. Chem.* **272**, 24308–24312.
21. Cohen, G. M. (1997) *Biochem. J.* **326**, 1–16.
22. Kessel, D., and Luo, Y. (1999) *Cell Death Differ.* **6**, 28–35.
23. Smyth, M. J., Perry, D. K., Zhang, J., Poirier, G. G., Hannun, Y. A., and Obeid, L. M. (1996) *Biochem. J.* **316**, 25–28.
24. Zhang, P., Liu, B., Jenkins, G. M., Hannun, Y. A., and Obeid, L. M. (1997) *J. Biol. Chem.* **272**, 9609–9612.
25. Escargueil-Blanc, I., Andrieu-Abadie, N., Caspar-Bauguil, S., Brossmer, R., Levade, T., Negre-Salvayre, A., and Salvayre, R. (1998) *J. Biol. Chem.* **273**, 27389–27395.
26. Bilderback, T. R., Grigsby, R. J., and Dobrowsky, R. T. (1997) *J. Biol. Chem.* **272**, 10922–10927.
27. Liu, Y.-Y., Han, T.-Y., Giuliano, A. E., and Cabot, M. C. (1999) *J. Biol. Chem.* **274**, 1140–1146.
28. Spiegel, S., and Merrill, A. H. J. (1996) *FASEB J.* **10**, 1388–1397.
29. Garcia-Ruiz, C., Colell, A., Mari, M., Morales, A., and Fernandez-Checa, J. C. (1997) *J. Biol. Chem.* **272**, 11369–11377.
30. Coroneos, E., Wang, Y., Panuska, J. R., Templeton, D. J., and Kester, M. (1996) *Biochem. J.* **316**, 13–17.
31. Klotz, L. O., Fritsch, C., Briviba, K., Tsacmacidis, N., Schliess, F., and Sies, H. (1998) *Cancer Res.* **58**, 4297–4300.
32. Gudz, T. I., Tserng, K.-Y., and Hoppel, C. L. (1997) *J. Biol. Chem.* **272**, 24154–24158.
33. Chen, L., Kim, T. J., and Pillai, S. (1998) *Mol. Immunol.* **35**, 195–205.
34. Genestier, L., Prigent, A.-F., Paillot, R., Quemeneur, L., Durand, I., Banchereau, J., Revillard, J. P., and Bonnefoy-Berard, N. (1998) *J. Biol. Chem.* **273**, 5060–5066.

[CANCER RESEARCH 59, 3972–3979, August 15, 1999]

Delayed Apoptotic Responses Associated with Radiation-induced Neoplastic Transformation of Human Hybrid Cells[1]

Marc S. Mendonca,[2] Kelly L. Howard, Daphne L. Farrington, Lael A. Desmond, Toni M. Temples, Brendan M. Mayhugh, John J. Pink, and David A. Boothman

Radiation and Cancer Biology Laboratory, Department of Radiation Oncology, Indiana University School of Medicine, Indianapolis, Indiana 46202 [M. S. M., K. L. H., D. L. F., L. A. D., T. M. T., B. M. M.], and Department of Radiation Oncology, Case Western Reserve University, Cleveland, Ohio 44106-4942 [J. J. P., D. A. B.]

ABSTRACT

HeLa X human skin fibroblast hybrid cells have been developed into a model for radiation-induced neoplastic transformation of human cells. Previous studies indicate that the appearance of neoplastically transformed foci in this system is delayed for several population doublings after irradiation and appears to involve the loss of putative tumor suppressor loci on fibroblast chromosomes 11 and 14. We now show that after treatment with 7 Gy of X-rays, transformed foci initiation correlates with delayed apoptosis initiated in the progeny of the irradiated cells after 10–12 cell divisions and with reduced plating efficiency (delayed death). The cells develop classic apoptotic morphology, positive terminal deoxynucleotidyl transferase-mediated nick end labeling and phosphatidylserine (annexin V) staining, and cleavage of poly(ADP-ribose) polymerase. In addition, a delayed induction of the p53 protein and the proapoptotic Bax protein is evident over a week after radiation exposure. We propose that a delayed build-up of mitosis-dependent genomic DNA damage or a loss of genetic material over time (10–12 cell divisions postirradiation) has two relevant outcomes: (*a*) cell death due to the delayed induction of a p53-dependent apoptosis; and (*b*) neoplastic transformation of a minor subset of survivors that has lost fibroblast chromosomes 11 and 14 (tumor suppressor loci for this system) and has either evaded apoptosis or not acquired enough genetic damage to induce apoptosis. It is postulated that both phenomena result from X-ray-induced, translesion-mediated genomic instability.

INTRODUCTION

Loss of heterozygosity of tumor suppressor loci has been proposed to be involved in radiation-induced neoplastic transformation of human cells (1–6). Human hybrid cells have proven useful for the identification of tumor suppressor loci and have been subsequently developed into a model of radiation-induced neoplastic transformation *in vitro* (7–10). Radiation-induced, neoplastically transformed cell lines from irradiated CGL1 human HeLa X fibroblast hybrid cells have been isolated and characterized (5, 6, 9, 11). Loss of heterozygosity at putative tumor suppressor loci located on chromosomes 11 and 14 of fibroblast origin correlates strongly with radiation-induced neoplastic transformation of the hybrid cells (5, 6). The mechanism of loss of these tumor suppressor loci on chromosomes 11 and 14 is important for understanding IR[3]-induced carcinogenesis.

We have previously shown that the appearance of IR-induced neoplastically transformed foci using CGL1 hybrid cells takes several population doublings to develop, with no foci appearing for several days after irradiation, followed by a gradual random appearance of foci over time (5, 6, 12). This suggests that IR-induced neoplastic transformation is not the result of immediate damage and the loss of chromosome 11 and 14 suppressor genes but rather the consequence of some kind of delayed onset genetic instability that may take several population doublings to develop after irradiation (12, 13). Similar mechanisms of neoplastic carcinogenesis after IR treatment have been proposed by others but have not been demonstrated directly in a neoplastic transformation system (14, 15).

Because our analysis indicated that the appearance of neoplastically transformed foci is delayed, we investigated the growth kinetics of the cells to search for other indications of instability in the progeny of CGL1 cells that have survived IR. Growth curve analysis of CGL1 cells from the neoplastic transformation assay flasks showed that both irradiated and control cells established a high-density plateau phase in transformation flasks by day 10 (12, 16). However, viability studies of irradiated and control CGL1 cells from the neoplastic transformation assay flasks performed by replating of the cells to determine PE indicated that the progeny of the irradiated cells never recover to the unirradiated control PEs of 60–85% (12, 13, 16). Instead, they initially recover to 35–45% PE by day 9, level off for 2 days, and then steadily decline from days 12–18 after irradiation. The delayed loss of PE in the progeny of irradiated cells weeks to months after treatment has been attributed to the expression of delayed death or lethal mutations (12, 16–19). We and others proposed that the expression of delayed death is a result of genomic instability (12, 20–22). Whether delayed death is a consequence of an increase in mitotic or necrotic cell death in the irradiated cell progeny or perhaps the result of the delayed onset of apoptosis remained to be investigated.

In this report, we demonstrate that the failure of progeny of the irradiated CGL1 cells to reach the control PE levels, due to a leveling off and reduction in PE, correlates with the onset of a delayed apoptosis. The data indicate that apoptotic cells arise in the progeny of the original irradiated CGL1 cells after more than 8 days of growth in the transformation assay flasks, which is equivalent to 10–12 cell divisions after irradiation. This process continues for about 10 days or for an additional 12 cell divisions.

Because apoptosis is a genetically controlled mode of cell death with distinct morphological features (for reviews, see Refs. 23 and 24) and a series of specific biochemical steps for induction, control, and progression after IR exposure (25–31), we decided to look for molecular evidence of the delayed onset of apoptosis in the progeny of irradiated cells. p53 appears to play a role in the induction of apoptosis in heavily damaged cells (25, 28–30, 32) and may also trigger the downstream transcriptional regulation of Bax and/or Bcl-2 (29, 33, 34), two opposing apoptotic-regulatory proteins. We therefore investigated the steady-state levels of the p53, Bax, and Bcl-2 proteins in IR-treated *versus* nontreated CGL1 hybrid cells during our 21-day neoplastic transformation assay. Our molecular analyses suggest that the delayed apoptotic response may be p53 dependent and caspase mediated and may involve alterations in Bax levels. It is postulated

Received 2/8/99; accepted 6/18/99.

The costs of publication of this article were defrayed in part by the payment of page charges. This article must therefore be hereby marked *advertisement* in accordance with 18 U.S.C. Section 1734 solely to indicate this fact.

[1] Supported primarily by in-house grants from the Department of Radiation Oncology, Indiana University School of Medicine (to M. S. M.). Other support for this work was provided by Grant DE-FG02-91ER61256-03 from the Department of Energy (to D. A. B.) and a Department of the Army, Department of Defense Human Breast Cancer Fellowship (to J. J. P.).

[2] To whom requests for reprints should be addressed, at Radiation and Cancer Biology Laboratory, Department of Radiation Oncology, 975 West Walnut Street, IB-346, Indiana University School of Medicine, Indianapolis, IN 46202. Phone: (317) 278-0404; Fax: (317) 278-0405; E-mail: mmendonc@iupui.edu.

[3] The abbreviations used are: IR, ionizing radiation (X-rays); DAPI, diamidino-2-phenylindole; IAP, intestinal alkaline phosphatase; PARP, poly(ADP-ribose) polymerase; PE, plating efficiency; PS, phosphatidylserine; TUNEL, terminal deoxynucleotidyl transferase-mediated nick end labeling; PI, propidium iodide.

that this novel, delayed apoptotic process may be a consequence of X-ray-induced, translesion-mediated genomic instability that we believe is also responsible for radiation-induced tumor suppressor gene loss on chromosomes 11 and 14 and the neoplastic transformation of these cells (13).

MATERIALS AND METHODS

Cell Lines. The derivation of cell lines CGL1 and CGL3 has been described previously (35). Briefly, a single fusion between the D98/AH-2 HeLa tumorigenic cell line (a HGPRT− variant) and the GM00077 normal human skin nontumorigenic fibroblast cell line was performed and designated ESH5. CGL1 cells were subsequently isolated from the third serial subclone of ESH5 in methycellulose growth selection. The CGL1 cell line is nontumorigenic when inoculated into nude mice and is IAP negative (35). CGL3 cells are IAP positive, spontaneous tumorigenic segregants that arose from the original cell hybrid fusion (ESH5) after more than 200 population doublings (35). This cell line is used as the IAP-positive control in the IR-induced neoplastic transformation assays described below. All hybrid cell lines were grown as adherent monolayers *in vitro*.

Culture Conditions. Cells were grown in Eagle's modified minimal essential medium (Flow Labs, Inc.) supplemented with 5% bovine calf serum (JRH Biosciences), 2 mM glutamine (Sigma), nonessential amino acids (Sigma), and 100 IU/ml penicillin (Sigma; Refs. 9 and 36). Sodium bicarbonate (20 mM) was added to the medium to maintain a pH of 7.2 in a 95.5% air:4.5% CO_2 humidified atmosphere.

IR Treatments. CGL1 cells were plated into several 75-cm^2 tissue culture flasks (Corning) containing complete growth medium 3–4 days before the experiment so that cultures were ~80% confluent at the time of IR treatment. Cells were then irradiated with 250 kVp X-rays at room temperature (20°C) at a dose rate of 80 cGy/min. All experiments described below were performed using 0- and 7-Gy treatments. After IR exposure, cells were incubated for 6 h at 37°C to allow for the repair of potentially lethal damage (12, 36).

Neoplastic Transformation Assays. Irradiated and nonirradiated CGL1 cells were assessed for neoplastic transformation (foci formation) as follows. After IR treatment and subsequent time for the repair of potentially lethal damage (described above), cells in 75-cm^2 flasks were trypsinized and counted. Cells receiving 7 Gy were plated at 25,000–50,000/75-cm^2 tissue culture flasks containing 15 ml of pre-equilibrated medium (pH 7.2). Multiple replica flasks (30–60) were prepared. For nonirradiated controls, 30–60 tissue culture flasks (75 cm^2) were plated with 5,000 cells in 15 ml of pre-equilibrated medium to maintain cell densities comparable to those of the surviving irradiated cells discussed above. This procedure allowed irradiated and control flasks to be plated at 50 viable cells/cm^2 (8). After 7 or 8 days, all transformation flasks were fed twice per week for the remainder of the 21-day expression period (8, 36). On day 21, the cultures were fixed with 2% paraformaldehyde/PBS for 20 min and rinsed with PBS. The flasks were stained simultaneously and assayed for IAP-positive foci by adding 2 ml of Western Blue reagent to each flask for 7 min. Blue foci were scored against a white high-density cell monolayer background as described previously (37). Control cultures were incubated, fed, and stained for IAP expression in an identical manner. PEs for the irradiated and unirradiated cells were also plated on day 0, scored 8–9 days after treatment, and used in the final transformation frequency calculations (8). It should be noted that to demonstrate that the appearance of radiation-induced neoplastically transformed foci was a delayed event after irradiation, Western Blue staining of sets of 30 T-75 flasks of irradiated and control cells was performed on days 4, 6, 8, 11, 13, 15, 18, 20, and 21 as described above (38).

PE Assays of CGL1 Cells in the Transformation Flasks. Irradiated and nonirradiated PEs were measured during the 21-day neoplastic transformation assay as follows. Measurements of changes in clonogenic PEs of control and irradiated CGL1 cells in the transformation flasks on days 4, 6, 8, 11, 13, 15, 18, 20, and 21 were performed as described previously (38). The adherent cells in 75-cm^2 transformation flasks were washed gently with PBS, trypsinized, and counted. From the single cell suspensions, irradiated and nonirradiated cells were plated at 100–500 cells/25-cm^2 tissue culture flask (six flasks/point); the flasks contained 5 ml of pre-equilibrated medium (pH 7.2). The PE flasks were incubated for 7–10 days to assess colony-forming ability. Colonies were stained with a solution containing 0.35% crystal violet in 35% ethanol as described previously (9, 36). Colonies with >50 normal-appearing cells were counted as survivors. All experiments described were performed a minimum of three times, using six replicate plates/condition. PEs for irradiated and control samples were calculated by dividing the average number of colonies in the six flasks by the number of cells initially plated (9, 36).

Detection of Apoptotic Cells. To assess apoptotic responses during the 21-day neoplastic transformation assays described above, adherent irradiated and nonirradiated CGL1 cells in the transformation flasks were investigated with DAPI morphology staining, TUNEL, PS (annexin V), and PARP cleavage assays (all described in detail below) on days 4, 6, 8, 11, 13, 15, and 18. Cells from the control and irradiated CGL1 cell transformation flasks were also replated to assess PEs on the same days.

DAPI Staining for Changes in Morphology. Adherent CGL1 cells in the 0 or 7 Gy neoplastic transformation 75-cm^2 flasks were analyzed for changes in cell and nuclear morphology (*i.e.*, the appearance of abnormal nuclear blebbing, apoptotic bodies) by staining cultures with the DNA-specific dye DAPI (Sigma), as described previously (23). Irradiated and nonirradiated cultures were rinsed with 1× PBS, fixed with 2% paraformaldehyde/PBS for 1 h, and stained for 20 min with DAPI. Cells were rinsed with PBS and viewed under a fluorescent inverted phase-contrast Leitz microscope with a camera attachment (Olympus OM4 T). Representative fields at ×200 and ×400 magnification were photographed with slide film. The number of normal and apoptotic cells was scored. Data from 10 microscopic fields containing a total of 300-2000 cells from four independent experiments were used to calculate the percentage of apoptotic cells on the designated days.

TUNEL Assays. Apoptotic-mediated, endonuclease-induced DNA strand breaks were detected by the addition of fluorescence-labeled dUTPs by the TUNEL assay (39). The *in situ* cell death detection kit TUNEL assay (Boehringer Mannheim) was used. On designated days, adherent cells in the irradiated and control transformation flasks were fixed with 4% paraformaldehyde for 30 min, rinsed with 1× PBS, and permeabilized with Triton X-100. Cells were rinsed twice with PBS, 50 μl of TUNEL reaction mixture were added, the cells were coverslipped with Parafilm, and the reactions were incubated for 1 h at 37°C in a humidified chamber. TUNEL-positive cells were viewed by inverted phase-contrast fluorescence microscopy, and matching phase-contrast and fluorescence photographs were recorded.

Genomic DNA Assays. Cell pellets from adherent CGL1 cells were isolated on designated days from the transformation flasks (see above) and stored at −20°C. Genomic DNA was isolated using a standard phenol/chloroform extraction and ethanol precipitation method (40) and resuspended in TE buffer [10 mM Tris (pH 8) and 1 mM EDTA]. RNase A treatment was performed overnight at 50°C. DNA was quantitated with a Shimadzu spectrophotometer, and aliquots (20 μg) were brought to a volume of 20 μl with TE buffer. Samples were heated to 70°C, and 10 μl of 10 mM EDTA containing 1% (w/v) low-melting temperature agarose (Sea Kem LE; FMC BioProducts), 0.25% (w/v) bromphenol blue (Sigma), and 40% (w/v) sucrose (Sigma) were added. Samples were dry loaded onto a 1% (w/v) agarose gel (Sea Kem LE; FMC Bio Products) and allowed to solidify (41). Electrophoresis was conducted in 1× TAE [0.04 M Tris-acetate and 0.001 M EDTA (pH 7.5)] for 4 h at 60 V. Genomic DNA was visualized under UV light after staining with 5 μg/ml ethidium bromide, and gels were photographed. A 1-kb DNA ladder (Life Technologies, Inc.) was included as a molecular weight control.

PS (Annexin V) Studies. Adherent apoptotic cells in the transformation flasks with translocated PS on their surfaces were detected by FITC-conjugated M_r 36,000 protein annexin V (42). The Clonetech Apoalert Annexin V Apoptosis Kit (Clonetech Laboratories, Inc.) was used. Briefly, the adherent cells in the irradiated or nonirradiated transformation flasks were trypsinized and treated for flow cytometry analysis as follows. Aliquots of 10^6 cells were washed with PBS and resuspended in binding buffer, equal volumes of annexin V-FITC/PI were added, and reactions were incubated at room temperature in the dark. Cellular fluorescence was detected using an Epics Profile I (Coulter) flow cytometer with an excitation wavelength of 488 nm. The number of cells that were negative for PI (red fluorescence) and positive for PS (green fluorescence) was measured by flow cytometry and scored as apoptotic. Quantitation and annexin V analysis were also performed on the floating cells in the irradiated and control transformation flasks.

Western Blot Analyses. For p53, Bax, Bcl-2, and α-tubulin steady-state analyses, protein from whole cell extracts was isolated from the transformation

flasks on designated days after treatment by adding 1 ml of radioimmunoprecipitation assay lysis buffer [150 mM NaCl, 1.0% NP40, 0.05% sodium deoxycholate, 0.1% SDS, and 50 mM Tris (pH 8.0)] on ice for 30 min. Lysates were scraped and collected in microcentrifuge tubes and centrifuged at 10,000 × *g* for 10 min, and supernatants were frozen at −80°C. Protein concentrations in supernatants were quantified by standard methods, and equivalent amounts (100 μg) were loaded (43) and then separated by SDS-PAGE. All separated proteins, including the PARP blots described below, were transferred to Immobilon-P membranes (Millipore, Danvers, MA). Equivalent protein loading was confirmed by Ponceau S staining [0.2% Ponceau S (w/v) in 3% trichloroacetic acid (w/v) and 3% sulfosalicylic acid (w/v); Sigma) using standard techniques.

For PARP cleavage analyses, cells were washed twice with ice-cold PBS and lysed in loading buffer [62.5 mM Tris (pH 6.8), 6 M urea, 10% glycerol, 2% SDS, 0.003% bromphenol blue, and 5% 2-mercaptoethanol (freshly added)]. Samples were sonicated with a Fisher Scientific Sonic Dismembrator (model 550) fitted with a microtip probe and stored at −20°C for later analyses. Equivalent amounts of protein (50 μg) were incubated at 65°C for 15 min, and proteins were separated by SDS-PAGE. PARP immunoblots were treated with PBS containing 0.2% Tween 20 and 10% fetal bovine serum for 1 h to prevent nonspecific binding. Membranes were then incubated overnight with primary anti-PARP C-2-10 antibody (Enzyme Systems Products, Dublin, CA) diluted in the same buffer at 4°C. Membranes were washed in PBS containing 0.2% Tween and then incubated with horseradish peroxidase-conjugated secondary antibody (Santa Cruz Biotechnology, Santa Cruz, CA) for 1 h.

For p53, Bax, Bcl-2, and α-tubulin analyses, membranes were blocked for 1 h with 2% blocking agent in Tris-saline buffer (Boehringer Mannheim), washed, and immunoblotted with primary antibodies to p53 (clone D0-1; Oncogene Research Products), Bax (clone YTH-2D2; Trevigen, Gaithersburg, MD), Bcl-2 (clone Bcl-2-100; Sigma), or α-tubulin (clone B-5-1-2; Sigma). Primary and secondary antibodies were diluted according to the manufacturer's recommendation in blocking buffer. After incubation for 1 h at room temperature and repeated washing, the appropriate horseradish peroxidase-conjugated secondary antibodies were added and incubated for 1 h at room temperature.

All Western blots were washed in PBS containing 0.2% Tween, developed with enhanced chemiluminescence substrate (Amersham, Arlington Heights, IL), and exposed to X-ray film. Autorads were examined visually and digitized (EDAS 120; Kodak Digital Science). Protein band intensities were quantitated by computerized densitometry with image analysis software (1D Analysis; Kodak Digital Science).

RESULTS

The Expression of Delayed Death and the Development of Neoplastically Transformed Foci in Irradiated CGL1 Cells. CGL1 cells were irradiated with 0 or 7 Gy of 250 KvP X-rays and plated at appropriate cell densities in T-75 flasks for a standard 21-day neoplastic transformation assay. Beginning on day 4, 0 and 7 Gy transformation flasks were removed, the adherent cells were trypsinized and counted, and 200-1000 cells were replated to assess the PE of CGL1 cells in the irradiated and control transformation flasks during the 21-day neoplastic transformation assay (Fig. 1). The cell counts also allowed us to calculate the number of population doublings that occurred in the unirradiated and 7 Gy transformation flasks (12, 13). The PE of unirradiated CGL1 cells from control transformation flasks remained between 60% and 85% during the 21-day assay period. However, the PE of CGL1 cells from the 7 Gy transformation flasks from day 4 (five population doublings after irradiation) to day 18 (22 population doublings after irradiation) was quite different (Fig. 1). The PE of the cells in the irradiated transformation flasks was initially 11% on day 4 and recovered up to 35–45% by day 9 (11 population doublings after irradiation). It then leveled off for 2 days and declined from days 12–18 postirradiation. We have attributed the lower PEs observed in CGL1 cells from the irradiated transformation flasks to the onset of delayed death (12, 13, 16). The appearance of radiation-induced neoplastically transformed foci was also delayed and correlated with the reduced PE in these cells (Fig. 1; Refs. 12 and 13). To investigate whether the leveling off and subsequent decline of PE in the irradiated CGL1 cells were the result of a delayed onset of apoptosis, several apoptotic end points, including gross changes in CGL1 cell morphology, TUNEL analysis, genomic DNA degradation, and altered annexin V expression, were examined during the 21-day assay period.

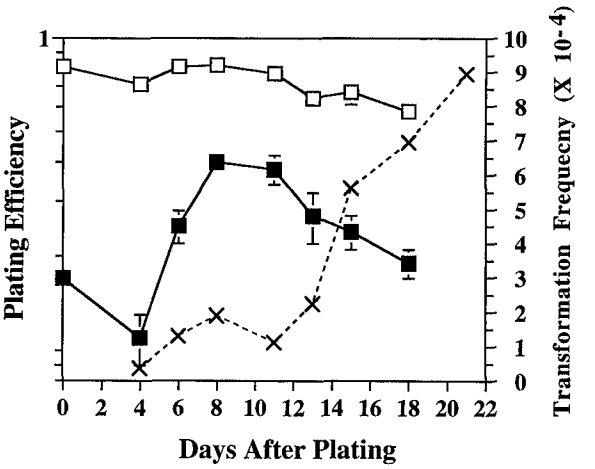

Fig. 1. Transformation frequency (*X*) and PE of irradiated CGL1 cells (■) as a function of time after a 7-Gy exposure to X-rays. The PE of control unirradiated CGL1 cells in the transformation flasks (□) is shown as a control. The data shown were accumulated from three independent neoplastic transformation experiments and are consistent with previously published observations (12).

Apoptotic Morphology Correlates with Onset of Delayed Death. Phase-contrast and matching DAPI-stained fluorescence photomicrographs of irradiated CGL1 cells during the course of a standard neoplastic transformation experiment demonstrated a significant number of apoptotic bodies between days 10 and 18 postirradiation (Fig. 2*A*). Numerous morphologically abnormal, apoptotic-like cells/nuclei were evident on days 10 and 15. Counting of adherent apoptotic *versus* normal cell nuclear morphology from days 4–20 indicates that between days 10 and 18, 25–50% of the attached cells were undergoing apoptosis, and by day 20, many of the apoptotic bodies disappeared (Fig. 2, *A* and *B*). This is the time scale during which the leveling and reduction in PE of the cells in the irradiated transformation flasks occur (Fig. 1). In contrast, nonirradiated control cells had few apoptotic bodies between days 4 and 15, with a small increase evident only after day 17 (Fig. 2), and a consistently higher overall PE (Fig. 1). These data indicate a possible relationship between the failure of the PE of progeny of the irradiated cells to fully recover to unirradiated PE levels, due to the leveling off and reduction in PE, and the appearance of apoptosis.

TUNEL-positive Cells and Genomic DNA Degradation Correlate with the Onset of Delayed Death. TUNEL assays were used to confirm that delayed apoptotic responses were occurring in irradiated CGL1 cells. In Fig. 3*A*, phase-contrast and fluorescence photomicrographs of adherent irradiated and control CGL1 cells on days 15 and 18 posttreatment in the transformation flasks are shown as examples. TUNEL-positive CGL1 cells with corresponding apoptotic morphology were evident in irradiated cells, but not in unirradiated control cells (*e.g.,* see day 15 control cells). The appearance of TUNEL-positive cells was concurrent with the appearance of apoptotic bodies identified by DAPI staining (Fig. 2, *A* and *B*) and with reduced PE (Fig. 1).

The integrity of genomic DNA was then examined because the caspase-dependent apoptotic endonuclease can be activated in some but not all cells (44, 45). Genomic DNA was isolated at various times

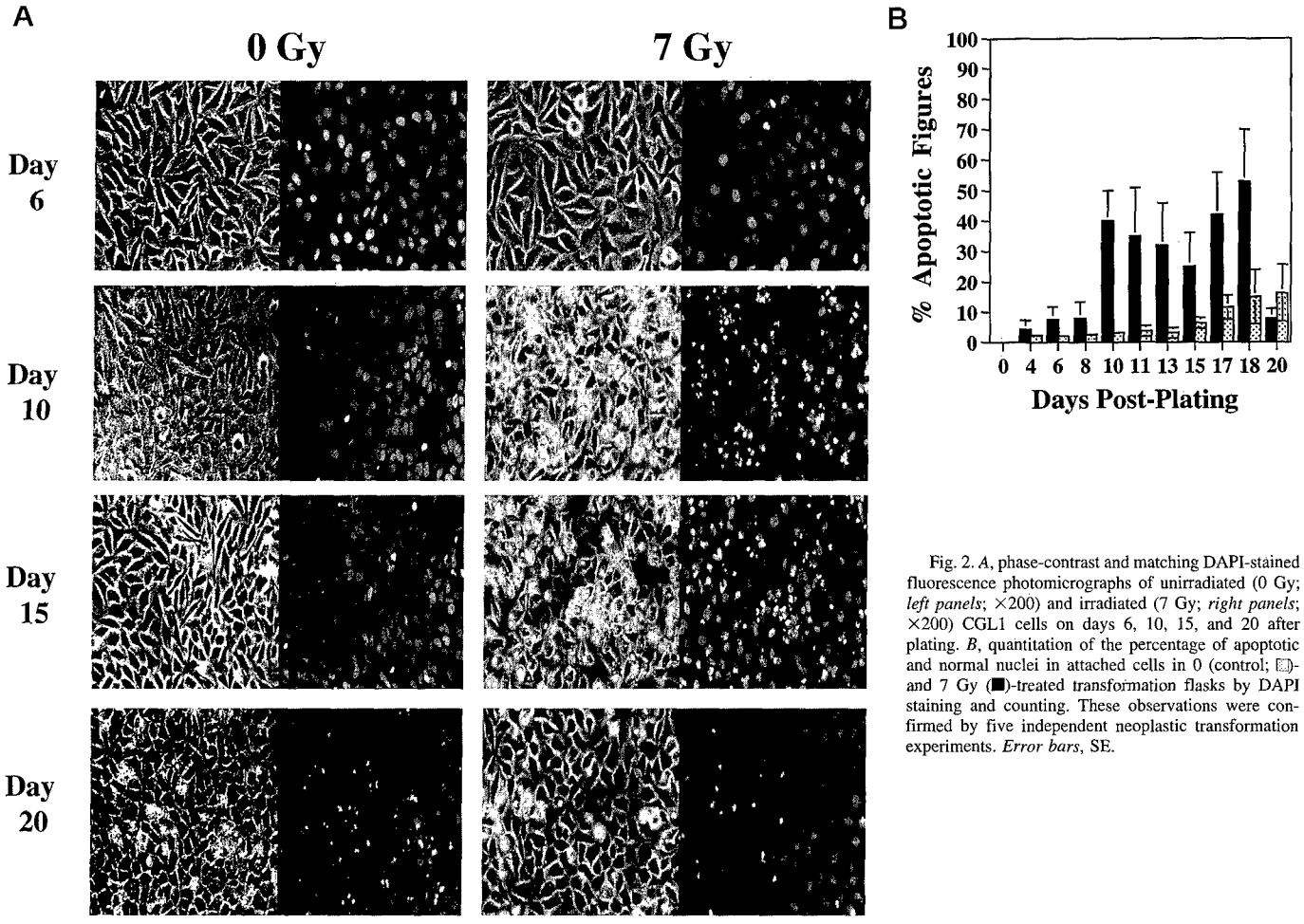

Fig. 2. *A*, phase-contrast and matching DAPI-stained fluorescence photomicrographs of unirradiated (0 Gy; *left panels*; ×200) and irradiated (7 Gy; *right panels*; ×200) CGL1 cells on days 6, 10, 15, and 20 after plating. *B*, quantitation of the percentage of apoptotic and normal nuclei in attached cells in 0 (control; ▨)- and 7 Gy (■)-treated transformation flasks by DAPI staining and counting. These observations were confirmed by five independent neoplastic transformation experiments. *Error bars*, SE.

after irradiation (7 Gy) from cells in transformation flasks to look for evidence of DNA degradation and the possible appearance of oligonucleosomal DNA ladders (46, 47). A delayed degradation of DNA, beginning on day 8 after irradiation and ending by day 19 or 20, was noted (Fig. 3*B*). DNA degradation was not accompanied by the appearance of a 180–200-bp DNA ladder (Fig. 3*B*), an observation also reported by others in a number of epithelial and fibroblast cells (46, 48, 49). However, the presence of degraded genomic DNA correlated with the delayed appearance of morphologically apoptotic and TUNEL-positive cells at this postirradiation time and with the reduction of PE (Figs. 1–3).

Increase in Annexin V-positive Cells Correlates with the Onset of Delayed Death. The translocation of PS (a membrane phospholipid) to the cell surface is a method of detecting apoptosis that is not dependent on morphology or genomic DNA integrity changes and can be quantitated by flow cytometry; it is detectable by adding FITC-labeled annexin V to cells (42). Flow cytometric analyses of the adherent cells in control and irradiated transformation flasks were therefore conducted by staining single cell suspensions of each with FITC-labeled annexin V on days 4–18 (Fig. 4). A significant increase in annexin V-positive cells in irradiated CGL1 cells above the unirradiated control average of 9 ± 6% was not noted until day 8 (35 ± 5%). The percentage of PS-positive CGL1 cells increased to 45 ± 5% on days 11 and 13 and increased to 51 ± 9% on day 15 after irradiation. The delay in the appearance of significant annexin V-positive cells until day 8–18 after irradiation was in quantitative agreement with DAPI morphology quantitation shown in Fig. 2*B* and in general agreement with the genomic DNA degradation data shown in Fig. 3*B*. The nonirradiated cells in the control transformation flasks stayed within an average value 9 ± 6% from days 4–13 and then increased slightly on days 15 and 18 after plating.

It should be noted that the analysis of annexin V staining and all of the other methods to measure apoptosis were done with the attached cells in the transformation flasks, because these are the cells that were replated in the PE studies reported here. However, analysis of the floating cells by annexin V staining also demonstrated a consistently larger amount of late-arising apoptotic/necrotic (annexin V- and PI-positive) cells in the irradiated transformation flasks than in the control transformation flasks. For example, the percentage of floating late apoptotic cells in the 0 Gy transformation flasks from days 4–12 was 4.0 ± 3.2% (range, 1.2% on day 4 to 9.0% on day 12). By comparison, the percentage of floating late apoptotic cells in the irradiated 7 Gy transformation flasks from days 4–12 was 27.3 ± 16.0% (range, 8% on day 4 to 50% on day 12).

Delayed Apoptosis Correlates with PARP Cleavage. Cleavage of PARP, a known apoptotic death substrate, by caspases activated during apoptosis commonly results in a decrease of the PARP protein from M_r 113,000 to a characteristic M_r 89,000 product (50). Treatment of CGL1 cells with 7 Gy resulted in a delayed PARP cleavage reaction *in vivo*, beginning at day 8 after irradiation and continuing to day 18 (Fig. 5). In contrast, the PARP polypeptide was essentially intact in unirradiated cells from days 6–15, with only a minor degree of spontaneous cleavage evident on days 11–13.

Delayed Increase in p53 Correlates with the Onset of Delayed Apoptosis. We next examined whether the delayed apoptosis we observed was associated with increased expression of p53, which is thought to regulate many apoptotic responses (28, 51). HeLa cells have wild-type p53, are human papillomavirus positive, and express

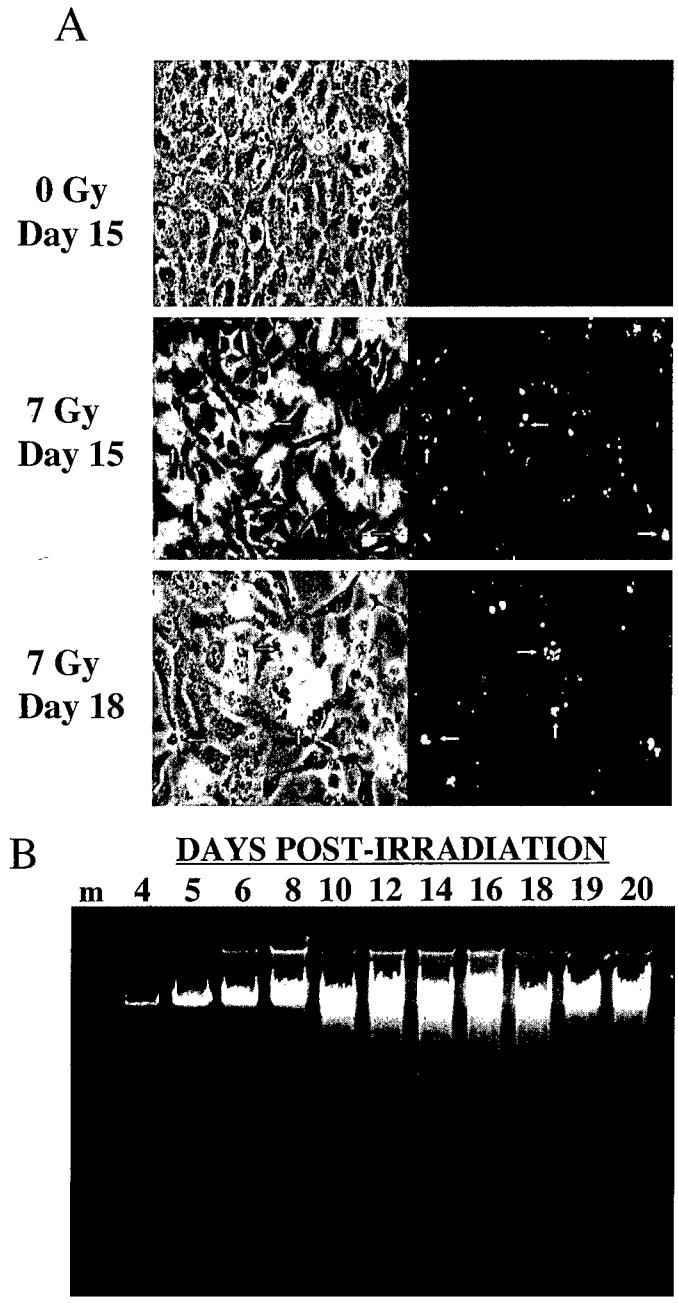

Fig. 3. *A*, phase-contrast and matching TUNEL photomicrographs of unirradiated (0 Gy) CGL1 control on day 15 (*top panel*) and 7 Gy-irradiated (*middle* and *bottom panels*) CGL1 cells on days 15 and 18 after plating. TUNEL-positive cells are detectable in the day 15 and day 18 (7 Gy) postirradiation transformation flask (*bottom two panels*). The day 15 unirradiated cells are TUNEL negative. *Arrows* indicate the same cells in the matching phase-contrast and fluorescence photomicrographs. The results have been confirmed by four independent neoplastic transformation experiments. *B*, agarose gel of genomic DNA isolated from irradiated CGL1 cells in transformation flasks on days 4–20 after irradiation. DNA (10 μg) was dry loaded into a 1% agarose gel and electrophoresed for 4 h at 60 V. These observations were confirmed in five independent transformation experiments. A 1-kb marker lane (*Lane m*) is also shown.

E6, but they remain partially responsive to DNA damage (52). We postulated that the fusion of HeLa with a wild-type p53 human fibroblast cell line to create the whole cell hybrid CGL1 might further dilute the relative amount of E6 protein and also allow a p53 response. Steady-state expression changes in p53 after IR were examined using Western immunoblot analyses (Fig. 6). p53 expression was monitored in CGL1 cells after treatment with 7 Gy in standard neoplastic transformation/PE studies by analyzing protein from the cells on days 4, 6, 8, 11, 13, 15, and 18 after irradiation. Significant increases in p53 were noted only after 6 days postirradiation. Densitometry indicated a progressive increase in p53 protein from 4- to 10- fold on days 6–15 after irradiation compared to day 4. Peak levels of p53 protein were noted at day 15 but completely disappeared by day 18 after irradiation (Fig. 6).

IR Induction of Bax Correlates with Delayed Apoptosis Onset. p53 is known to stimulate the downstream expression of the apoptotic-inducing protein Bax, which is thought to open pores in the mitochondrial outer membranes, causing a loss of membrane potential and the induction of apoptosis (29, 33, 34, 53). The ratio of proapoptotic Bax to antiapoptotic Bcl-2 protein appears to be important in the decision to undergo apoptosis (54–56). We examined the steady-state level of Bax and Bcl-2 using the same protein extracts and the same Western immunoblots originally used to probe for p53 expression (Fig. 6). A delayed increase in the steady-state level of the Bax protein was observed, with the maximum level of Bax occurring on day 15 after irradiation. This increase was concomitant with p53 expression. Densitometry indicated a 1.5–2.5 increase in Bax protein on days 6–15 after irradiation compared to day 4. As with p53, the levels of Bax decreased to control levels on day 18 (Fig. 4). Bcl-2 levels remained at a constant low level during most of this time period. These data suggest that a delayed p53 damage response pathway is activated in the progeny of irradiated CGL1 cells during standard neoplastic transformation assays (Fig. 1). Variations in p53 and Bax levels after day 6 were not the result of loading, because equivalent levels of α-tubulin were noted on days 6–18 (Fig. 6).

DISCUSSION

Our previous studies using CGL1 cells as an *in vitro* model of radiation-induced neoplastic transformation of human cells suggested that two important consequences of IR exposure may be a prolonged reduction in PE (the onset of delayed death) and neoplastic transformation (the appearance of neoplastically transformed foci; Fig. 1; Refs. 12 and 13). We hypothesized that the onset of delayed death is either a consequence of an increase in mitotic cell death in the irradiated cell progeny or perhaps the result of the onset of apoptosis.

In this report, we show that the failure of progeny of the irradiated CGL1 cells to reach the control PE levels during the 21-day assay period, due to the leveling off and reduction in PE, and the appearance of neoplastically transformed foci correlate with the onset of delayed apoptosis (Figs. 1–6). Counting the apoptotic figures by DAPI nuclear staining and the measurement of the number of PS-positive cells with

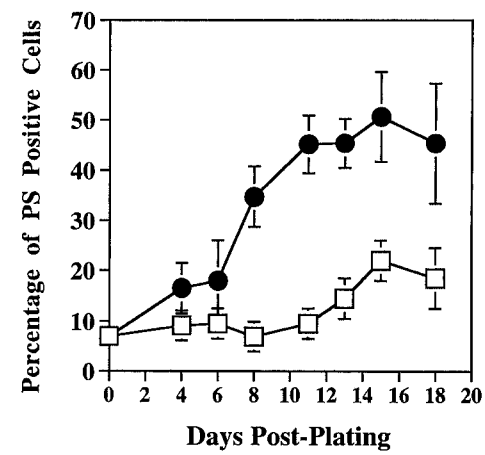

Fig. 4. Flow cytometric analysis of 7 Gy X-irradiated (●) and control (□) CGL1 cells assayed for the presence of PS by FITC-labeled annexin V on days 4, 6, 8, 11, 13, 15, and 18 postirradiation during a standard neoplastic transformation experiment. The time points were accumulated from four independent experiments. *Error bars*, SE.

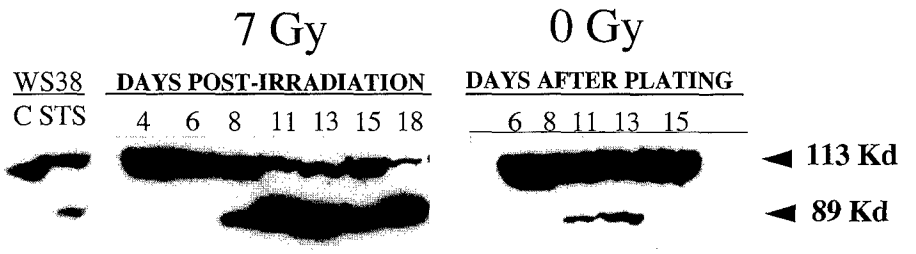

Fig. 5. Western blot of PARP from protein isolated from the 7 Gy-irradiated transformation flasks on days 4–18 after irradiation and from unirradiated control (*0 Gy*) transformation flasks on days 6–15 after plating. Untreated MCF-7 cells (*C*) and cells treated with staurosporine (*STS*), a universal apoptosis inducer, are shown as controls. Intact PARP runs at M_r 113,000, and the caspase-cleaved product runs at M_r 89,000. These observations were confirmed in two independent transformation experiments.

annexin V indicated that >40% of the population appears to be undergoing apoptosis on days 11–18, when the plateau and reduction in PE occurs. This suggests that the onset of delayed apoptosis plays a role in the expression of delayed death in the irradiated CGL1 cells observed in Fig. 1. It is important to note that the PE of unirradiated CGL1 cells from control transformation flasks remained between 60% and 85% during the 21-day assay period, and evidence of a relatively small amount of apoptosis is seen only near the end of this period (Figs. 1–5).

The delayed-onset apoptosis was characterized by changes in cell and nuclear morphology characteristic of apoptosis (Ref. 23; Fig. 2, *A* and *B*), the appearance of TUNEL-positive cells (Ref. 57; Fig. 3*A*), genomic DNA degradation (Fig. 3*B*), and the externalization of PS detected by reactivity with the annexin V antibody (Ref. 42; Fig. 4). The eventual disappearance of the apoptotic cells [seen in Fig. 2, *A* and *B* and by the disappearance of genomic DNA degradation (Fig. 3*B*)] suggests that the induction of apoptosis is transient and/or perhaps that severely genomically altered cells were selected from the population and removed.

Because apoptosis is a genetically controlled mode of cell death with distinct morphological features (for reviews, see Refs. 23 and 24) and a series of specific biochemical steps for induction, control, and progression after IR exposure (25–31), experiments to detect molecular evidence of the delayed apoptosis were undertaken. One of the important pathways in the execution phase of apoptosis is the activation of a series of apoptotic cellular proteases referred to as caspases, which are activated zymogens that cleave key cell death substrates such as the PARP DNA repair protein (50, 58, 59). In Fig. 5, we demonstrated that the M_r 113,000 PARP protein was intact in irradiated cells until day 8 after irradiation. However, from days 8–18 after irradiation, the intact PARP polypeptide decreased dramatically, and a corresponding increase in its M_r 89,000 fragment was observed. Such cleavage *in vivo* is diagnostic for the activation of a select number of caspases, including caspases 3 and 6 (60–62). In samples from nonirradiated CGL1 cells, on the other hand, the full-length PARP polypeptide remained essentially intact from days 6–15, with only minor increases in the M_r 89,000 apoptotic PARP fragment. The extent to which PARP cleavage occurred *in vivo* closely paralleled the overall amount of apoptosis that was observed using a variety of other cellular end points. These data support our proposal that the onset of apoptosis is delayed after IR exposure and begins after more than 8 days postirradiation. This is in contrast with other examples of IR-induced apoptosis and associated PARP cleavage that are evident within several hours after irradiation (63). These data, together with the other end points assayed above, suggest that delayed, IR-induced, caspase-mediated apoptosis occurs at a time consistent with the lower PE of the cells from the irradiated transformation flasks.

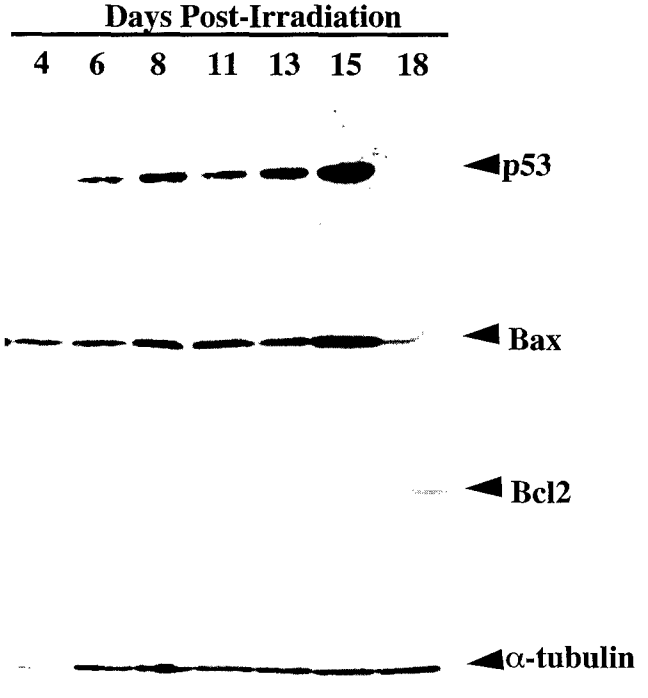

Fig. 6. Western blots of total protein isolated from cells on days 4, 6, 8, 11, 13, 15, and 18 after irradiation and probed for p53, Bax, and Bcl-2. α-Tubulin is shown as a loading control. Densitometry confirms a 4–10- fold increase in p53 protein from days 6–15 and a 1.5 -2-fold increase in the level of the Bax protein during this time period. These observations were confirmed in three independent transformation experiments.

How IR-induced DNA damage and genomic instability may be linked to apoptosis is currently under intense investigation. Because the tumor suppressor gene p53 may control apoptosis in many systems (28, 32, 64, 65), the steady-state levels of p53 protein in IR-treated *versus* nontreated CGL1 hybrid cells over a 21-day period were investigated. HeLa cells have wild-type p53, are human papillomavirus positive, and express E6, but they remain partially responsive to DNA damage (52). Steady-state expression changes in p53 after IR show a delayed, slow increase in p53 protein levels after day 6 postirradiation, which peaked by day 15 and disappeared by day 18 (Fig. 6). These data suggest that a delayed increase in the steady-state level of p53 in the progeny of irradiated CGL1 cells correlates with delayed-onset apoptosis. Furthermore, the fact that increased levels of p53 were apparent for more than 15 days after irradiation and then disappeared after day 18 (which appeared to correlate with the disappearance of apoptotic cells in Fig. 2) strongly suggests a p53-dependent apoptotic response pathway. We hypothesize that the emergence of genomically unstable cells may have triggered the delayed p53 induction response, perhaps as a result of a delayed production of DNA double-strand breaks. p53 induction responses have been linked to the production of double-stranded DNA breaks (32). Because the progeny of the irradiated CGL1 cells continue to cycle, either replication past unrepaired or misrepaired sites (*i.e.,* translesion DNA synthesis) after radiation damage or IR-induced error-prone repair could result in instability and the delayed production of double strand

breaks (28, 32, 64, 65). Studies to investigate the nature of the delayed DNA damage are in progress.

Data from a number of laboratories have indicated that p53 induction responses may play a major role in apoptosis in heavily damaged cells (25, 28–30, 32). In certain cells, p53 may trigger the downstream transcriptional regulation of Bax and/or Bcl-2, two opposing apoptotis-regulatory proteins (29, 33, 34, 66). Bax appears to stimulate the initiation of apoptosis (54, 67) by altering mitochondrial function (29, 68, 69). The majority of these molecular studies on the mechanism(s) of induction of apoptosis following IR have focused on the first few cell cycles (<96 h) posttreatment (25, 51, 64, 70–74). Therefore, we investigated whether the delayed transient increase in p53 results in increased steady-state levels of the Bax proapoptotic protein. A moderate increase in Bax protein levels was observed, which peaked 15 days postirradiation, concomitant with p53 increases. Both Bax and p53 levels then returned to basal levels by day 18 postirradiation. Low constant levels of Bcl-2 protein were evident during these time periods. These data suggest that IR-induced, delayed apoptosis in CGL1 cells involves the delayed induction of the p53 damage response pathway that subsequently up-regulated Bax and signaled apoptosis.

The delayed appearance of neoplastic foci in the CGL1 human hybrid cell system may be the result of the delayed onset of genomic instability with resultant damage to alleles on both chromosomes 11 and 14 in the same cell (6, 12). However, we have isolated eight radiation-induced neoplastically transformed hybrid cell lines (GIMs) that demonstrated stable PEs and long-term chromosomal stability in culture (6, 9, 16). This suggests that any radiation-induced genomic instability that produced the GIMs may be transient. The data reported here indicate that the delayed apoptosis seen in this system may also be a transient phenomenon postirradiation.

A potential link between the expression of delayed heritable damage and genomic instability with the induction of apoptosis was recently suggested as a method to rid the population of poorly repaired or "unstable" cells that might progress to cancer (21). Very recently, a link between reproductive failure, apoptosis, and compromised genomic integrity in a human/hamster cell line has been reported (75). In our cell system, the mechanisms for either escaping death or controlling genomic instability may lie on chromosomes 11 and/or 14 because maintaining these chromosomes allows the suppression of neoplastic transformation (5, 6, 13). Very recently, we have shown that previous loss of chromosome 11 in the CGL1 cells increases radiation sensitivity and neoplastic transformation frequency (76). We propose that IR-induced instability in this system has two relevant outcomes: (*a*) delayed cell death by p53-dependent postmitotic apoptosis in cells that have developed large-scale genomic damage or loss through misrepair or translesion DNA synthesis; and (*b*) neoplastic transformation of a subset of survivors that have lost fibroblast chromosomes 11 and 14 (tumor suppressor loci) but have not acquired enough genetic damage to induce apoptosis or have found pathways for avoidance of apoptosis, perhaps by mutation of genes involved in its regulation.

We and others have proposed that the consequences of exposing mammalian cells to IR can be examined and divided into three categories: (*a*) short term (several hours to a few days); (*b*) intermediate term (weeks to months); and (*c*) long term or late (month to years) post-irradiation. Death after IR exposure in many mammalian cells is postmitotic and can take a few rounds of cell division to be manifested postirradiation (72, 77, 78). In some cells mitotic death or postmitotic catastrophe may also be accompanied by the onset of programmed cell death or apoptosis during the first few cell cycles after IR (31, 65, 71, 72, 79, 80). It has been shown here that the expression of delayed death after irradiation appears to be the result of apoptotic death, with the onset of significant apoptosis not appearing until more than 8 days after irradiation, which is equivalent to 10 cell population doublings in these cells. We and others have hypothesized that the induction of genomic instability leading to chromosome and chromatid aberrations in the progeny of the irradiated cells may provide the link(s) between short-term and long-term consequences of IR exposure (12, 20, 22, 81, 82).

A novel, IR-induced apoptotic process has been described that develops in the progeny of the irradiated CGL1 cells more than 9 days or 12 cell divisions after irradiation. This process correlates in time with the appearance of neoplastically transformed foci in these cells. A deeper understanding of the molecular pathways being activated during the onset of this delayed apoptosis and the nature of the DNA damage triggering this response should give us further insight into the molecular mechanism of radiation-induced neoplastic transformation in human cells.

ACKNOWLEDGMENTS

We thank Caroline Weissman Derrow for editorial assistance and Drs. Joë Dynlacht, Dan Spandau, and Zvi Fuks for critical comments and suggestions.

REFERENCES

1. Weichselbaum, R. R., Beckett, M. A., and Diamond, A. A. An important step in radiation carcinogenesis may be inactivation of cellular genes. Int. J. Radiat. Oncol. Biol. Phys., *16:* 277–282, 1989.
2. Thraves, P., Salehi, Z., Dritschilo, A., and Rhim, J. S. Neoplastic transformation of immortalized human epidermal keratinocytes by ionizing radiation. Proc. Natl. Acad. Sci. USA, *87:* 1174–1177, 1990.
3. Willey, J. C., Hei, T. K., Piao, C. Q., Madrid, L., Willey, J. J., Apostolakos, M. J., and Hukku, B. Radiation-induced deletion of chromosomal regions containing tumor suppressor genes in human bronchial epithelial cells. Carcinogenesis (Lond.), *14:* 1181–1188, 1993.
4. Pazzaglia, S., Chen, X-R., Aamodt, C. B., Wu, S-Q., Kao, C., Gilchrist, K. W., Oyasu, R., Reznikoff, C. A., and Ritter, M. A. *In vitro* radiation-induced neoplastic progression of low-grade uroepithelial tumors. Radiat. Res., *138:* 86–92, 1994.
5. Mendonca, M. S., Fasching, C. L., Srivatsan, E. S., Stanbridge, E. J., and Redpath, J. L. Loss of a putative chromosome 11 tumor suppressor locus after γ-ray-induced neoplastic transformation of HeLa X fibroblast human cell hybrids. Radiat. Res., *143:* 34–44, 1995.
6. Mendonca, M. S., Howard, K., Fasching, C. L., Farrington, D. L., Desmond, L. A., Stanbridge, E. J., and Redpath, J. L. Loss of suppressor loci on chromosomes 11 and 14 may be required for radiation-induced neoplastic transformation of HeLa X fibroblast human cell hybrids. Radiat. Res., *149:* 246–255, 1998.
7. Stanbridge, E. J. Suppression of malignancy in human cells. Nature (Lond.), *260:* 17–20, 1976.
8. Sun, C., Redpath, J. L., Colman, M., and Stanbridge, E. J. Further studies on the radiation-induced expression of a tumor-specific antigen in human cell hybrids. Radiat. Res., *114:* 84–93, 1988.
9. Mendonca, M. S., Antoniono, R. J., Latham, K. M., Stanbridge, E. J., and Redpath, J. L. Characterization of intestinal alkaline phosphatase expression and the tumorigenic potential of γ-irradiated HeLa X fibroblast cell hybrids. Cancer Res., *51:* 4455–4462, 1991.
10. Redpath, J. L., Mendonca, M., Sun, C., Antoniono, R., Colman, M., Latham, K. M., and Stanbridge, E. J. Tumor suppressor gene inactivation and radiation-induced neoplastic transformation *in vitro*: model studies using human hybrid cells. *In:* W. C. Dewey, M. Edington, R. J. M. Fry, E. J. Hall, and G. Whitmore (eds.), Radiation Research: A Twentieth-Century Perspective, Proceedings of the 9th International Congress of Radiation Research, Vol. II, pp. 342–347. San Diego, CA: Academic Press, 1992.
11. Mendonca, M. S., and Redpath, J. L. Isolation of human cell hybrids (HeLa X skin fibroblast) expressing a radiation-induced tumour-associated antigen. Br. J. Cancer, *60:* 324–326, 1989.
12. Mendonca, M. S., Antoniono, R. J., and Redpath, J. L. Delayed heritable damage and epigenetics in radiation-induced neoplastic transformation of human hybrid cells. Radiat. Res., *134:* 209–219, 1993.
13. Mendonca, M. S., Temples, T. M., Farrington, D. L., and Bloch, C. Evidence for a role of delayed death and genomic instability in radiation-induced neoplastic transformation of human hybrid cells. Int. J. Radiat. Biol., *74:* 755–764, 1998.
14. Limoli, C. L., Kaplan, M. I., Corcoran, J., Meyers, M., Boothman, D. A., and Morgan, W. F. Chromosomal instability and its relationship to other end points of genomic instability. Cancer Res., *57:* 5557–5563, 1997.
15. Little, J. B., Nagasawa, H., Pfenning, T., and Vetrovs, H. Radiation-induced genomic instability: delayed mutagenic and cytogenic effects of x rays and α particles. Radiat. Res., *148:* 299–307, 1997.
16. Mendonca, M. S., Kurohara, W., Antoniono, R., and Redpath, J. L. Plating efficiency as a function of time post-irradiation: evidence for the delayed expression of lethal mutations. Radiat. Res., *119:* 389–393, 1989.
17. Seymour, C. B., Mothersill, C., and Alper, T. High yields of lethal mutations in somatic mammalian cells that survive ionizing radiation. Int. J. Radiat. Biol. Relat. Stud. Phys. Chem. Med., *50:* 167–179, 1986.

18. Gorgojo, L., and Little, J. B. Expression of lethal mutations in progeny of irradiated mammalian cells. Int. J. Radiat. Biol., *55:* 619–630, 1989.
19. Chang, W. P., and Little, J. B. Delayed reproductive death in X-irradiated Chinese hamster ovary cells. Int. J. Radiat. Biol., *60:* 483–496, 1991.
20. Morgan, W. F., Day, J. P., Kaplan, M. I., McGhee, E. M., and Limoli, C. L. Genomic instability induced by ionizing radiation. Radiat. Res., *146:* 247–258, 1996.
21. Mothersill, C., Lyng, F., O'Reilly, S., Harney, J., and Seymour, C. B. Expression of lethal mutations is suppressed in neoplasically transformed cells and after treatment of normal cells with carcinogens. Radiat. Res., *145:* 714–721, 1996.
22. Murnane, J. P. Role of induced genetic instability in the mutagenic effects of chemicals and radiation. Mutat. Res., *367:* 11–23, 1996.
23. Kerr, J. F. R., Wyllie, A. H., and Currie, A. R. Apoptosis: a basic biological phenomenon with wide ranging implications in tissue kinetics. Br. J. Cancer, *26:* 239–257, 1972.
24. Hoffman, B., and Liebermann, D. A. Molecular controls of apoptosis: differentiation/ growth arrest primary response genes, proto-oncogenes, and tumor suppressor genes as positive and negative modulators, Oncogene, *9:* 1807–1812, 1994.
25. Levine, A. J. p53, the cellular gatekeeper for growth and division. Cell, *88:* 323–331, 1997.
26. Zhan, Q., Carrier, F., and Fornace, A. J., Jr. Induction of cellular p53 activity by DNA-damaging agents and growth arrest. Mol. Cell. Biol., *13:* 4242–4250, 1993.
27. Zhan, Q., Fan, S., Bae, I., Guillouf, C., Liebermann, D. A., O'Connor, P. M., and Fornace, A. J., Jr. Induction of bax by genotoxic stress in human cells correlates with normal p53 status and apoptosis. Oncogene, *9:* 3743–3751, 1994.
28. Kastan, M. B., Canman, C. E., and Leonard, C. J. p53, cell cycle control and apoptosis: implications for cancer. Cancer Metastasis Rev., *14:* 3–15, 1995.
29. Green, D. R. Apoptotic pathways: the roads to ruin. Cell, *94:* 695–698, 1998.
30. Evan, G. I., and Littlewood, T. A matter of life and cell death. Science (Washington DC), *281:* 1317–1322, 1998.
31. Blank, K. R., Rudoltz, M. S., Kao, G. D., Muschel, R. J., and Mckenna, W. G. The molecular regulation of apoptosis and implications for radiation oncology. Int. J. Radiat. Biol., *71:* 455–466, 1997.
32. Nelson, W. G., and Kastan, M. B. DNA strand breaks: the DNA template alterations that trigger p53-dependent DNA damage response pathways. Mol. Cell. Biol., *14:* 1815–1823, 1994.
33. Miyashita, T., Krajewski, S., Krajewska, M., Wang, H. G., Lin, H. K., Liebermann, D. A., Hoffman, B., and Reed, J. C. Tumor suppressor p53 is a regulator of Bcl-2 and Bax gene expression *in vitro* and *in vivo*. Oncogene, *9:* 1799–1805, 1994.
34. Adams, J. M., and Cory, S. The bcl-2 protein family: arbiters of cell survival. Science (Washington DC), *281:* 1322–1326, 1998.
35. Stanbridge, E. J., Flandemeyer, R. R., Daniels, D. W., and Nelson-Rees, W. A. Specific chromosome loss associated with expression of tumorigenicity in human cell hybrids. Somatic Cell Genet., *7:* 699–712, 1981.
36. Redpath, J. L., Sun, C., Colman, M., and Stanbridge, E. J. Neoplastic transformation of human hybrid cells by irradiation: a quantitative assay. Radiat. Res., *110:* 468–472, 1987.
37. Mendonca, M. S., Antoniono, R. J., Sun, C., and Redpath, J. L. A simplified and rapid staining method for the HeLa X skin fibroblast human hybrid cell neoplastic transformation assay. Radiat. Res., *131:* 345–350, 1992.
38. Mendonca, M. S., Sun, C., and Redpath, J. L. Suppression of radiation-induced neoplastic transformation of human cell hybrids by long term incubation at low extracellular pH. Cancer Res., *50:* 2123–2127, 1990.
39. Gorczyca, W., Gong, J., and Darzynkiewicz, Z. Detection of DNA strand breaks in individual apoptotic cells by the *in situ* terminal deoxynucleotidyl transferase and nick translation assays. Cancer Res., *53:* 1945–1951, 1993.
40. Sambrook, J., Fritsch, E. F., and Maniatis, T. Molecular Cloning: A Laboratory Manual, 2nd ed. Cold Spring Harbor, NY: Cold Spring Harbor Laboratory Press, 1989.
41. Smith, C. A., Williams, G. T., Kingston, R., Jenkinson, E. J., and Owen, J. J. T. Antibodies to CD3/T-cell receptor complex induce death by apoptosis in immature T cells in thymic cultures. Nature (Lond.), *337:* 181–184, 1989.
42. Martin, S. J., Reutelingsperger, C. P. M., McGahon, A. J., Rader, J. A., van Schie, R. C. A. A., LaFace, D. M., and Green, D. R. Early redistribution of plasma membrane phosphatidylserine is a general feature of apoptosis regardless of the initiating stimulus: inhibition by overexpression of bcl-2 and abl. J. Exp. Med., *182:* 1545–1556, 1995.
43. Harlow, E., and Lane, D. Antibodies: A Laboratory Manual. Cold Spring Harbor, NY: Cold Spring Harbor Laboratory, 1988.
44. Sakahira, H., Enari, M., and Nagata, S. Cleavage of CAD inhibitor in CAD activation and DNA degradaton during apoptosis. Nature (Lond.), *391:* 96–99, 1998.
45. Enari, M., Sakahira, H., Yokoyama, H., Okawa, K., Iwamatsu, A., and Nagata, S. A caspase-activated DNase that degrades DNA during apoptosis, and its inhibitor ICAD. Nature (Lond.), *391:* 43–50, 1998.
46. Cohen, G. M., Sun, X-M., Snowden, R. T., Dinsdale, D., and Skilleter, D. N. Key morphological features of apoptosis may occur in the absence of internucleosomal DNA fragmentation. Biochem. J., *286:* 331–334, 1992.
47. Collins, R. J., Harmon, B. V., Gobe, G. C., and Kerr, J. F. Internucleosomal DNA cleavage should not be the sole criterion for indentifying apoptosis. Int. J. Radiat. Biol., *61:* 451–453, 1992.
48. Tomei, L. D., Shapiro, J. P., and Cope, F. O. Apoptosis in C3H/10T 1/2 mouse embryonic cells: evidence for internucleosomal DNA modification in the absence of double-strand cleavage. Proc. Natl. Acad. Sci. USA, *90:* 853–857, 1993.
49. Schulze-Osthoff, K., Walczak, H., Droge, W., and Krammer, P. H. Cell nucleus and DNA fragmentation are not required for apoptosis. J. Cell Biol., *127:* 15–20, 1994.
50. Lazebnik, Y. A., Kaufmann, S. H., Desnoyers, S., Poirier, G. G., and Earnshaw, W. C. Cleavage of poly(ADP-ribose) polymerase by a proteinase with properties like ICE. Nature (Lond.), *371:* 346–347, 1994.
51. Lowe, S. W., Schmitt, E. M., Smith, S. W., Osborne, B. A., and Jacks, T. p53 is required for radiation-induced apoptosis in mouse thymocytes. Nature (Lond.), *362:* 847–852, 1993.
52. Butz, K., Shahabedin, L., Geisen, C., Spitkovsky, D., Ullmann, A., and Hoppe-Seyler, F. Functional p53 protein in human papillomavirus-positive cancer cells. Oncogene, *10:* 927–936, 1995.
53. Reed, J. C. Double identity for proteins of the Bcl-2 family. Nature (Lond.), *387:* 773–776, 1997.
54. Oltvai, Z. N., Milliman, C. L., and Korsmeyer, S. J. Bcl-2 heterodimerizes *in vivo* with a conserved homolog, bax, that accelerates programmed cell death. Cell, *74:* 609–619, 1993.
55. Yin, X-M., Oltvai, Z. N., and Korsmeyer, S. J. BH1 and BH2 domains of Bcl-2 are required for inhibition of apoptosis and heterodimerization with Bax. Nature (Lond.), *369:* 321–323, 1994.
56. Yin, C., Knudson, C. M., Korsmeyer, S. J., and Van Dyke, T. Bax suppresses tumorigenesis and stimulates apoptosis *in vivo*. Nature (Lond.), *385:* 337–340, 1997.
57. Gavrieli, Y., Sherman, Y., and Ben Sasson, S. A. Identification of programmed cell death *in situ* via specific labeling of nuclear DNA fragmentation. J. Cell Biol., *119:* 493–501, 1992.
58. Steller, H. Mechanisms and genes of cellular suicide. Science (Washington DC), *267:* 1445–1449, 1995.
59. Casciola-Rosen, L., Nicholson, D. W., Chong, T., Rowan, K. R., Thornberry, N. A., Miller, D. K., and Rosen, A. Apopain/CPP32 cleaves proteins that are essential for cellular repair: a fundamental principle of apoptotic death. J. Exp. Med., *183:* 1957–1964, 1996.
60. Waterhouse, N., Kumar, S., Song, Q., Strike, P., Sparrow, L., Dreyfuss, G., Ahemri, E. S., Litwack, G., Lavin, M., and Watters, D. Heteronuclear ribonucleoproteins C1 and C2, components of the spliceosome, are specific targets of interleukin1β-converting enzyme-like proteases in apoptosis. J. Biol. Chem., *271:* 29335–29341, 1996.
61. Villa, P., Kaufmann, S. H., and Earnshaw, W. C. Caspases and caspase inhibitors. Trends Biochem. Sci., *22:* 388–393, 1997.
62. Salvesen, G. S., and Dixit, V. M. Caspases. Intracellular signaling by proteolysis. Cell, *91:* 443–446, 1997.
63. Kharbanda, S., Pandey, P., Schofield, L., Ireals, S., Rocincske, R., Yoshida, K., Bharti, A., Yuan, Z-M., Saxena, S., Weichselbaum, R. R., Nalin, C., and Kufe, D. Role of Bcl-x_L as an inhibitor of cytosolic cytochrome *c* accumulation in DNA damage-induced apoptosis. Proc. Natl. Acad. Sci. USA, *94:* 6939–6942, 1997.
64. Smith, M. L., and Fornace, A. J., Jr. Genomic instability and the role of p53 mutations in cancer cells. Curr. Opin. Oncol., *7: 69–75, 1995.*
65. Wahl, G. M., Linke, S. P., Paulson, T. G., and Huang, L-C. Maintaining genetic stability through TP53 mediated checkpoint control. Cancer Surv., *29:* 183–219, 1997.
66. White, E. Life, death, and the pursuit of apoptosis. Genes Dev., *10:* 1–15, 1996.
67. Boise, L. H., Gonzalez-Garcia, M., Postema, C. E., Ding, L., Lindsten, T., Turka, L. A., Mao, X., Nunez, G., and Thompson, C. B. bcl-x, a bcl-2 related gene that functions as a dominant regulator of apoptotic cell death. Cell, *74:* 597–608, 1993.
68. Reed, J. C. Cytochrome *c*: can't live with it–can't live without it. Cell, *91:* 559–562, 1997.
69. Green, D. R., and Reed, J. C. Mitochondria and apoptosis. Science (Washington DC), *281: 1309–1312, 1998.*
70. Kastan, M. B., Zhan, Q., El-Deiry, W. S., Carrier, F., Jacks, T., Walsh, W. V., Plunkett, B. S., Vogelstein, B., and Fornace, A. J. J. A mammalian cell cycle checkpoint pathway utilizing p53 and GADD45 is defective in ataxia-telangiectasia. Cell, *71:* 587–597, 1992.
71. King, K. L., and Cidlowski, J. A. Cell cycle and apoptosis: common pathways to life and death. J. Cell. Biochem., *58:* 175–180, 1995.
72. Dewey, W. C., Ling, C. C., and Meyn, R. E. Radiation-induced apoptosis: relevance to radiotherapy. Int. J. Radiat. Oncol. Biol. Phys., *33:* 781–796, 1995.
73. Algan, O., Stobbe, C. C., Helt, A. M., Hanks, G. E., and Chapman, J. D. Radiation inactivation of human prostate cancer cells: the role of apoptosis. Radiat. Res., *146:* 267–275, 1996.
74. Zhan, Q., Alamo, I., Yu, K., Boise, L. H., Cherney, B., Tosato, G., O'Connor, P. M., and Fornace, A. J., Jr. The apoptosis-associated γ-ray response of BCL-X_L depends on normal p53 function. Oncogene, *13:* 2287–2293, 1997.
75. Limoli, C. L., Hartmann, A., Shephard, L., Yang, C-R., Boothman, D. A., Bartholomew, J., and Morgan, W. F. Apoptosis, reproductive failure, and oxidative stress in Chinese hamster ovary cells with compromised genomic integrity. Cancer Res., *58:* 3712–3718, 1998.
76. Mendonca, M. S., Howard, K., Desmond, L. A., and Derrow, C. Previous loss of chromosome 11 containing a suppressor locus increases radiosensitivity, neoplastic transformation frequency, and delayed death in HeLa X fibroblast human hybrid cells. Mutagenesis, in press, 1999.
77. Elkind, M. M., and Whitmore, G. F. The Radiobiology of Cultured Mammalian Cells. New York: Gordon and Breach, 1967.
78. Hall, E. J. Radiobiology for the Radiobiologist, Ed. 4. Philadelphia: J. B. Lippincott Co., 1994.
79. Vidair, C. A., Chen, C. H., Ling, C. C., and Dewey, W. C. Apoptosis induced by X-irradiation of rec-myc cells is postmitotic and not predicted by the time after irradiation or behavior of sister cells. Cancer Res., *56:* 4116–4118, 1996.
80. Ianzini, F., and Mackey, M. A. Spontaneous premature chromosome condensation and mitotic catastrophe following irradiation of HeLa S3 cells. Int. J. Radiat. Biol., *72:* 409–421, 1997.
81. Cheng, K. C., and Loeb, L. A. Genomic instability and tumor progression: mechanistic considerations. Adv. Cancer Res., *60:* 121–156, 1993.
82. Kronenberg, A. Radiation-induced genomic instability. Int. J. Radiat. Biol., *66:* 603–609, 1994.

DEPARTMENT OF THE ARMY
US ARMY MEDICAL RESEARCH AND MATERIEL COMMAND
504 SCOTT STREET
FORT DETRICK, MARYLAND 21702-5012

REPLY TO
ATTENTION OF:

MCMR-RMI-S (70-1y) 26 Aug 02

MEMORANDUM FOR Administrator, Defense Technical Information Center (DTIC-OCA), 8725 John J. Kingman Road, Fort Belvoir, VA 22060-6218

SUBJECT: Request Change in Distribution Statement

1. The U.S. Army Medical Research and Materiel Command has reexamined the need for the limitation assigned to technical reports written for this Command. Request the limited distribution statement for the enclosed accession numbers be changed to "Approved for public release; distribution unlimited." These reports should be released to the National Technical Information Service.

2. Point of contact for this request is Ms. Kristin Morrow at DSN 343-7327 or by e-mail at Kristin.Morrow@det.amedd.army.mil.

FOR THE COMMANDER:

Encl

PHYLIS M. RINEHART
Deputy Chief of Staff for
Information Management

ADB274369
ADB256383
ADB264003
ADB274462
ADB266221
ADB274470
ADB266221
ADB274464
ADB259044
ADB258808
ADB266026
ADB274658
ADB258831
ADB266077
ADB274348
ADB274273
ADB258193
ADB274516
ADB259018
ADB231912
ADB244626
ADB256677
ADB229447
ADB240218
ADB258619
ADB259398
ADB275140
ADB240473
ADB254579
ADB277040
ADB249647
ADB275184
ADB259035
ADB244774
ADB258195
ADB244675
ADB257208
ADB267108
ADB244889
ADB257384
ADB270660
ADB274493
ADB261527
ADB274286
ADB274269
ADB274592
ADB274604
ADB274596
ADB258952
ADB265976
ADB274350
ADB274346
ADB257408
ADB274474
ADB260285
ADB274568
ADB266076
ADB274441
ADB253499
ADB274406
ADB262090
ADB261103
ADB274372